



Technical University of Crete

Dept: Production Engineering and Management

Master Thesis Subject:

**Off-line Application of the
Motorway Traffic Surveillance Tool RENAISSANCE to a
Motorway Network Around Antwerp**

Antonis F. Lentzakis

Supervising Professor: Markos Papageorgiou

Chania, February 2009

Acknowledgements

I would like to thank my supervising professor Markos Papageorgiou, professor Ioannis Papamichael, professor Ilias Kosmatopoulos, Dr. Chris Tampere, Dr. Albert Messmer, Dr. Yibing Wang, Thomas Verbaken, Katia Organe as well as all the members of the DSSL laboratory. I would also like to thank Athena Tzimitsi, whose help at the beginning of my thesis has been invaluable, since, a lot of the progress I made in the initial stages of this project can be attributed to her. Last, but not least, I would like to thank my family and friends for supporting me throughout my studies.

Table of Contents

1. Introduction	1
1.1. Introduction to the RENAISSANCE Tool	1
1.2. Scope of the Reported Work	3
2. An Overview of RENAISSANCE	5
2.1. Modelling of RENAISSANCE	5
2.1.1 Macroscopic motorway network traffic flow model.....	5
2.1.2 Model of traffic measurements	8
2.1.3 Dynamic system model of RENAISSANCE	9
2.2. Traffic Surveillance Tasks of RENAISSANCE.....	10
2.2.1 Traffic state estimation and prediction.....	10
2.2.2 Travel time estimation and prediction.....	12
2.2.3 Queue tail and head tracking	13
2.2.4 Incident report processing and incident alarm	14
2.3. Functional Architecture of RENAISSANCE.....	15
2.3.1 User options.....	15
2.3.2 Data input and output of RENAISSANCE	18
2.4. Versions of RENAISSANCE.....	20
3. The Application Network in Antwerp.....	21
3.1. Basic RENAISSANCE Settings.....	22
4. Estimation Results.....	30
4.1. Use of a Single Fundamental Diagram for the Entire Network	30
4.2. Use of Multiple Fundamental Diagrams	35
4.3. Evaluation at Non-Measurement Locations	48
4.4. Multiple Day Assessment.....	59
4.5. Impact of Faulty Detectors and Replacement of Faulty Data	65
4.6. Incident Detection	67
4.7. Less-Loops Scenario	81
5. Prediction Results.....	88
5.1. Prediction Parameters.....	88
5.2. Boundary Variable Prediction.....	89
5.3. Prediction Results with Use of Historical Data.....	91
5.4. Prediction Results with Extrapolation Only	100
5.5. Travel Time Prediction.....	107

5.6. Prediction under Incidents.....	111
5.6.1 General considerations	111
5.6.2 Prediction Results for Incident 1	113
5.6.3 Prediction Results for Incident 3	113
5.6.4 Prediction Results for Incident 4.....	115
5.6.5 Conclusions on Prediction under Incidents.....	116
6. Conclusions and Recommendations.....	117
6.1. Traffic state estimation and travel time prediction capabilities of RENAISSANCE on the Antwerp Ring network in regular conditions	117
6.2. Incident detection capability of RENAISSANCE on the Antwerp Ring network.....	118
6.3. Traffic state estimation capability of RENAISSANCE on the Antwerp Ring network in incident conditions	119
6.4. Traffic state prediction capability of RENAISSANCE on the Antwerp Ring network in regular conditions.....	119
6.5. Traffic state prediction capability of RENAISSANCE on the Antwerp Ring network in incident conditions	121
6.6. Conclusion and recommendations on applicability of RENAISSANCE on the Antwerp Ring network	121

List of Figures

Figure 1: The role of RENAISSANCE in on-line case.....	2
Figure 2: Queue tracking.....	14
Figure 3: Functionalities of RENAISSANCE.....	16
Figure 4: The application network (Source: Google Earth).....	21
Figure 5: The overall network model.....	27
Figure 6: Speed measurements in R1 Inner Ring.....	28
Figure 7: Speed measurements in R1 Outer Ring.....	28
Figure 8: Speed measurements in E313 (one direction).	29
Figure 9: Flow and mean speed estimates for R1 Inner Ring for case of single FD.....	31
Figure 10: Flow and mean speed estimates for R1 Outer Ring for case of single FD.....	31
Figure 11: Flow and mean speed estimates for E313 for case of single FD.....	32
Figure 12: Flow and mean speed estimates for E313 connections to R1 Inner and Outer Ring and for A12 Motorway for case of single FD.	33
Figure 13: Fundamental Diagram model parameter estimates for entire network for case of single FD.	34
Figure 14: Application network layout with multiple Fundamental Diagram clusters, R1 Ring both directions.	35
Figure 15: Application network layout with multiple Fundamental Diagram clusters, E313 and A12.	36
Figure 16: Flow, mean speed and Fundamental Diagram model parameter estimates for R1 Inner Ring for case of multiple FDs.....	40
Figure 17: Flow, mean speed and Fundamental Diagram model parameter estimates for R1 Outer Ring for case of multiple FDs.	43
Figure 18: Flow, mean speed and Fundamental Diagram model parameter estimates for E313 for case of multiple FDs.	44
Figure 19: Flow, mean speed and Fundamental Diagram model parameter estimates for E313 connections to R1 Inner and Outer Ring and for A12 Motorway for case of multiple FD.....	47
Figure 20: Congestion propagation examples to assess estimation quality at non-measurement locations.	51
Figure 21: Representative examples of AID measured versus estimated speed trajectories. ..	53
Figure 22: Part of the network for Case 1.	54
Figure 23: AID measured versus estimated speed trajectories for Case 1.	56

Figure 24: Part of the network for Case 2.	57
Figure 25: AID measured versus estimated speed trajectories for Case 2.	57
Figure 26: Part of the network for Case 3.	57
Figure 27: AID measured versus estimated speed trajectories for Case 3.	58
Figure 32: Examples of 5-day estimation results.	63
Figure 33: Examples of steady changes of FD parameter estimates.	64
Figure 34: Impact of faulty data in R1 tunnel (inner and outer).	66
Figure 35: Impact of faulty data at LE11_o.	67
Figure 36: Part of network for Incident 1.	68
Figure 37: Capacity estimates indicating occurrence of Incident 1 at around 7:00 a.m. of day 1.	69
Figure 38: Time derivative of capacity estimates for Incident 1.	69
Figure 39: Speed measurements confirming the occurrence of Incident 1.	69
Figure 40: Zooming-in of Figure 39.	70
Figure 41: Zooming-in of Figure 38.	70
Figure 42: Network part for Incident 2.	71
Figure 43: Capacity estimates for Incident 2 (around 14:00 h of day 3).	71
Figure 44: Time derivative of capacity estimates for Incident 2.	72
Figure 45: Speed measurements at the upstream detector _77.	72
Figure 46: Zooming-in of Figure 44.	72
Figure 47: Flow and speed measurements for Incident 3.	74
Figure 48: Capacity estimates for Incident 3.	74
Figure 49: Time derivative of capacity estimates for Incident 3.	75
Figure 50: Zooming-in of Figure 49.	75
Figure 51: Flow and speed measurements for Incident 4.	76
Figure 52: Capacity estimates for Incident 4.	77
Figure 53: Time derivative of capacity estimates for Incident 4.	77
Figure 54: Zooming-in of Figure 51.	77
Figure 55: Zooming-in of Figure 53.	78
Figure 56: Speed measurement for Incident 5.	79
Figure 57: Capacity estimates for Incident 5.	79
Figure 58: Time derivative of capacity estimates for Incident 5.	79
Figure 59: Zooming in of Figure 56.	80
Figure 60: Zooming-in of Figure 58.	80

Figure 61: Dropped detectors (red-coloured) and modified link clusters for the less-loops scenario.	83
Figure 62: Inner ring less-loop scenario results.	84
Figure 63: Outer ring less-loop scenario results.....	85
Figure 64: E313 less-loop scenario results.....	86
Figure 65: Impact of dropped off-ramp measurements.....	87
Figure 66: Inflow predictions with extrapolation only (left column) and with historical data combined with extrapolation (right column).....	90
Figure 67: Turning rate predictions.....	90
Figure 68: Destination (off-ramp) density predictions with extrapolation only (left column) and with historical data combined with extrapolation (right column).	92
Figure 69: Inner ring prediction results using historical data and extrapolation.....	96
Figure 70: Outer ring prediction results using historical data and extrapolation.	98
Figure 71: E313 prediction results using historical data and extrapolation.	99
Figure 72: Inner ring prediction results using extrapolation only.....	103
Figure 73: Outer ring prediction results using extrapolation only.	105
Figure 74: E313 prediction results using extrapolation only.	106
Figure 75: Instantaneous and predicted travel times on 3 network routes with use of historical data and extrapolation.	109
Figure 76: Instantaneous and predicted travel times on 3 network routes with use of extrapolation only.....	111
Figure 77: Mean speed predictions for Incident 1.....	114
Figure 78: Flow measurements and estimates for Incident 1.....	114
Figure 79: Mean speed predictions for Incident 3.....	115
Figure 80: Mean speed predictions for Incident 4.....	115

1. Introduction

1.1. Introduction to the RENAISSANCE Tool

Motorway networks are usually equipped with a number of measurement devices of various kinds (inductive loops, video sensors, radar detectors) that deliver real-time information about the current traffic conditions in corresponding locations. However, if the density of available traffic detectors is not very high (e.g. lower than one sensor per 0.5 or 1 km), the delivered real-time information may not be complete due to significant space inhomogeneities. This creates the need for a traffic state estimator that would deliver in real time the complete traffic state for an entire motorway network based on a more or less limited amount of traffic measurements. Moreover, a number of further real-time traffic surveillance tasks including traffic state prediction, travel time estimation and prediction, queue tail/head estimation and prediction (queue tracking), and incident alarm are of interest to the traffic operators for various uses. More precisely, the **traffic state estimation** refers to estimating all traffic variables of a motorway network at each current time instant based on a **limited** amount of **local** real-time traffic measurements available up to now; the short-term **traffic state prediction** delivers at each current time instant the traffic variables within the motorway network over a future time horizon. The **travel time estimation (prediction)** refers to estimating (predicting) the instantaneous (experienced) travel time along any specified route inside the network at each time instant. Finally, the **queue tail and head estimation (prediction)** aims at estimating (predicting) the locations of any queue tail and head existing (to appear) along any specified route within the network at each time instant (over a future time horizon). With the identified locations of queue tails and heads, the queue lengths are readily estimated and predicted.

The **REal-time motorway Network trAffic State SurveillANCE (RENAISSANCE)** tool has been developed within the European project RHYTHM to address these traffic surveillance tasks in a unified approach. As illustrated in Figure 1, in real life application RENAISSANCE is an intermediate layer between real-time traffic measurements and various driver information, guidance, and control systems, or between real-time traffic measurements and traffic operators. The real-time information, extended and enriched by RENAISSANCE, may be exploited for more efficient operations in motorway networks (e.g. traffic control, route guidance, etc.) or for real-time decision-making of traffic operators. More specifically, RENAISSANCE has the following noteworthy features:

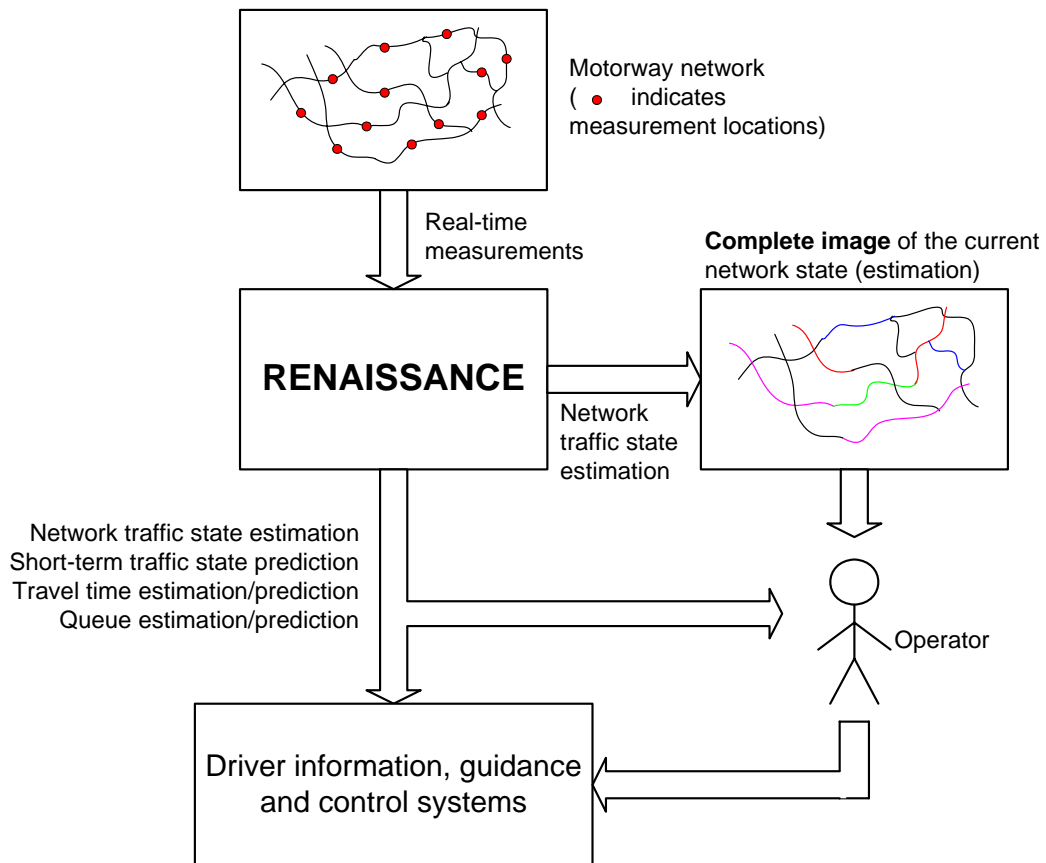


Figure 1: The role of RENAISSANCE in on-line case.

- RENAISSANCE delivers a **complete real-time image** of the network traffic conditions, especially in case of sparse detector installation and also in case of detector faults; see Figure 1, where the colours of motorway links inside the estimated network block represent different traffic conditions (e.g. free, dense, congested, etc.) identified by RENAISSANCE in real-time.
- RENAISSANCE delivers in real time **short-term predictions** of traffic state, travel times, and queues within the network.
- RENAISSANCE is applicable for motorway networks of arbitrary size, topology, and characteristics, with any suitable traffic detector configuration.
- RENAISSANCE is able to handle in an efficient way real-time measurements collected via inductive loops, radar detectors, video sensors, or via any combination of those. Parallel to the on-line usage, the unprocessed measurement data (exactly as they were received) are recorded for possible later replay.

- The RENAISSANCE software can be easily integrated into a motorway traffic control centre. Any further extensions of the infrastructure, sensors, etc. can be easily accommodated.
- RENAISSANCE is also available in an off-line version where the detector data are user-provided in a general off-line format via input file. The off-line version may be used for studies by researchers, traffic engineers, consultants, or authority employees, based on historical measurement data or even simulated data. This is the version used in the present study.

RENAISSANCE also includes an integrated graphical user-friendly interface (GUI), which allows for, e.g.

- visualization of the estimation and prediction results in a form of network overview which displays traffic variables and queues with certain attributes on the links (colour and width);
- plotting over time any detector measurement, any traffic variable of each network segment as well as travel time and queue variables along pre-defined routes;
- indication of program running status and display of warning/error messages.

1.2. Scope of the Reported Work

This report reflects the results of a project aiming at applying and testing in off-line mode the RENAISSANCE tool for the motorway network around Antwerp, Belgium.

The specific tasks that were agreed to be completed were the following:

One network definition is used, in which three test sections are included. The overall network is defined as:

- R1 in both driving directions, i.e. from Interchange St.-Anna LO (location_ID 76) to Antwerp North (location_ID 101) with total length of 17 km + 17 km (for both directions)
- E313 Westbound, starting downstream from Interchange Ranst (location_ID 58), length 7 km.

Altogether this network is approximately 44 km long (including the modeling of some on-ramp and off-ramp parts beyond the motorway mainstream).

The test sections are:

- E313 Westbound, length 7 km

- R1 Inner ring, length 17 km
- R1 Outer ring, length 17 km.

Variants to be analyzed on this network are:

- In-depth analysis of estimation and prediction using only the double loop detectors in a range of traffic conditions, including:
 - morning peak
 - evening peak
 - off-peak periods: evening, night, between peaks
 - 2 incidents, one peak and one off-peak.
- Variable detector spacing variants:
- AID variants, i.e. by using additional speed measurements stemming from installed AID cameras.

The work actually carried out extends to some further interesting tasks as reported in the following chapters.

2. An Overview of RENAISSANCE

2.1. Modelling of RENAISSANCE

2.1.1 Macroscopic motorway network traffic flow model

A motorway network may be represented as a directed graph. More precisely, bifurcations, junctions, on-ramps, and off-ramps are represented by the **nodes**, whereas the motorway stretches between these locations are represented by the **links** of the graph. The two directions of a motorway stretch are modelled as separate links with opposite directions. Inside each link we suppose homogeneous geometric characteristics such as number of lanes, grade, curvature, etc. An inhomogeneous motorway stretch is represented by two or more consecutive links separated by nodes at the locations where a geometrical change occurs. At the bounds of the network, origin or destination links are added where traffic enters or leaves the considered network.

A validated second-order macroscopic network traffic flow model is employed in RENAISSANCE to describe the traffic flow dynamics in motorway networks. The model describes traffic flow dynamics within each motorway link, while the distribution of traffic flow at bifurcation nodes is modelled in terms of **turning rates**. This model can simulate all kinds of traffic conditions (free, dense, and congested) and model capacity-reducing events (incidents) with prescribed characteristics (location, intensity, and duration).

Based on a macroscopic approach, the dynamic behaviour of traffic flow along motorway links can be described in terms of appropriate aggregated traffic flow variables that are **space mean speed**, **traffic density**, and **flow**. For the convenience of modelling and digital computation, the aggregated traffic flow variables are presented in a space-time discretized form. More specifically, for the space discretisation any motorway link m is sub-divided into a number of **segments**, each with a length Δ_m (about 500 m), while the time discretisation is based on a time step T (e.g. 10 s) and the discrete time indices $k = 0, 1, 2, \dots$. The aggregated traffic flow variables defined in this discrete space-time frame are:

- traffic density $\rho_{m,i}(k)$ (in veh/km/lane) is defined as the number of vehicles in segment i of link m at time instant $t = kT$, divided successively by the segment length Δ_m and number of lanes λ_m ;
- space mean speed $v_{m,i}(k)$ (in km/h) is the average speed of all vehicles included in segment i of link m at time instant $t = kT$;

- traffic flow $q_{m,i}(k)$ (in veh/h) is the number of vehicles leaving segment i of link m during the time period $[kT, (k+1)T]$, divided by T .

For a segment i of a link m , the stochastic nonlinear difference equations of the second-order macroscopic traffic flow model are as follows:

$$\rho_{m,i}(k+1) = \rho_{m,i}(k) + \frac{T}{\Delta_m \lambda_m} [q_{m,i-1}(k) - q_{m,i}(k)] \quad (1)$$

$$\begin{aligned} v_{m,i}(k+1) = & v_{m,i}(k) + \frac{T}{\tau} [V(\rho_{m,i}(k)) - v_{m,i}(k)] \\ & + \frac{T}{\Delta_m} v_{m,i}(k) [v_{m,i-1}(k) - v_{m,i}(k)] - \frac{\nu T}{\tau \Delta_m} \frac{[\rho_{m,i+1}(k) - \rho_{m,i}(k)]}{\rho_{m,i}(k) + \kappa} + \xi_{m,i}^v(k) \end{aligned} \quad (2)$$

$$V(\rho) = v_{f,m} \exp \left[-\frac{1}{a_m} \left(\frac{\rho}{\rho_{cr,m}} \right)^{a_m} \right] \quad (3)$$

$$q_{m,i}(k) = \rho_{m,i}(k) v_{m,i}(k) \lambda_m + \xi_{m,i}^q(k) \quad (4)$$

where equations (1)-(4) are the well-known conservation equation, dynamic speed equation, stationary speed equation (to be replaced in (2)), and transport equation (to be replaced in (1)), respectively; τ , ν , κ are model parameters which are given the same values for the whole network, while $v_{f,m}$ denotes the free speed, $\rho_{cr,m}$ the critical density, and a_m the exponent of the stationary speed equation for link m ; $\xi_{m,i}^v(k)$ and $\xi_{m,i}^q(k)$ denote noise acting on the empirical speed equation and approximate transport equation, respectively, to reflect the modelling inaccuracies. Note that (1) is not corrupted by noise as it reflects the conservation of vehicles, which holds strictly in any case. The model parameters may be identified via an off-line calibration procedure, but they may change values in real-time due to changing environmental conditions (darkness, rain, etc.); hence it would be best to estimate them on-line. It is known that the model results are most sensitive to variations of the free speed, critical density, and exponent. Based on the fundamental diagram $Q(\rho) = \rho V(\rho)$, the capacity of a link m (per lane) may be deduced from (3) as $q_{cap,m} = v_{f,m} \cdot \rho_{cr,m} \cdot \exp[-1/a_m]$.

Clearly, the complete macroscopic model of link m can be built upon a chain of interconnected segment models with a total of $2N_m$ dynamic equations for the segment state variables $\rho_{m,1}, v_{m,1}, \rho_{m,2}, v_{m,2}, \dots, \rho_{m,N_m}, v_{m,N_m}$; this model includes three boundary variables: (a) flow $q_{m,0}$ at the upper boundary of link m (needed in (1) for $i=1$); (b) speed $v_{m,0}$ at the upper boundary of link m (needed in (2) for $i=1$); (c) density ρ_{m,N_m+1} at the lower boundary of link m (needed in (2) for $i=N_m$).

Links are interconnected via nodes. Traffic enters a node n through a number of inflowing links according to

$$Q_n(k) = \sum_{\mu \in I_n} q_{\mu, N_\mu}(k) \quad (5)$$

where I_n denotes the set of the links entering node n , and $Q_n(k)$ is the total traffic volume reaching node n at time period $[kT, (k+1)T]$. On the other hand, the outflow that leaves a node n via a link m is given by

$$q_{m,0}(k) = Q_n(k) \beta_n^m(k), \quad \forall m \in O_n \quad (6)$$

where O_n is the set of links leaving node n , $q_{m,0}(k)$ is the traffic volume leaving node n via link m during time period $[kT, (k+1)T]$, and the turning rate $\beta_n^m(k)$ is defined as the percentage of $Q_n(k)$ that leaves node n via exiting link m during the same time period. A turning rate at a bifurcation node immediately upstream of an off-ramp is also called the exiting rate at the off-ramp.

At a network node n , the upstream influence of the downstream-link density (e.g., in case of congestion spillback) has to be taken into account in the last segment of the incoming links (see (2) for $i = N_m$). This is provided via

$$\rho_{m, N_{m+1}}(k) = \sum_{\mu \in O_n} \rho_{\mu,1}^2(k) / \sum_{\mu \in O_n} \rho_{\mu,1}(k) \quad (7)$$

where $\rho_{m, N_{m+1}}(k)$ is the virtual density downstream of any entering link m to be used in (2) for $i = N_m$ and $\rho_{\mu,1}(k)$ is the density of the first segment of the leaving link μ . The quadratic form is used to account for the fact that congestion on one leaving link may spill back into the entering link even if there is free flow in the other leaving links.

The use of the quadratic average in (7) does not allow for a model calibration so as to better fit the field phenomena at bifurcation nodes where one of the out-links may occasionally carry a traffic congestion that spills back onto the in-link(s). As a matter of fact, it is easy to prove that the quadratic average of (7) is always greater than or equal to the arithmetic average $\rho_{\mu,A} = \left(\sum_{\mu \in O_n} \rho_{\mu,1} \right) / |O_n|$. Also, the quadratic average of (7) is always less than or equal to the infinity norm $\rho_{\mu,\infty} = \max_{\mu \in O_n} \rho_{\mu,1}$. (In fact, equality of all averages is encountered if all $\rho_{\mu,1}$ are equal among them $\forall \mu \in O_n$.) This creates a possibility to replace (7) by an alternative weighted combination formula

$$\rho_{m, N_{m+1}}(k) = \alpha \rho_{m,\infty}(k) + (1 - \alpha) \rho_{m,A}(k) \quad (8)$$

with a constant parameter $\alpha \in [0,1]$ that may be selected at each bifurcation node for better adjustment to the corresponding real observed phenomena.

On the other hand, at a network node n the downstream influence of the upstream-link speed has to be taken into account according to (2) for $i = 1$. The required upstream mean speed value is calculated from the flow-weighted average

$$v_{m,0}(k) = \sum_{\mu \in I_n} v_{\mu, N_\mu}(k) q_{\mu, N_\mu}(k) / \sum_{\mu \in I_n} q_{\mu, N_\mu}(k) \quad (9)$$

where $v_{m,0}(k)$ is the virtual speed upstream of any leaving link m that is needed in (2) for $i = 1$.

2.1.2 Model of traffic measurements

Traffic detectors are installed along motorway stretches at a separation of several kilometres as a main tool for obtaining real-time traffic measurements. Consider a traffic detector installed at the boundary of two adjacent segments i and $i + 1$. For the flow measurement, we have, via (4),

$$y_{m,i}^q(k) = \rho_{m,i}(k) v_{m,i}(k) \lambda_{m,i} + \xi_{m,i}^q(k) + \gamma_{m,i}^q(k) \quad (10)$$

where $y_{m,i}^q(k)$ denotes the flow measurement and $\gamma_{m,i}^q(k)$ the flow measurement noise. For the mean speed measurement, we have

$$y_{m,i}^v(k) = v_{m,i}(k) + \gamma_{m,i}^v(k) \quad (11)$$

where $y_{m,i}^v(k)$ denotes the speed measurement and $\gamma_{m,i}^v(k)$ the speed measurement noise. The flow measurement $y_o^q(k)$ at an on-ramp o can be expressed as

$$y_o^q(k) = q_o(k) + \gamma_o^q(k) \quad (12)$$

where $\gamma_o^q(k)$ denote the corresponding measurement noise. For an off-ramp d with its upstream bifurcation node n , the off-ramp flow measurement $y_d^q(k)$ can be modelled, via (6), as

$$y_d^q(k) = \beta_n^d(k) Q_n(k) + \gamma_d^q(k) \quad (13)$$

where $\gamma_d^q(k)$ denotes the corresponding measurement noise.

If an off-ramp is known to carry congested traffic that may spill back onto the motorway, it is advisable to also use speed measurements (if available) from the off-ramp; in this case a boundary density is calculated (using flow and speed measurements) for the off-ramp; this boundary density is then used at the off-ramps bifurcation node according to (7) or (8).

If a considered motorway network is homogeneous in terms of traffic characteristics, the RENAISSANCE model can simulate the network traffic dynamics with one fundamental diagram (i.e. with one single group of model parameters free speed, critical density, and

capacity). If a considered motorway network is inhomogeneous in terms of traffic characteristics, the model is also able to simulate the network traffic dynamics with multiple fundamental diagrams (i.e. with multiple groups of model parameters), each for a separate subset of motorway links with the same or similar traffic characteristics. In fact, the user may even specify a separate fundamental diagram for each motorway link, if necessary.

2.1.3 Dynamic system model of RENAISSANCE

The overall network traffic flow model (1)-(9) can be expressed in a compact state-space form:

$$\mathbf{z}(k+1) = \mathbf{h}[\mathbf{z}(k), \mathbf{d}(k), \mathbf{p}(k), \xi_1(k)] \quad (14)$$

where \mathbf{h} is a nonlinear differentiable vector function corresponding to a number of model equations, vector \mathbf{z} includes all segment speeds and densities, vector \mathbf{d} includes all the network boundary variables (origin inflows, origin inflow speeds, destination densities, turning rates), vector \mathbf{p} includes all important model parameters (free speed, critical density, and capacity of each considered fundamental diagram), and vector ξ_1 includes all modelling noise. Considering that $\mathbf{d}(k)$ may not be fully measured (some of its elements may not even be measurable) and that $\mathbf{p}(k)$ are normally unknown, two random-walk equations are introduced

$$\mathbf{d}(k+1) = \mathbf{d}(k) + \xi_2(k) \quad (15)$$

$$\mathbf{p}(k+1) = \mathbf{p}(k) + \xi_3(k). \quad (16)$$

The combination of equation (14) and both random-walk equations (15) and (16) leads to the following augmented state-space model

$$\mathbf{x}(k+1) = \mathbf{f}[\mathbf{x}(k), \xi(k)] \quad (17)$$

where state vector $\mathbf{x} = [\mathbf{z}^T \ \mathbf{d}^T \ \mathbf{p}^T]^T$, state noise $\xi = [\xi_1^T \ \xi_2^T \ \xi_3^T]^T$, and the nonlinear differentiable vector function \mathbf{f} can be determined accordingly. As a consequence, all boundary variables and important model parameters are included as a part of the augmented model state \mathbf{x} . The state vector \mathbf{x} is referred to as the **traffic state** of the considered motorway network, which is what the RENAISSANCE traffic state estimator addresses. Traffic measurements within a motorway network depend on the traffic state \mathbf{x} via an output equation

$$\mathbf{y}(k) = \mathbf{g}[\mathbf{x}(k), \boldsymbol{\eta}(k)] \quad (18)$$

where vector \mathbf{y} consists of all available measurements of flow and mean speed; \mathbf{g} is a nonlinear differentiable vector function; vector $\boldsymbol{\eta}$ is a function of modelling noise and measurement noise. Equations (17) and (18) constitute a complete motorway traffic dynamic system.

2.2. Traffic Surveillance Tasks of RENAISSANCE

RENAISSANCE incorporates a number of traffic surveillance algorithms and performs the corresponding traffic surveillance tasks in a unified macroscopic model-based approach. This section briefly introduces the RENAISSANCE traffic surveillance tasks.

2.2.1 Traffic state estimation and prediction

The **traffic state estimation** refers to estimating all traffic state variables of a considered motorway network at each current time instant based on real-time traffic measurements available up to now, while the short-term **traffic state prediction** refers to predicting at each current time instant the segment speeds and densities over a future time horizon. Note that **the number of traffic state variables to be estimated and predicted within a motorway network may be much larger than those that can be directly measured**, especially when the detectors are sparsely installed within the network. In addition, the traffic state estimation and prediction algorithms build the operating foundation of RENAISSANCE, i.e. all other surveillance tasks are performed on the basis of the results of the traffic state estimation and/or prediction.

Since the dynamic system model (17) and (18) is highly nonlinear, the extended Kalman filter (EKF) is used to design the traffic state estimator

$$\hat{\mathbf{x}}(k+1/k) = \underbrace{\mathbf{f}[\hat{\mathbf{x}}(k/k-1), \mathbf{0}]}_{\text{model}} + \underbrace{\mathbf{K}(k)[\mathbf{y}(k) - \mathbf{g}[\hat{\mathbf{x}}(k/k-1), \mathbf{0}]]}_{\text{correction}} \quad (19)$$

where $\hat{\mathbf{x}}(k+1/k)$ denotes the traffic state estimation for time instant $k+1$ based on the traffic measurements available up to time instant k ; $\mathbf{K}(k)$ is the gain matrix calculated on-line based on the linear Taylor expansion of \mathbf{f} and \mathbf{g} at $\hat{\mathbf{x}}(k/k-1)$. Because these calculations are recursive, $\mathbf{K}(k)$ is actually calculated based (implicitly) on traffic measurements at all previous time instants $k-1, k-2, \dots$.

A particular feature of this estimator is the real-time estimation not only of the segment speeds and densities, but also of some important model parameters. RENAISSANCE is able to handle the model parameters in two alternative approaches: (a) RENAISSANCE keeps the parameter values constant at some pre-specified values; (b) RENAISSANCE estimates the model parameter values on-line. In order to apply approach (a), a tedious model calibration

work may have to be conducted beforehand based on available off-line data in order to get accurate parameter values; else the segment speed/flow/density estimates may be biased. With approach (b), the user only has to specify the initial values for the parameters to be estimated. In case that the user does not have proper knowledge of the model parameter values, these initial values can be given quite arbitrarily, because RENAISSANCE is capable of identifying the actual model parameter values and even tracking parameter changes based on real-time traffic measurements. It is known that the model parameter values may be different from site to site, and even for a given site, they may change in real-time, due to environmental impact (weather and light conditions) or due to changing traffic composition (percentage of trucks), or specific control measures (e.g. variable speed limits). Therefore, approach (b) nicely leads to a general and flexible way to tackle the model parameters issue.

The RENAISSANCE traffic state prediction is performed by use of the motorway network traffic flow model, on the basis of the traffic state estimates available at the current time instant and of boundary value prediction over the prediction horizon. More precisely, neglecting the impact of unpredictable noise ξ_1 , the network traffic flow model (14) is written as

$$\mathbf{z}(k+1) = \mathbf{h}[\mathbf{z}(k), \mathbf{d}(k), \mathbf{p}(k), \mathbf{0}] \quad (20)$$

Let $\hat{\mathbf{z}}(k)$, $\hat{\mathbf{d}}(k)$, and $\hat{\mathbf{p}}(k)$ denote, respectively, the estimates of $\mathbf{z}(k)$, $\mathbf{d}(k)$, and $\mathbf{p}(k)$ at the current time instant k . Let $\mathbf{d}^p(\kappa)$ and $\mathbf{p}^p(\kappa)$, $\kappa = k+1, k+2, \dots, k+K_p-1$, denote the prediction of \mathbf{d} and \mathbf{p} for the future K_p-1 steps. Note that at each current time instant k ,

- (1) The values $\hat{\mathbf{z}}(k)$, $\hat{\mathbf{d}}(k)$, and $\hat{\mathbf{p}}(k)$ are available from $\hat{\mathbf{x}}(k)$ that is delivered by the traffic state estimator.
- (2) $\mathbf{d}^p(\kappa)$ is available for $\kappa = k+1, \dots, k+K_p-1$ via the boundary value prediction (see below).
- (3) The model parameters are not strongly time-varying, hence the predicted parameters $\mathbf{p}^p(\kappa)$ are set equal to $\mathbf{p}^p(k)$, for $\kappa = k+1, \dots, k+K_p-1$;

Thus, running the dynamic model (20) for K_p steps produces $\mathbf{z}^p(\kappa)$, $\kappa = k+1, \dots, k+K_p$, i.e. the pursued traffic state prediction.

As indicated above, the boundary value prediction is indispensable to the traffic state prediction. Two cases need to be distinguished while performing the boundary value prediction:

- (1) No historical data for the boundary variables (to be predicted) are available.

(2) Such historical data is available.

In case (1), the boundary value prediction is performed based on the trend-extrapolation of the boundary variable estimates that are available up to the current time instant. In case (2), the boundary value prediction can be performed either by use of (typically smoothed) historical data or based on an appropriate combination of both historical data and trend extrapolation. The basic idea of this combined approach is that the closer a future time instant is to the current time instant, the more the boundary value prediction (for this future time instant) relies on the trend-extrapolation of the boundary variable estimates available up to the current time instant, while the farther from the current time instant, the more the boundary value prediction relies on the historical data (corresponding to this future time instant).

2.2.2 Travel time estimation and prediction

A **route** within a motorway network is a sequence of adjacent links that connect two specific network nodes. The **instantaneous** travel time along a route is an ideal travel time spent by an ideal vehicle traversing that route under the currently prevailing traffic conditions. In other words, the instantaneous travel time at any time instant is calculated based on an assumption that, when a vehicle starts its trip along the route at that time instant, all segment speeds along the route are ‘frozen’ at the values they have. Consider any route r including M consecutive links (each link m with N_m segments). Then the instantaneous travel time along this route at any time instant k can be expressed as

$$\tau_{r,i}(k) = \sum_{m=1}^M \sum_{i=1}^{N_m} \frac{\Delta_m}{v_{m,i}(k)} \quad (21)$$

For the same route and the same time instant k , the travel time **estimation** can be expressed as

$$\hat{\tau}_{r,i}(k) = \sum_{m=1}^M \sum_{i=1}^{N_m} \frac{\Delta_m}{\hat{v}_{m,i}(k)} \quad (22)$$

where $\hat{\tau}_{r,i}(k)$ denotes the travel time estimation at k and $\hat{v}_{m,i}(k)$ the estimation of $v_{m,i}(k)$.

On the other hand, the **experienced** travel time along a route is the real travel time that a vehicle traversing the route will actually experience. Consider the same route as above (with total length $\sum_{m=1}^M N_m \Delta_m$); we denote by $\tau_{r,e}(k)$ the experienced travel time of vehicles starting their trip at time instant k , and $v_{r,k}(t)$, $t \geq k$ the speed trajectory of these vehicles during the trip. Then we have

$$\sum_{m=1}^M N_m \Delta_m = \int_{kT}^{kT + \tau_{r,e}(k)} v_{r,k}(t) dt \quad (23)$$

The travel time **prediction** refers to predicting the **experienced** travel time. Corresponding to (23), we have

$$\sum_{m=1}^M N_m \Delta_m = \int_{kT}^{kT + \hat{\tau}_{r,e}(k)} \hat{v}_{r,k}(t) dt \quad (24)$$

where $\hat{\tau}_{r,e}(k)$ and $\hat{v}_{r,k}(t)$ denote, respectively, the travel time prediction at time instant kT and the prediction of $v_{r,k}(t)$ over a future time horizon equal to or longer than $[kT, kT + \hat{\tau}_{r,e}(k)]$. In order to deliver travel time prediction, the virtual-car technique is employed by RENAISSANCE. A virtual car starts at the route origin at time k and is moved along the route according to the mean speeds predicted to prevail in corresponding motorway segments at the time they are reached by the virtual vehicle. In case the predicted travel time exceeds the prediction horizon K_p , there are no according predicted speeds to be used; in this case RENAISSANCE uses as segment speed values beyond K_p , the corresponding segment speed averages predicted for the last 5 minutes of the prediction horizon.

It should be noted that, in case of low speeds a slight underestimation may produce major travel time overestimation due to the specific nonlinear (hyperbolic) form of (22), and its counterpart in the virtual vehicle movement. Therefore, the user is offered the possibility to limit the speed value to be used in the travel time formulas; this option may be used by setting relatively high lower limits (e.g. 8-10 km/h) so as to avoid major travel time overestimation (for the price of possible but less strong travel time underestimation).

It is noted that RENAISSANCE performs travel time estimation/prediction only for the routes that are pre-specified by the user.

2.2.3 Queue tail and head tracking

RENAISSANCE defines a vehicle queue as a platoon of vehicles moving at a speed lower than a certain threshold value. A vehicle queue has a queue head and a queue tail. A queue tail is normally a congestion shockwave, while a queue head is normally where the traffic congestion originates, e.g. a bottleneck, or a traffic incident location, etc. Once a queue builds up within a motorway network, traffic operators at the traffic control centre need to track its evolution and in particular track how the queue tail will be propagating, so as to inform drivers, through VMS or other means, of the existence, extent and propagation of the queue in real time. Also, based on the obtained queue information, the traffic control centre may instruct the drivers to use a speed that would prevent shockwave crashes. Moreover, accurate

information on the existing queues or any queue to appear may help traffic operators or automatic traffic control algorithms to make more confident decisions on possible control actions to improve the overall traffic conditions.

Queue tail and head estimation (prediction) aims at estimating (predicting) the locations of any queue tail and head existing (to appear) at the current (future) time instant(s). With the identified locations of queue tails and heads, the queue lengths are readily estimated and predicted. The queue tail and head estimation (prediction) is based on the segment speed estimation (prediction). As illustrated in Figure 2, when mean speeds of some segments along a route are below a threshold value, one (or several) vehicular queue(s) is (are) considered to exist along that route (within the corresponding segments). It is noted that RENAISSANCE performs queue tracking only for the routes that are pre-specified by the user. The utilized speed threshold value can also be pre-specified by the user.

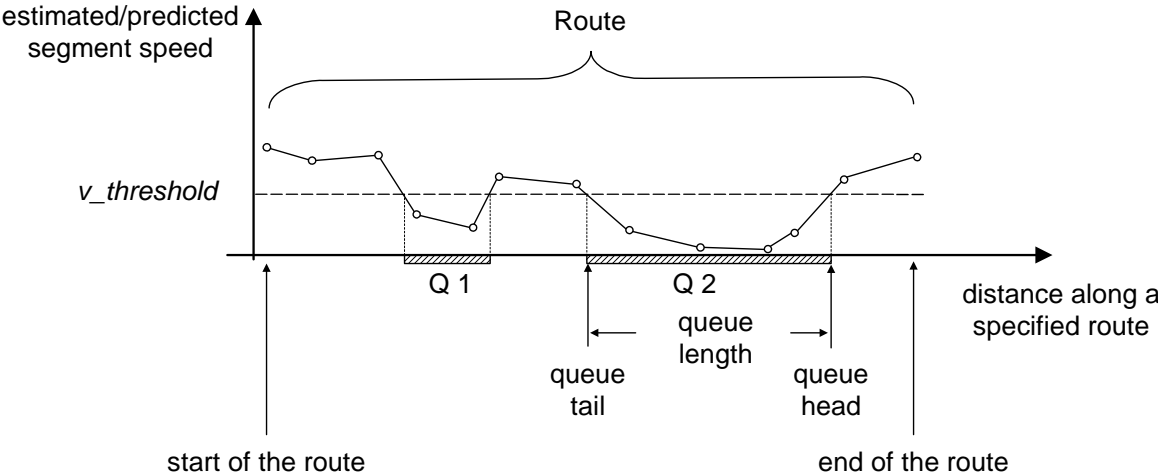


Figure 2: Queue tracking.

2.2.4 Incident report processing and incident alarm

Two complementary approaches are available in RENAISSANCE to deal with traffic incidents: (a) incident report processing, and (b) incident alarm. When RENAISSANCE receives an external incident report issued by a traffic operator, containing the location and severity (in terms of capacity reduction) of an incident, the incident is modelled in RENAISSANCE until the ending of this incident is reported by the traffic operator. On the other hand, incident alarm aims to indicate a possible incident occurrence that may be missing

from the incident report. The incident alarm intends to issue a warning regarding an abnormal traffic phenomenon, which could be a traffic incident. The incident alarm is performed based on the on-line model parameter estimation. The basic idea is that any abnormal traffic flow behaviour may be reflected in a strong variation of the estimated model parameters. Since the model parameter variation can be tracked on-line by the RENAISSANCE traffic state estimator, the model parameter estimates can be used as indicators of abnormal traffic phenomena.

2.3. Functional Architecture of RENAISSANCE

Figure 3 displays the functional architecture of the RENAISSANCE software. The highlighted central block represents the main body of RENAISSANCE. The included sub-blocks represent RENAISSANCE's various functional modules, most of which correspond to the specific traffic surveillance tasks. The directed lines between the functional modules represent the signal flows. Each module has both input and output. The input to a module can be from outside or inside of RENAISSANCE. If it is from inside, this input must be the output of another module. The external inputs to RENAISSANCE include real-time traffic measurements (flow and mean speed or occupancy) and, possibly, incident reports from the traffic operators. The outputs of RENAISSANCE correspond to its various traffic surveillance tasks. In addition, RENAISSANCE provides the users with quite a few user options in order for the traffic surveillance tasks to be performed according to the specific user needs and application requirements.

2.3.1 User options

RENAISSANCE provides to the user a number of options regarding

- network to be addressed by RENAISSANCE;
- detector configuration
- RENAISSANCE operation control
- RENAISSANCE inputs;

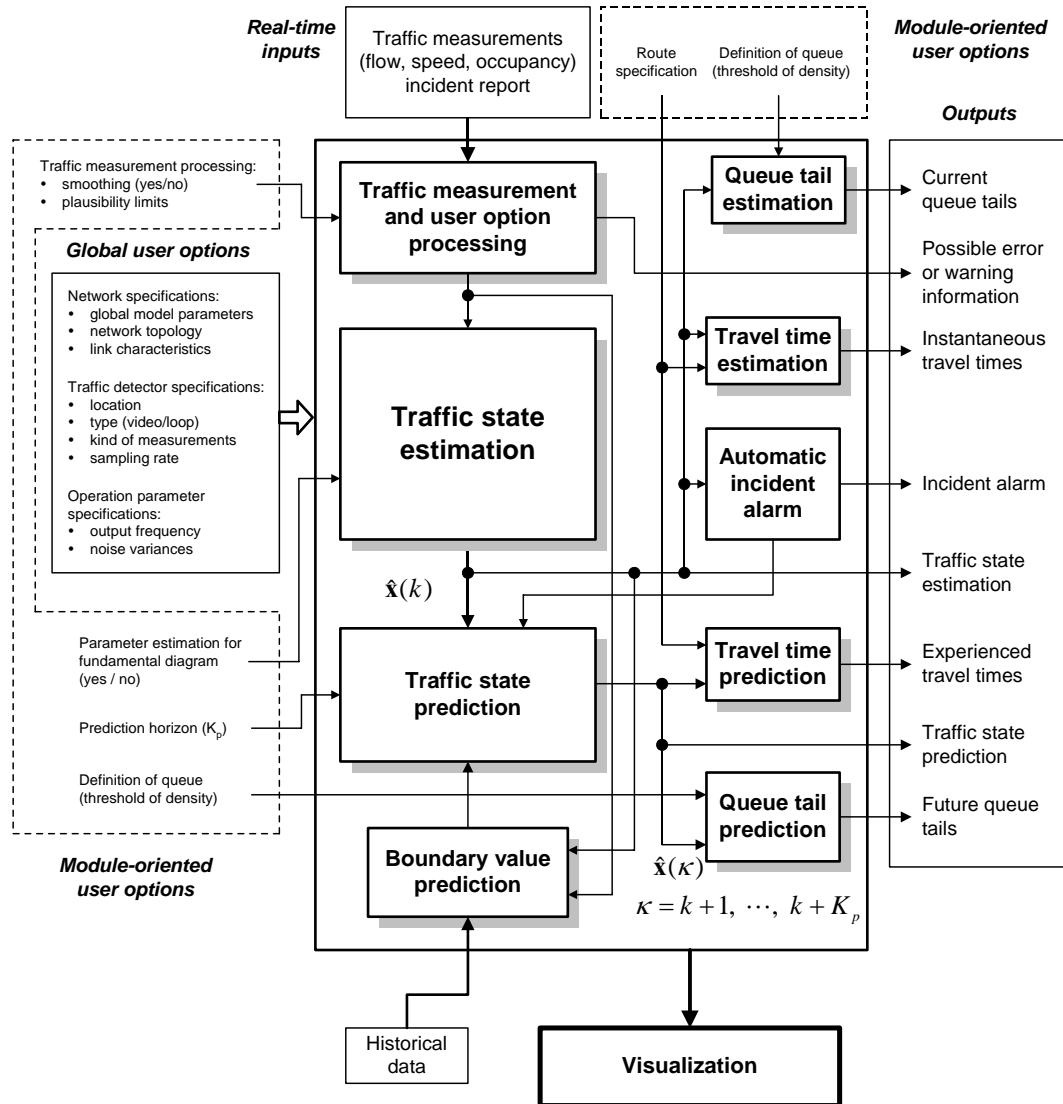


Figure 3: Functionalities of RENAISSANCE.

➤ RENAISSANCE outputs.

Each user option is either mandatory or optional. A mandatory option must be specified by the user in order to run RENAISSANCE, while an optional one can be ignored by the user if e.g. the user does not have sufficient related knowledge, in which case RENAISSANCE takes automatically a default value for the unspecified option.

Network description

This set of user options specifies an existing (or hypothetical) motorway network for which the RENAISSANCE-targeted traffic surveillance tasks are to be performed. The network specification options address:

- Network topology (i.e. nodes, links, origins, and destinations as well as the corresponding connection between them).
- Global model parameters (the macroscopic model parameters other than the free speed, critical density, and capacity).
- Link characteristics (for each link)
 - number of lanes
 - capacity (with a default value of 2000 veh/h/lane)
 - free speed (with a default value of 120 km/h)
 - critical density (with a default value of 33.5 veh/km/lane)
 - length
 - number of segments.

Detector configuration

For each available detector, the following information has to be specified:

- name (as given by the user)
- its location (in terms of link name and km-position inside the link)
- type (video, loop, or radar)
- availability of speed measurement (flow measurement is assumed to be always available for all detectors)
- usage flag, i.e. used for the estimation process or not (if not used for estimation, data are nevertheless processed for the sake of visualisation and comparison).

Operation control

These user options address parameters as

- model time step T
- measurement aggregation interval (specifying how frequently the traffic measurements are updated), typically considerably bigger than T
- name and path for detector data input file (used by the off-line version and in replay mode by on-line versions)
- prediction frequency (specifying how often the prediction tasks are performed)

- prediction time horizon (specifying over how long a time period the prediction tasks are performed each time)
- On-line estimation of the free speed, critical density, capacity
 - yes or no?
 - if yes, for a unique group or multiple groups of model parameter estimation?
- standard deviations for modelling noise and for measurement noise
- route specification for travel time estimation and prediction as well as queue tracking
- speed threshold for queue tracking
- boundary value prediction method
- RENAISSANCE outputs.

2.3.2 Data input and output of RENAISSANCE

As illustrated in Figure 3, RENAISSANCE needs (besides user options, i.e. configuration) two kinds of data input, which are (real-time) traffic measurement data and historical boundary data. Traffic measurement data include flow and/or speed measurements from all detectors installed within the network addressed by RENAISSANCE and are used by the traffic state estimator of RENAISSANCE if selected for usage. Considering that the traffic state estimation lays the operational foundation of RENAISSANCE, traffic measurement data is actually indispensable to all RENAISSANCE functionalities. On the other hand, the historical boundary data refer to the historical measurement data or typical recurrent patterns from (some) network boundary locations, and may be utilized optionally for the traffic state prediction task of RENAISSANCE. More precisely, the boundary data may include flow and speed measurements at the network origins and destinations, inflow measurements at on-ramps, outflow (and speed) measurements at off-ramps, and turning rates at bifurcation nodes. Note that the provision of the historical data is not mandatory. As already mentioned RENAISSANCE can still perform its prediction tasks even without any historical data. In that case, the currently estimated boundary values are extrapolated. Providing historical data may, however, help improving the RENAISSANCE prediction accuracy.

The RENAISSANCE output corresponds to its various functionalities. More precisely, the traffic state estimation module delivers, besides the GUI display features, the following variables on files:

- estimation of all segment variables

- flows
 - speeds
 - densities
- estimation of all boundary variables (whether measured/measurable or not):
- origin inflows and speeds
 - destination densities
 - on-ramp inflows
 - off-ramp outflows
 - turning rates
- model parameter estimation (depending on the relevant user option);
- free speeds
 - critical densities
 - capacities

The travel time estimator and queue tail/head/length estimator deliver their corresponding results for all user-specified routes. Over the user-specified prediction time horizon, the boundary value prediction module delivers the prediction of all boundary variables, based on which the traffic state prediction module delivers the prediction of all segment variables. Over the same prediction time horizon, the queue tail/head/length predictor delivers the corresponding results for all user-specified routes. Finally, the predicted travel times for all user-specified routes are calculated based on the predicted segment speeds.

When RENAISSANCE runs in the off-line mode, some *performance criteria* are calculated¹ over “surveillance_horizon” (specified in the Operation Control file). More specifically, both absolute and relative performance indices are calculated for each measurement location. For example, regarding a detector installed at the boundary between segments i and $i+1$ of link m , the absolute performance index calculated over the time horizon K reads

$$E_{m,i}^a = \frac{1}{K} \sum_{k=0}^K |x_{m,i}(k) - \hat{x}_{m,i}(k)| \quad (25)$$

where x represents the measured flow or speed, \hat{x} represents the estimated flow or speed. On the other hand, the **relative** performance index is defined as:

¹ Only in the off-line case.

$$E_{m,i}^r = \frac{1}{K} \sum_{k=0}^K \frac{|x_{m,i}(k) - \hat{x}_{m,i}(k)|}{x_{m,i}(k)} \quad (26)$$

Note that these indices are calculated for all available measurement locations, whether the corresponding measurements are used to feed RENAISSANCE or not. The calculated criteria can be found in the output file “PI.txt”.

2.4. Versions of RENAISSANCE

Each on-line application of RENAISSANCE is site-specific in terms of detector data interfacing. Specific modules are linked to the RENAISSANCE core, in order to realise the according interfacing and data processing functionalities. These site-specific issues have to be treated in dedicated documentations as a supplement to the general RENAISSANCE manual. In order to provide the user with a tool for studies independent from on-line application, an off-line version of RENAISSANCE is also available and was actually used in the present study.

3. The Application Network in Antwerp

The overall network is defined as:

- R1 in both driving directions, i.e. from Interchange St.-Anna LO (location_ID 76) to Antwerp North (location_ID 101); length 17 km + 17 km (for both directions).
- E313 Westbound, starting downstream from Interchange Ranst (location_ID 58); length 7 km.

Altogether this network is approximately 44 km long (including the modeling of some on-ramp and off-ramp parts beyond the motorway mainstream) and is divided in the following sections:

1. E313 Westbound, length 7 km
2. R1 Inner ring, length 17 km
3. R1 Outer ring, length 17 km

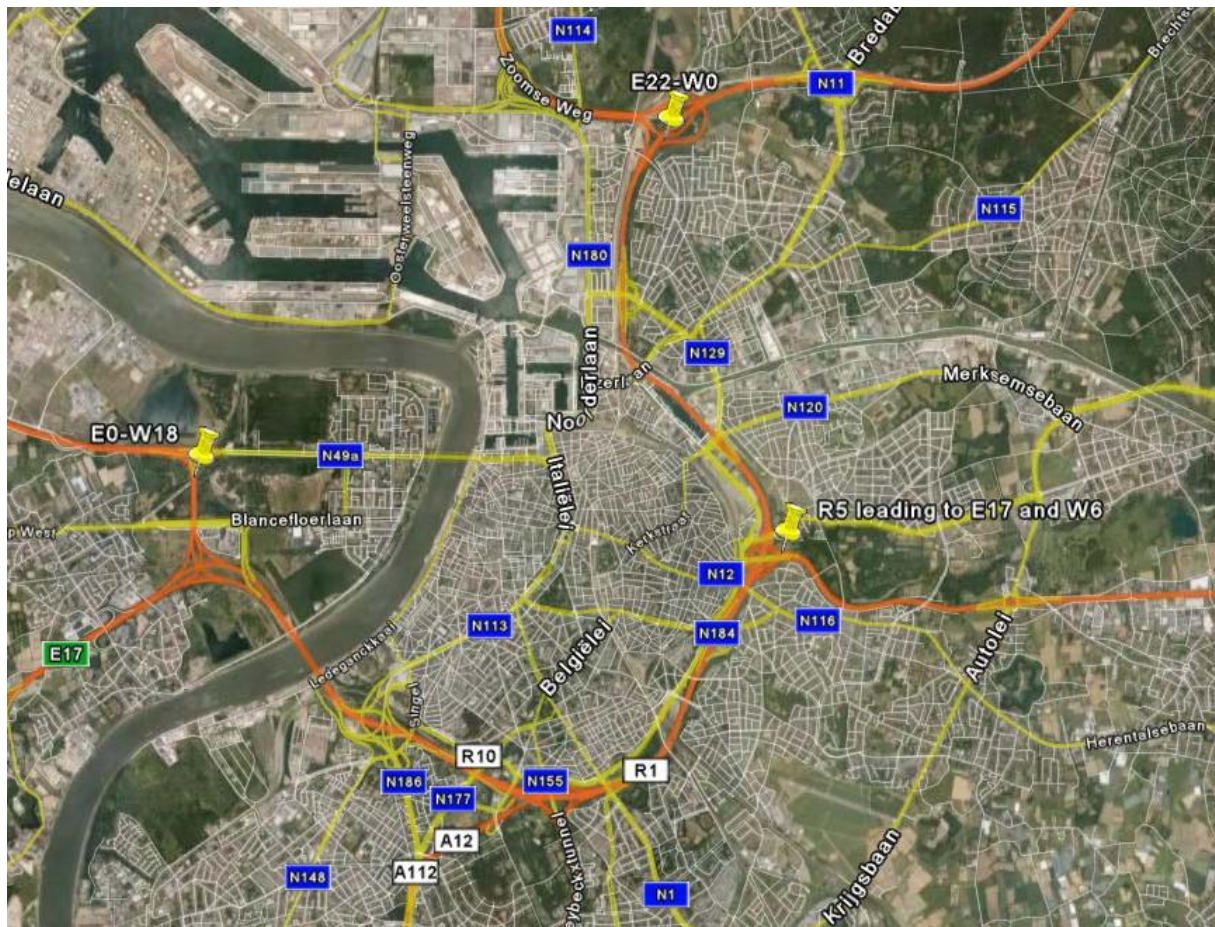


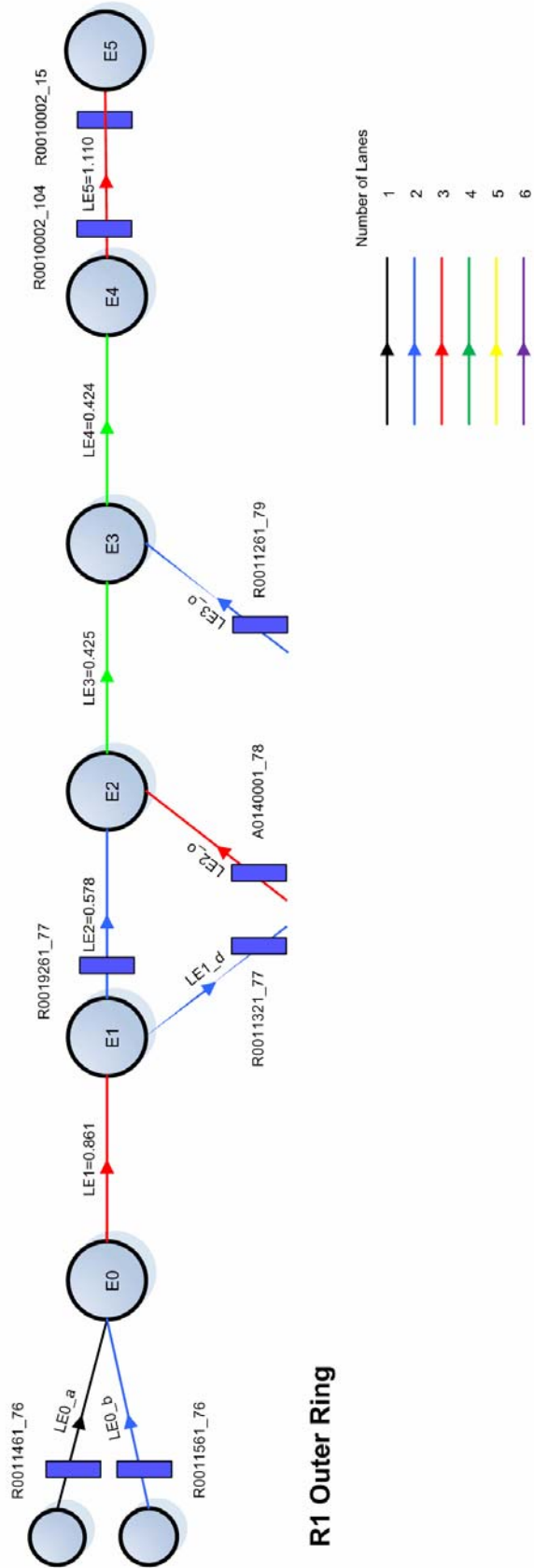
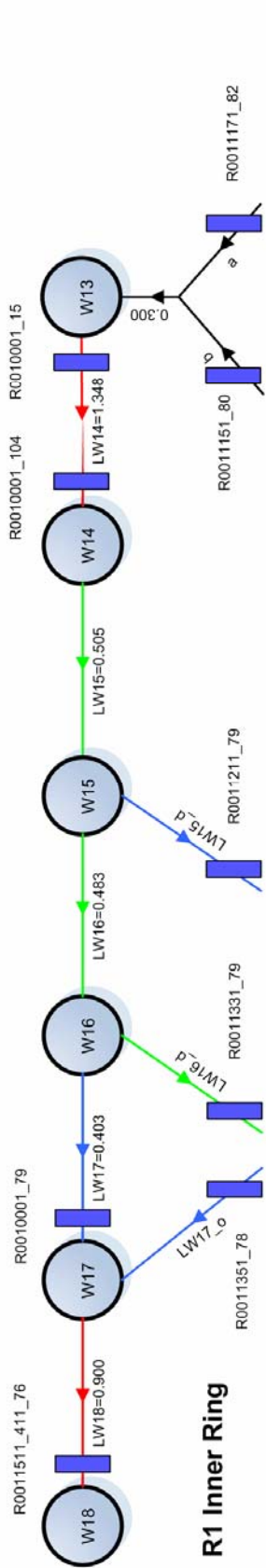
Figure 4: The application network (Source: Google Earth)

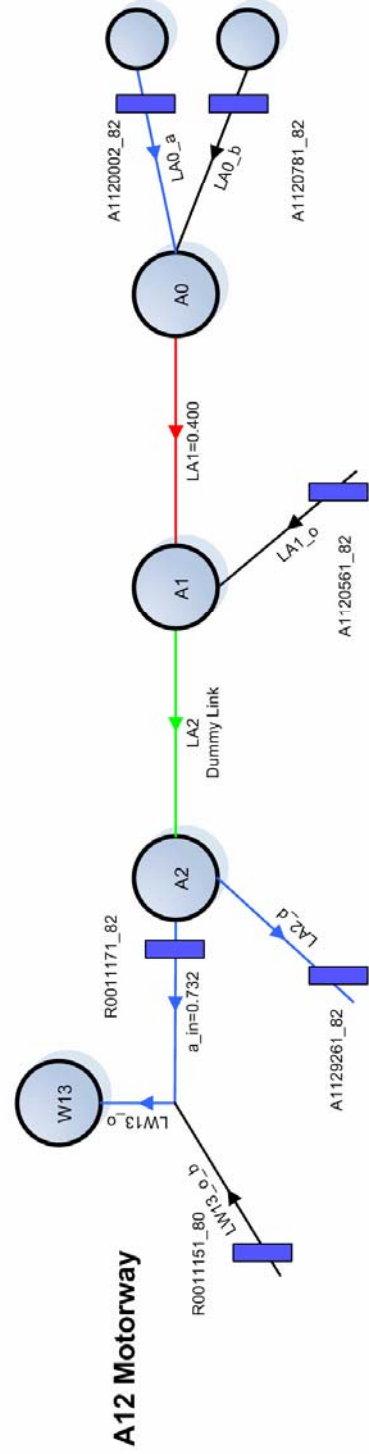
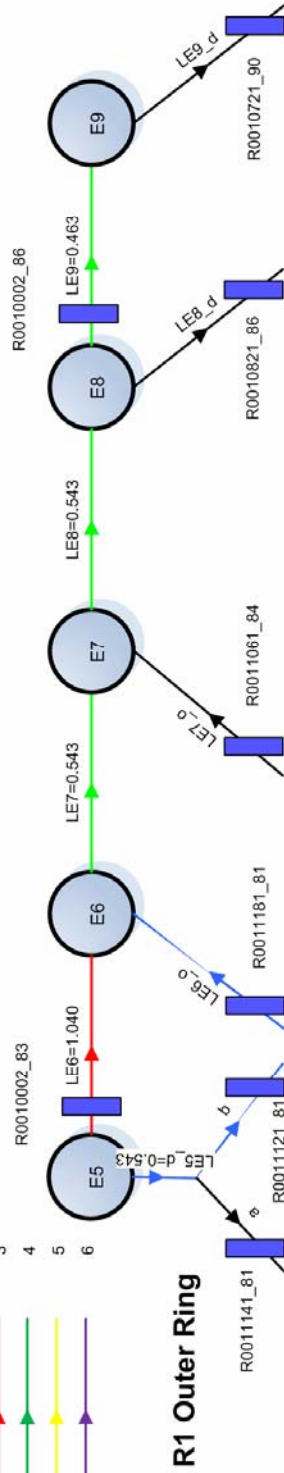
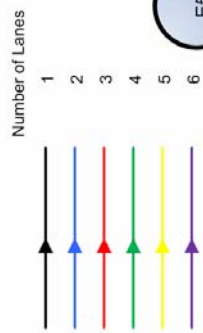
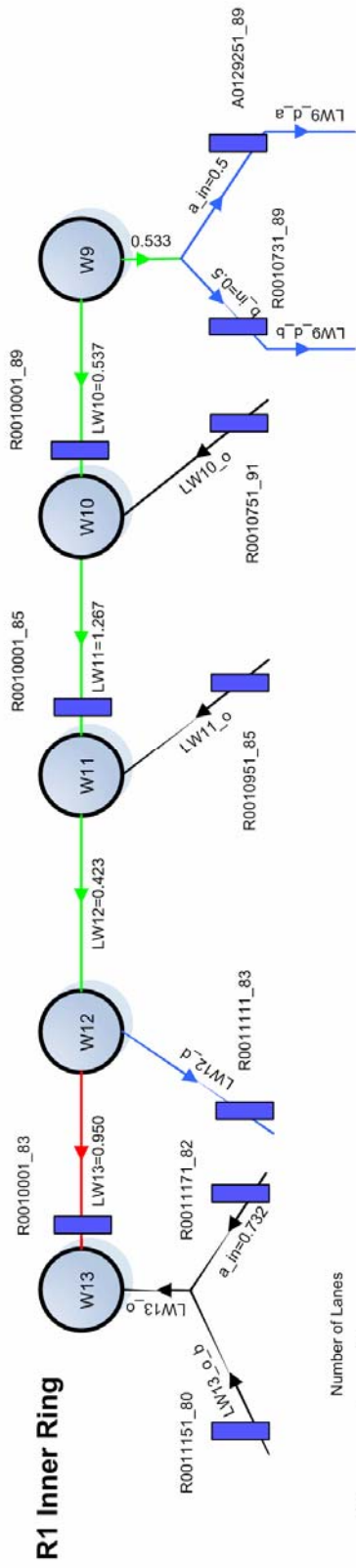
3.1. Basic RENAISSANCE Settings

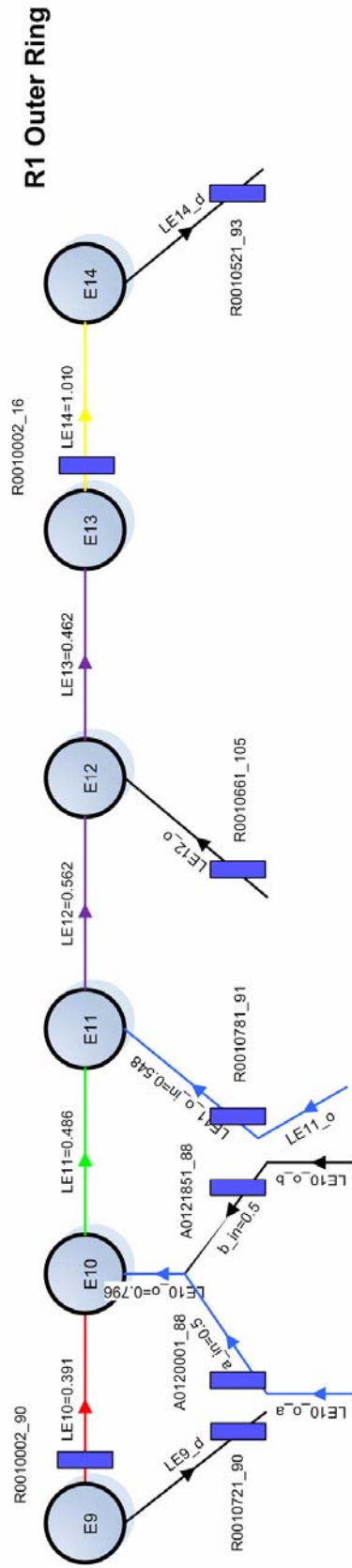
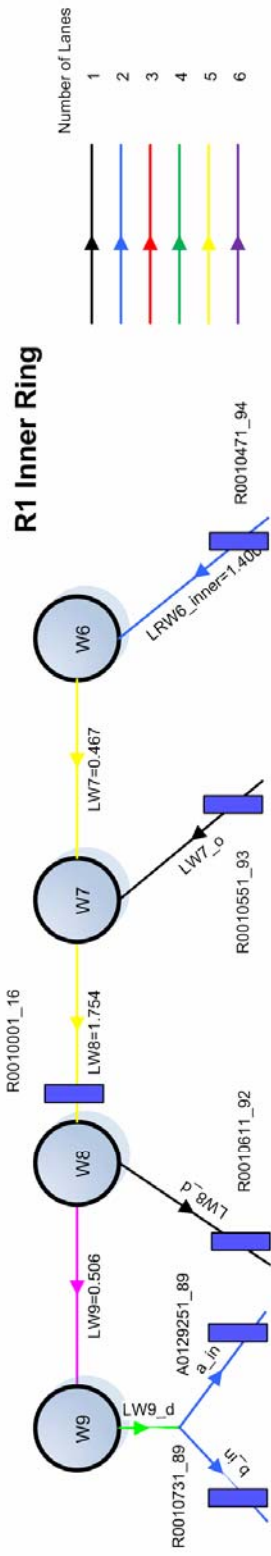
The RENAISSANCE network segmentation follows the segmentation defined in the GIS file (provided by the Antwerp Authorities) as much as possible. The overall network model for RENAISSANCE, including the links and nodes, link lengths (in km) and widths (number of lanes) and available detectors is displayed in Figure 5. The standard deviations needed in RENAISSANCE were initially the same as in previous implementations but were roughly fine-tuned after several tests to reach a more satisfactory degree of estimation accuracy. The time step T was set to 5 s. The model parameters, which are not in the Fundamental Diagram Equation, i.e. Tau, Kappa, Nue, Phi, Delta, had values roughly according to previous studies but ν and τ were eventually roughly fine-tuned so as to improve the estimation results.

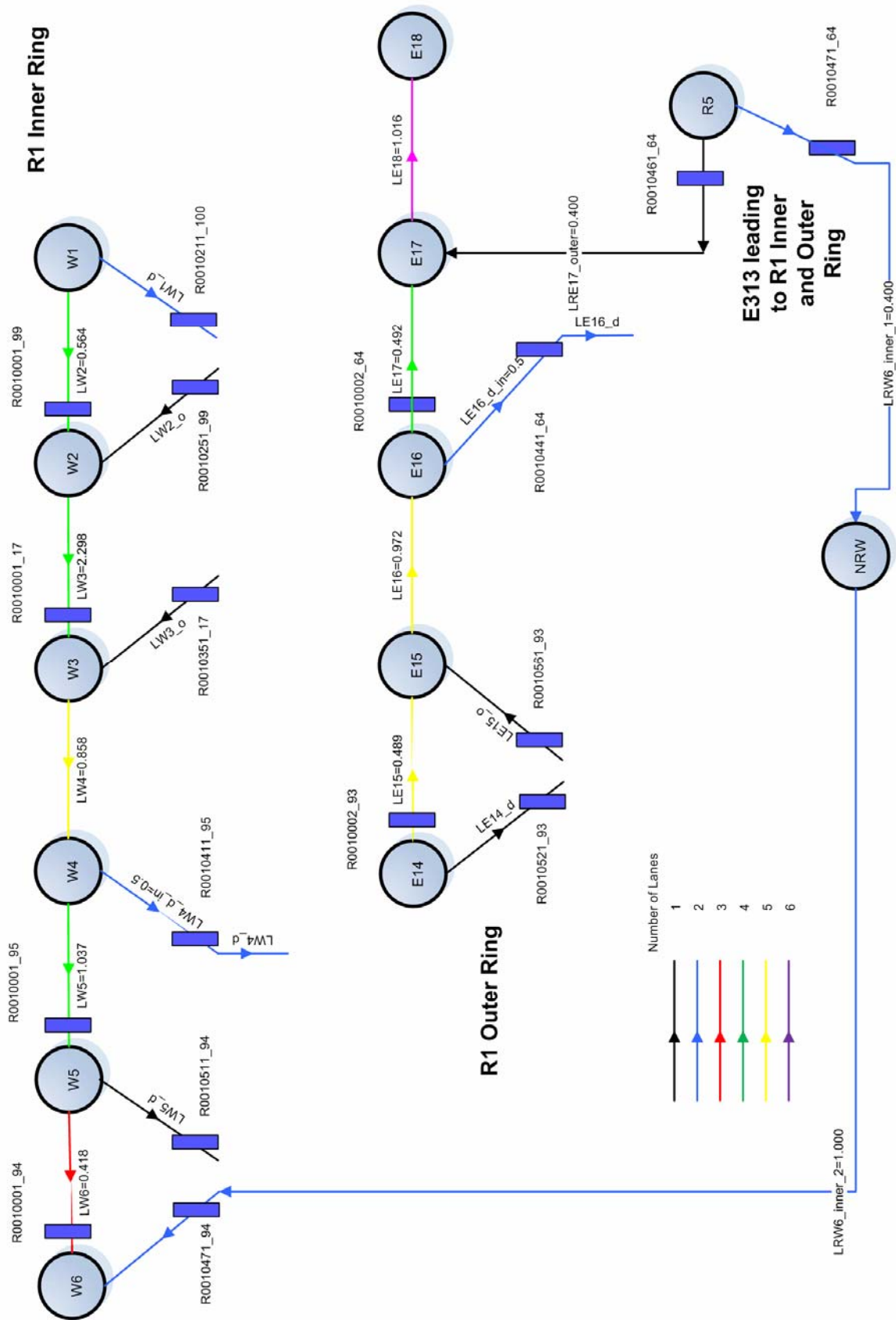
Figures 6-8 display loop detector measurements for speeds, collected at different locations of the three included mainline stretches, respectively. It is obvious by inspection of the displayed curves that:

- There are two peak periods with low speeds at different locations, a morning peak at 6:30-9:00 a.m. and an afternoon peak at 3:00-6:00 pm.
- The differences in mean speeds at different locations during the off-peak periods (e.g. 9:00 a.m. – 3:00 pm), ranging from 70 km/h to 100 km/h, indicate that there are structural inhomogeneities in the considered stretches and call for the use of multiple fundamental diagrams in RENAISSANCE.









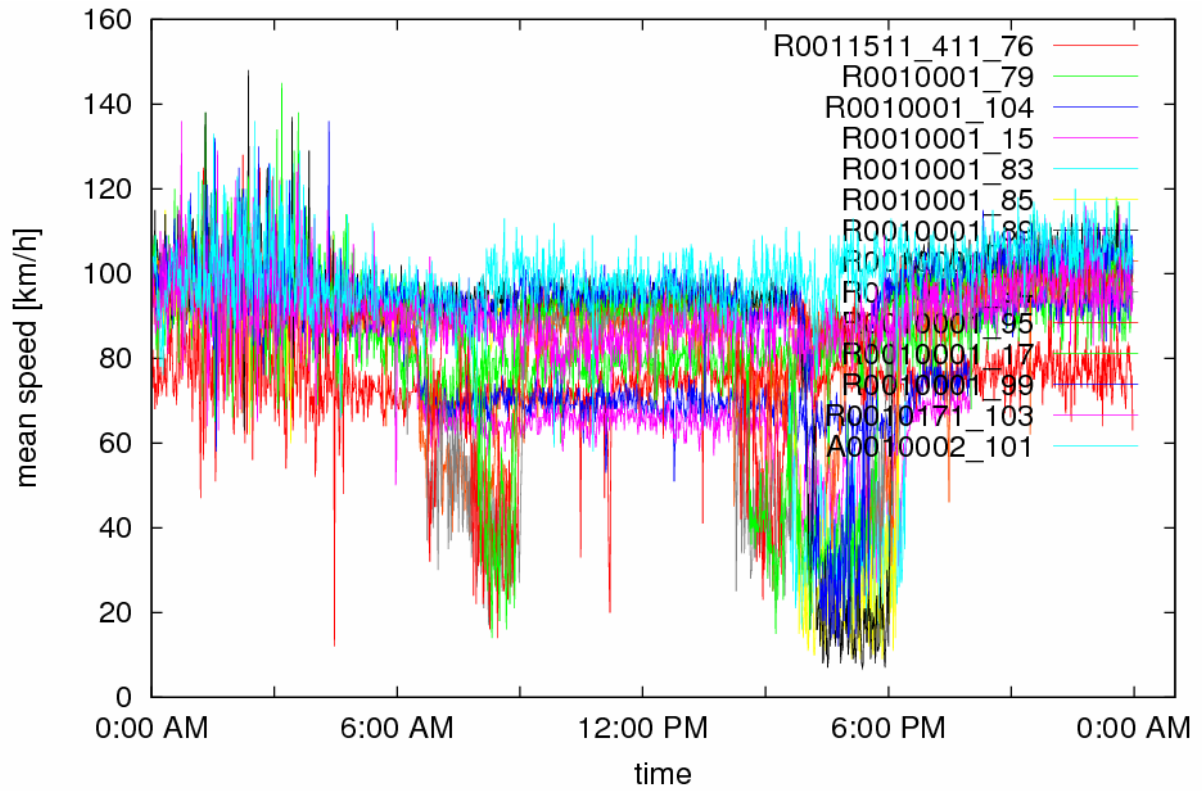


Figure 6: Speed measurements in R1 Inner Ring.

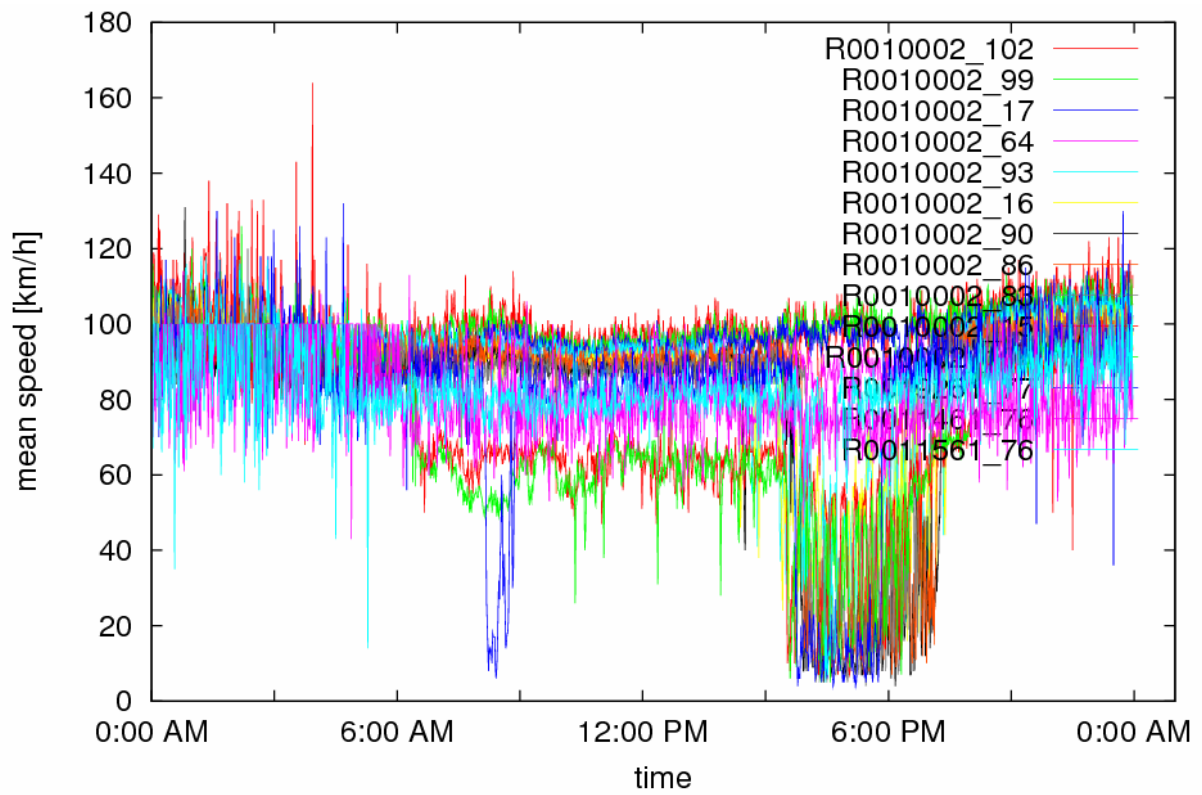


Figure 7: Speed measurements in R1 Outer Ring.

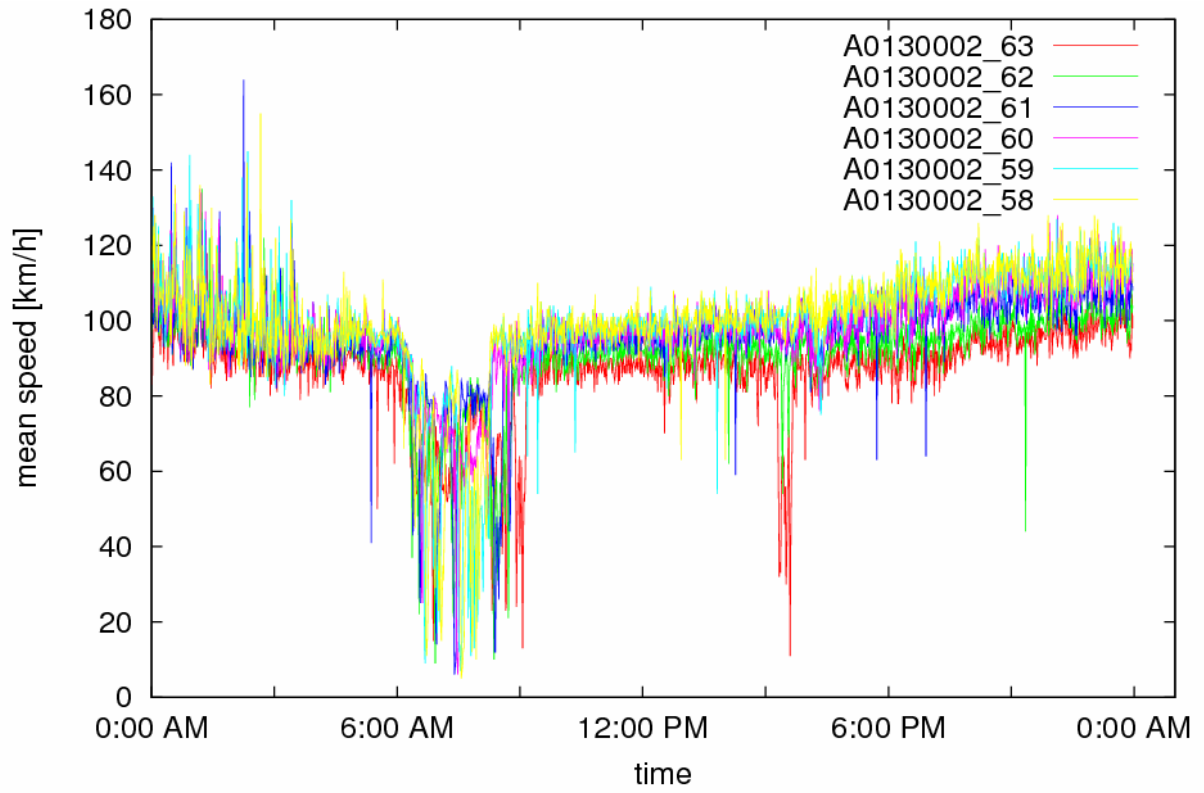


Figure 8: Speed measurements in E313 (one direction).

4. Estimation Results

The estimation results reported in this section refer to the current state reconstruction by RENAISSANCE, based on a limited amount of available measurement data from mainstream detectors as well as from on-ramps and off-ramps. Note that the estimation covers:

- Estimation of traffic flow variables (mean speeds and flows) at the measurement locations.
- Estimation of traffic flow variables (densities, mean speeds, flows) at locations (segments) without measurement devices.
- Estimation of boundary variables (on-ramp and mainstream origin flows, origin speeds, destination densities, turning rates at off-ramps or bifurcations), some of which may be measured while others are not.
- Estimation of the parameters of the fundamental diagrams.
- Detection of incidents.

Several variations in the estimation specifications or the utilised data are reported in the following sub-sections separately, for better result presentation and analysis.

4.1. Use of a Single Fundamental Diagram for the Entire Network

Despite the structural speed differences at off-peak periods visible in Figures 6-8, which indicate inhomogeneous traffic flow characteristics along the network stretches, a first application was carried out by use of one single fundamental diagram, common for all network links. Figures 9-12 display the estimation results obtained for 24 h of data of Friday 23 November 2007. Each figure contains the estimation results on a corresponding motorway stretch, starting from its downstream end and progressing towards the upstream end of the stretch. Each line of diagrams corresponds to one detector, noted on the top of the diagram; the left diagrams are flows while the right diagrams are mean speeds. The red curves are measurements while the green curves are estimates.

The obtained results may be commented as follows:

- Flow estimates are very good, virtually at all detector locations.
- Speed estimates are mostly very good during congestion. In contrast, positive or negative bias appears at many locations during the off-peak period. This is because the estimation of the (one single) fundamental diagram parameters leads to (spatially) average values over several motorway stretches with different flow characteristics. Thus, positive

estimation bias appears at relatively low-speed stretches (e.g. tunnel, off-ramps etc.) and vice versa.

Figure 13 displays the resulted estimated parameter values of the (one single) fundamental diagram. It may be seen that the estimates are reasonable and, despite some fluctuations during the day, quite stable.

The obtained results can be clearly improved by use of multiple fundamental diagrams within RENAISSANCE.

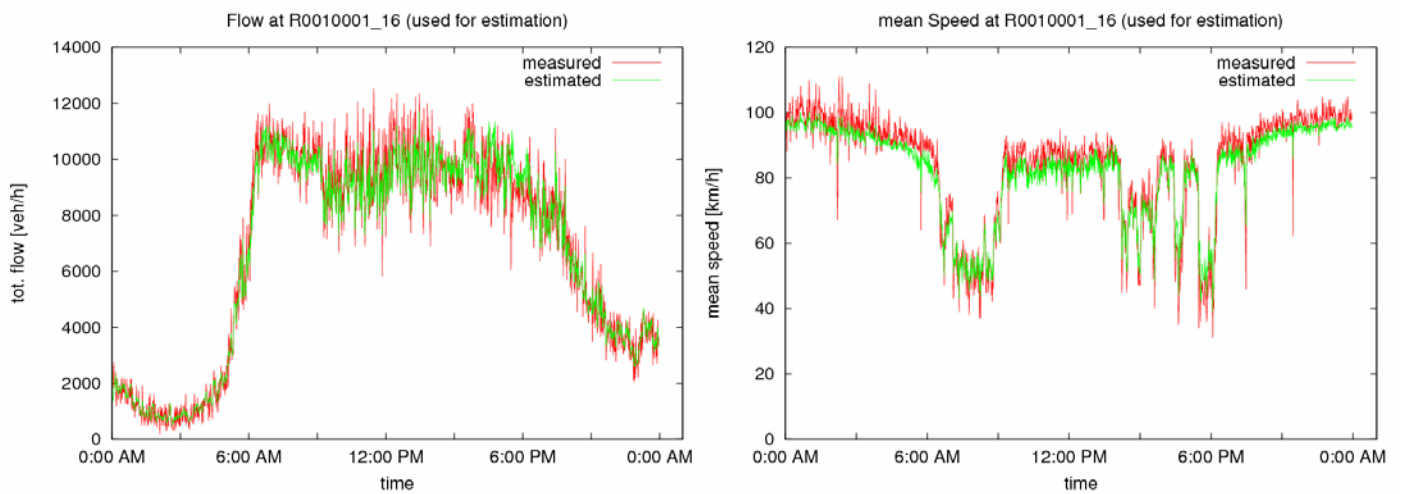


Figure 9: Flow and mean speed estimates for R1 Inner Ring for case of single FD.

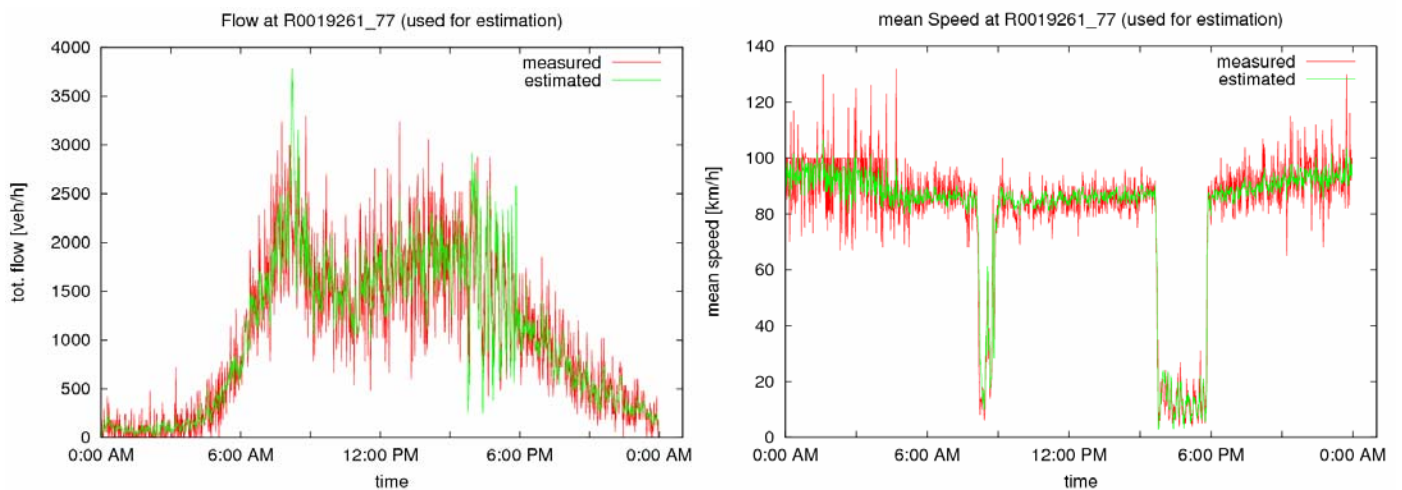


Figure 10: Flow and mean speed estimates for R1 Outer Ring for case of single FD.

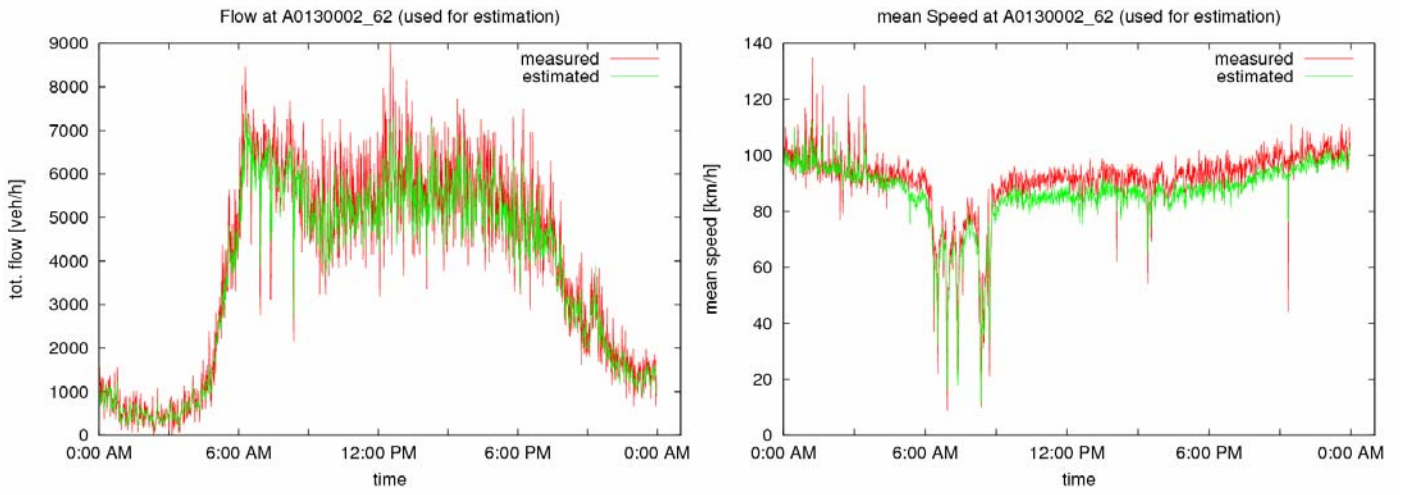


Figure 11: Flow and mean speed estimates for E313 for case of single FD.

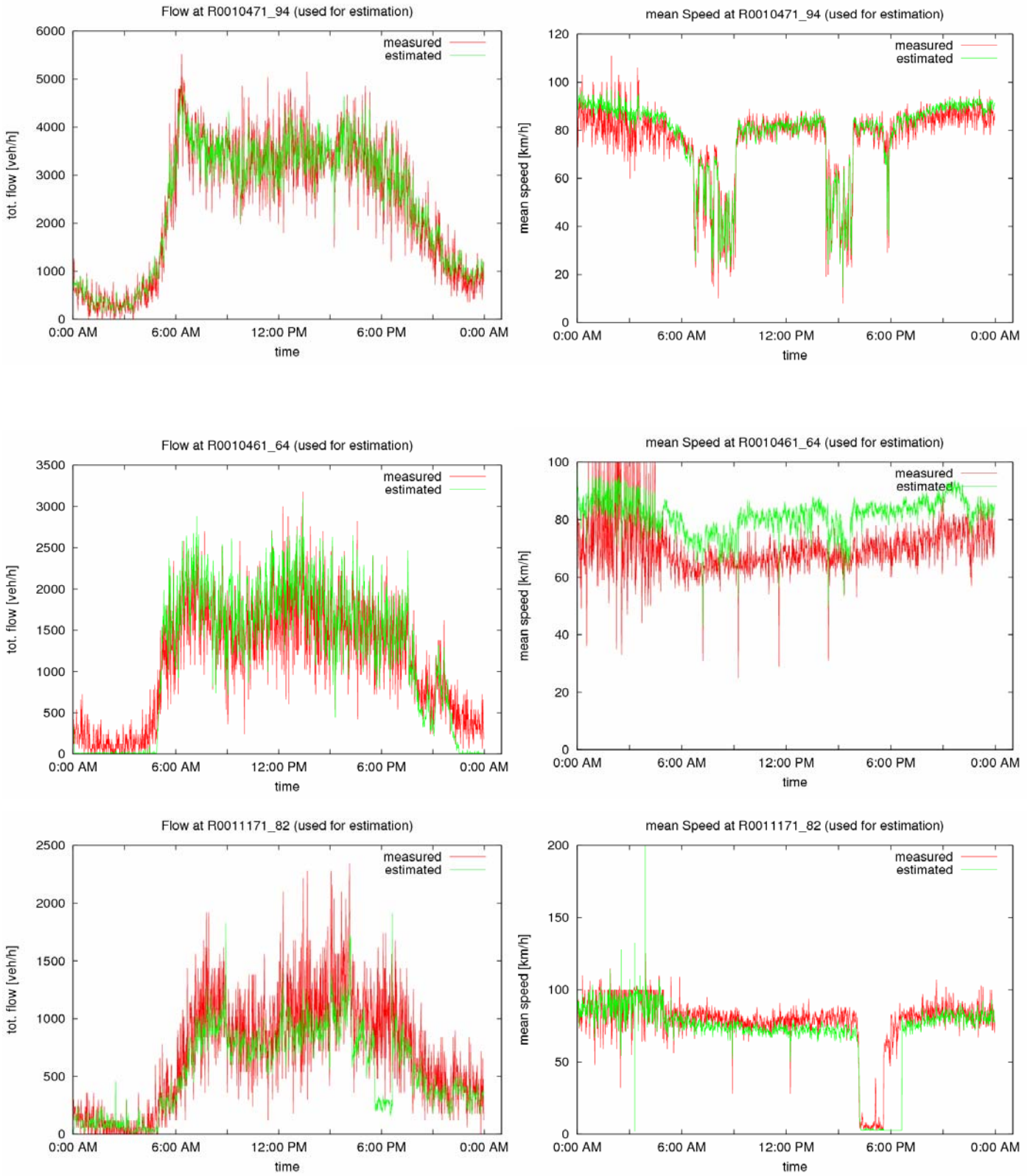


Figure 12: Flow and mean speed estimates for E313 connections to R1 Inner and Outer Ring and for A12 Motorway for case of single FD.

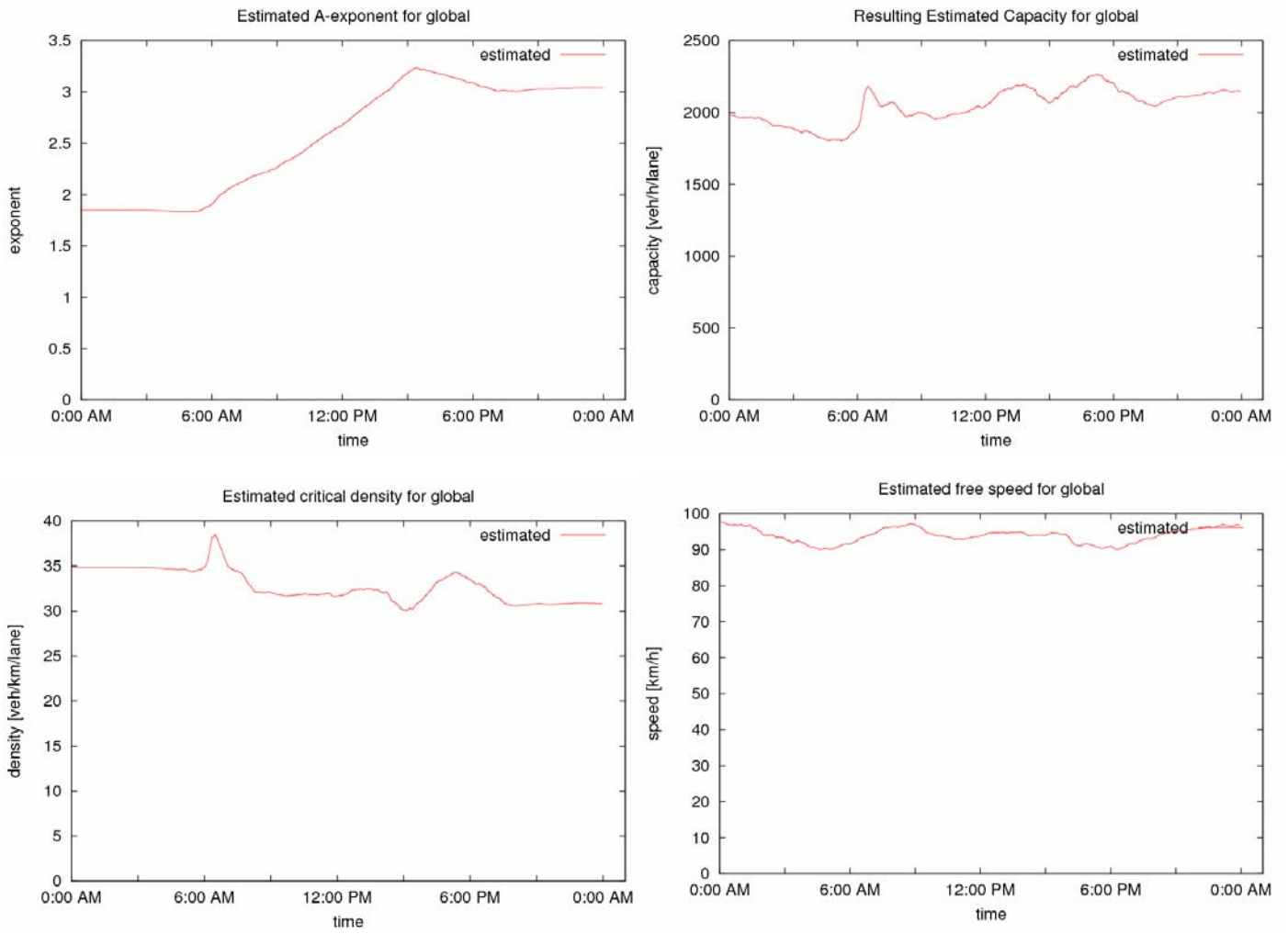


Figure 13: Fundamental Diagram model parameter estimates for entire network for case of single FD.

4.2. Use of Multiple Fundamental Diagrams

There are two main reasons for introducing multiple fundamental diagrams (FD) in the case of medium or large scale motorway networks as the application network of the present study:

1. In order to obtain better estimation results, i.e. essentially in order to avoid speed estimation bias in case of spatial inhomogeneity along or across the network stretches.
2. A possible incident may be detected via a relatively significant and abrupt drop of the estimated capacity. However, in case of one single FD, the incident impact on the parameter estimates is likely to be minor (hence hardly detectable) because the incident affects only the traffic characteristics of a small part (around the incident location) of the overall network; moreover, even if the incident impact on parameter estimates would be detectable, it would not be possible to make any statement regarding the incident location within the network.

We define **clusters** to be sets of links, each set with a common FD for all included links. It should be noted that, for proper production of parameter estimates, at least one mainline detector station should be included in each link cluster.

Figures 14 and 15 display the utilised link clusters, each usually containing one mainline detector station; merely for motorway E313, one single FD was used for the sake of simplicity.

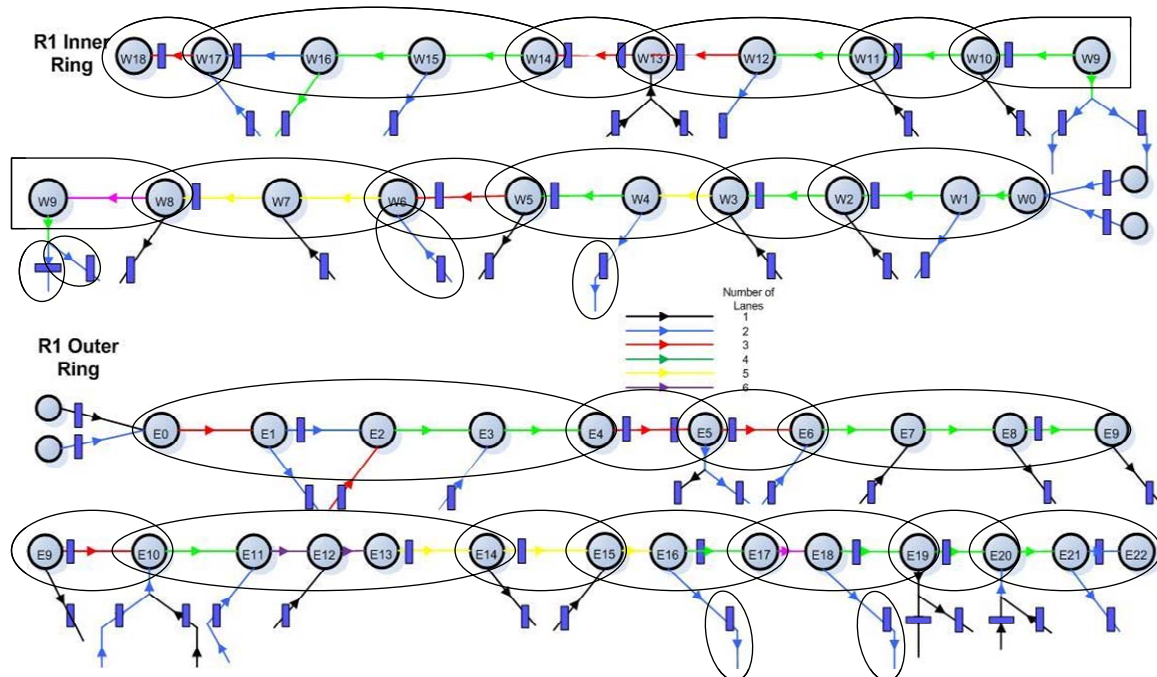


Figure 14: Application network layout with multiple Fundamental Diagram clusters, R1 Ring both directions.

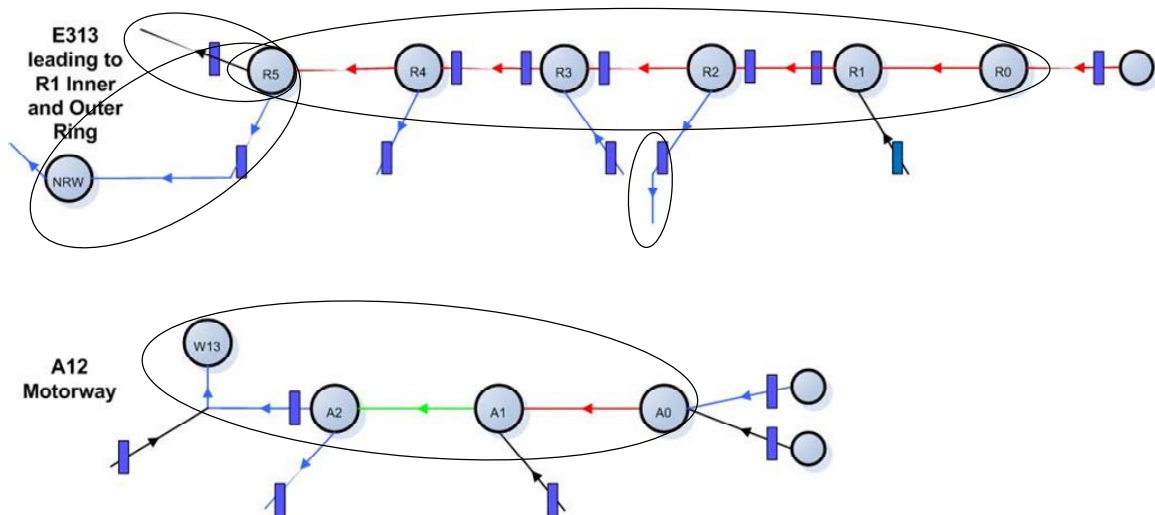


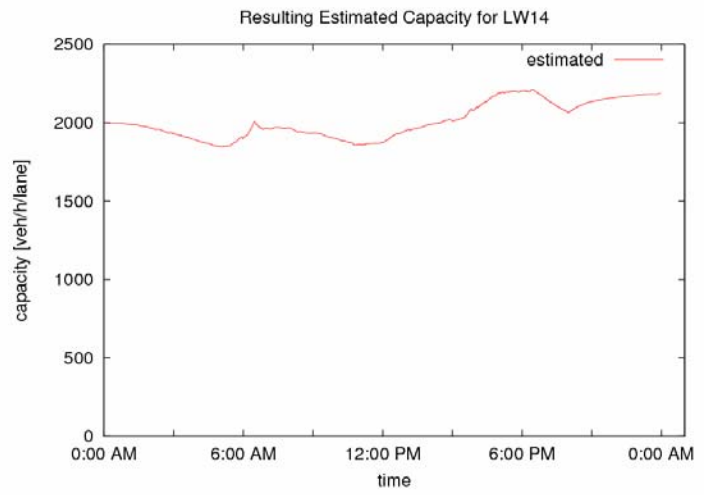
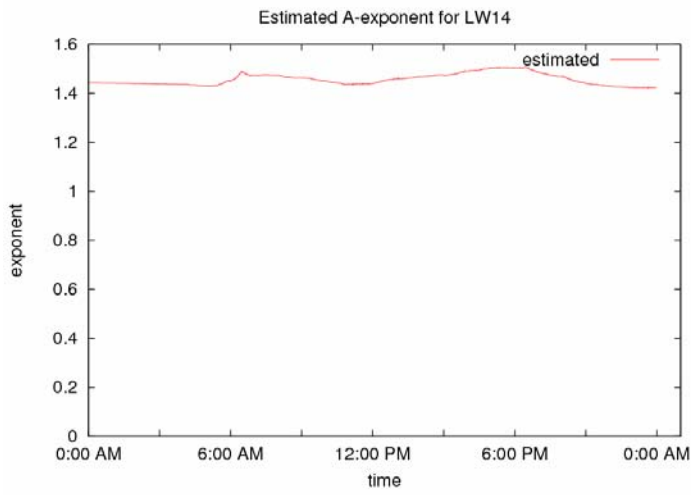
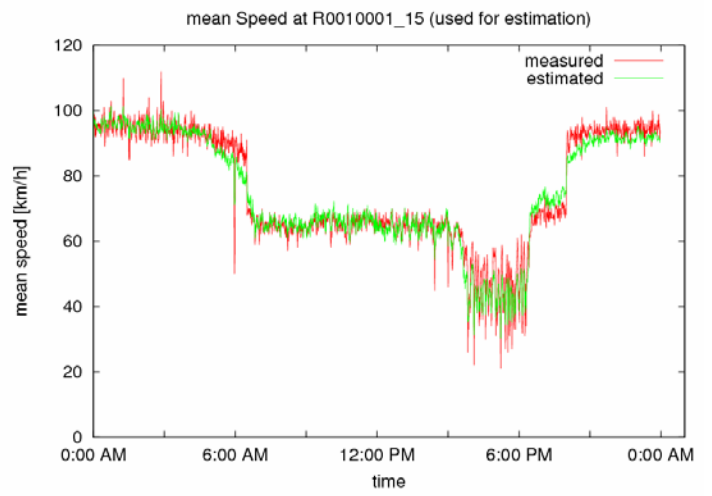
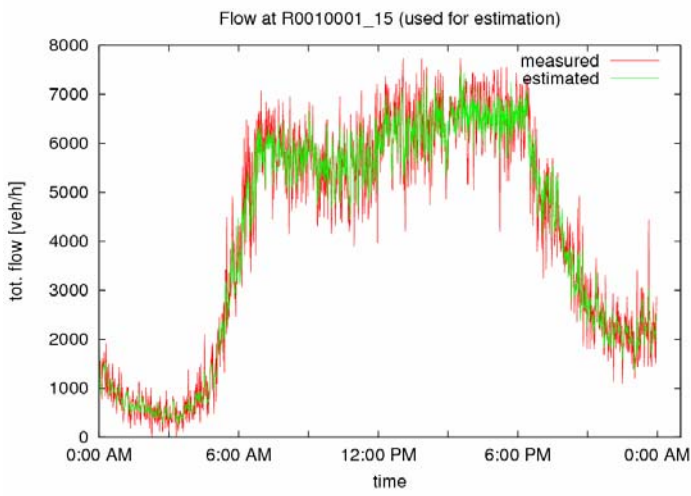
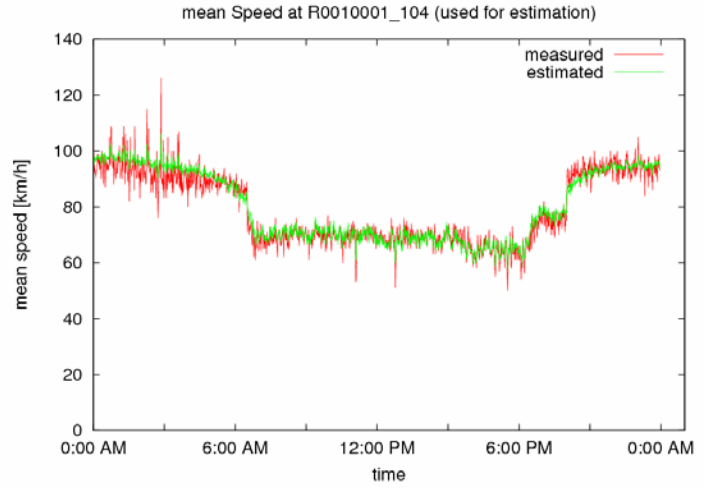
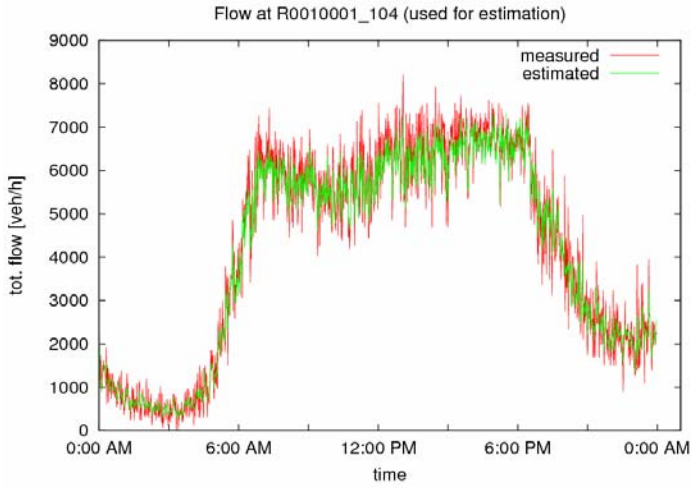
Figure 15: Application network layout with multiple Fundamental Diagram clusters, E313 and A12.

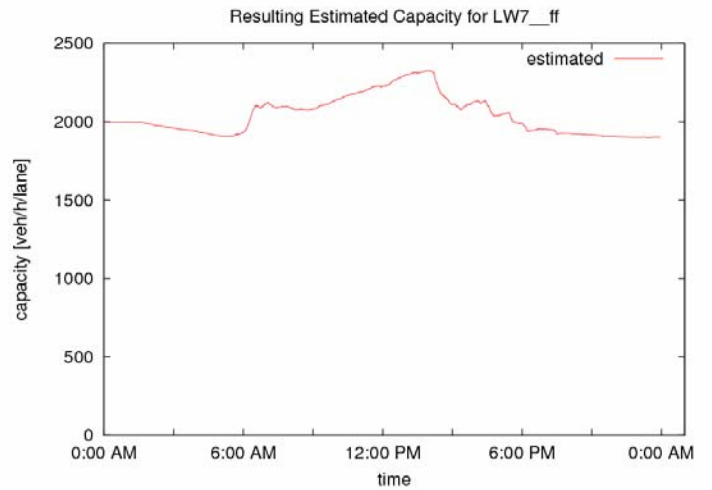
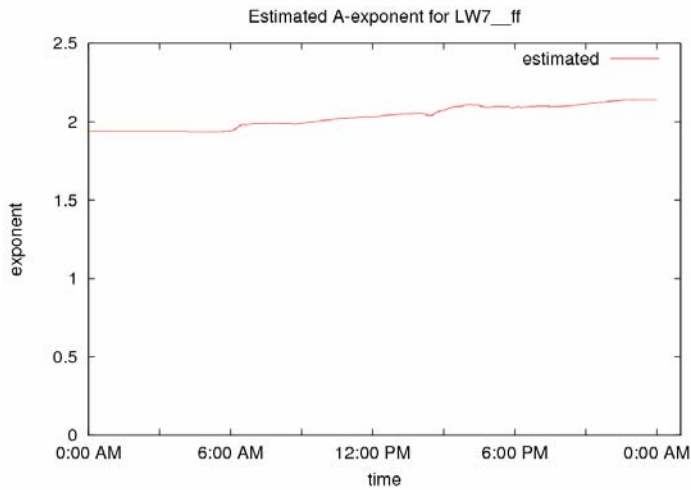
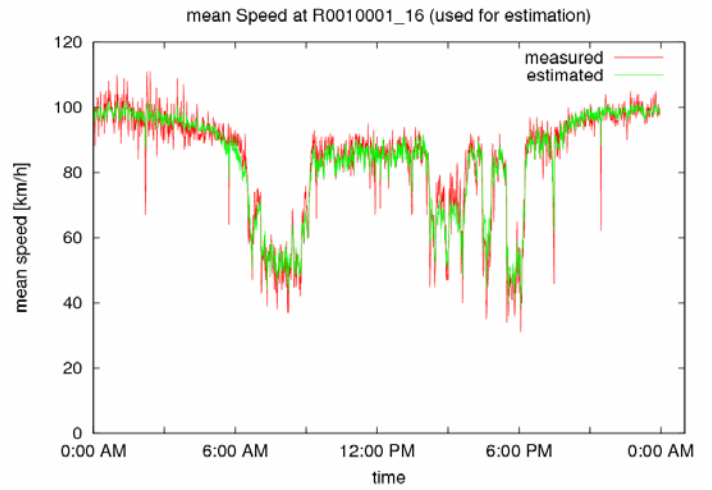
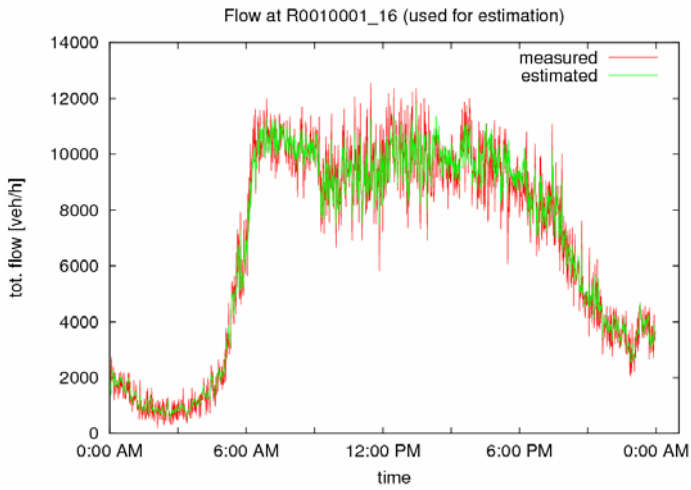
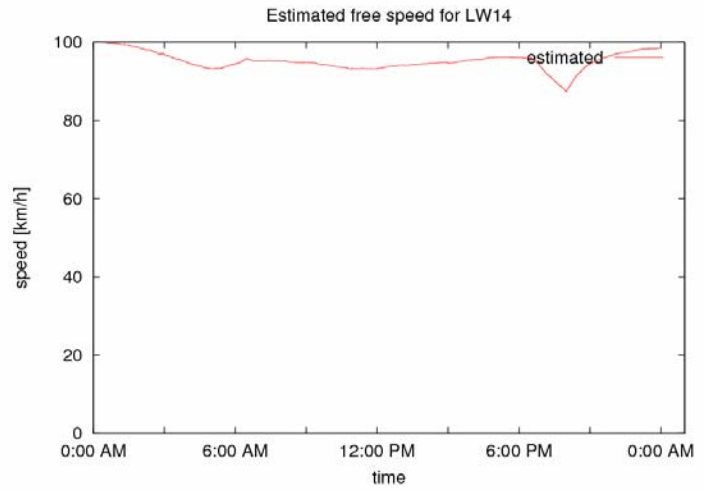
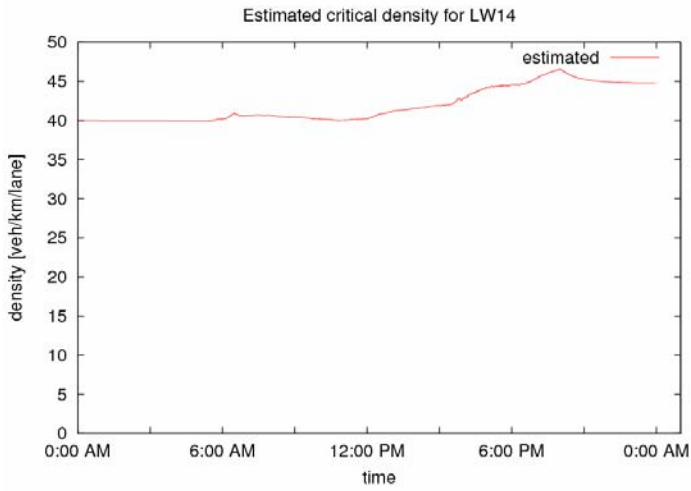
The obtained simulation results for the same 24 h data (23 November 2007) as in Section 4.1, are displayed on Figures 16-19 in a similar way as in Section 4.1, with the notable difference that the presentation of detector data of each cluster are immediately followed by the FD parameter estimate diagrams of the same cluster, before proceeding to the next cluster and so forth.

The obtained results may be commented as follows:

- Flow estimates are very good, virtually at all detector locations.
- Speed estimates are mostly very good, both during congestion and during off-peak periods. The observed bias of Section 4.1 during off-peak periods has largely disappeared thanks to the use of multiple FD. An initial bias observed at some locations up to 6:00 a.m. is due to the inaccurate initial values of the FD parameters (mainly the free speed) and is seen to essentially vanish after 6:00 am.
- The FD parameter estimates take reasonable values; variation of the estimates over the 24 h is moderate and appears mostly stable. Some observed, relatively strong and abrupt, drops of the estimated capacity may indicate the occurrence of an incident, see e.g. detector_99 of the outer R1 ring.
- The observed speed drop (from around 85 km/h to around 65 km/h) within the Ring tunnel (detectors _104 and _15, inner ring and outer ring) from 6:00 a.m. to 6:00 p.m. is due to displayed variable speed limits during this time period. Although the reduced speed is estimated properly, the related decrease of the free speed is not really captured by the free speed estimates.

Clearly, the good match of flow and speed estimates at detector locations is a necessary but not a sufficient condition for overall good estimation results. More specifically, it is much more interesting to check whether the delivered estimates are reasonably accurate also at motorway links and segments without loop detectors. This investigation is carried out in the next section.





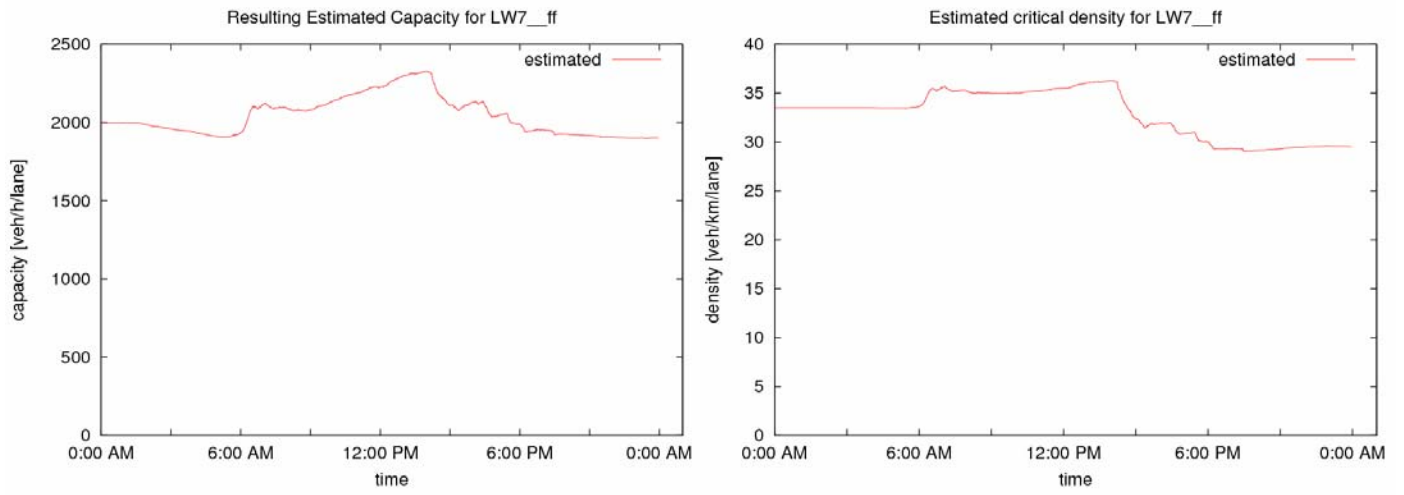
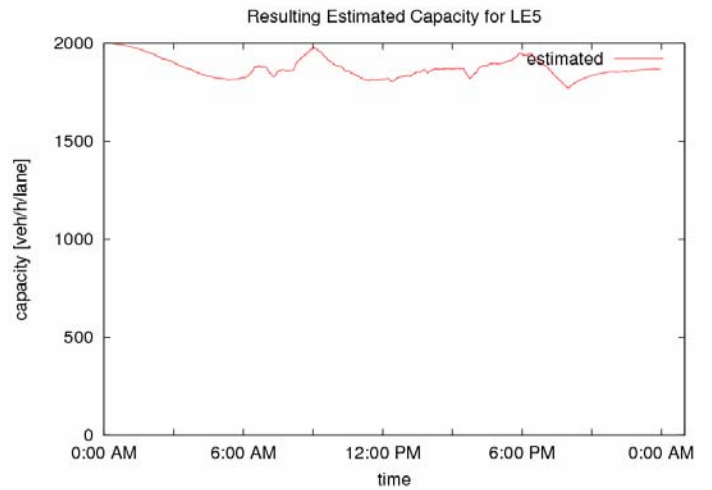
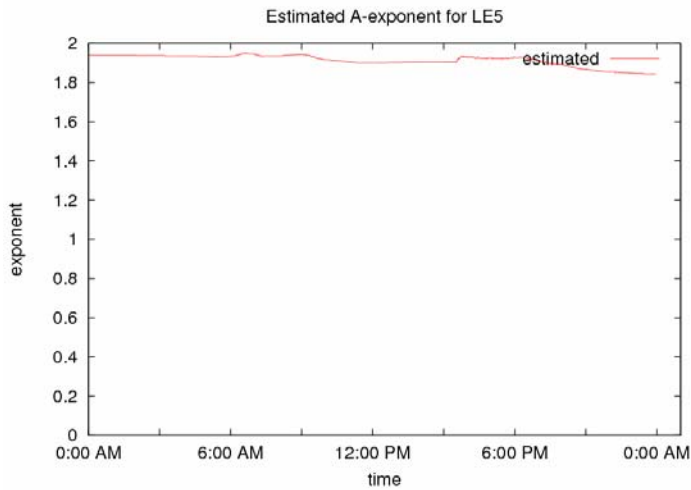
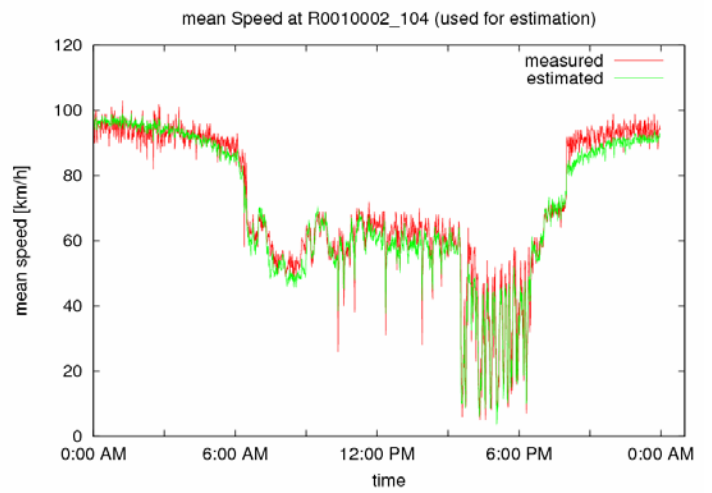
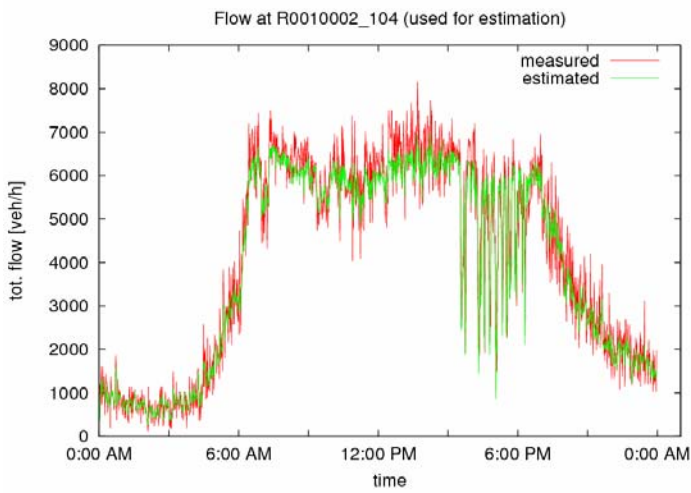
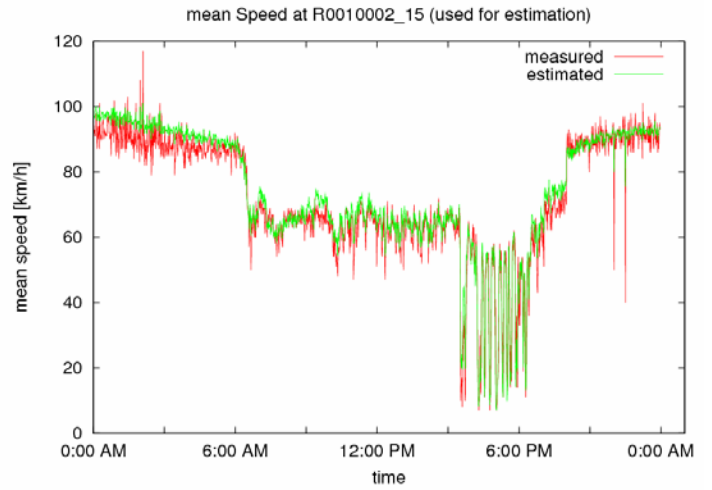
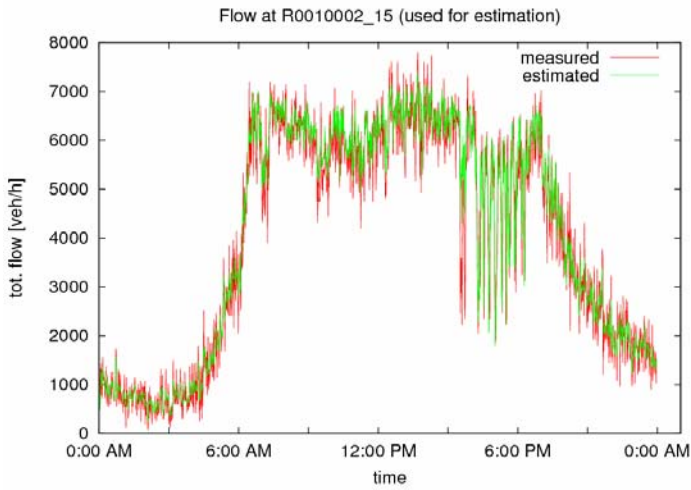
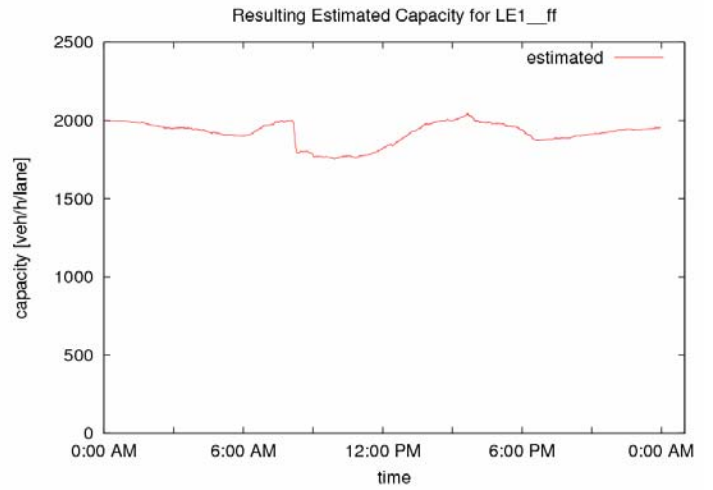
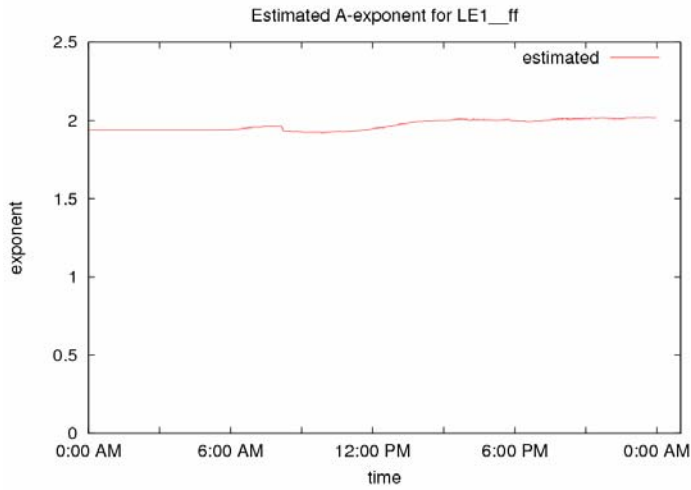
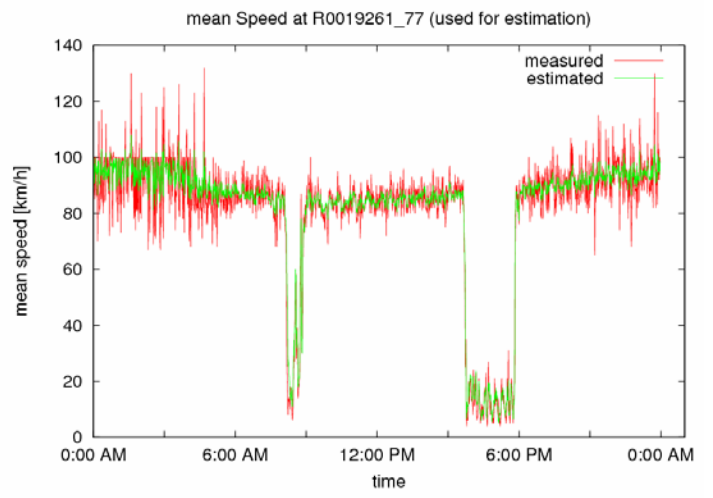
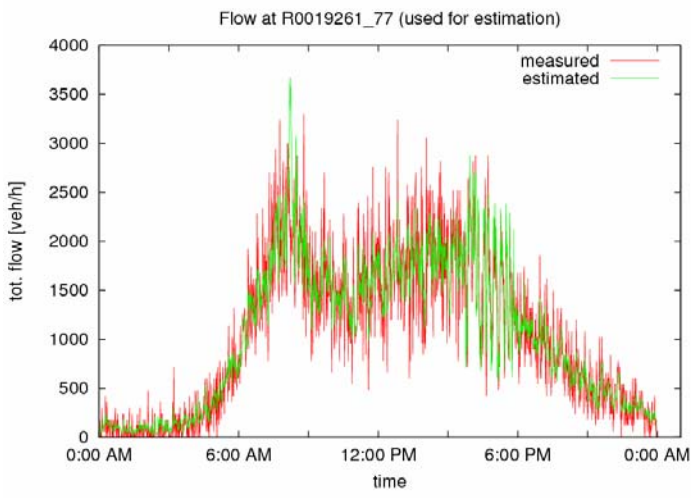
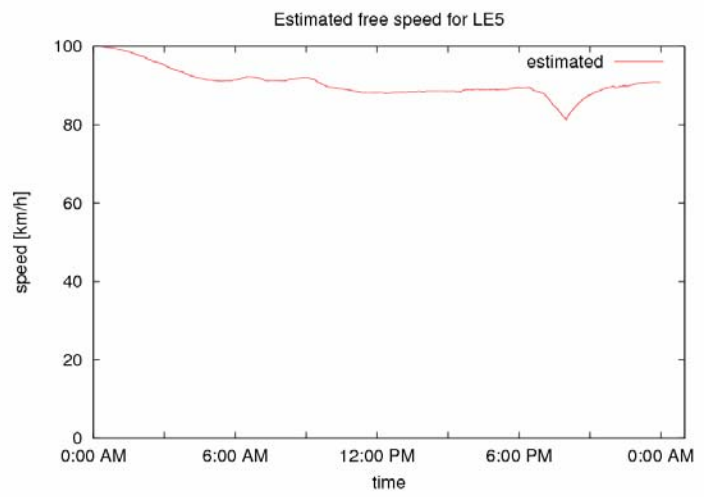
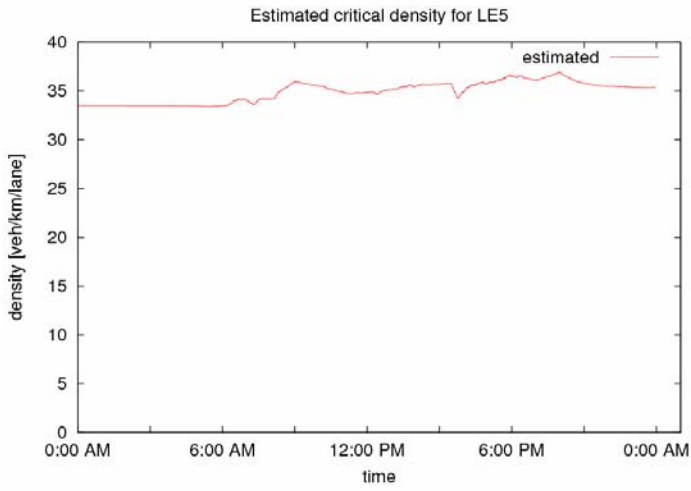


Figure 16: Flow, mean speed and Fundamental Diagram model parameter estimates for R1 Inner Ring for case of multiple FDs.





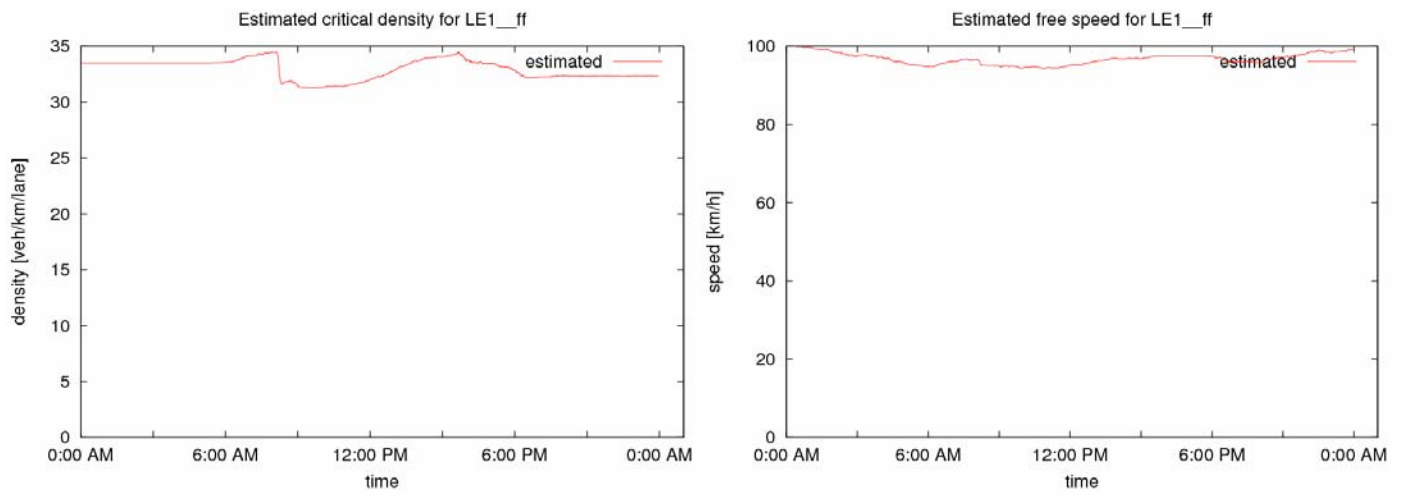


Figure 17: Flow, mean speed and Fundamental Diagram model parameter estimates for R1 Outer Ring for case of multiple FDs.

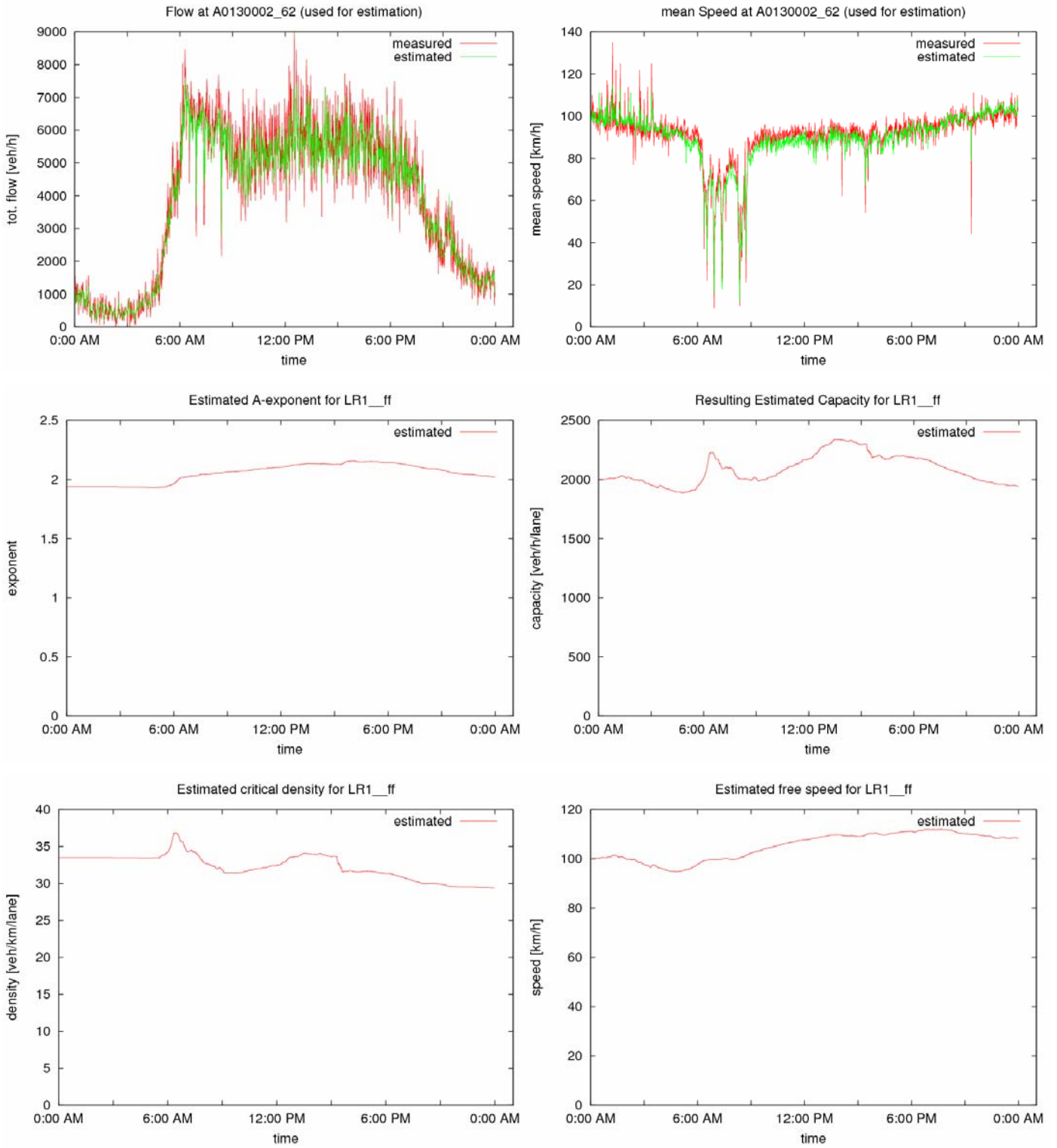
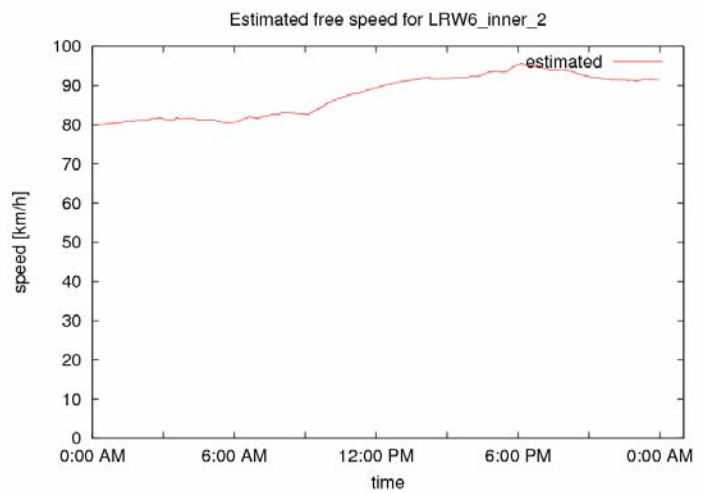
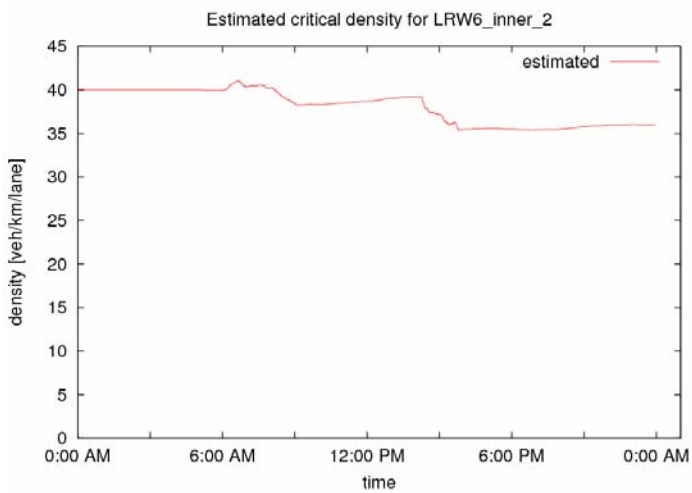
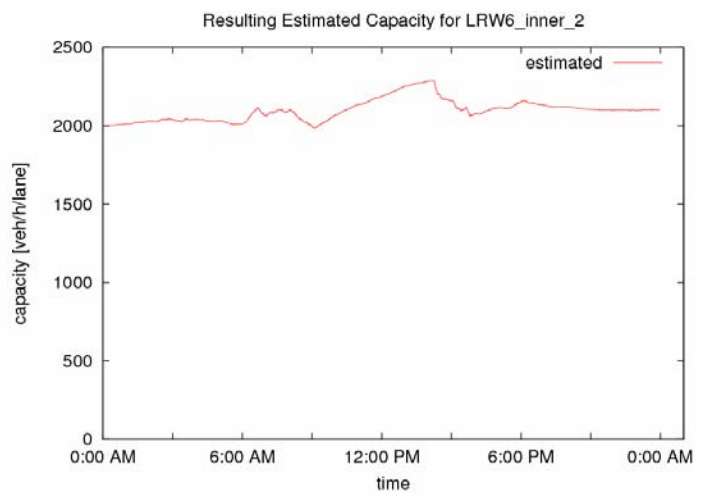
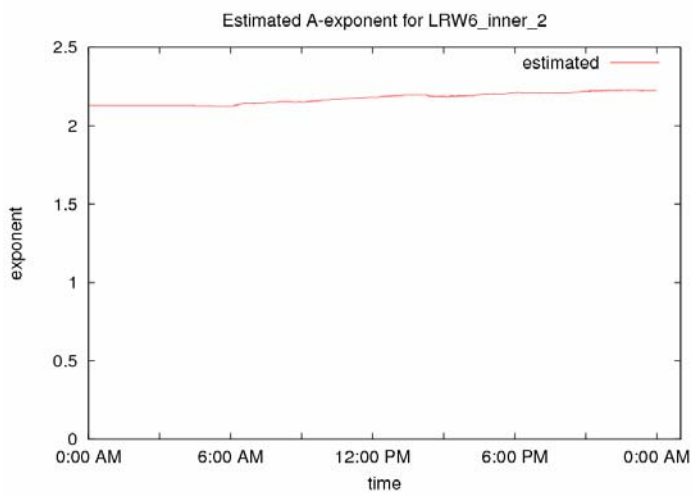
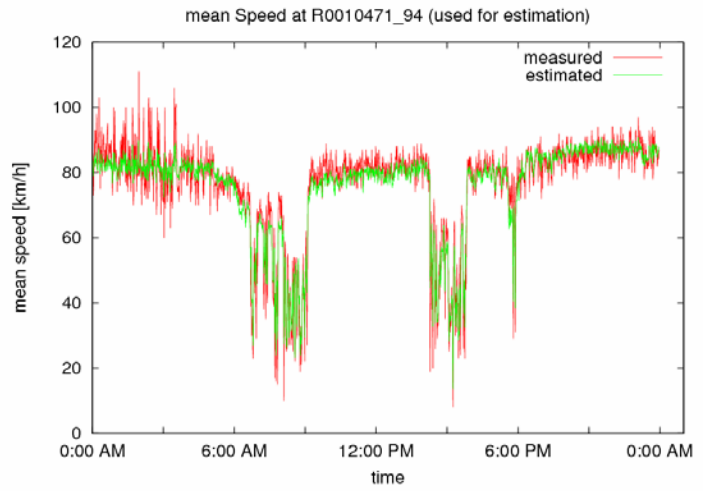
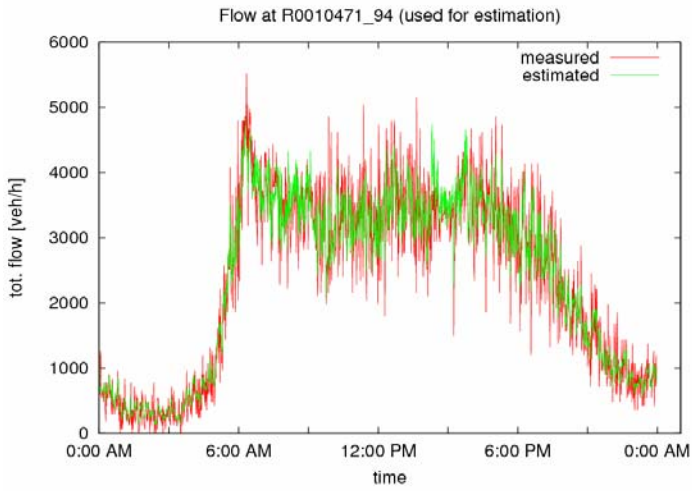
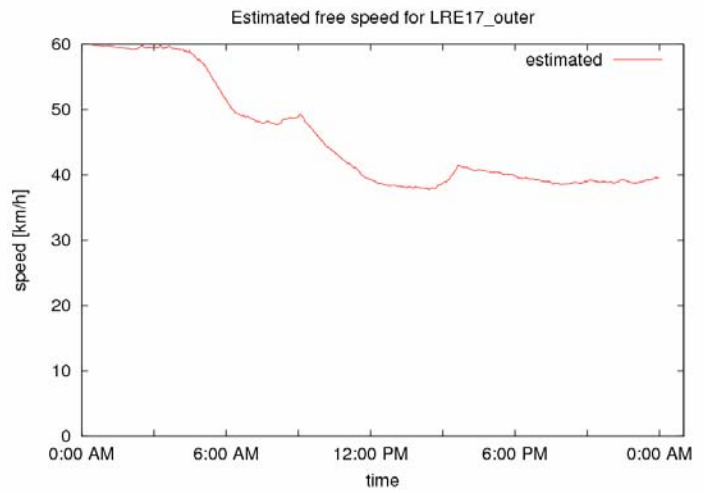
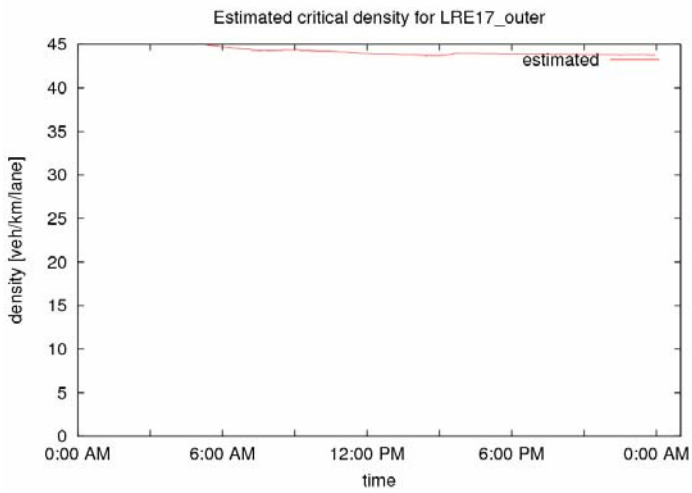
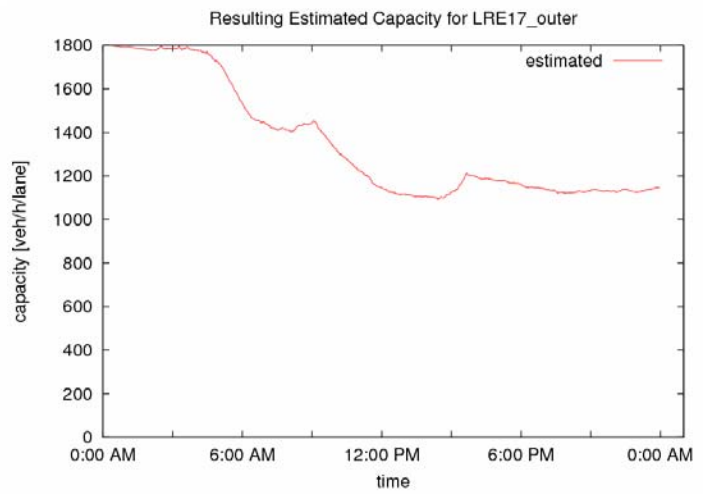
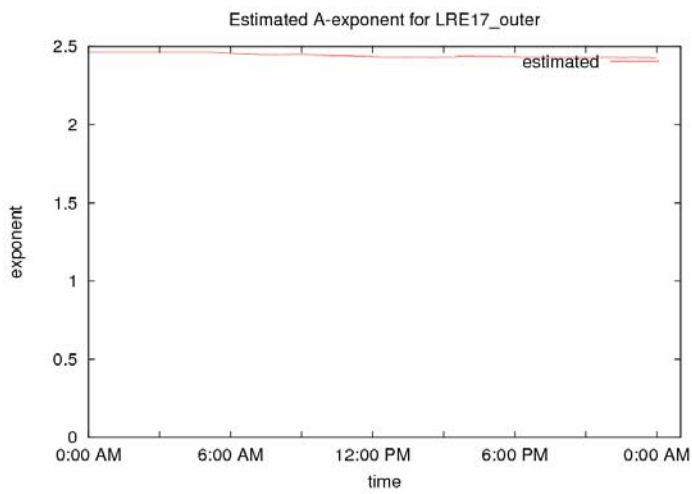
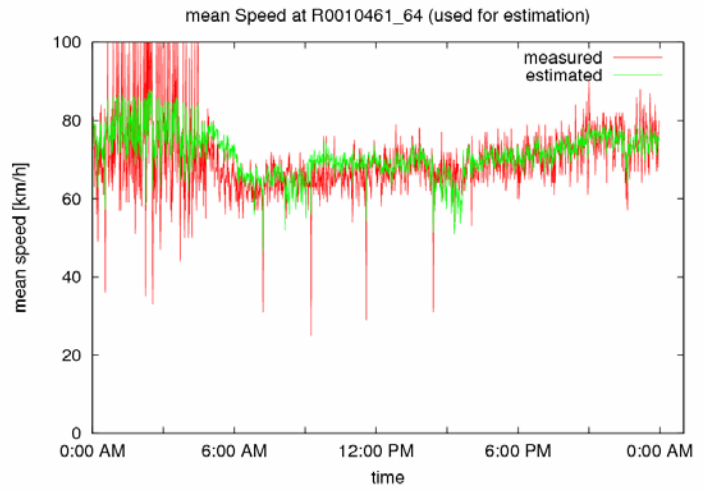
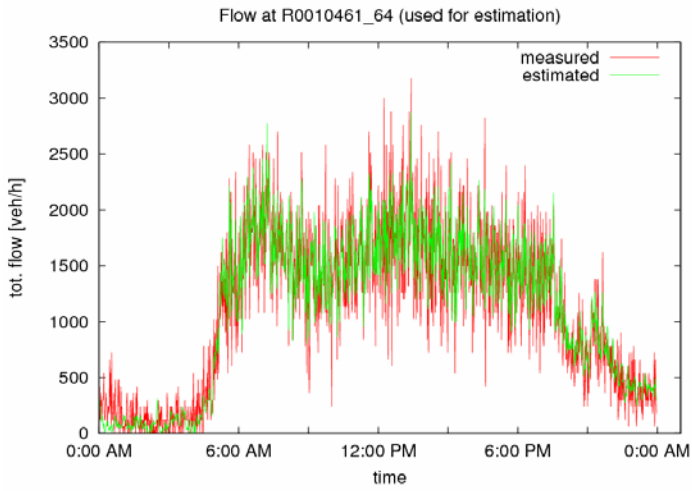


Figure 18: Flow, mean speed and Fundamental Diagram model parameter estimates for E313 for case of multiple FDs.





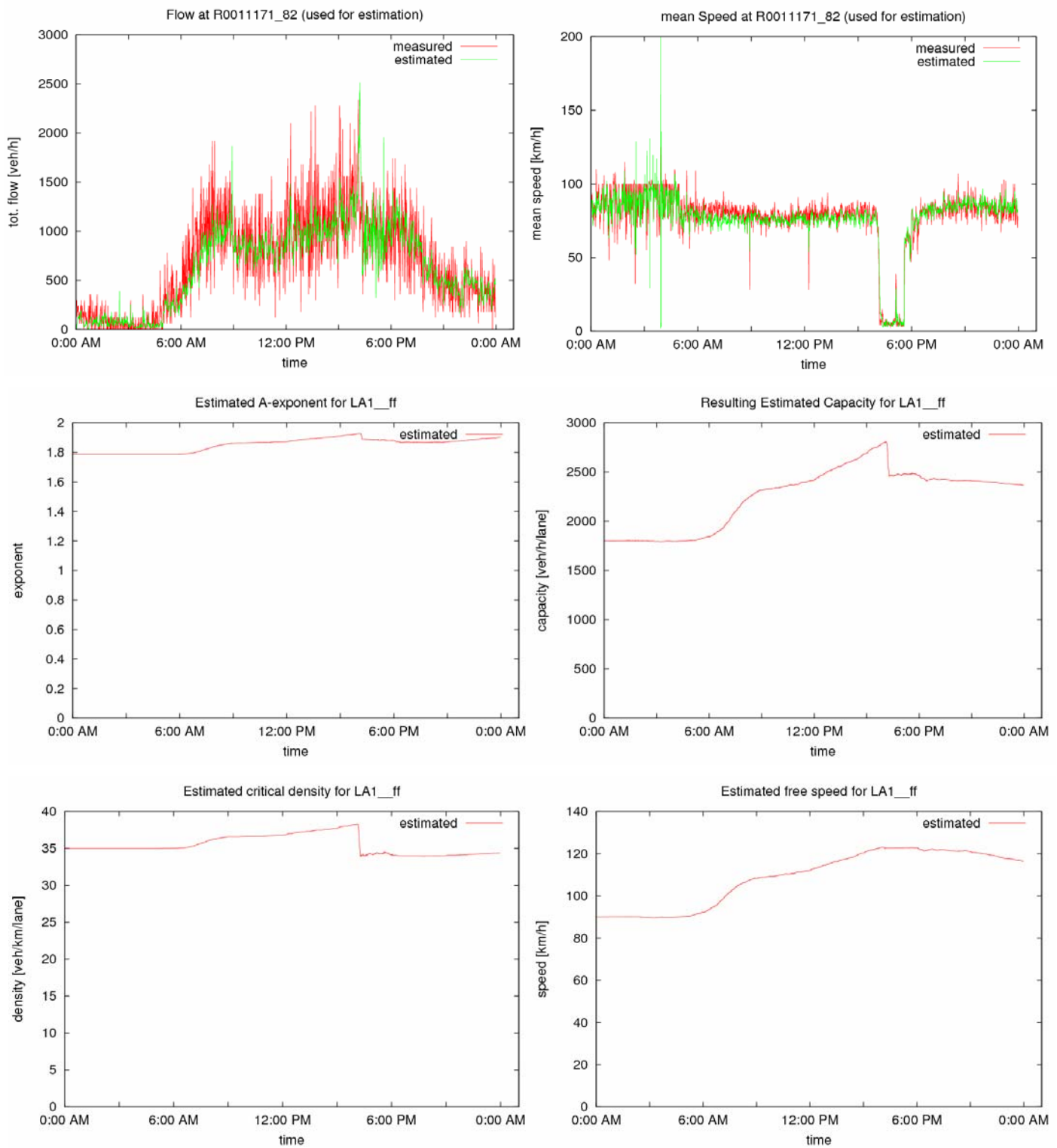


Figure 19: Flow, mean speed and Fundamental Diagram model parameter estimates for E313 connections to R1 Inner and Outer Ring and for A12 Motorway for case of multiple FD.

4.3. Evaluation at Non-Measurement Locations

The evaluation of estimation accuracy at links and segments that do not contain a detector measurement is most interesting in the case of appearing or propagating congestions, e.g. during the peak periods. This is because in periods of high speeds prevailing, the estimated mean speeds are likely to be similar to the speeds measured (and largely successfully estimated, see Section 4.2) at specific locations in the corresponding links or link clusters.

The evaluation of estimation accuracy at segments without detectors can be carried out for the present application in two ways:

- (1) When a congestion tail moves upstream or downstream along the motorway, the related speed drop or rise, respectively, should be visible in subsequent segments in the proper order in time. If this proper order of speed drops or rises is not visible in the estimation results for subsequent segments, it is quite likely that the RENAISSANCE traffic flow model does not propagate upstream or downstream moving congestion tails as it should, i.e. estimations are likely to be flawed.
- (2) The application network includes many so-called AID cameras that measure mean speed; these mean speed measurements are not used by RENAISSANCE, hence they can be used for evaluating the estimation results in segments without loop detectors. A potential difficulty is due to the fact that the cameras measure time mean speeds that were found to be roughly 10% higher than the space mean speeds measured by loop detectors. This implies that the comparison of camera-measured versus estimated (or loop-measured) speeds cannot be quantitatively accurate, particularly at high speeds (off-peak). Nevertheless, this comparison is very helpful in evaluating the estimation accuracy in cases of congestion and their propagation along the motorways.

Using the approach (1) above, all appearing congestions of 23 November 2007 were closely observed as they crossed detector locations (where speed measurements are available) and intermediate segments without measurements. In all cases, the (upstream or downstream) movement of the congestion tails was found to be visible in intermediate segment estimates in the proper spatial order, which indicates a (at least) reasonable estimation quality.

Figure 20 displays three representative examples of this investigation. Each diagram of Figure 20 presents the mean speed trajectories of:

- Two (boundary) detector measurements
- Estimates for all segments included in the motorway stretch between both boundary detectors.

The spatial order of trajectories (and specific detector and segment locations) are given on the legend (top right) of each diagram. Note that each diagram zooms on the period of the day and range of speed values that are of interest for this investigation.

The trajectories of the diagrams of Figure 20 indicate a very reasonable estimation quality even under quite complex stop-and-go traffic conditions. When the congestion tail moves upstream or downstream (towards the start or the end, respectively, of the diagram), the speed drop or rise are indeed visible in the spatially subsequent locations in the proper order.

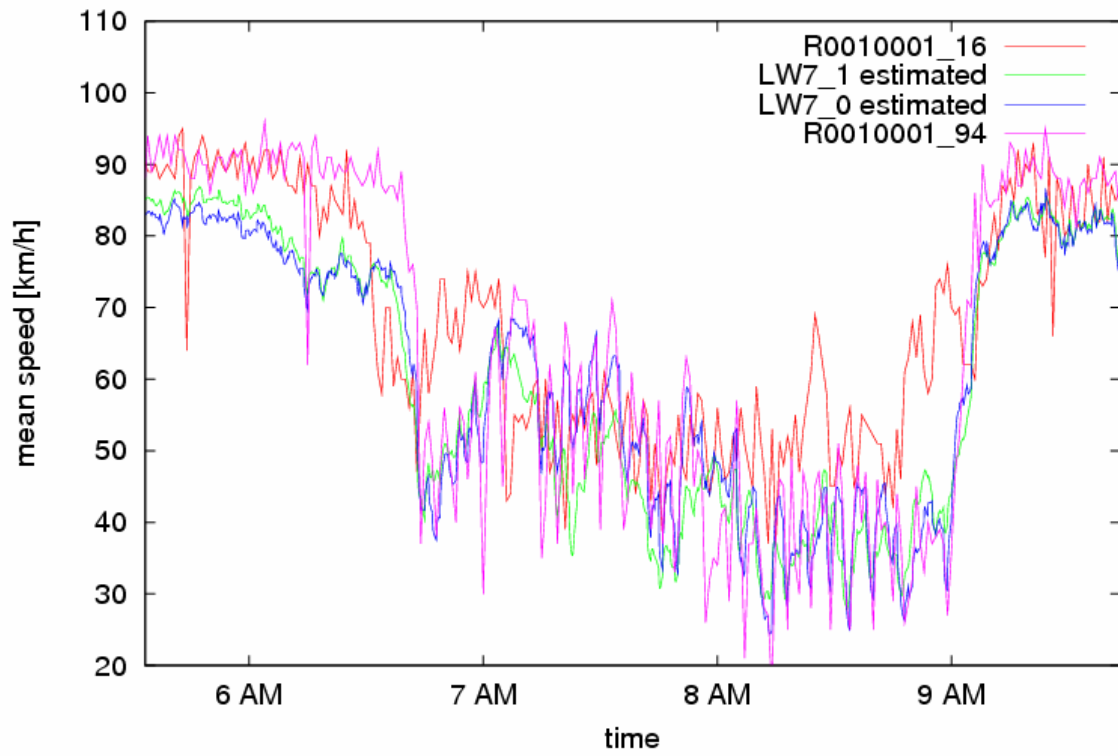
Using the approach (2), all available AID speed measurements of 23 November 2007 were compared with corresponding speed estimates for virtually all segments without detector measurements. The main findings were:

- At high speeds, AID measurements are mostly higher (by some 10%) than the corresponding mean speed estimates, as expected.
- Speed drops and rises (due to generated and propagating congestions) were mostly similar (in magnitude and time of occurrence) in AID measurements as in speed estimates. Some few identified exceptions are commented further below.
- AID speeds and estimates were quite similar within the congestion periods, despite some quite intensive stop-and-go or strongly oscillating phenomena.

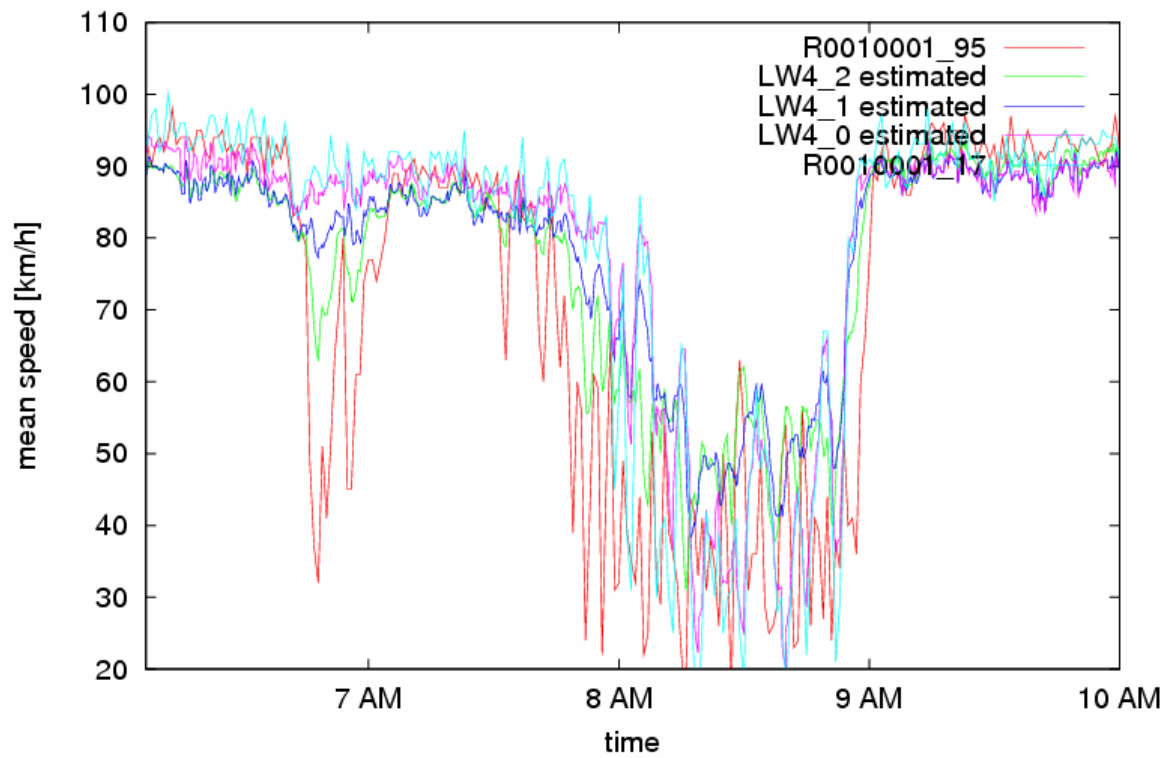
These findings confirm that the produced RENAISSANCE estimates are quite reasonable, not only at the utilised detector locations, but also at quite long motorway stretches that do not include detectors.

Figure 21 displays for illustration four representative examples of measured AID versus estimated speed trajectories at four different network locations.

R1 Inner CP pt3 mean speed zoom 1



R1 Inner CP pt4 mean speed zoom 1



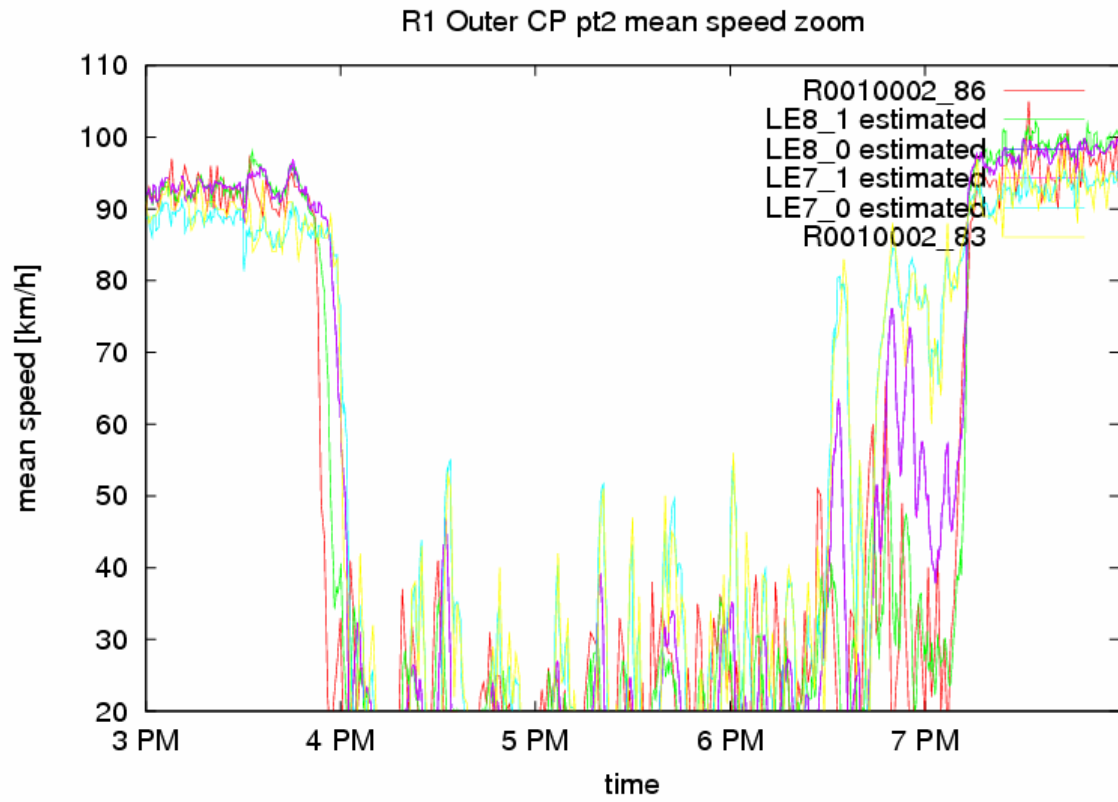
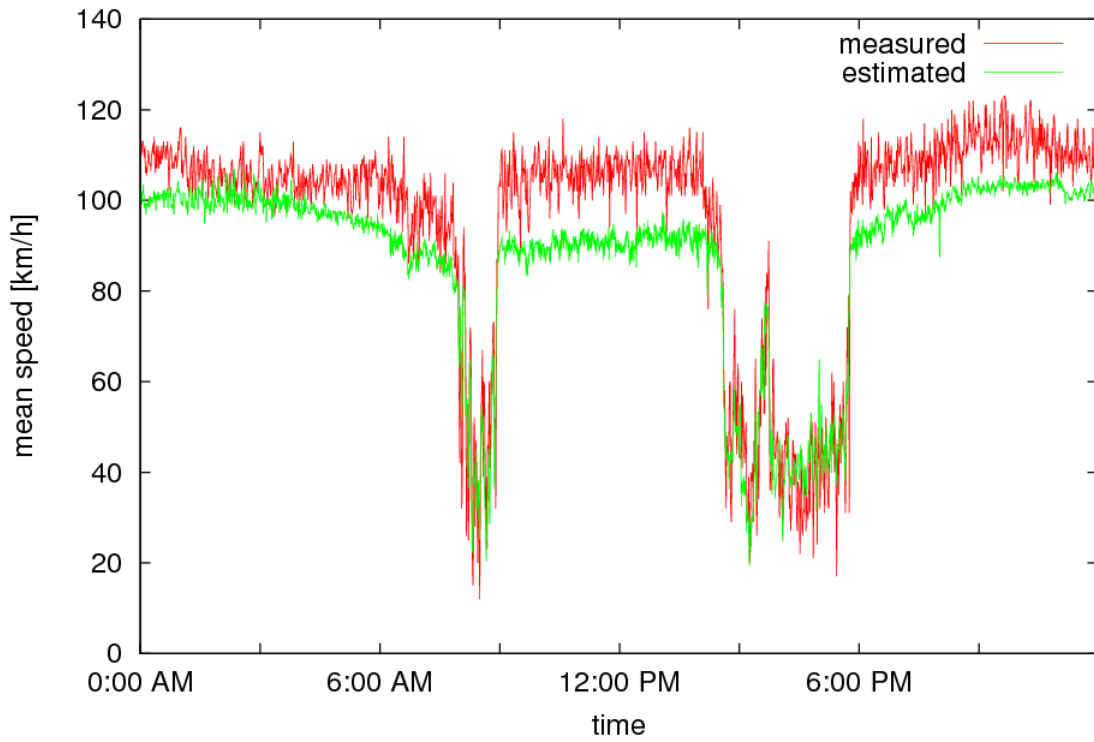


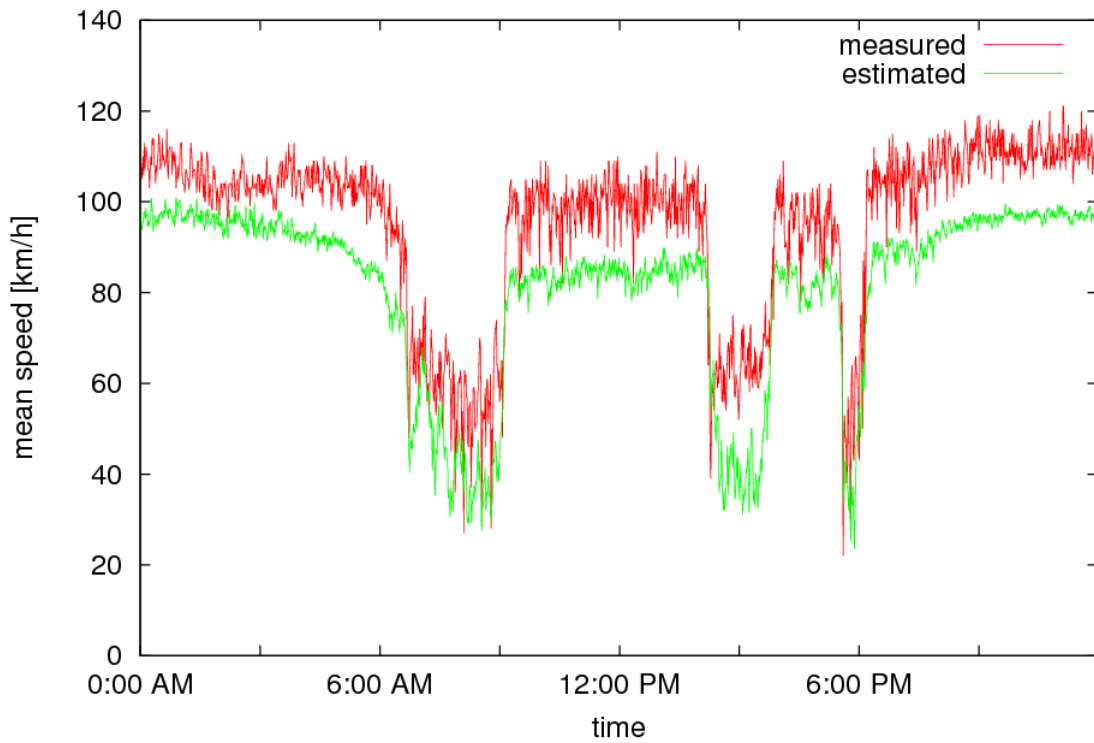
Figure 20: Congestion propagation examples to assess estimation quality at non-measurement locations.

mean Speed at 66 (not used for estimation)

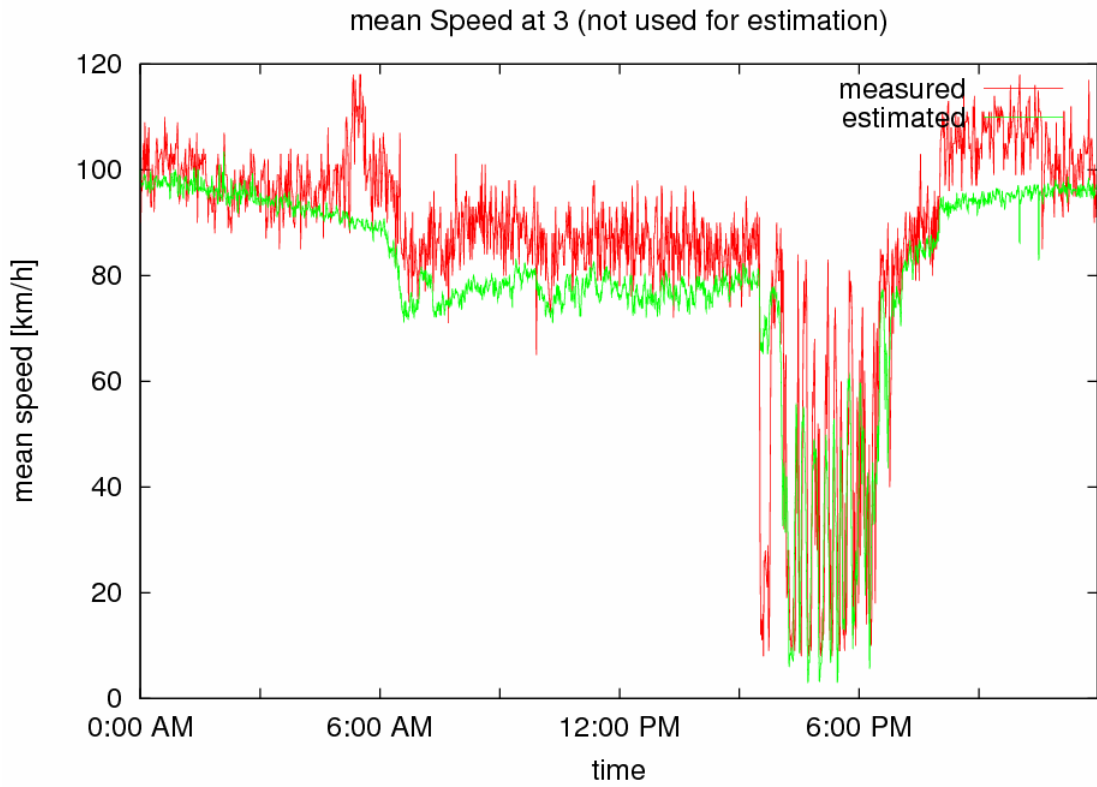


LW3 segment 4 (AID 66 used for assessment)

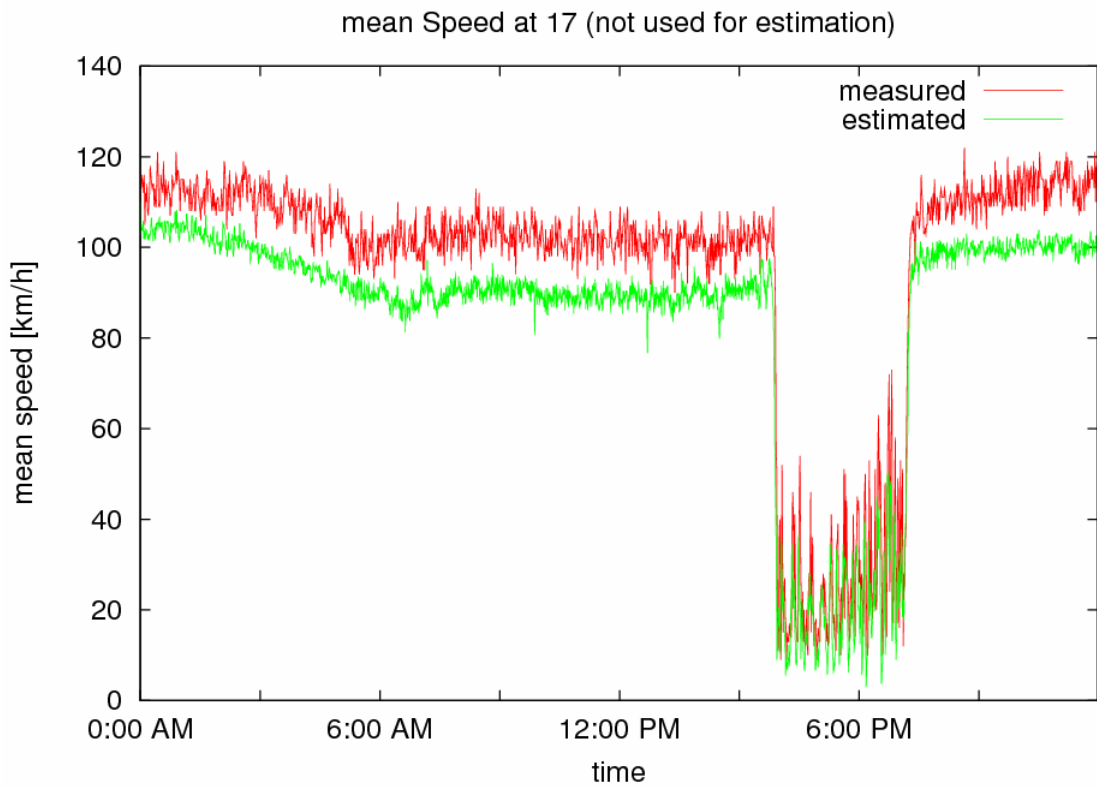
mean Speed at 43 (not used for estimation)



LW7 segment 1 (AID 43 used for assessment)



LE6 segment 1 (AID 3 used for assessment)



LE9 segment 1 (AID 17 used for assessment)

Figure 21: Representative examples of AID measured versus estimated speed trajectories.

In the following, we comment on a few identified cases where some of the above findings were not fully applicable.

Case 1

Figure 22 depicts, for convenience, the network part commented (upstream end of inner ring R1). Figure 23 displays the AID and estimated speed trajectories for the following subsequent segments (from downstream to upstream): segment 1 of the 1-segment link LW2 (where a loop detector is also available but not displayed here), and segments 3, 2 of the 3-segment link LW1. Note that the AID camera for segment 1 of LW1 was on failure on that day. It may be seen that the p.m. peak congestion was estimated very well in LW2 and was propagated reasonably well onto segment 3 of LW2, but was virtually resolved at segment 2 of LW2; while the real congestion reached segment 2 of LW2 and dissolved shortly after (as we know from the non-congested speed measurements at the upstream boundary detectors that were displayed in Figure 16). In summary, the estimation error in this case is that the mainstream congestion tail in the estimation reached upstream up to some 500 m less compared to the real congestion tail. Any increase of the traffic flow model parameter ν (NUE) would probably improve the estimation here.

Case 2

Figure 24 depicts, for convenience the network part commented. Figure 25 displays the AID and estimated speed trajectories for the one-segment link LE3. The visible morning-peak congestion is created due to traffic merging from on-ramp LE3_o. However, the next available upstream detector is located 1 km upstream, at link LE2. This means that the RENAISSANCE model must predict the congestion creation and duration by itself, i.e. without the help of a measurement. The result is visible in Figure 25 and indicates an initially correctly estimated speed decrease, but eventually the estimated low-speed congestion is shorter in time than the real congestion. Generally speaking, placing detectors at locations where congestion is known to appear first, is very helpful for better estimation quality.

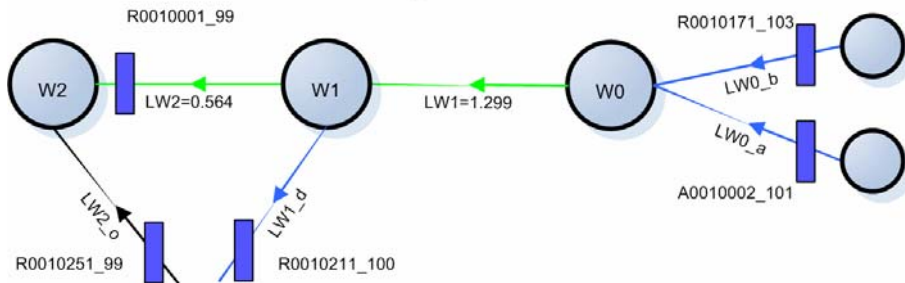
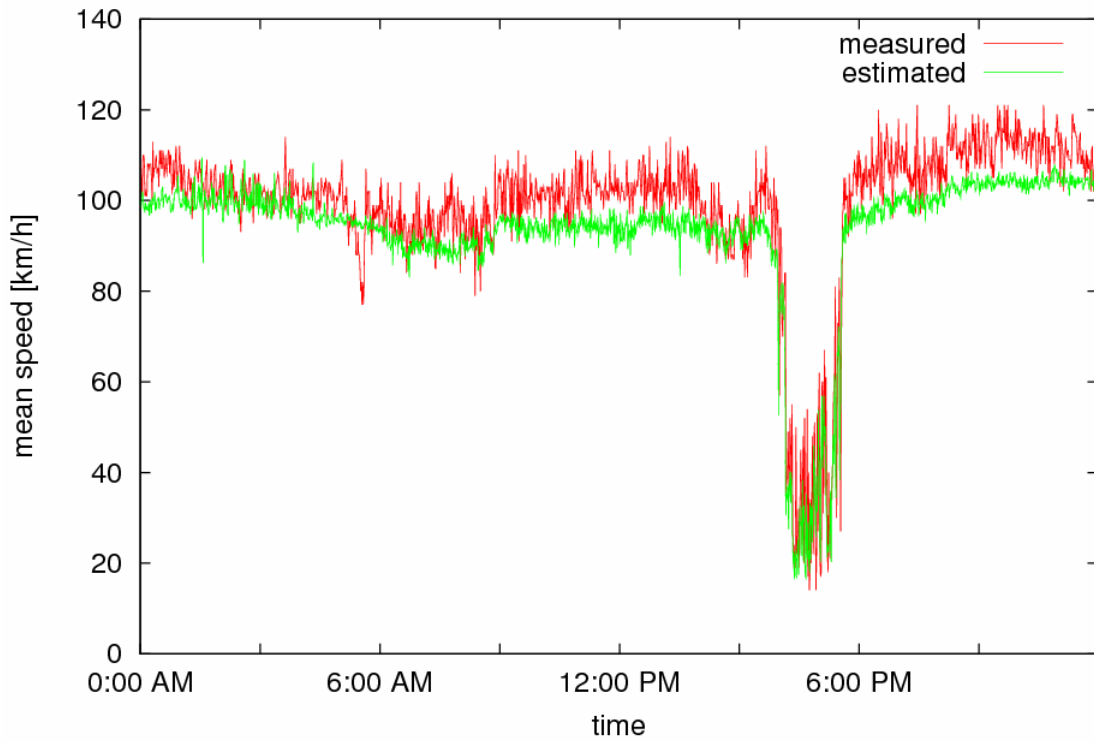


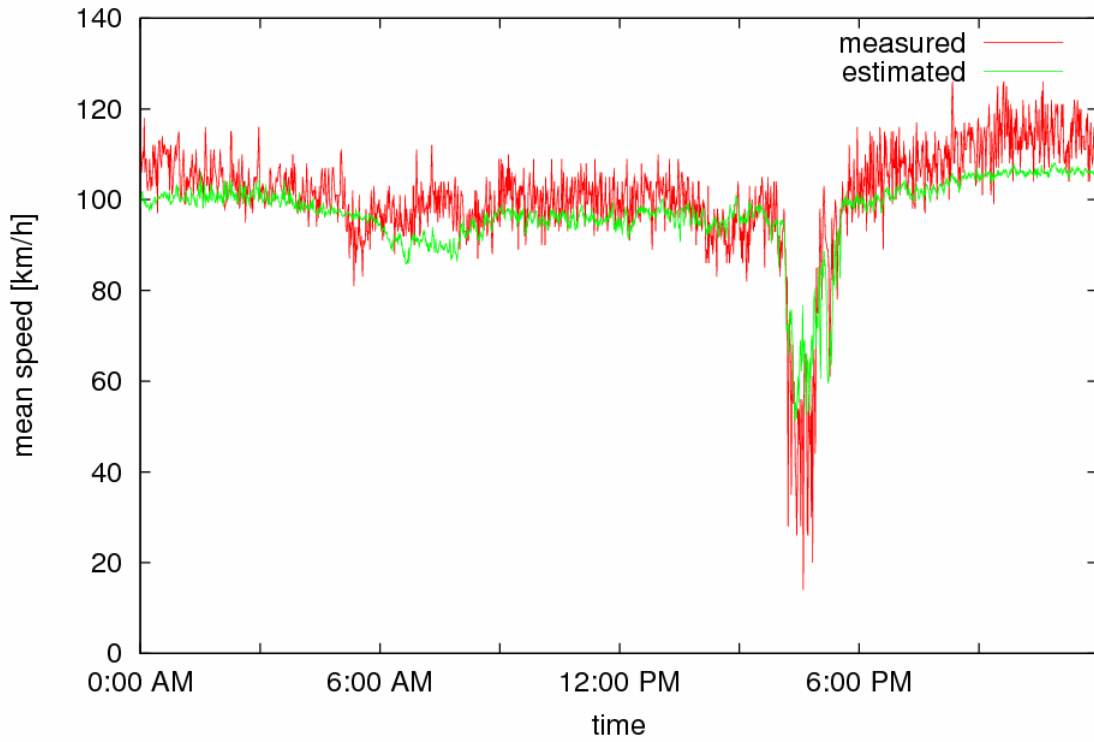
Figure 22: Part of the network for Case 1.

mean Speed at 103_M (not used for estimation)

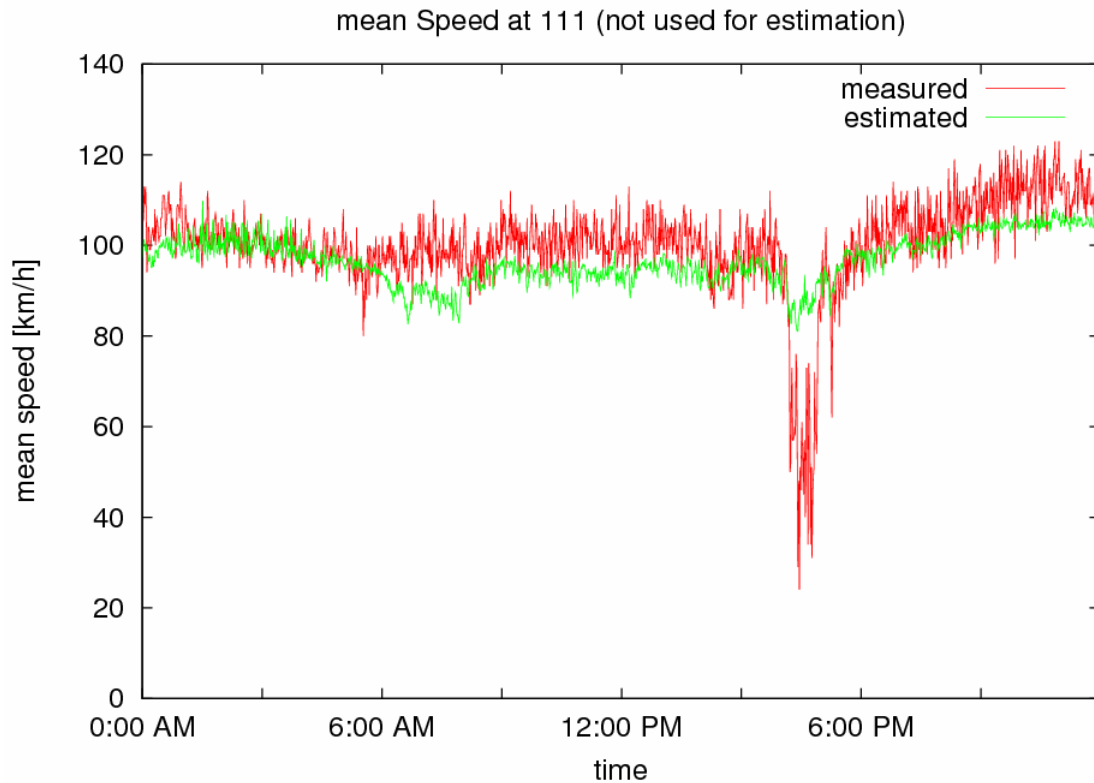


LW2 segment 1 (AID 103_M used for assessment)

mean Speed at 109 (not used for estimation)



LW1 segment 3 (AID 109 used for assessment)



LW1 segment 2 (AID 111 used for assessment)

Figure 23: AID measured versus estimated speed trajectories for Case 1.

Case 3

Figure 26 depicts, for convenience, the network part commented. Figure 27 displays the AID and estimated speed trajectories for the 1-segment links LE12 and LE13. Note that the available mainstream detectors in Figure 26 are some 2 km apart from each other and that there are 3 on-ramps between those detectors. Figure 27 shows a very short-lived real congestion at around 2:30 pm, visible in both diagrams, that is not properly estimated at LE12, LE13. Note that the short congestion is also visible and properly estimated at both boundary detectors (driven by the available measurements there, see Figure 17), but is too short for the RENAISSANCE model to actually propagate it to the links LE12, LE13 where no measurement is available.

We believe that the significance of the three identified and reported cases of less appropriate estimation results at locations without measurements is rather limited. Appropriate targeted measures or modifications could possibly improve the estimation quality for these cases as well.

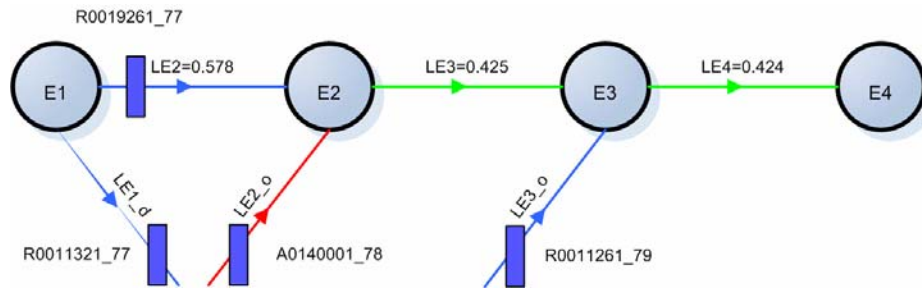
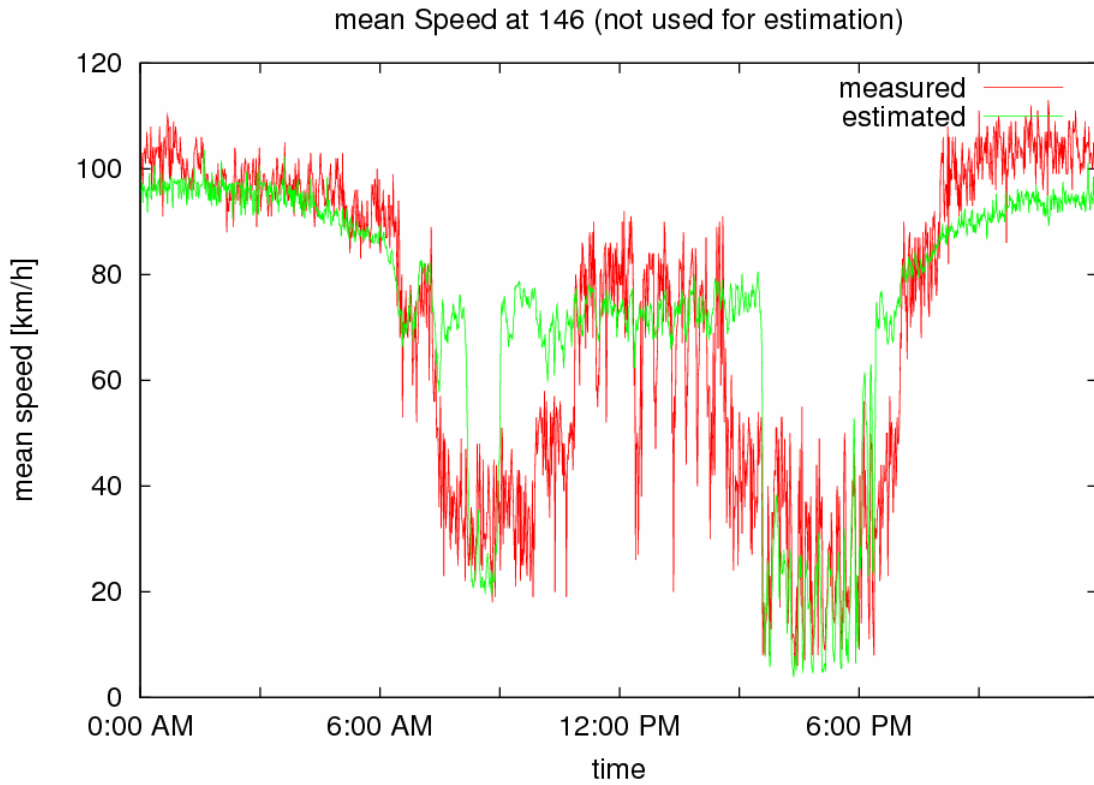


Figure 24: Part of the network for Case 2.



LE3 segment 1 (AID 146 used for assessment)

Figure 25: AID measured versus estimated speed trajectories for Case 2.

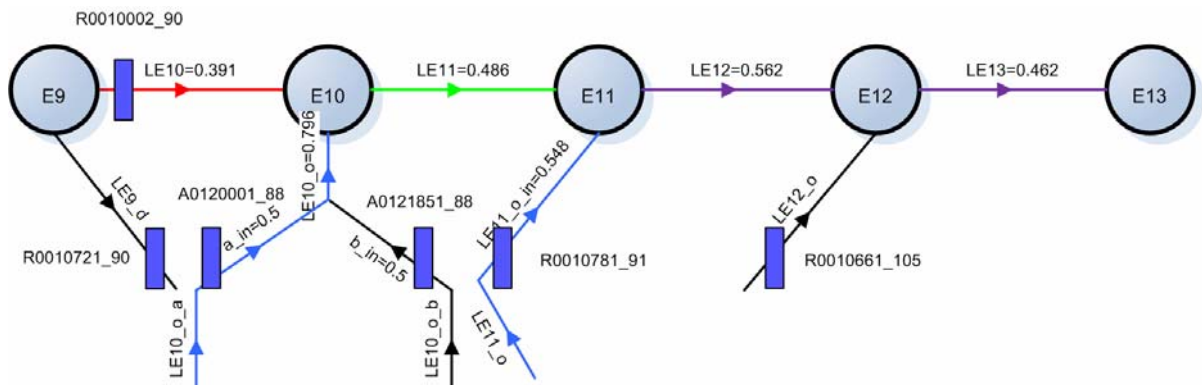
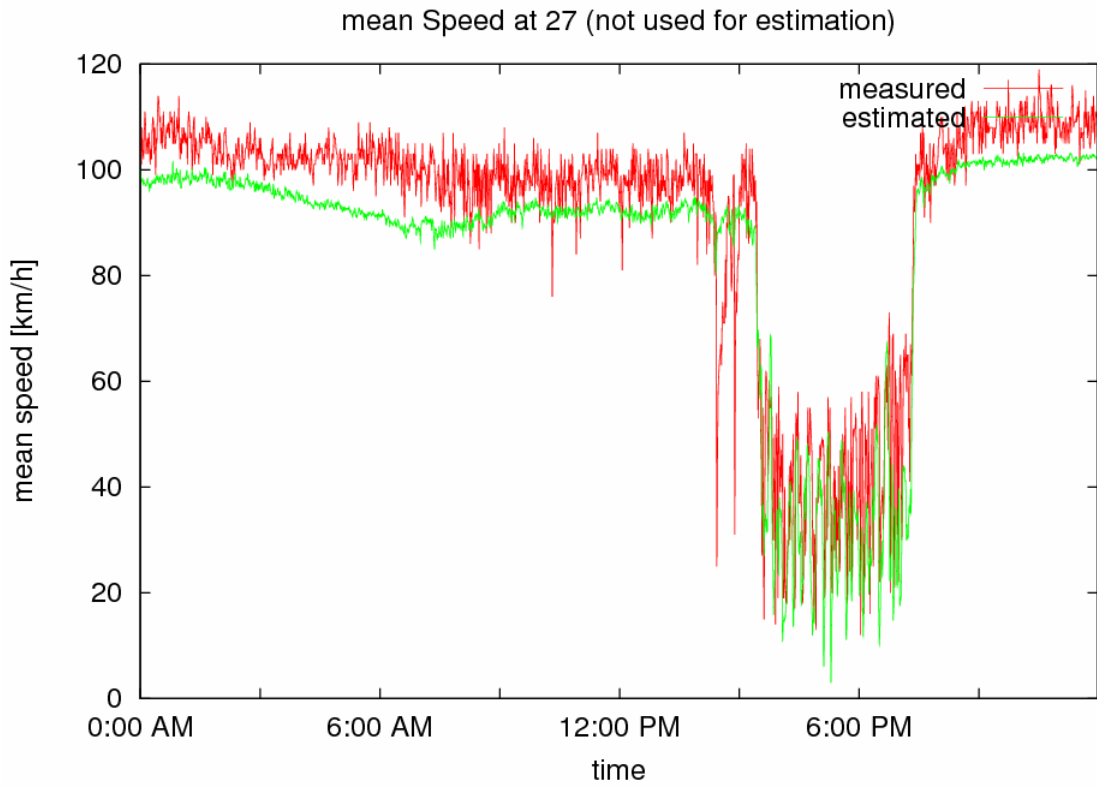
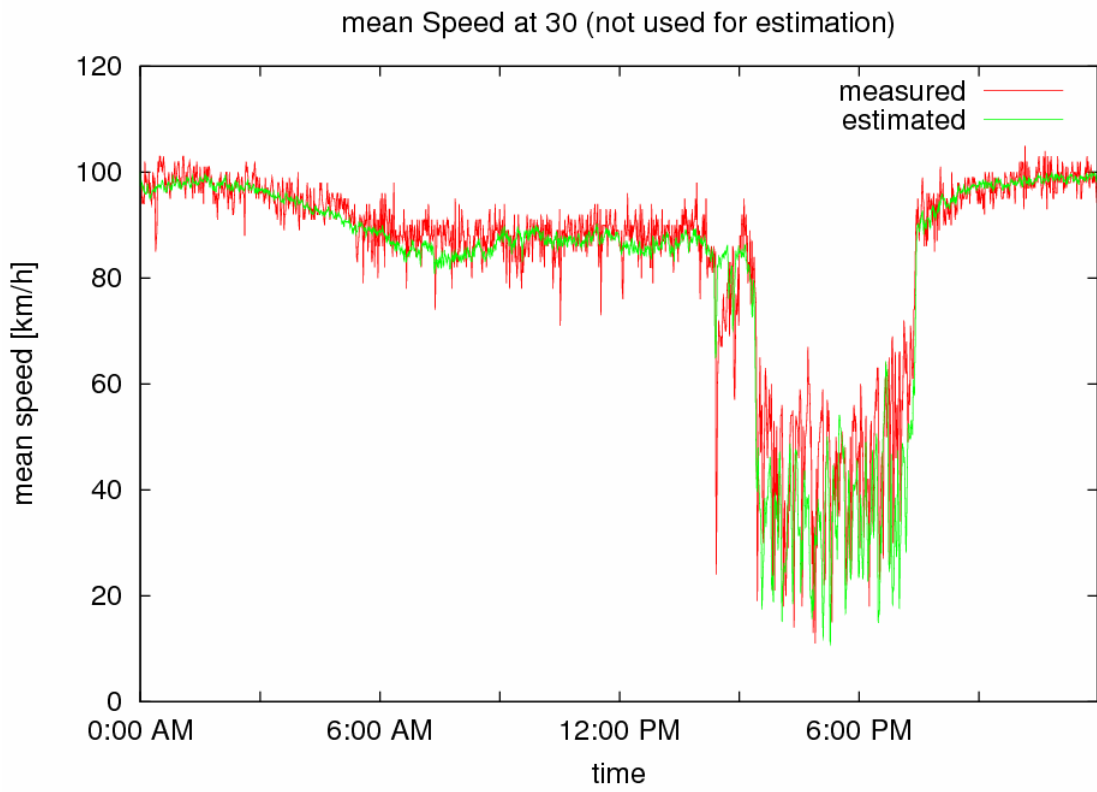


Figure 26: Part of the network for Case 3.



LE12 segment 1 (AID 27 used for assessment)



LE13 segment 1 (AID 30 used for assessment)

Figure 27: AID measured versus estimated speed trajectories for Case 3.

4.4. Multiple Day Assessment

This section presents estimation results obtained while running RENAISSANCE with field data from 5 consecutive days, 19-23 November 2007. The goals of this investigation are:

- (i) To check RENAISSANCE estimation performance on days different than the day used in previous sections.
- (ii) To check whether RENAISSANCE performance improves (or otherwise) in the medium term, i.e. after day one, which may be influenced to some extent by the utilised initial values of FD parameters (and of the \mathbf{P} -matrix in the EKF equations).
- (iii) To assess stability (or otherwise) of the FD parameter estimates in the medium term.

Figure 28 presents some examples of obtained 5-day estimation results, i.e. estimated flows and mean speeds along with the corresponding FD parameter estimates.

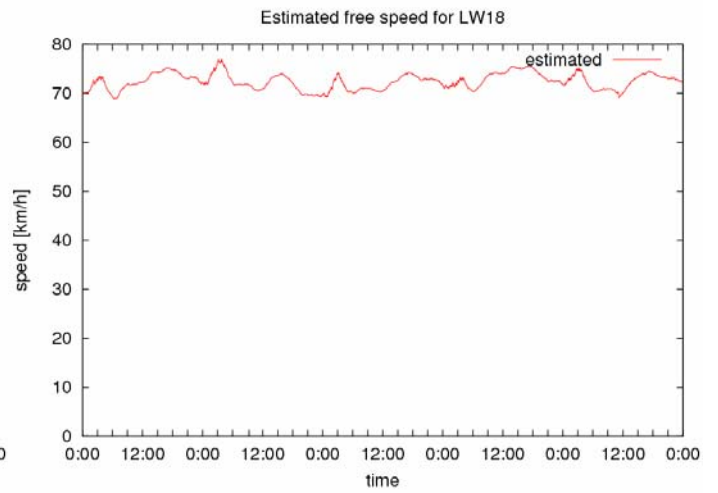
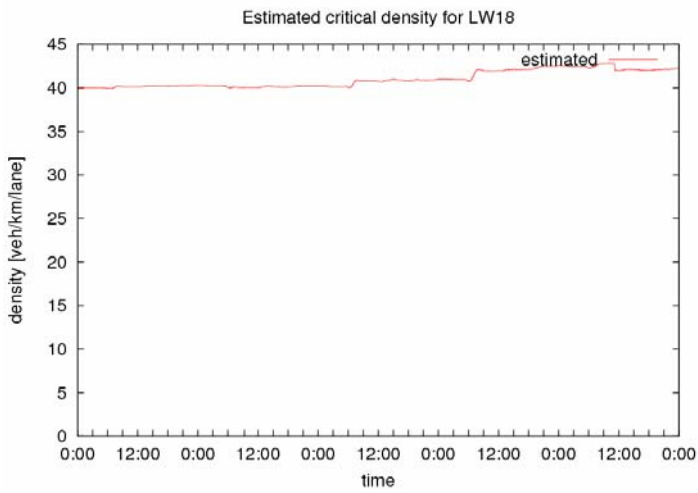
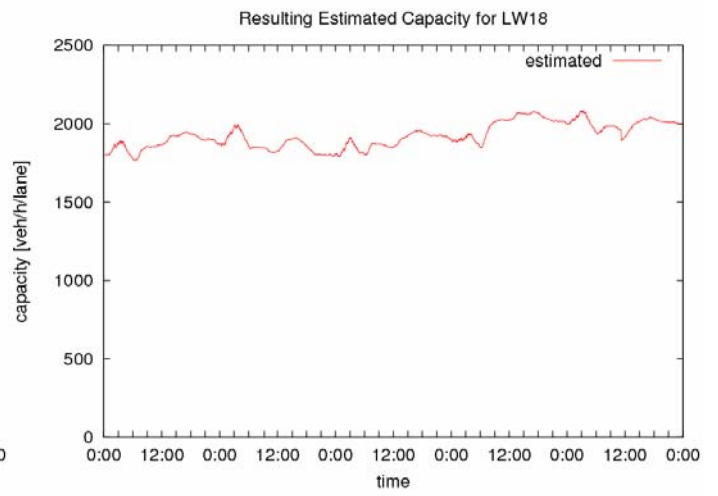
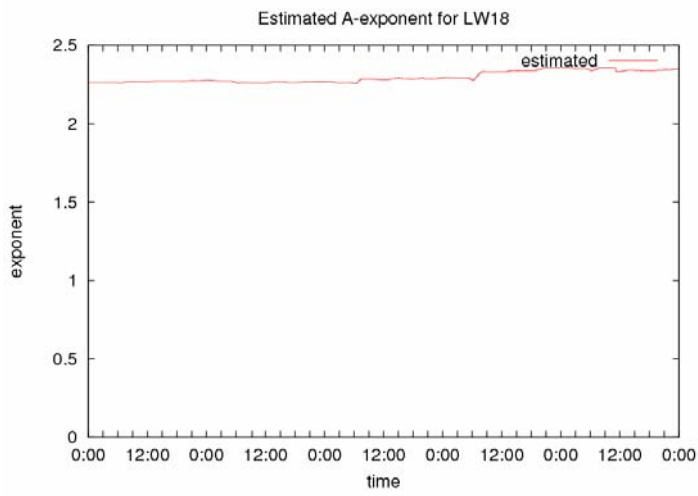
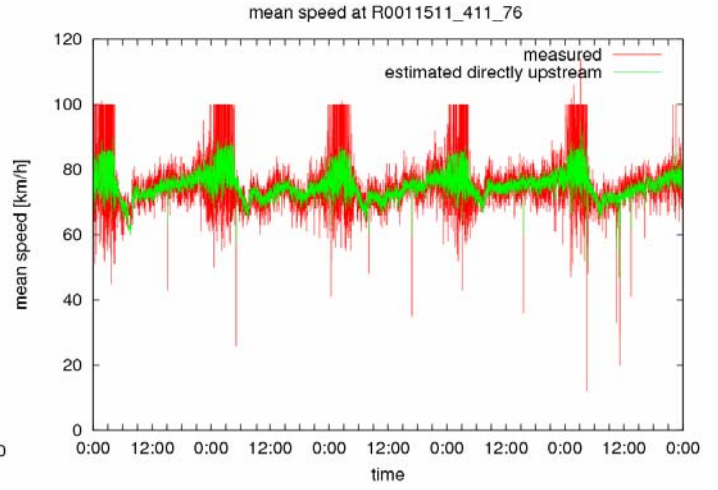
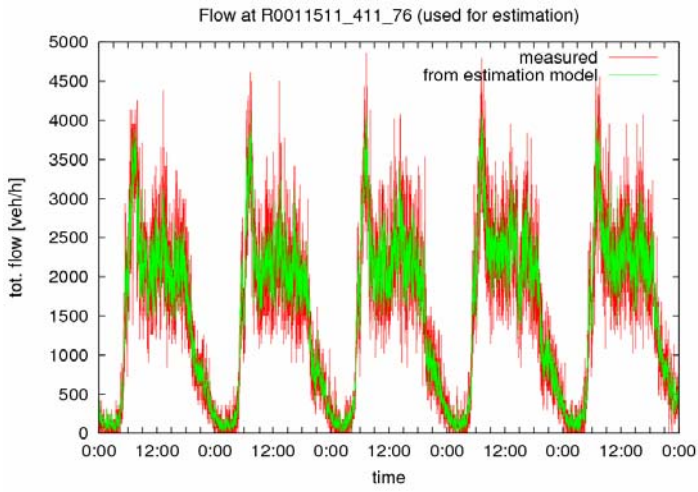
Regarding issue (i), the obtained estimation results indicate a very similar estimation behaviour and quality on days different than the one used in previous sections, which is encouraging for a potential on-line application of RENAISSANCE.

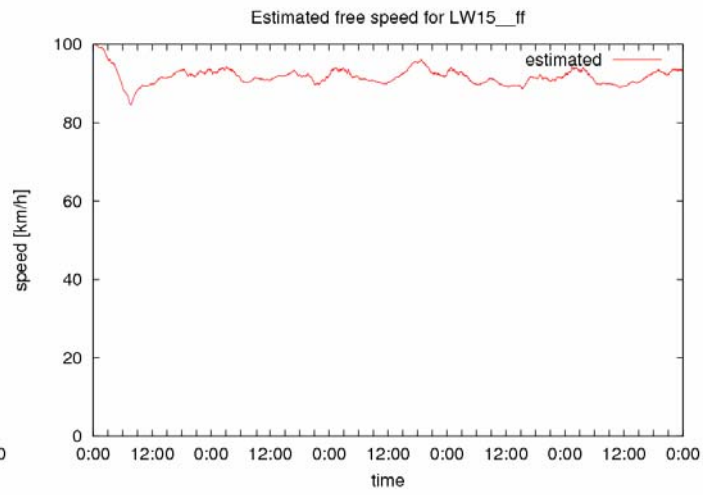
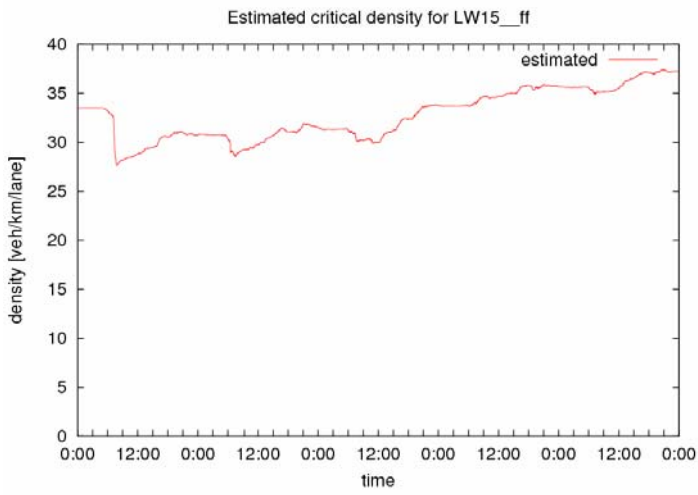
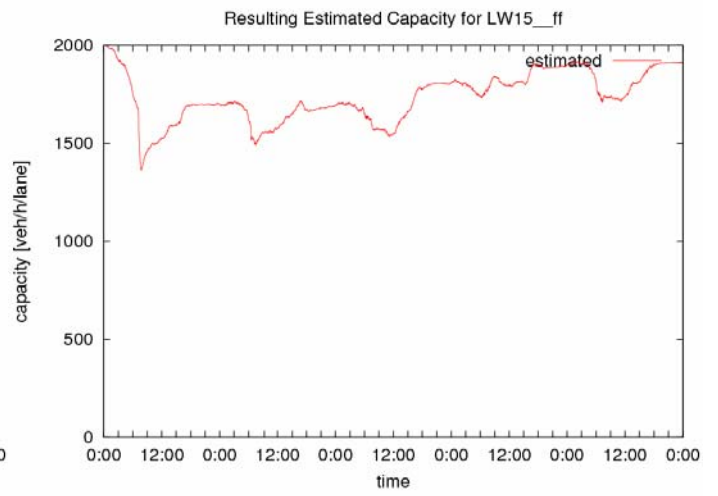
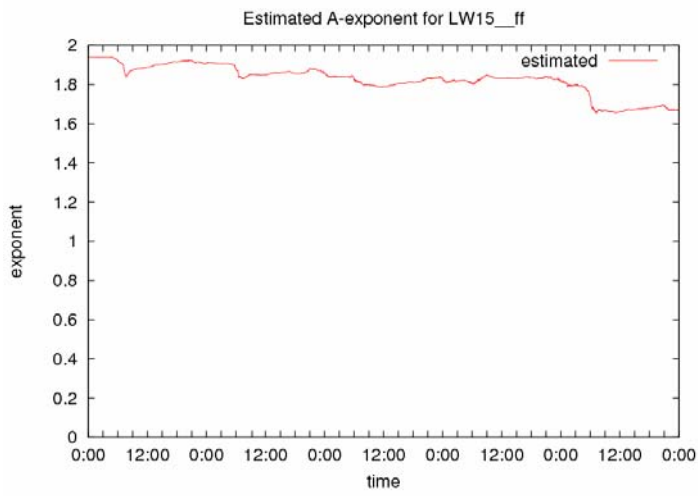
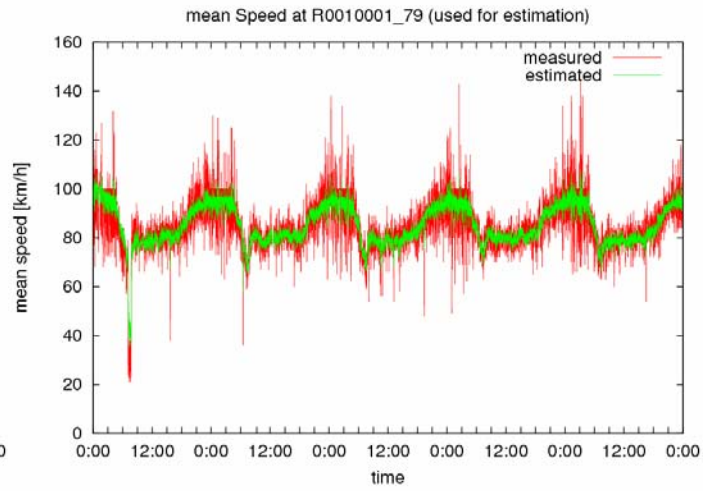
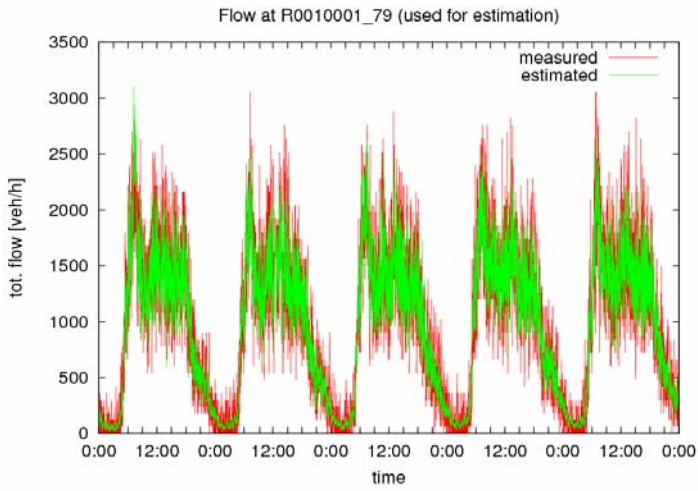
Regarding issue (ii), a careful inspection of the speed estimates indicates an improvement of estimation quality after day 1. For example, some estimation bias that was observed at some locations in the early morning hours in Section 4.2 and was attributed to the biased initial values of the free speed parameter is indeed seen to vanish on consecutive days, because the free speed has meanwhile reached a more appropriate value for the concerned locations.

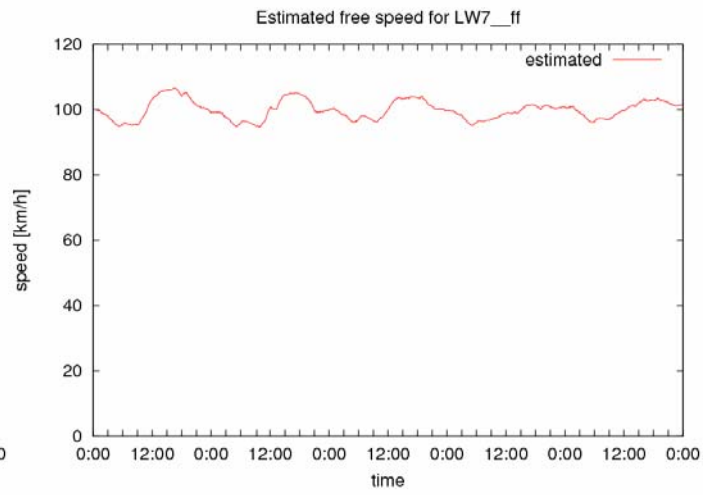
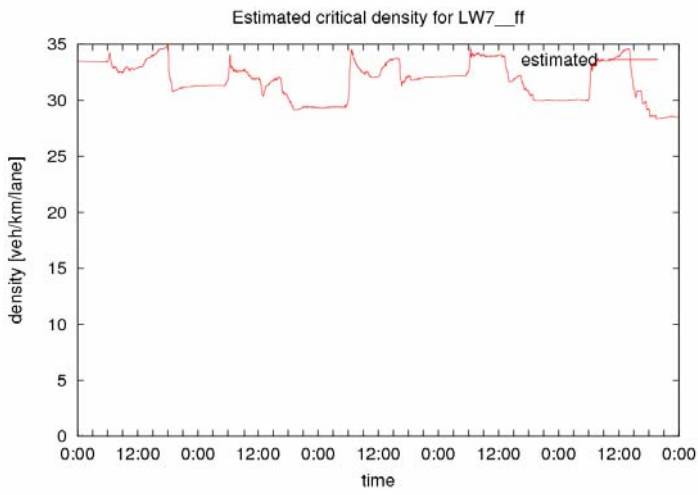
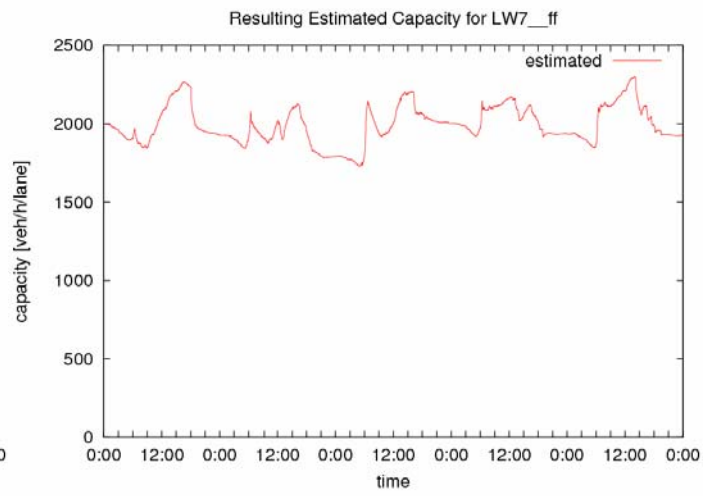
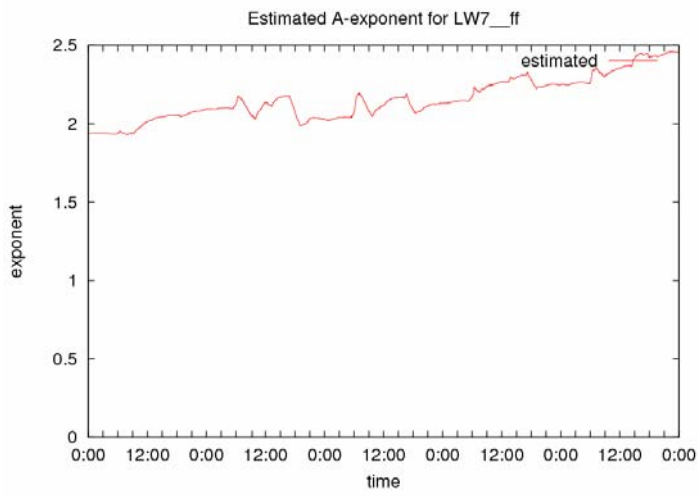
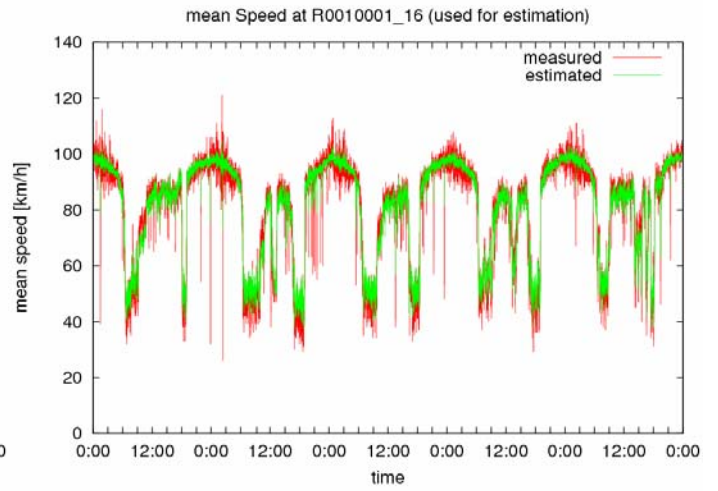
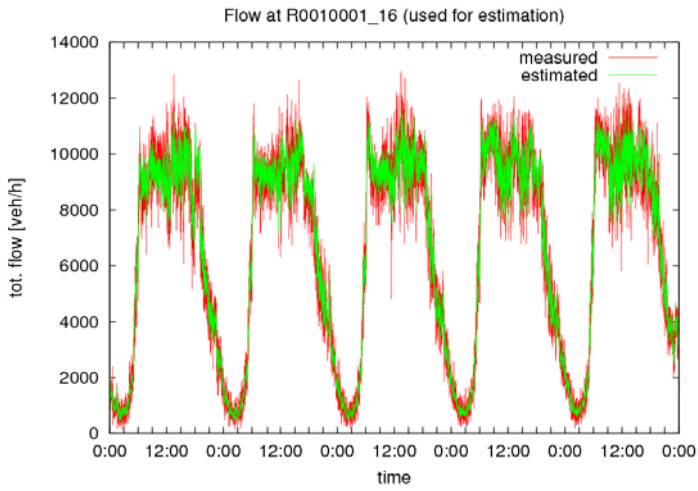
Regarding issue (iii), we may state the following:

- The estimated FD parameters exhibit some moderate variations during each day to better adapt to the received measurement data.
- All observed values of FD parameters (and their variations) are physically reasonable in terms of the parameters' physical significance (free speed, critical density, capacity) or usual range of values (alpha exponent). In other words, the estimator does not create physically meaningless, computational artefacts for FD parameters. Justified exceptions to this observation are cases of occurred incidents, that will be discussed in Section 4.6

Most estimated FD parameter values remain within a stable range of values from day to day, i.e. their trajectories do not indicate a steady increase or decrease that might lead (after more days) to physically little meaningful values. There are, however, some cases (see related examples in Figure 29), where a steady increase of parameter values is observed at least for







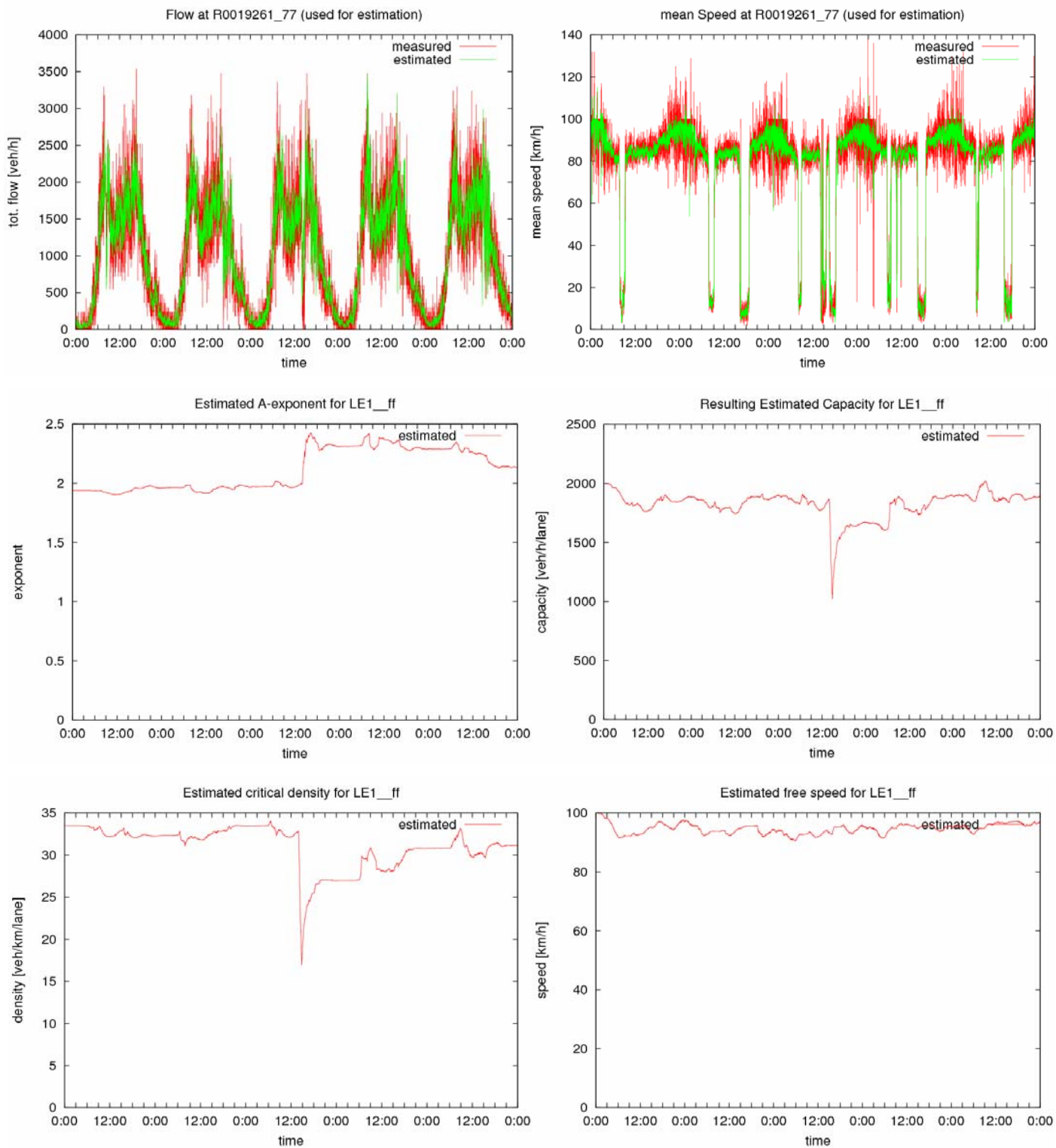


Figure 28: Examples of 5-day estimation results.

the first 4 days, albeit without really exceeding the range of physically meaningful values. To elaborate further on this issue, an additional 10-day run was carried out (not presented here), by doubling the current 5-day data. The 10-day investigation indicated some multiple-day periods of steady increase or decrease of some parameter values, after which the parameter values were stabilized while some others started changing etc. In summary, it was concluded that:

- The 5-day and 10-day investigation did not identify any periods of physically unacceptable FD parameter estimates.
- A full appreciation of the dynamic behaviour of FD parameter estimates is only possible in the long run, i.e. after on-line implementation.

Note that, in the unlikely case of encountering stability problems with the FD parameter estimates in the long run, there are several countermeasures that could be applied as a potential remedy.

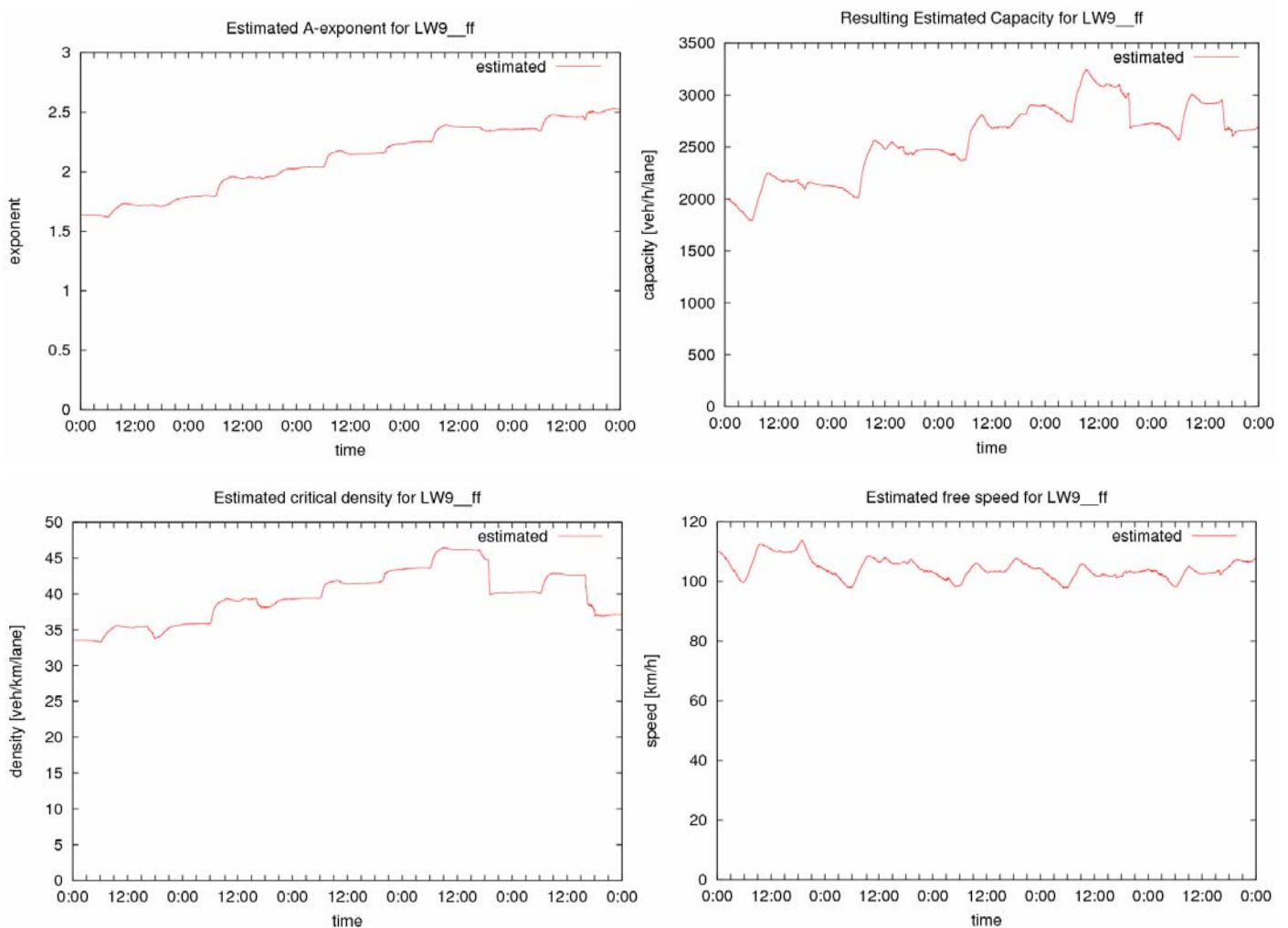


Figure 29: Examples of steady changes of FD parameter estimates.

4.5. Impact of Faulty Detectors and Replacement of Faulty Data

A common phenomenon during traffic operations is detector failure. Even in well-maintained systems, having at any time some 10% of available detectors in a faulty state is not uncommon. This fact, however, motivates the question on RENAISSANCE estimation performance in presence of detector failures.

To start with, any occurring detector failures should be known to RENAISSANCE, otherwise any arriving faulty measurements will be used by the tool and lead to a deterioration of the estimation accuracy, the level of which would depend on the specific values of the received faulty data. For example, faulty speed measurements of zero would lead the produced estimates to accordingly wrong paths etc. Fortunately, faulty data may be detected, either because the measurement device produces a corresponding flag or via appropriate (pre-RENAISSANCE) plausibility tests.

Assuming that RENAISSANCE is aware of the faulty data, the next question arising is how these data can be excluded from the estimation calculations without having to re-configure the tool which would be quite a cumbersome procedure in real time. The virtual exclusion of faulty data can indeed be automatically achieved via a gradual but rapid increase of the standard deviation of measurement data that are declared faulty, because a high value of standard deviation conveys to the estimator the message that the data in question are not trustworthy or even useless. The standard deviation is reset to its usual value when the correct data become again available. This procedure was successfully tested in the laboratory.

A final question concerns the estimation quality in (virtual) lack of the faulty data. Clearly, this question cannot be answered in a general way, because the level of deterioration of the estimation quality will depend on the amount of detectors available. Two distinct cases may be distinguished:

- Flow observability is lost due to the failed data, in which case no estimator is capable of identifying the proper values of flows in network links. Laboratory tests emulating this case indicate the appearance of (reasonable in size) flow estimation bias around the area of observability loss, while the impact may be negligible in other network areas.
- Flow observability is not lost. In this case, a deterioration of the estimation quality may appear to a larger or lesser degree, depending on the amount of available detectors.

Figure 30 presents two examples of faulty detector estimations (without loss of flow observability), that are taken from the 5-day run of Section 4.4. Each line of Figure 30 corresponds to a faulty detector, and both diagrams of each line refer to flow and mean speed,

respectively. The red curves are, as usual, measurements; it may be seen that there is a failure (corresponding to zero values for flows and speeds) during the first 1.5 days while proper measurement data become again available for the last 3.5 days. The green curves are, as usual, estimates, produced here without use of both (partially) faulty detectors; note that the specific measurement data are not used by the estimator even after they became available (on the last 3.5 days). This procedure allows us to assess, comparing the red and green curves during the last 3.5 days, the estimation quality of RENAISSANCE, should both detectors fail during online operation. It may be seen in Figure 30 that, despite the loss of the detectors, the estimation quality remains reasonably good for both flows and speeds.

Another example of faulty data replacement is provided in Figure 31. The faulty data now concern an on-ramp flow (at LW10_o). The interpretation of the curves of Figure 31 is the same as in Figure 30. It may be seen that RENAISSANCE, exploiting the flow information stemming from other available detectors, is capable also in this case to replace the faulty flow data with very reasonable (but much less oscillating) estimates.

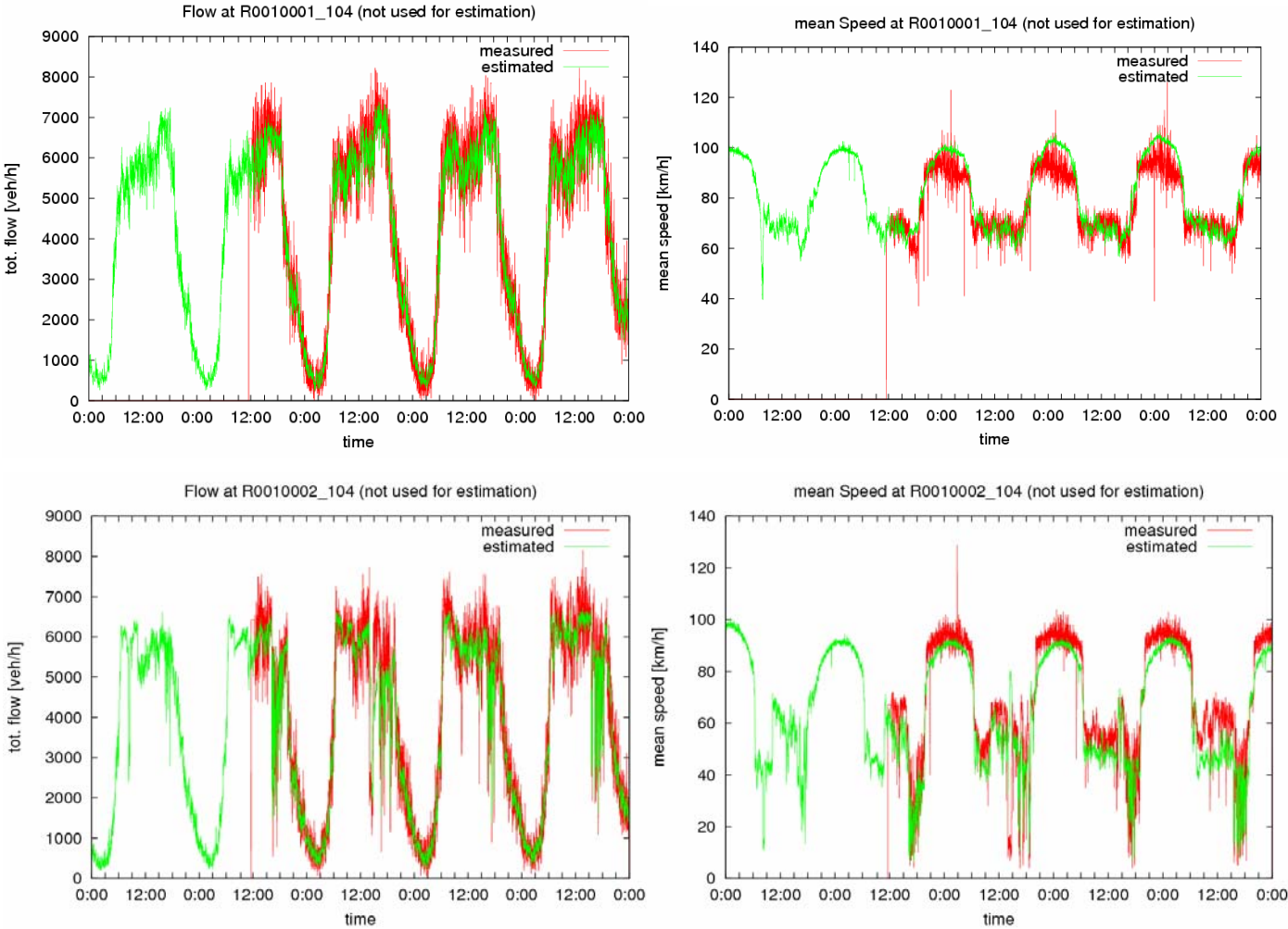


Figure 30: Impact of faulty data in R1 tunnel (inner and outer).

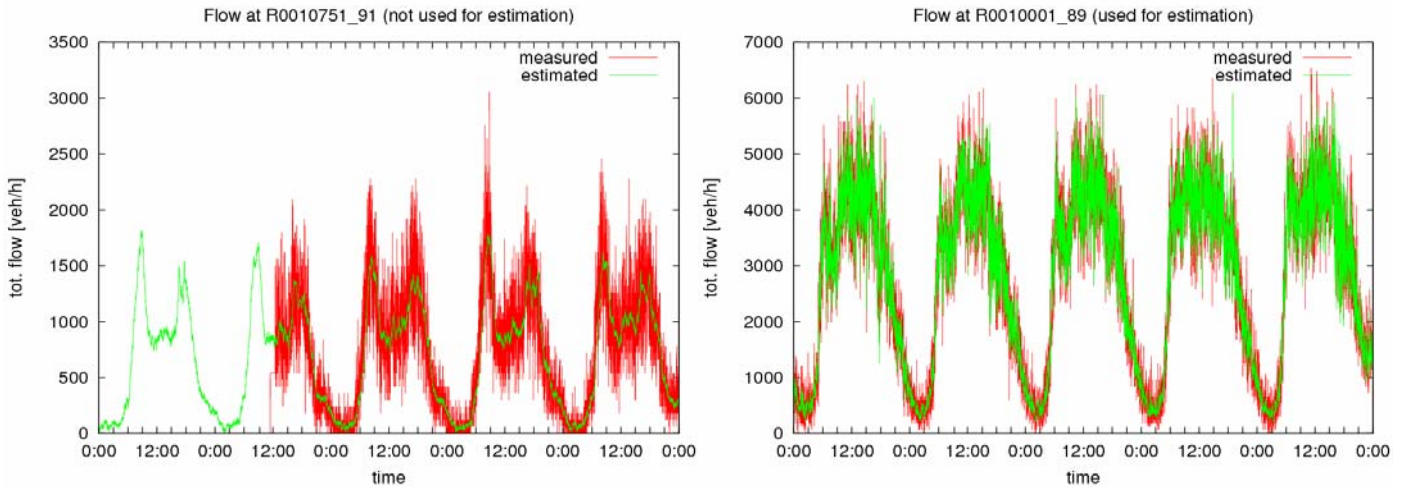


Figure 31: Impact of faulty data at LE11_o.

4.6. Incident Detection

Incidents are external capacity-reducing events, such as a disabled vehicle or an accident that blocks a part of the highway. Because the incident (in contrast to a regular congestion) is an external event, i.e. not explicable by the inherent traffic flow dynamics, it may create a traffic flow situation that cannot be described by a traffic flow model with the usual values of FD parameters. In fact, the capacity loss due to the incident implies that the FD parameter values should be changed appropriately at the incident location to reflect the real capacity loss, in lack of which the traffic flow model may not be able to describe the incident-affected traffic situation sufficiently accurately. Clearly, the incident impact may be minor (e.g. because the traffic flow is not high enough to be affected by the capacity loss), in which case the change of FD parameter values may not be necessary for accurate traffic flow description.

RENAISSANCE is fed with real data and includes a traffic flow model with FD parameter values that are estimated in real time such that the model calculations approximate the real data. In case of an incident with sufficiently significant impact on the traffic situation (and, hence, on the real data), the model calculations cannot match the real data unless the FD parameter values are changed accordingly. This forces the estimator to modify, relatively rapidly, the FD parameter estimates so as to better match the real data.

The most relevant parameter that needs to be changed for a better description of incident-affected traffic conditions is the capacity. As seen in previous sections, the capacity estimate of a link cluster is subject to continuous change. However, based on previous experience, an abrupt and/or significant change in the capacity estimate produced by RENAISSANCE is usually a sign for an occurred incident. Hence, the rate of (decreasing) capacity estimates (i.e. of its time derivative), possibly in combination with the magnitude of (decreasing) capacity

estimates, may be used to detect incidents with sufficiently high impact. This section provides some examples of detected (initially unknown) incidents as well as of known (reported by the authorities) incidents.

Incident 1

Figure 32 displays a part of the network (outer ring) that includes Incident 1. The first hint about the incident was gained by visual inspection of the produced capacity estimates for link LE20 during the multiple-day investigation of Section 4.4; in fact Figure 33 indicates at around 7:00 a.m. of day 1, an abrupt capacity loss (from around 2000 veh/h/lane to 1200 veh/h/lane). Figure 34 displays (over 24 h of day 1) the corresponding time-derivative (of capacity estimates) that confirms the unusually abrupt capacity drop, since the time-derivative value at around 7:00 a.m. is much lower (negative) than at any other time during the 24 h displayed. Note that the time-derivative (in veh/h²/lane) is calculated as the difference of the capacity estimates of two subsequent time steps, divided by T . The capacity estimate is seen (Figure 33) to slowly recover after 7:00 a.m..

The incident occurred somewhere between detectors R0010002_99 and R0010002_102 (Figure 32) as clearly indicated by the much lower speeds in the former compared to the speeds of the latter detector around 7:00 a.m. of day 1, see Figure 35. Note that the visible strong congestion at location _99 at around 7:00 a.m. does not occur on any other day, which is a clear indication for a non-recurrent congestion caused by an incident. Remarkably, the abrupt drop of estimated capacity is observed in the link LE20 (although the real incident reportedly occurred just downstream of node E21), because link LE20 contains the first mainstream detector upstream of the incident that measures the sharp speed drop.

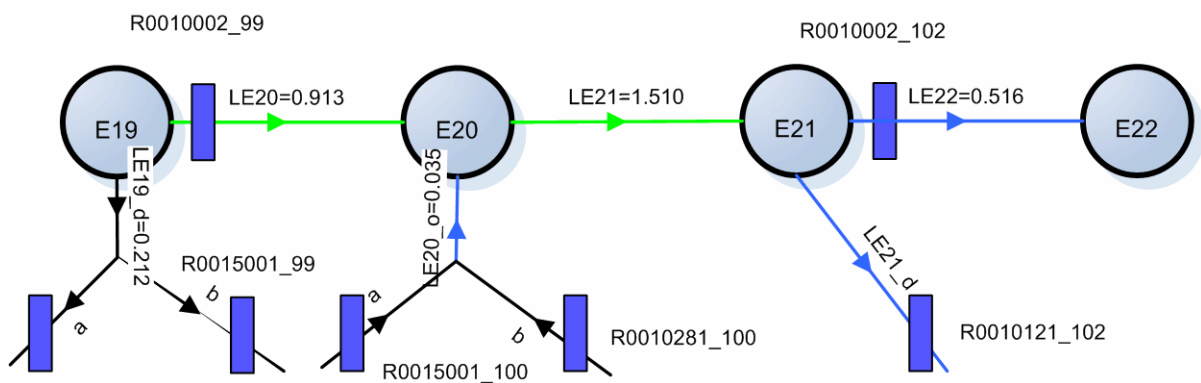


Figure 32: Part of network for Incident 1.

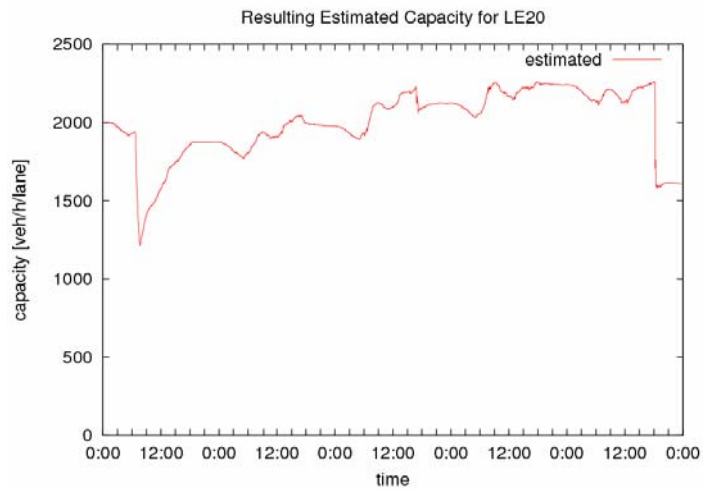


Figure 33: Capacity estimates indicating occurrence of Incident 1 at around 7:00 a.m. of day 1.

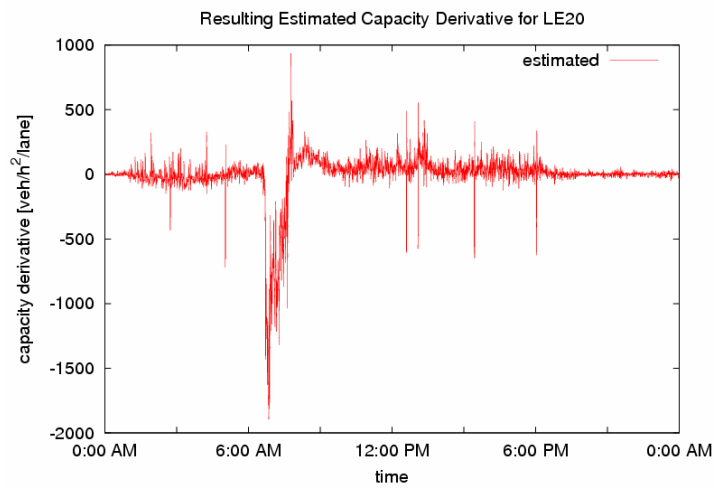


Figure 34: Time derivative of capacity estimates for Incident 1.

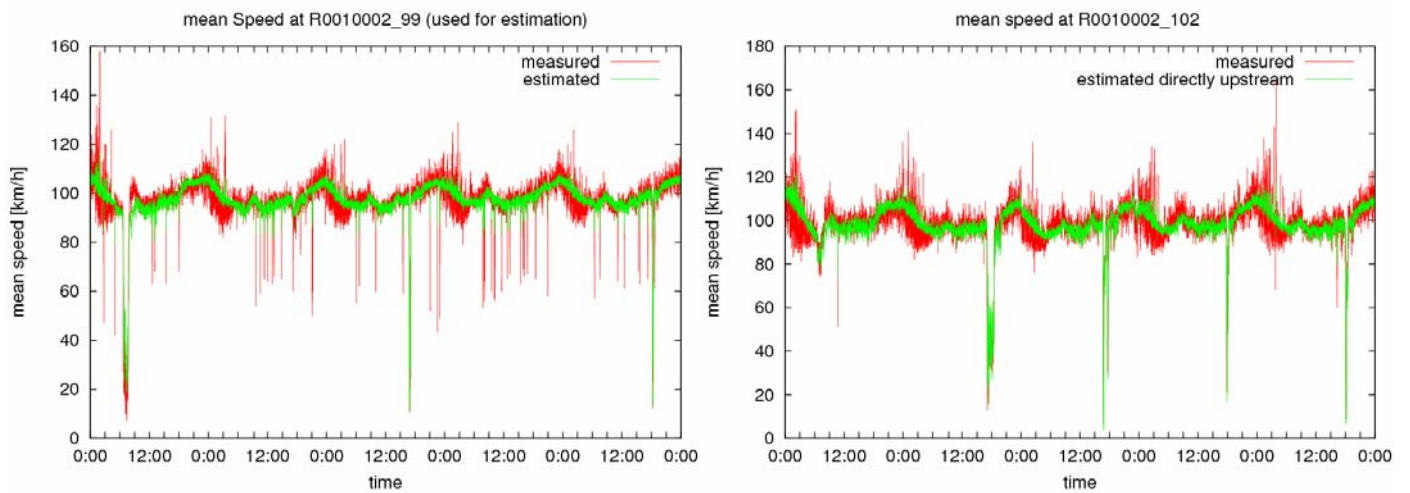


Figure 35: Speed measurements confirming the occurrence of Incident 1.

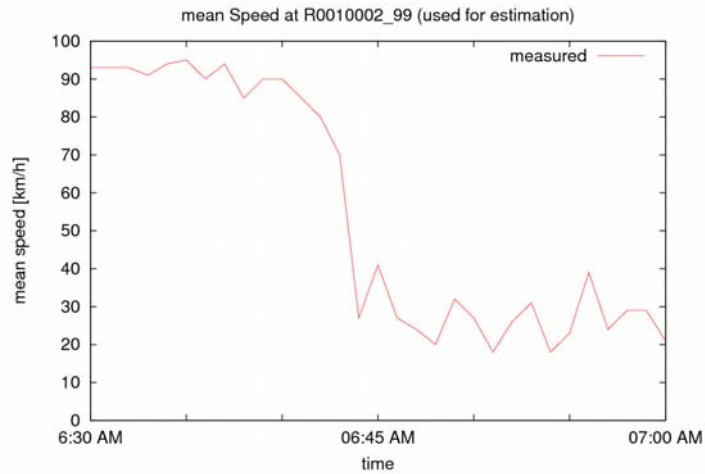


Figure 36: Zooming-in of Figure 35.

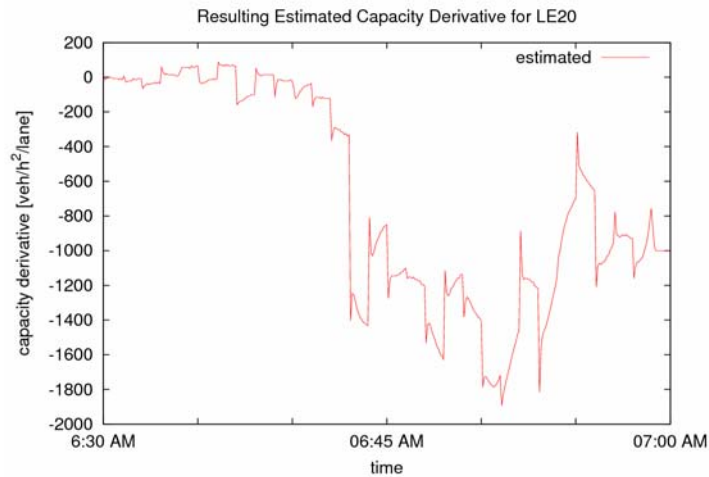


Figure 37: Zooming-in of Figure 34.

The incident occurred reportedly at 6:23 a.m.. Figure 36 however reveals that the corresponding shock wave reached the upstream detector _99 only 20 min later; this is partly due to the 2.4 km separating the incident location (reportedly just downstream of node E21) and detector _99. On the other hand, the capacity derivative on Figure 37 is seen to reach sufficiently low values for incident detection almost at the same time of shock-wave arrival at detector _99 which is deemed to be an excellent performance.

Incident 2

Figure 38 displays the network part (outer ring) that includes Incident 2. The first hint about the incident was gained by visual inspection of the produced capacity estimates for link LE2 during the multiple-day investigation of Section 4.4; in fact Figure 39 indicates at around 14:00 h of day 3, an abrupt capacity loss (from around 1900 veh/h/lane to 1000 veh/h/lane).

Figure 40 displays (over 24 h of day3) the corresponding time-derivative of capacity estimates that confirms the unusually abrupt capacity drop around 14:00 h of day 3 which is indeed stronger than any other drop during that day. The capacity estimate is seen in Figure 39 to start recovering after 15:00 h.

The incident occurred within the tunnel, between detectors _104 and _15 (Figure 38) as can be easily determined from the measured speed trajectories. However, detector _104 was not used in this run because it was faulty on the first 1.5 days (Section 4.5), hence the incident was detected further upstream, based on the measurements of detector _77. It might be interesting to repeat the run by use of only day-3 data (at that time detector _104 was functional again) and check which capacity estimates (at which link clusters) would be affected if all detectors (_77, _104, _15) are available.

The incident occurred reportedly at 2:01 pm. Figure 41 reveals that the corresponding shock wave reached the upstream detector _77 at around 2:08, after covering a distance of some 1.5 km between the incident location and the detector. Surprisingly, Figure 42 indicates that the capacity derivative:

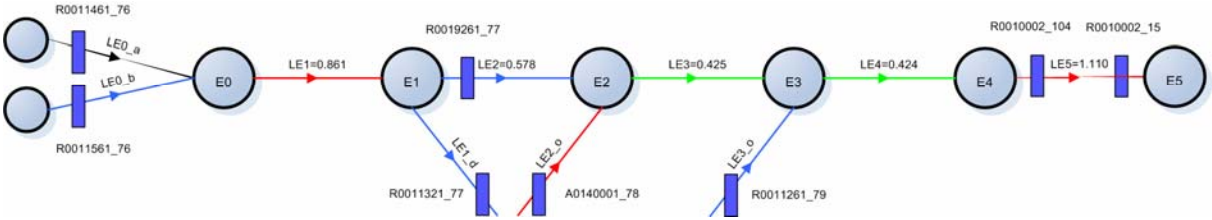


Figure 38: Network part for Incident 2.

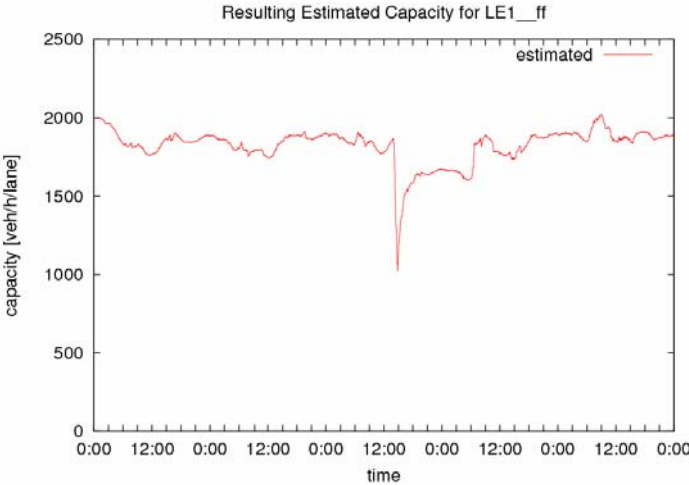


Figure 39: Capacity estimates for Incident 2 (around 14:00 h of day 3).

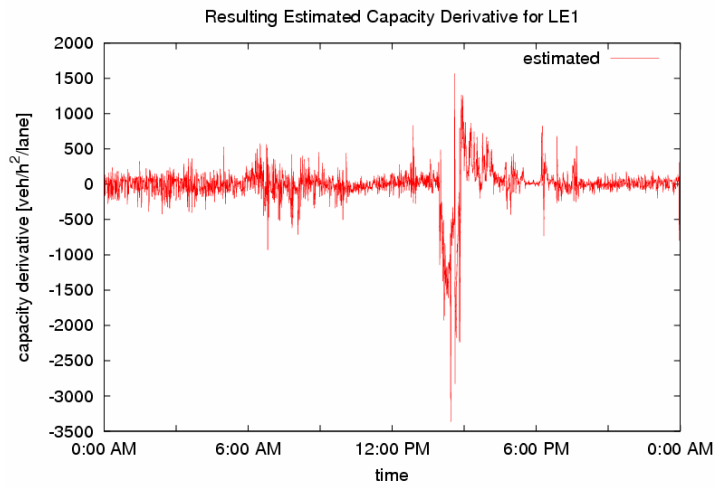


Figure 40: Time derivative of capacity estimates for Incident 2.

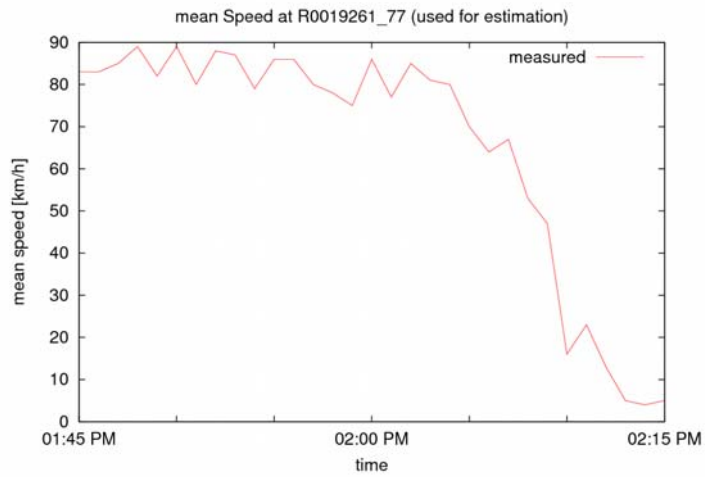


Figure 41: Speed measurements at the upstream detector _77.

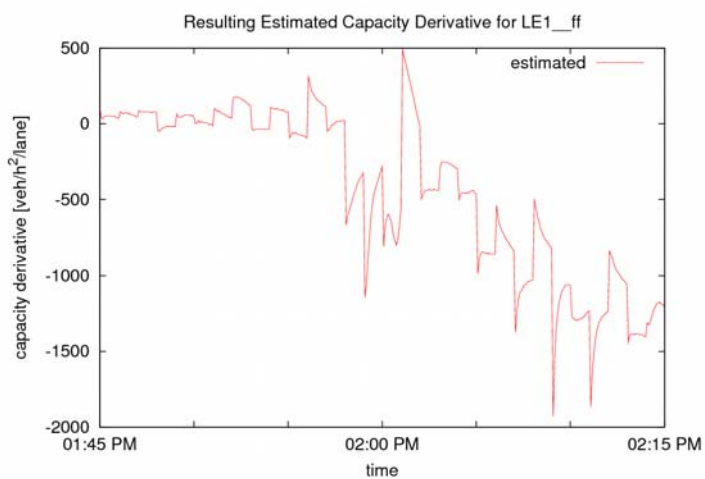


Figure 42: Zooming-in of Figure 40.

- reaches values lower than -1000 persistently, several minutes earlier than the shock wave arrival; this may indicate that an incident detection might be possible in some cases even before arrival of the shock wave at the upstream detector.
- exhibits some abnormal "turbulence", even featuring momentary values below -1000, already at 1:58 p.m., i.e. before the reported incident occurrence; this may be an indication that the reported incident occurrence time may be inaccurate; or that some other abnormal circumstance preceded the reported incident.

Incident 3

This incident was reported by the Antwerp road authority to have occurred on 17 January 2008 at 7:17 p.m. on the inner ring, between the off- and on-ramp for E19, just upstream of detector _89 (km 10.5) and about 1 km downstream of detector _16. Figure 43 displays the flow and speed trajectories at both detector locations (diagrams start at 10:00 a.m. due to detector failure before this time). A serious flow drop is indeed visible at both locations after 7:00 p.m.. At the same time, a serious speed drop is seen in the upstream detector _16 while the speeds at the downstream detector _89 are close to normal. This situation confirms that the incident occurred between detectors _89 and _16. Note also that, at the time just before the incident occurrence, the flow at the upstream detector is around 8000 veh/h, while, due to two important intermediate off-ramps, the monitored flow at the downstream detector at the same time is only around 3000 veh/h.

Figure 44 displays the produced capacity estimates for LW7-8 which includes a minor but abrupt capacity drop after 7:00 p.m.. Figure 45 indeed reveals a distinguished (although smaller in magnitude compared to previous incidents) negative peak of the time-derivative of the capacity estimates after 7:00 p.m.. The negative peak reaches a value of -900 which is smaller, but not much smaller than other negative peaks (most of which are probably not related to incidents) that are visible in the figure on the same day; this could of course be a difficulty for the specification of a proper incident-detection threshold at this location. The specific situation created by both intermediate off-ramps and the big difference in mainstream pre-incident flows upstream and downstream of the incident might be the reason for less pronounced detection results (including the minor capacity drop) in this case.

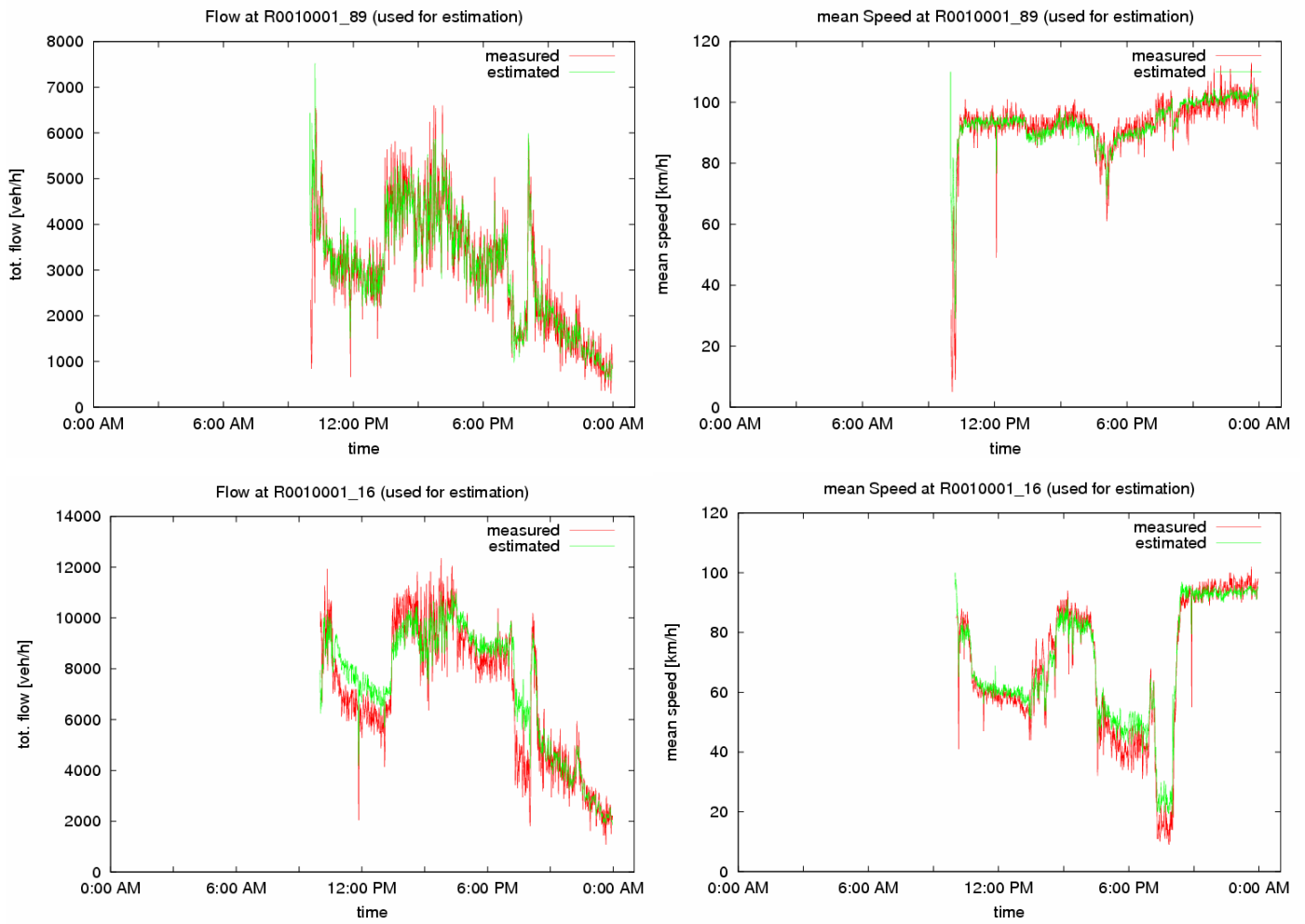


Figure 43: Flow and speed measurements for Incident 3.

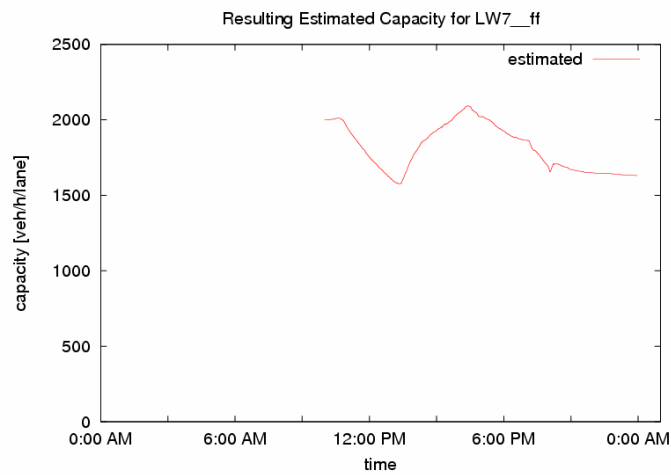


Figure 44: Capacity estimates for Incident 3.

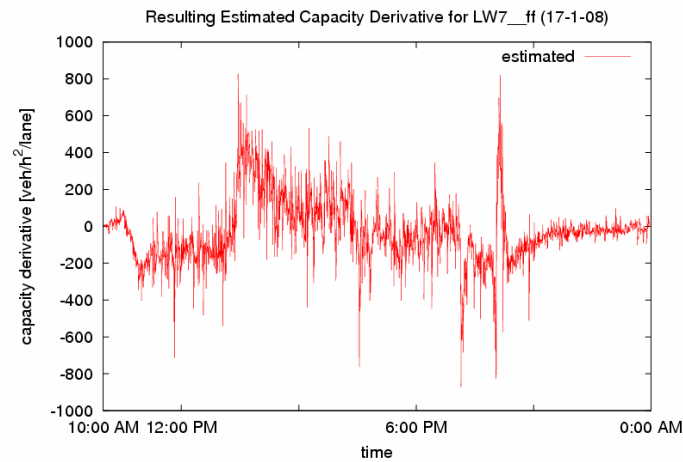


Figure 45: Time derivative of capacity estimates for Incident 3.

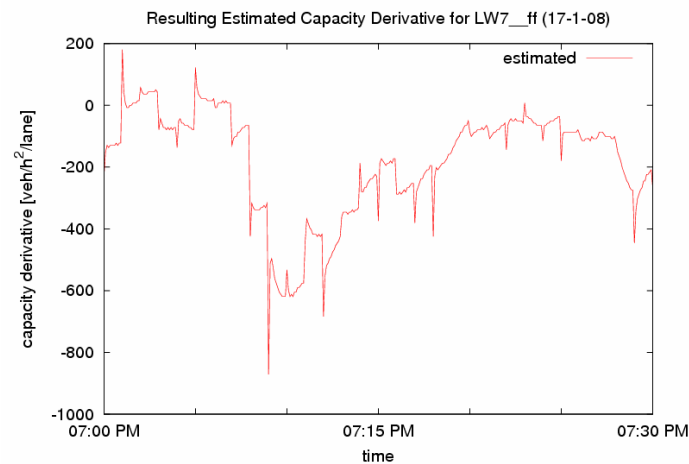


Figure 46: Zooming-in of Figure 45.

Figure 46 is a zoom-in of Figure 45, showing clearly the strong-negative values of the capacity time-derivative that, in fact, occurs earlier than the reported incident time of 7:17 p.m.; this may indicate a small inaccuracy in the recorded incident time or in the time-synchronisation with the detector data. Note that the strong-negative values of the time derivative due to the incident are quite persistent (over some 15 min); in contrast to other negative peaks of the capacity time-derivative on the same day (Figure 45) that are rather quasi-instantaneous. Thus, by smoothing the time-derivative signal, one could distinguish much more clearly between incident and non-incident situations, i.e. reduce the false alarm rate to virtually zero at this location as well.

Incident 4

This incident was also reported by the Antwerp road authorities to have occurred on 6 February 2008 at around 7:00 a.m. on the inner ring, reportedly between detectors _89 and

_85. Figure 47 displays the flow and speed trajectories at both detector locations. A serious speed and flow drop is indeed visible at both locations around 7:00 a.m., while speeds at the next downstream detector _83 are close to normal (not shown here). For the same reasons as in Incident 3, this incident probably occurred upstream but very close to the downstream detector _85.

Figure 48 displays the capacity estimates for LW11 while Figure 49 displays the corresponding time-derivative. Capacity estimates are seen to drop from 1900 veh/h/lane to 1500 veh/h/lane while their time-derivative exhibits a clear negative peak at around 7:00 am, much bigger in magnitude than at any other time of the day.

The incident occurred reportedly at 6:55 a.m. and Figure 50 shows that the corresponding shock wave reached the upstream detector _89 few minutes later. The capacity derivative is seen to drop at 6:54 and reach detection-relevant values after 6:55 (Figure 51). This indicates that the reported incident time may be slightly inaccurate (or not fully synchronized with the data time stamp). In any case, the incident detection performance is excellent.

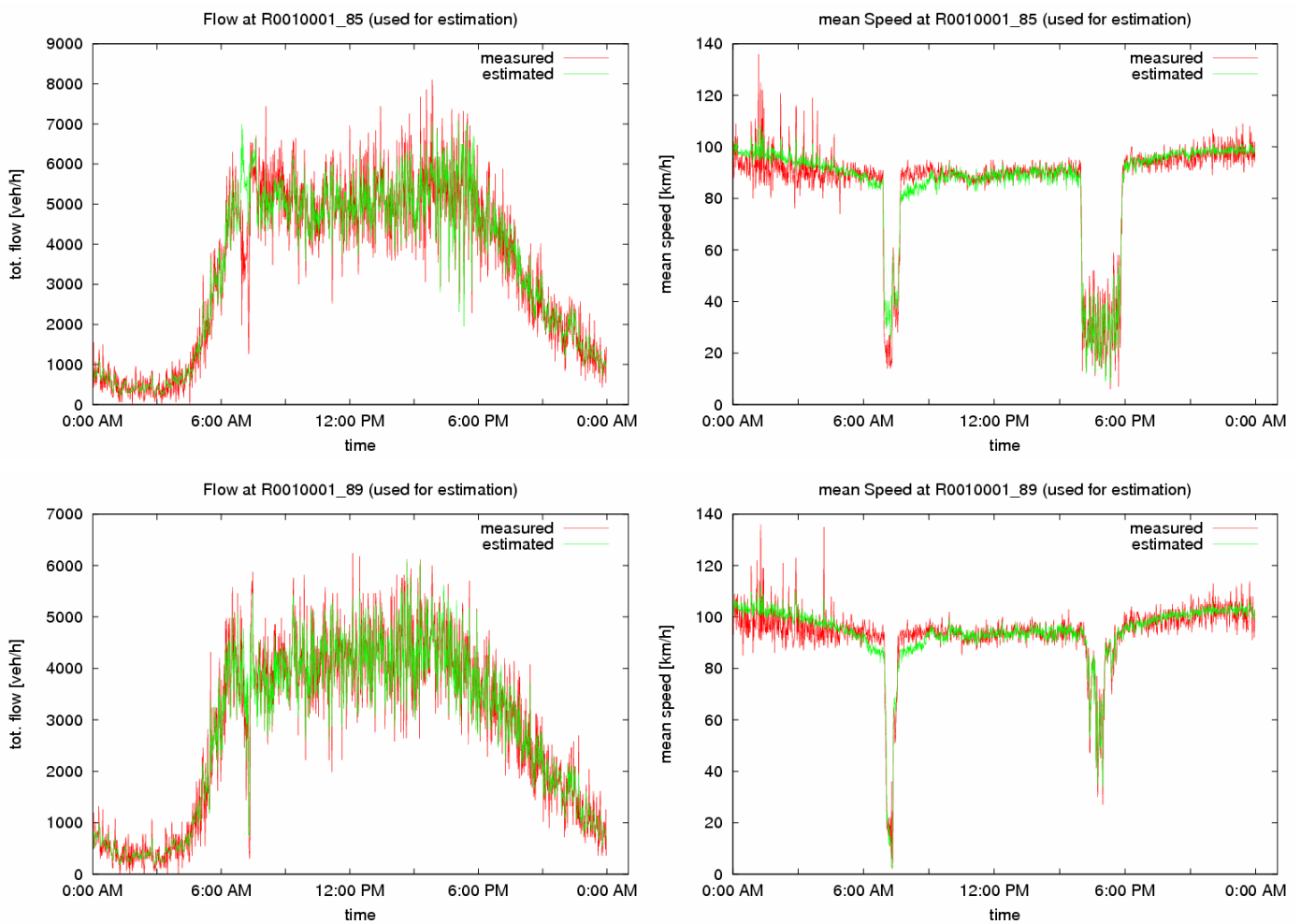


Figure 47: Flow and speed measurements for Incident 4.

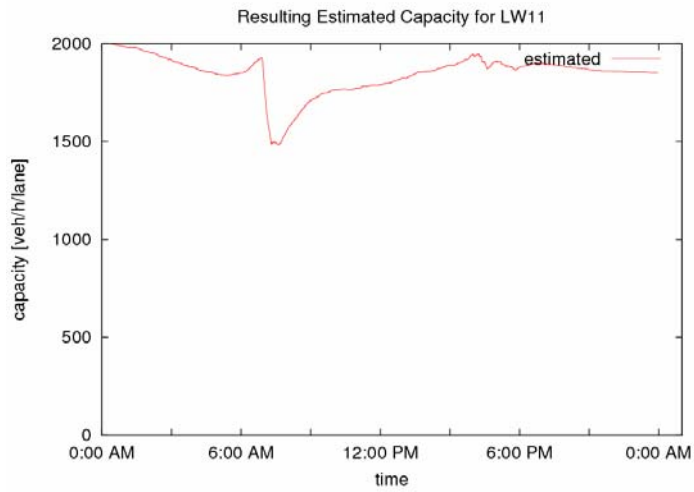


Figure 48: Capacity estimates for Incident 4.

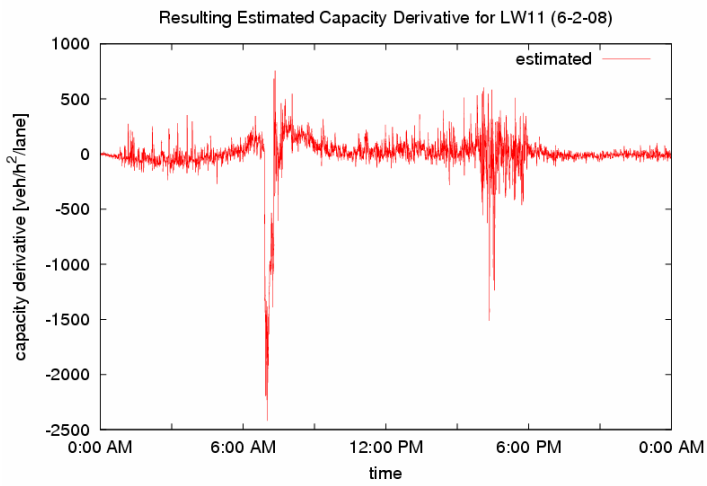


Figure 49: Time derivative of capacity estimates for Incident 4.

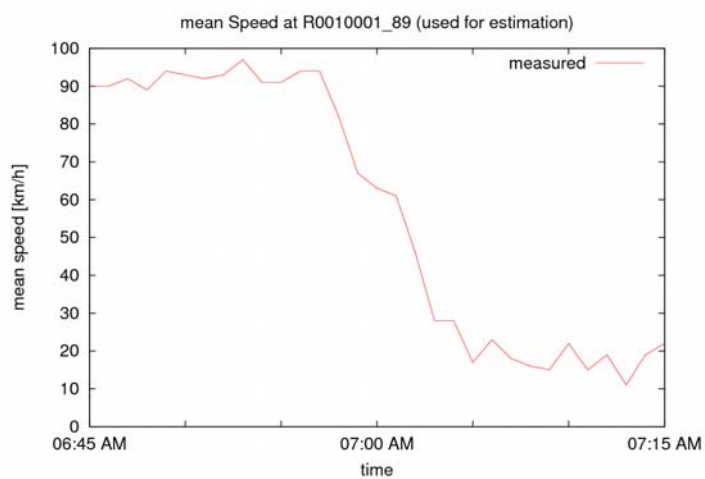


Figure 50: Zooming-in of Figure 47.

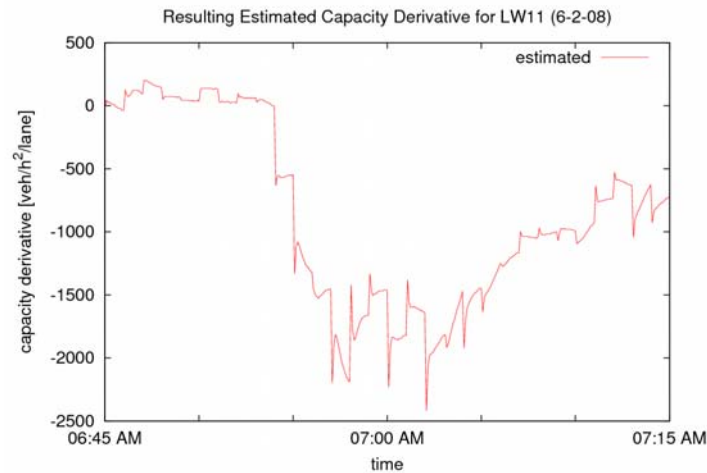


Figure 51: Zooming-in of Figure 49.

Incident 5

This slight and short-duration incident was accidentally discovered in the data of 6 February 2008 (received to investigate incident 4). Figure 52 displays the mean speed at detector _15 (inner ring), i.e. within the tunnel, where a short-lived speed drop at around 9:30 a.m. is clearly visible. The speed at the upstream detector _83 also decreases at the same time (not shown here), but to a lesser degree, which means that the slight created congestion barely reaches that location. On the other hand, the speed at the downstream detector _104 decreases very slightly at the same time (not shown here), apparently due to accelerating vehicles exiting the incident area. Thus, the incident location seems to be between detectors _15 and _104.

Figure 53 Indicates a minor but abrupt capacity drop at LW14 around 9:30 a.m. while the related time-derivative in Figure 54 exhibits a strong negative peak at the same time, much stronger than any other time-derivative value on the same day.

This short-lived incident was not registered by the responsible road authority. Figure 55 indicates that the shock wave reached the upstream detector _15 at 9:24 a.m. while Figure 56 indicates a quasi-instantaneous detection.

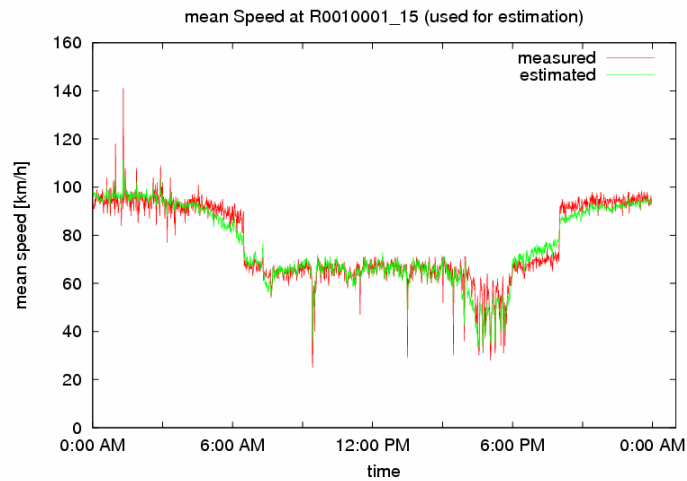


Figure 52: Speed measurement for Incident 5.

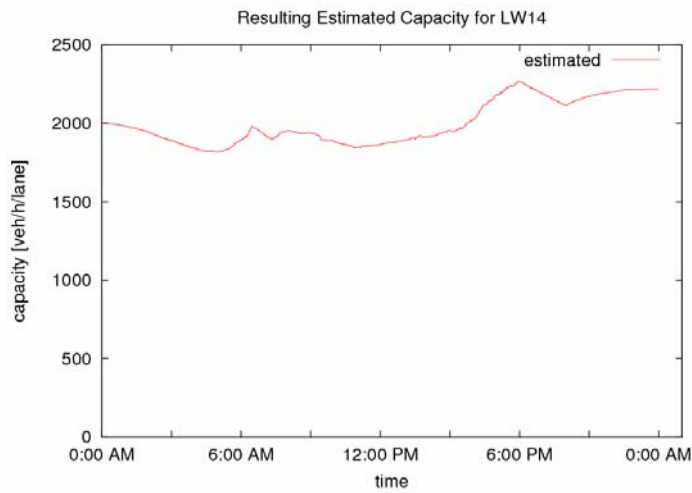


Figure 53: Capacity estimates for Incident 5.

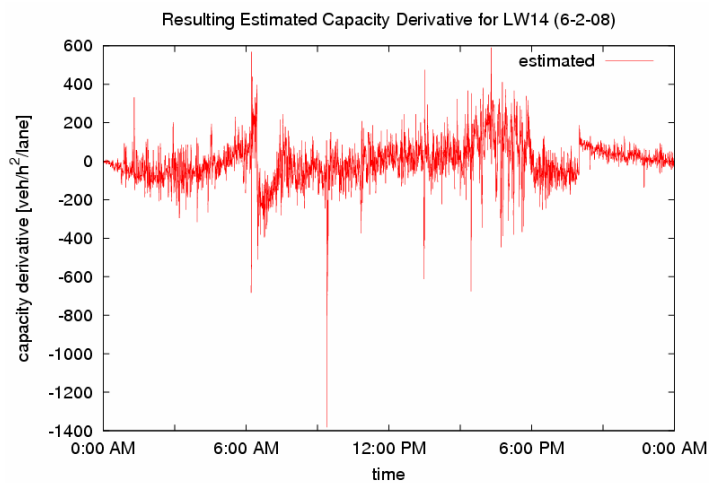


Figure 54: Time derivative of capacity estimates for Incident 5.

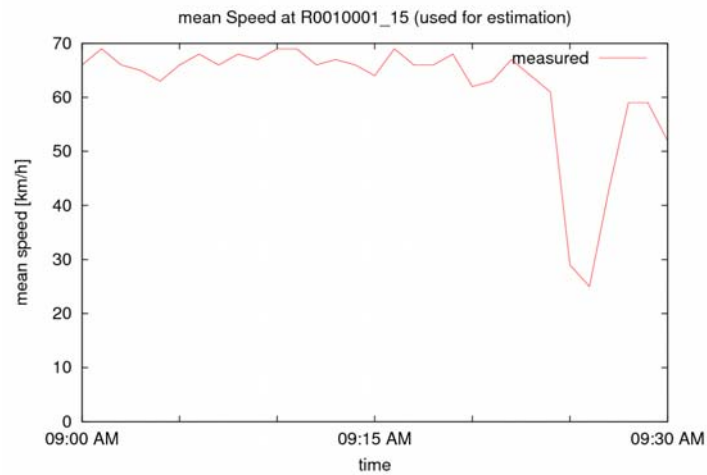


Figure 55: Zooming in of Figure 52.

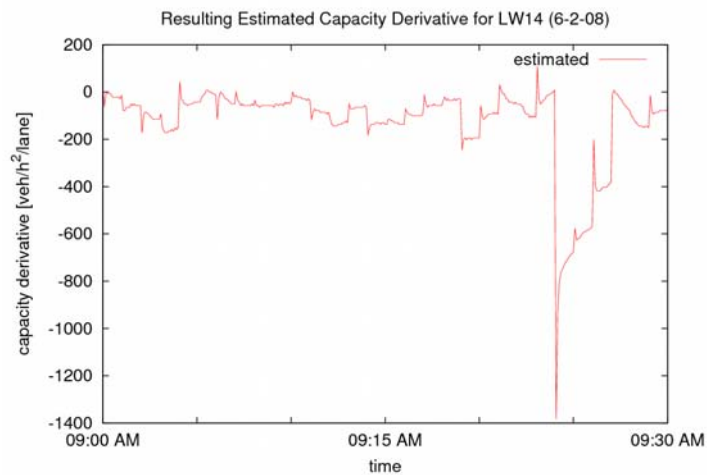


Figure 56: Zooming-in of Figure 54.

In conclusion, RENAISSANCE was found to produce excellent results regarding the detection of incidents. In fact, several unknown incidents could be identified in available data and two known incidents were seen to produce sufficiently strong (or more durable) negative peaks of the time-derivative of capacity estimates to be detected. Most importantly, the detected incidents produce time-derivative peaks that are much stronger (or durable) than the time-derivative values encountered in absence of incidents, which indicates an accordingly low (virtually zero) false alarm rate. Note that high false-alarm rates is the main obstacle towards operational use of virtually all known incident detection algorithms to date. Note also that the RENAISSANCE mechanism for detection of incidents does not call for detector installation every 500 m as most known incident detection algorithms; nor does it call for the absence of on-ramps and off-ramps between the adjacent (upstream and downstream) detectors of the incident location. The detected incidents in this report were mostly included

between two mainstream detectors at a distance of some 2 km, with on-ramps and off-ramps between them. On the other hand, the exact location of the detected incidents may not be based on a 500 m-resolution as with usual incident detection algorithms. Given these circumstances, the time-to-detect is deemed very satisfactory and, in several cases, actually quasi-instantaneous.

It is also interesting to note that an exponential smoothing of the time-derivative signal could increase the distance between incident and non-incident cases, at least for incidents of a certain duration. This is because the negative time-derivative values in cases of incidents persist over a period of time while other occasional negative peaks are very short-lived and would be reduced by the smoothing.

4.7. Less-Loops Scenario

RENAISSANCE reproduces (estimates) the full traffic state of the motorway based on a limited amount of available measurements. A natural question arising concerns the necessary amount of available measurements. The issue bears clear similarities with the discussion of faulty data in Section 4.5. The available measurements should, as a minimum, guarantee flow observability. However, two additional questions arise:

- (1) There may be different combinations of detector locations, all satisfying flow observability. Which out of those combinations is most preferable?
- (2) How much additional estimation quality is gained if more detectors are added (beyond flow observability)?

Based on previous experiences, but also experiences from the present project (see e.g. Section 4.3), detector availability is most valuable at (or closely upstream of) locations where congestion appears first. In cases of over-spilling off-ramps, a mainstream detector closely upstream of the off-ramp is also valuable. For the rest, mainstream detectors are usually more useful than the on-ramp or off-ramp detectors because they may help RENAISSANCE to more accurately follow and estimate moving congestion tails. Moreover, the real-time estimation of FD parameter values is not possible without mainstream measurements; in other words, less available mainstream measurements would lead to longer motorway stretches (link clusters) with common FD parameter estimates. This answers question (1) above.

Regarding question (2), the answer is less obvious because a quantitative assessment may strongly depend on the particular network and traffic characteristics. Section 4.5 reported on a couple of cases where the loss of specific detector measurements was found to only have a minor impact on estimation quality. To gain some further empirical insights related to this

issue, the amount of utilized detector measurements in the Antwerp network was strongly reduced (almost to a minimum level for flow observability) according to Figure 57 (where red-colored detectors were dropped). Note that most dropped detectors are from on-ramps and off-ramps. Note also that the removal of some mainstream detectors necessitates a modification (enlargement) of link clusters (marked in Figure 57) so as to have at least one mainstream measurement per cluster.

RENAISSANCE was run by use of the reduced amount of measurement data for 23 November 2007. Each of the diagrams below displays traffic variables as follows:

- Measurement data (in red) which may or may not have been used in the estimation procedure, as the case may be (noted on the top of the respective diagram).
- Estimation data (in green) with full detector utilization (as in Section 4.2).
- Estimation data (in blue) with less detector utilization (less-loops scenario).

Figure 58 displays the results at two mainstream dropped-detector locations (_104 and _85) of the inner ring. Note that the drop of detector _104 (_85) increases the local available inter-detector distance to some 2.7 km (2.5 km) with many intermediate on-ramps and off-ramps. Flow estimates are seen in Figure 58 to be similarly good with less loops as for the full-detector case, while the speed estimates are slightly worse at _85 when the mainstream loop is dropped. Note also the slower convergence towards the real speed values at the early morning period. The estimation of the congestion period at _104 is quite good, albeit with some delay during congestion recovery.

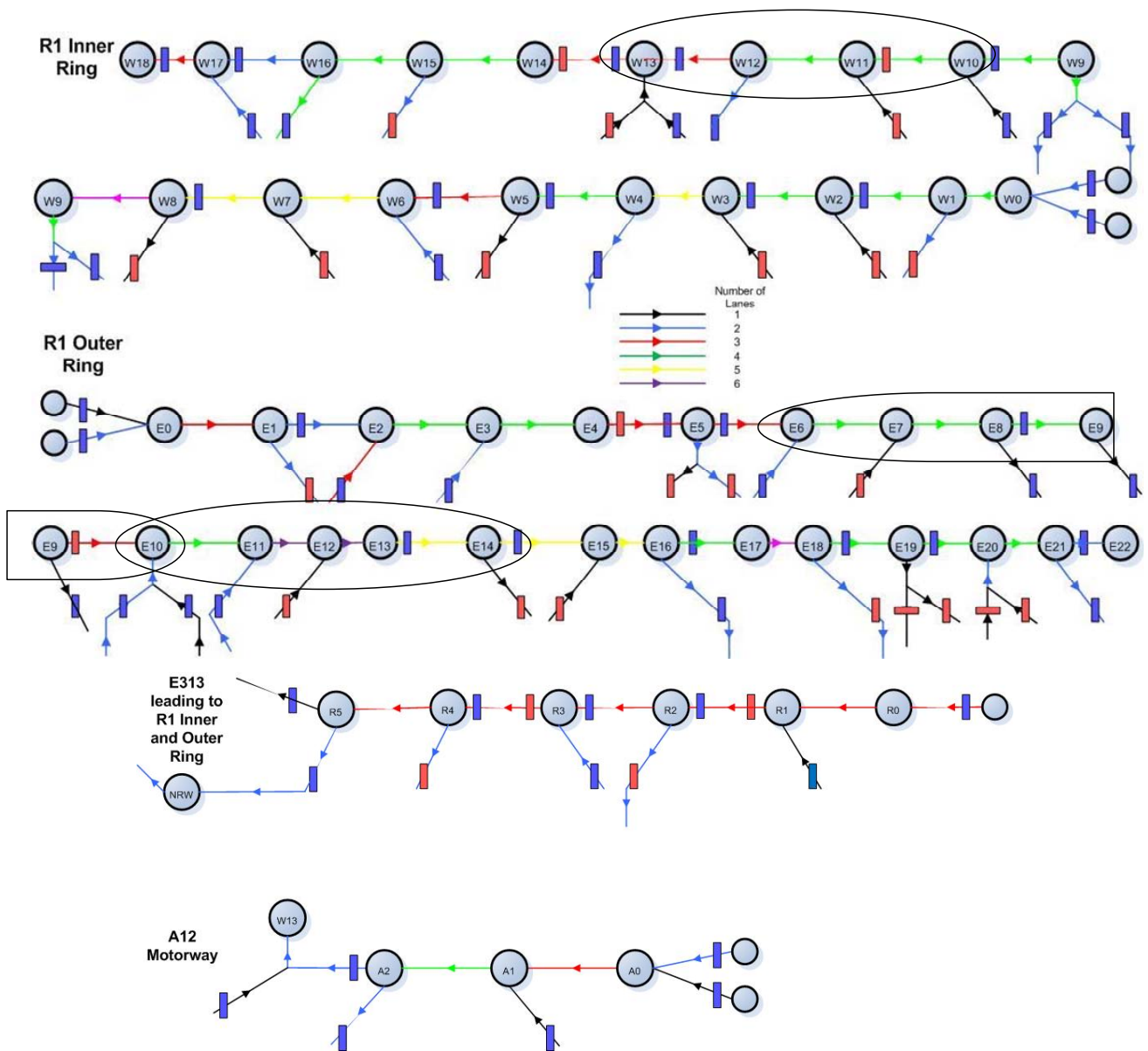


Figure 57: Dropped detectors (red-coloured) and modified link clusters for the less-loops scenario.

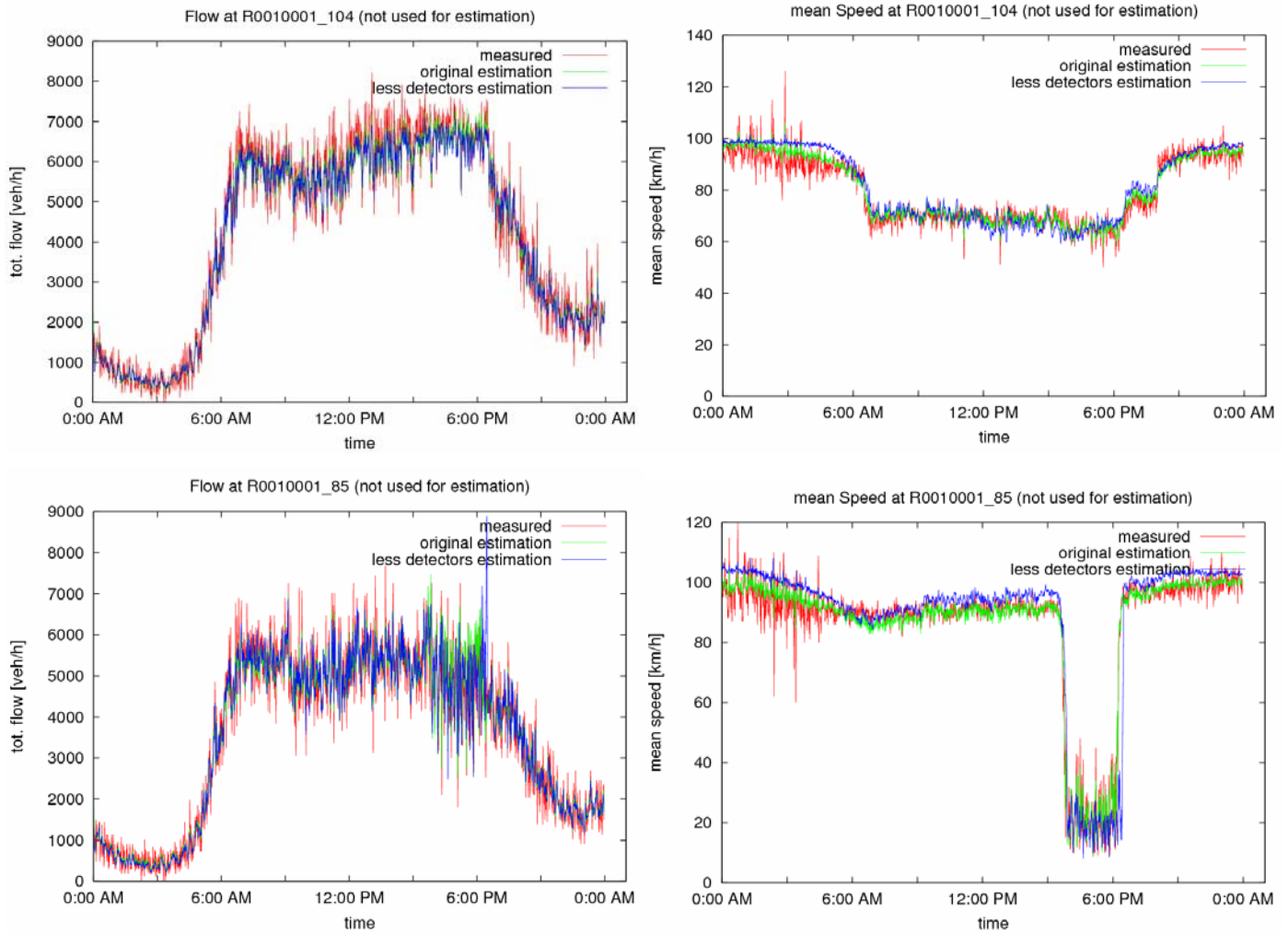


Figure 58: Inner ring less-loop scenario results.

Figure 59 displays the results at two mainstream dropped detector locations (_90 and _104) for the outer ring. Note that the drop of detector _90 (_104) increases the local available inter-detector distance to some 2.3 km (2.5 km) with many intermediate on-ramps and off-ramps. Flow estimates are again quite good. Speed estimates are very good during the afternoon peak period but include some estimation bias particularly during the off-peak period (possibly due to slower convergence of the FD parameter estimates).

Figure 60 displays the results at two mainstream dropped detector locations (_62 and _59) for E313. Note that the drop of detector _62 (_59) increases the local available inter-detector distance to some 2.5 km (3.2 km) with many intermediate on-ramps and off-ramps. Flow estimates are reasonably good. Speed estimates are good at _62, but, at _59 the low-speed morning period is only partly reproduced, probably due to the quite complex oscillatory phenomena on this motorway.

Figure 61 reflects the impact of an off-ramp measurement drop. The upper line of Figure 61 displays the flow and speed at the (dropped-measurement) off-ramp while the medium and lower lines display the flows and speeds at the next downstream and upstream, respectively, mainstream detector locations (which are not dropped). All flow diagrams indicate that the drop of the off-ramp measurement did not have any visible impact on the flow estimation quality, and in fact the same holds true for both mainstream speed estimates. In contrast, the speed estimate at the off-ramp itself (upper-right diagram) is strongly biased because, in lack of a local speed measurement and local FD, the estimates tend (via the model's speed convection term) towards the mainstream speed, as one would expect. Clearly, this bias is of minor importance if the off-ramp does not bear a particular interest for operators.

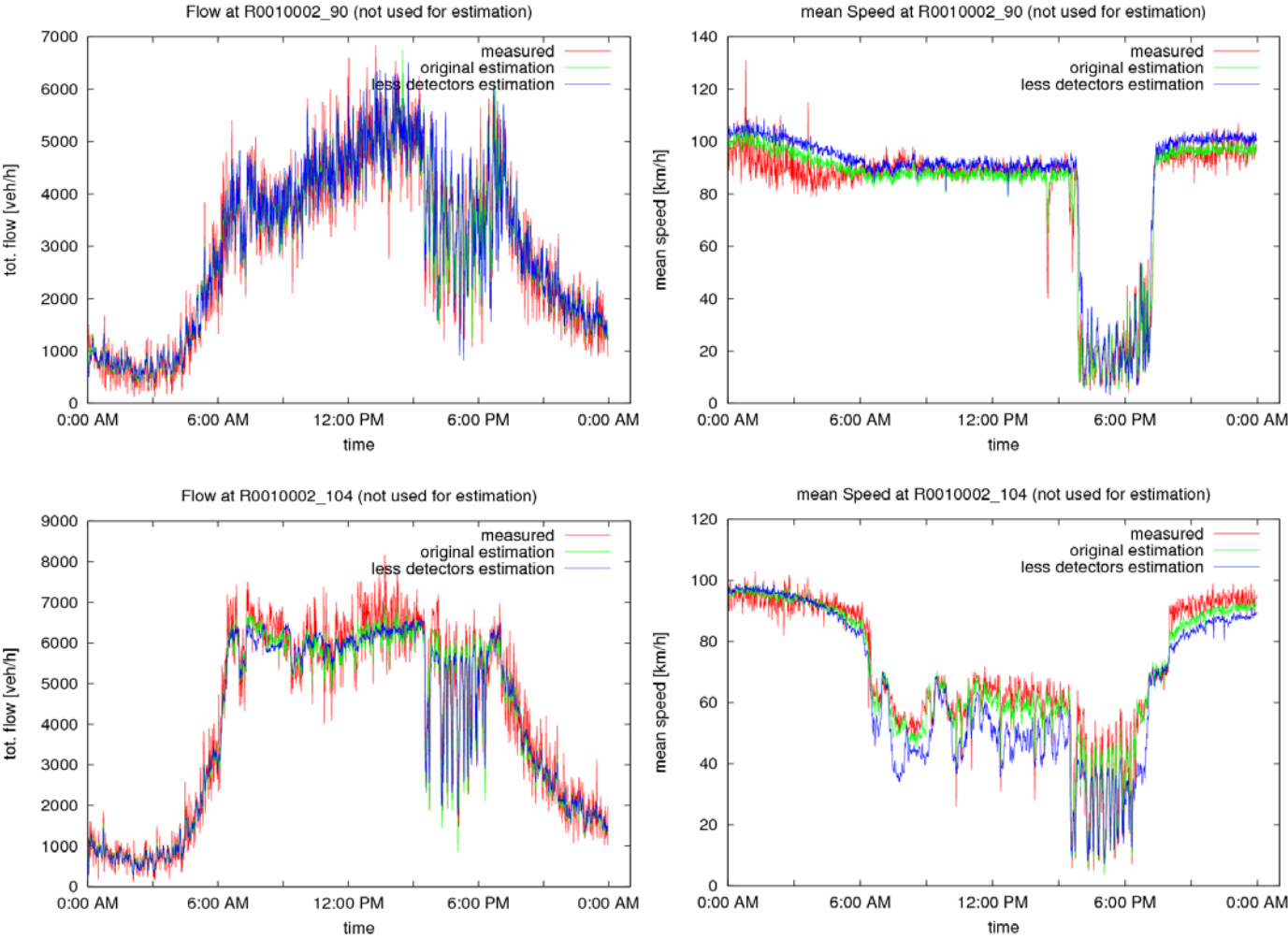


Figure 59: Outer ring less-loop scenario results.

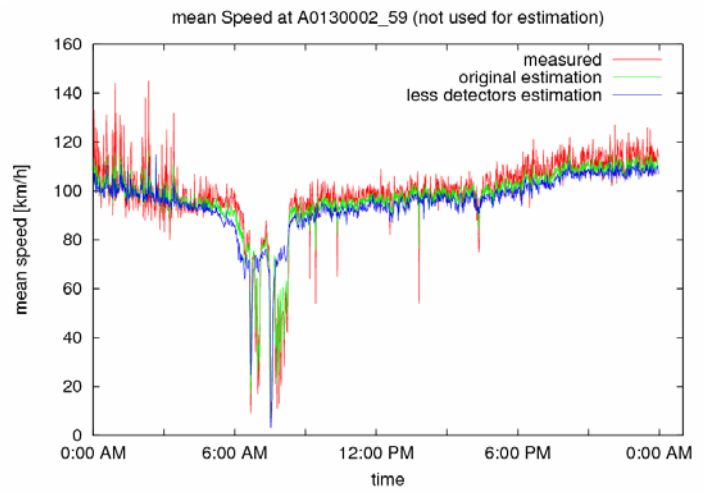
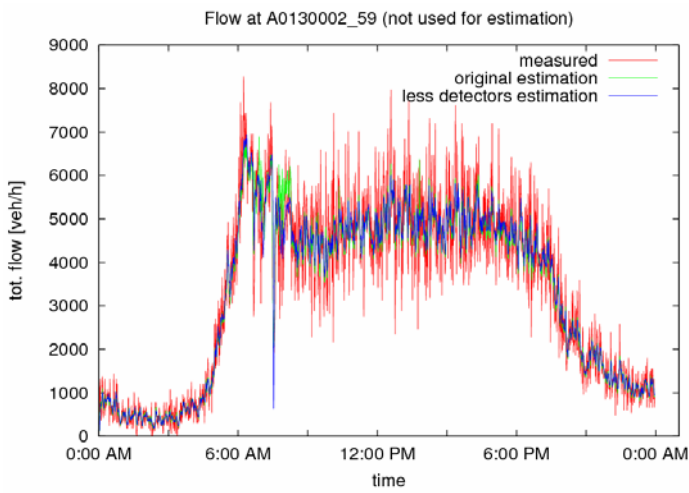
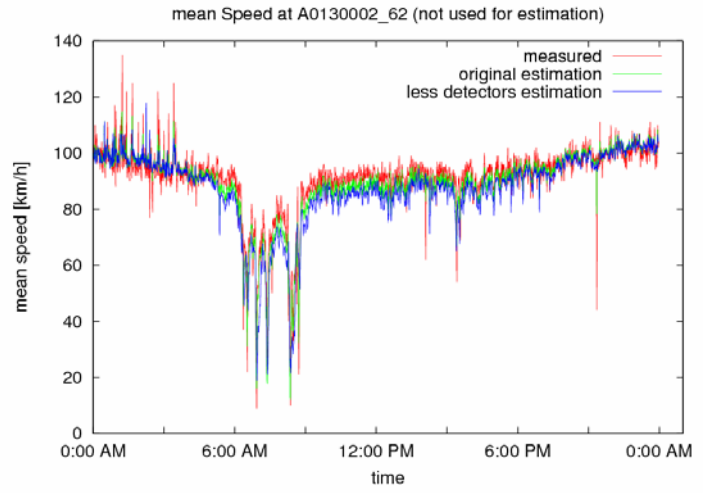
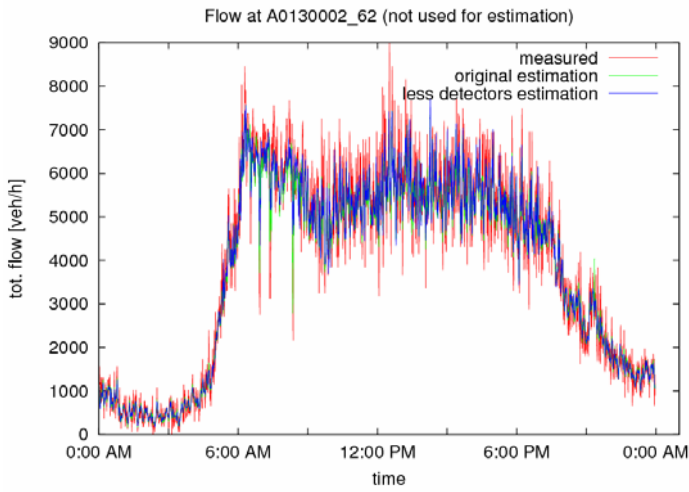


Figure 60: E313 less-loop scenario results.

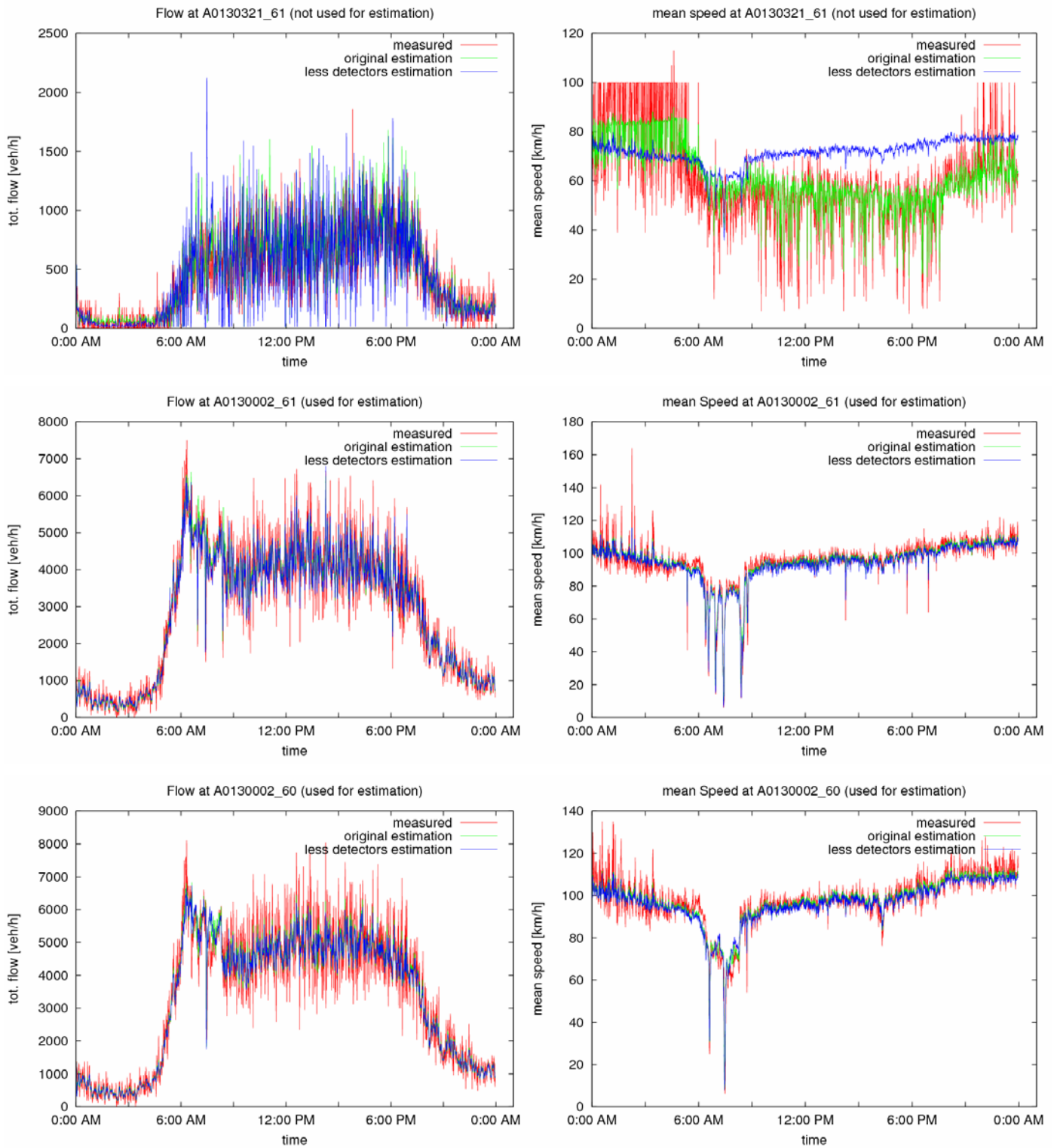


Figure 61: Impact of dropped off-ramp measurements.

5. Prediction Results

As indicated in Figure 3, the traffic state estimation results (Section 4) provide a basis (an initial condition) for predicting the evolution of the traffic state (densities, mean speeds and flows) and of route travel times and queues over a future short-term horizon (e.g. 30 min) via a corresponding run of the RENAISSANCE traffic flow model. To this end, the fundamental diagram parameters may be maintained at their latest estimated values; in addition, all required boundary variables, that are external variables for the traffic flow model, must also be predicted (Figure 3), and this is achieved via extrapolation (of the respective measured or estimated values) or via historical data (where available) or both, as described in Section 2.

5.1. Prediction Parameters

A number of parameters and settings must be selected according to the specifications of RENAISSANCE to enable the production of prediction results. To start with, the short-term prediction time horizon was set equal to 30 min. Regarding the extrapolation procedure for boundary variables, the necessary past-time window was set (after some rough fine-tuning) equal to 30 min as well, as this value was found to be a good compromise between

- smoothing of low-significance high-frequency “noise”
- relatively fast identification of significant trend changes (e.g. at the start of the peak period etc.)

in the past time-histories of boundary variables. For similar reasons, the trend compliance ε was set equal to 0.5, except for turning rates at bifurcations where $\varepsilon = 0$ was used; note that this latter value indicates the consideration of constant turning rates over the prediction horizon which is a reasonable assumption for these, quite stable in average, boundary variables.

When using historical data in combination with extrapolation for the boundary variable prediction, a “fade over time period” of 30 min (i.e., equal to the prediction horizon) is used.

The minimum and the maximum values for boundary variable prediction are used so as to exclude unrealistic predictions due to exaggerated trends. The utilized maximum value of each boundary variable is generally set equal to the maximum observed value of that variable, increased by 10-15%; while the utilized minimum values are typically equal to zero.

Predicted travel times along pre-specified routes are calculated on the basis of predicted (network-internal) segment mean speeds. To avoid potential strong overestimations of travel times due to very low predicted speeds (which might occur due to the strong non-linearity of

the speed-travel time relationship for low speeds), a relatively generous minimum admissible predicted speed value of 12 km/h is introduced when calculating predicted travel times.

Finally, some minor changes of ν and τ parameters of the traffic flow model were introduced for slightly better prediction results.

5.2. Boundary Variable Prediction

As mentioned earlier, boundary variables are external inputs for the network traffic flow model that must be entered to the model to enable the short-term prediction of the network traffic state. This implies that the boundary variables must also be predicted based on extrapolation or on historical data or a combination of both. In the following, some representative examples of boundary variable predictions are provided, using each prediction possibility for comparison, for the 24 h data of the 23 November 2007.

Figure 62 provides some typical inflow predictions with extrapolation only (left column) and with historical data combined with extrapolation (right column). The upper line in Figure 62 refers to a mainstream inflow with relatively high flows while the lower line in Figure 62 refers to an on-ramp inflow with lower values. Notice that:

- All predictions are fairly reasonable.
- Predictions based on extrapolation only are, by construction, straight lines; while combined predictions are generally nonlinear curves starting at the current estimate and ending at the respective historical value.
- Predictions involving historical data are generally better; for example, they are mostly contained within the (oscillation) “noise” of future values. Clearly, this indicates (and requires) very similar inflow values for every (working) day.
- Predictions based on extrapolation only, tend often outwards of the “noise band” of future values.

Figure 63 provides some typical turning rate predictions with extrapolation only (no historical data are required for turning rates). Note that:

- Turning rates are quite stable in average during the whole day.
- All prediction lines are horizontal because the trend compliance ε was set equal to zero in Section 5.1, due to the relatively stable behaviour of this type of boundary variables.

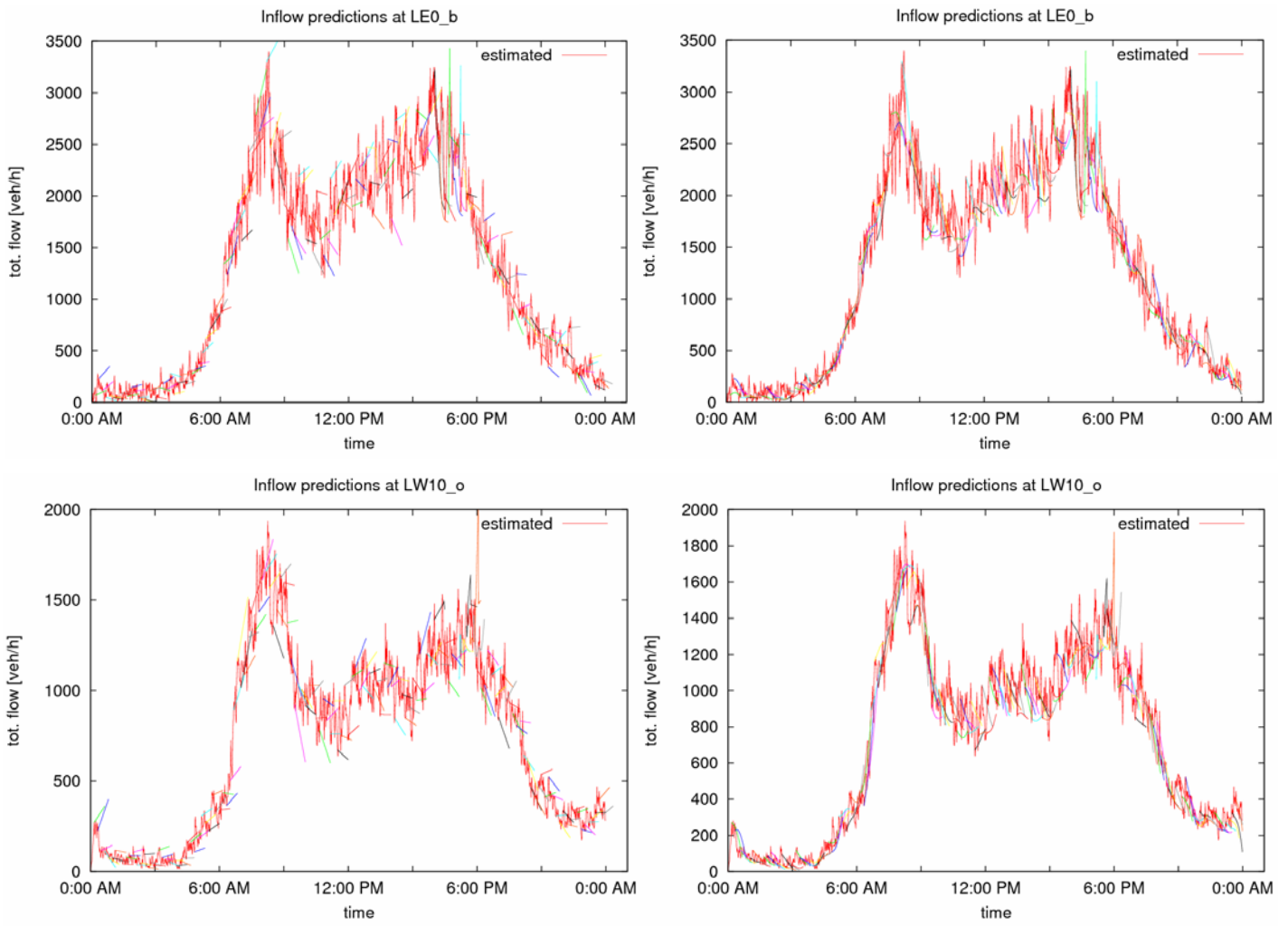


Figure 62: Inflow predictions with extrapolation only (left column) and with historical data combined with extrapolation (right column).

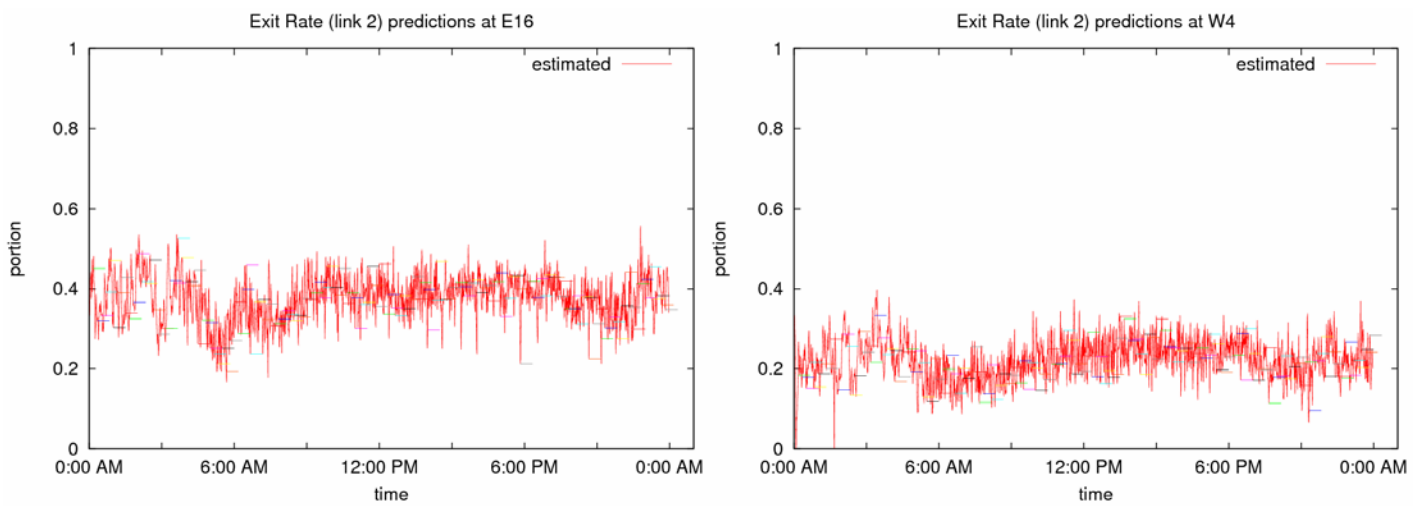


Figure 63: Turning rate predictions.

Figure 64 provides some typical destination density predictions at 2 off-ramps that are known to carry congestion that spills back onto the motorway mainstream. The left diagram for off-ramp LE16_d is based on extrapolation only while the right diagram is based on combined historical data and extrapolation. Specifically for the boundary density of off-ramp LW4_d, no historical data were available, hence only one single diagram (based on extrapolation) is included in Figure 64. Notice that:

- Predictions using historical data at LE16_d tend to higher values during 6:00 am-3:00 p.m.. This is because the historical data are consistently higher than the estimated boundary density on the specific day. Note, however, that the impact of this peculiar prediction on the traffic flow model calculations is minor as long as both the historical and the estimated density values are undercritical (i.e. below 35-40 veh/km).
- During congestion spillback (visible via the overcritical density values), the prediction at both off-ramps are reasonably good.

In conclusion, the quality of boundary variable prediction is quite good, although some methodological improvements could be envisaged to improve it further.

5.3. Prediction Results with Use of Historical Data

Smoothed historical data for most boundary variables, produced via averaging and smoothing of measured data for several days, were prepared in KU Leuven. The historical data were used in combination with extrapolation at all inflow locations as well as at the off-ramps that are known to carry congestion spillback onto the motorway mainstream.

Figures 65-67 display the prediction results for the mean speeds (flow prediction are usually very good) at all network-internal measurement locations for the 24-h data of 23 November 2007, using the multiple fundamental diagrams as in Section 4.2. Each diagram of Figures 65-67 includes the measurements and the estimates (as in Section 4); in addition, prediction curves (over 30 min in future) are displayed every 10 min in order to facilitate reasonable visibility.

Figure 65 displays the inner-ring results (from downstream to upstream), that may be commented as follows:

- Predictions are fairly good at those locations that are not explicitly mentioned in the following comments.

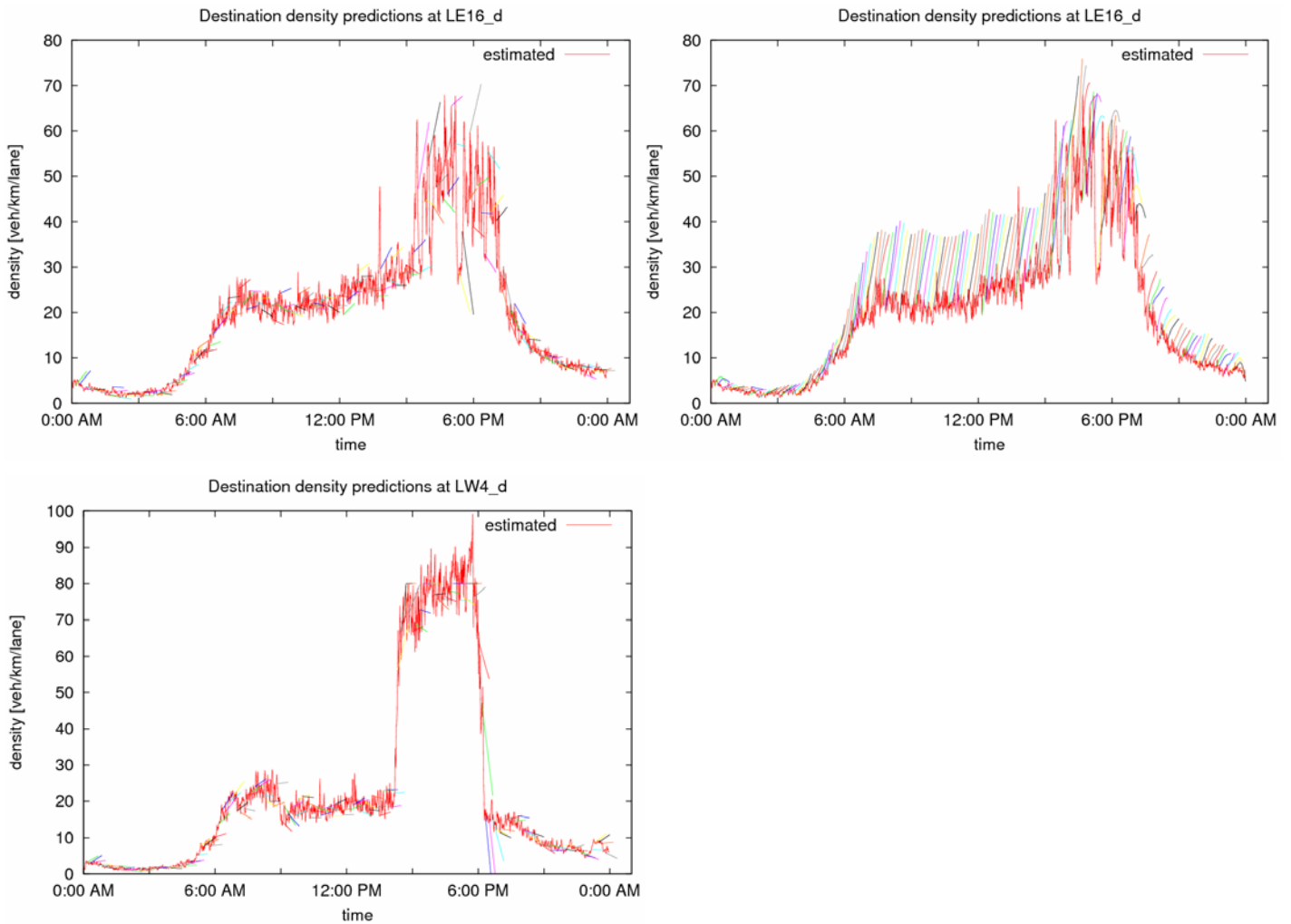
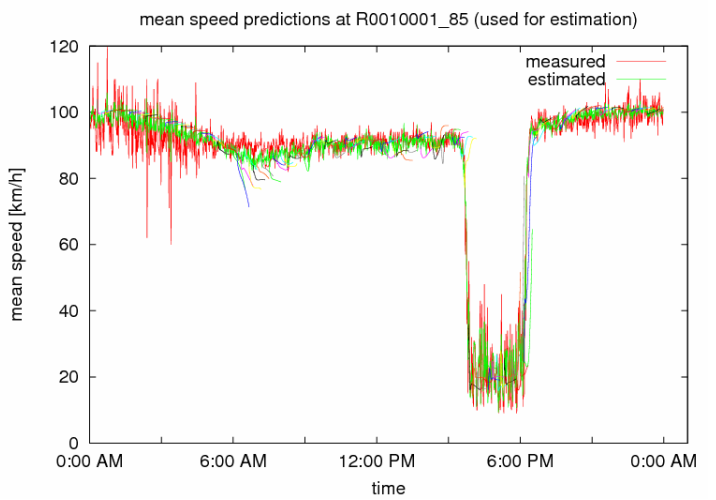
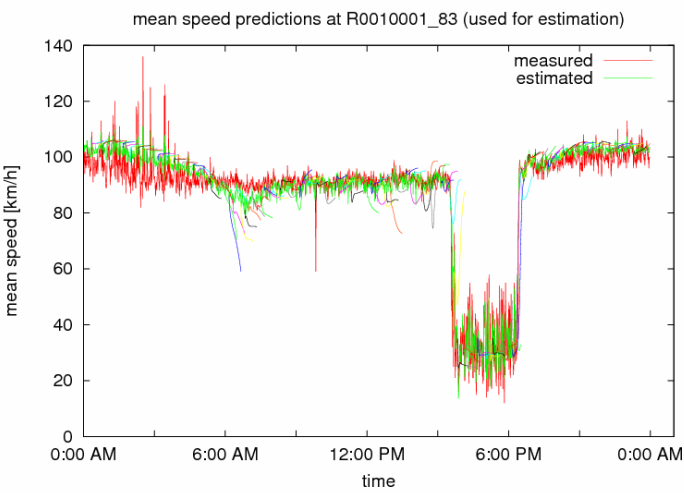
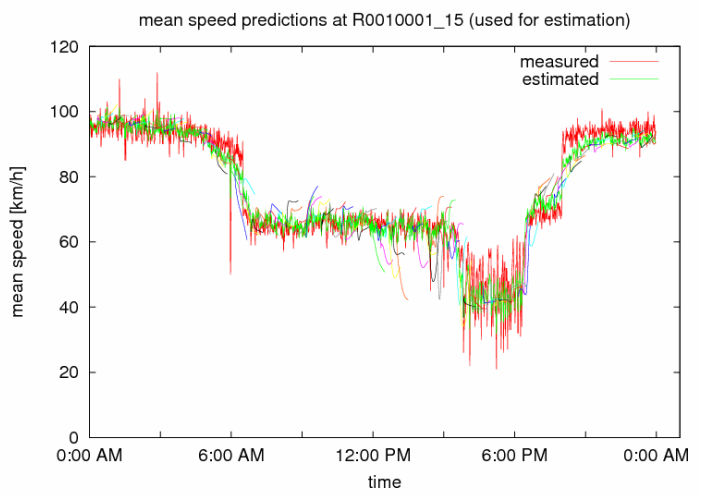
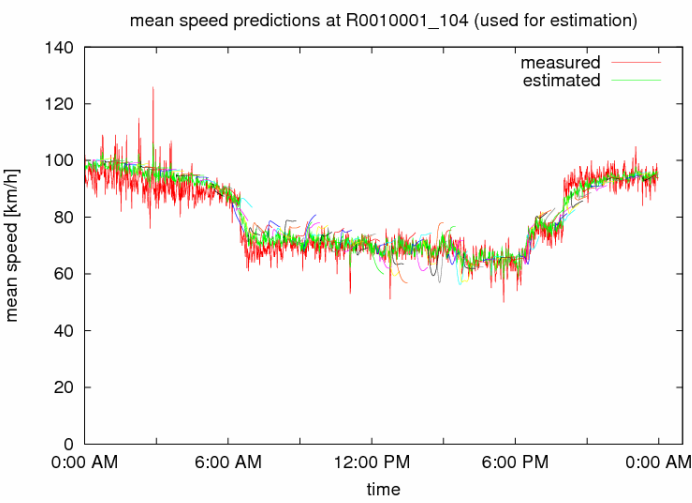
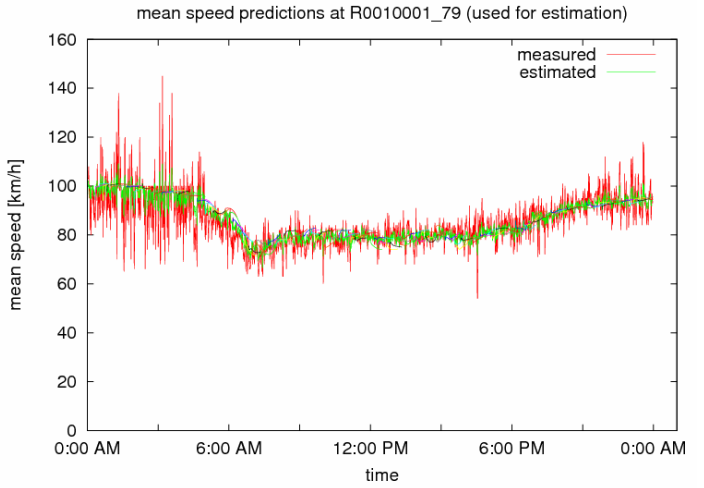
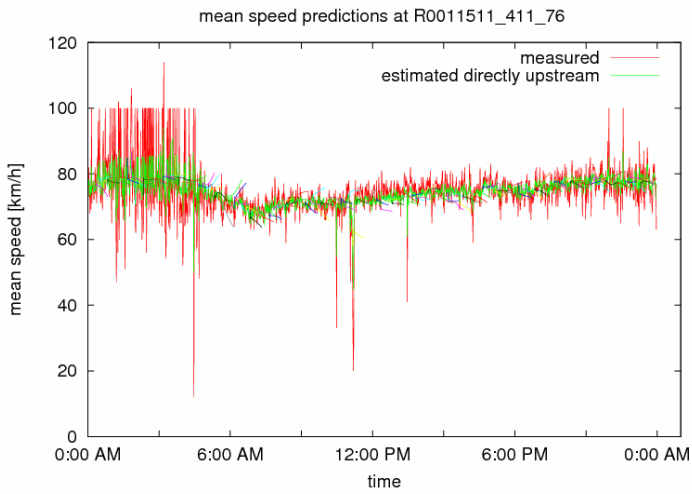


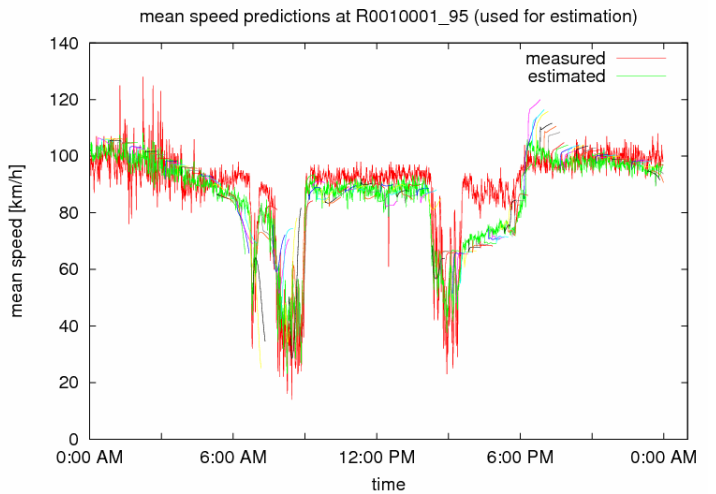
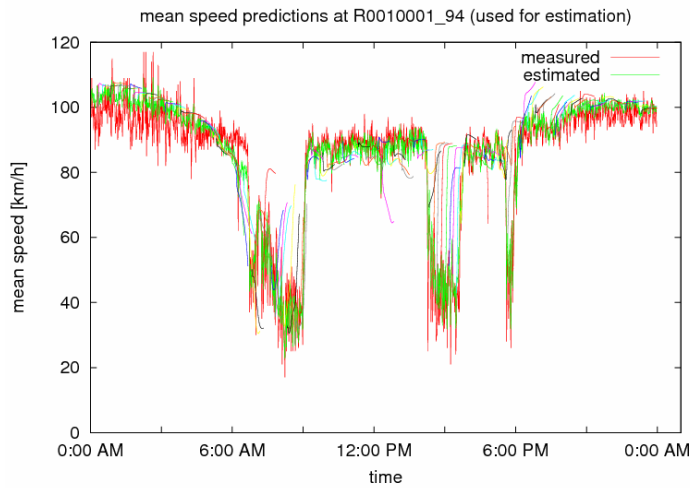
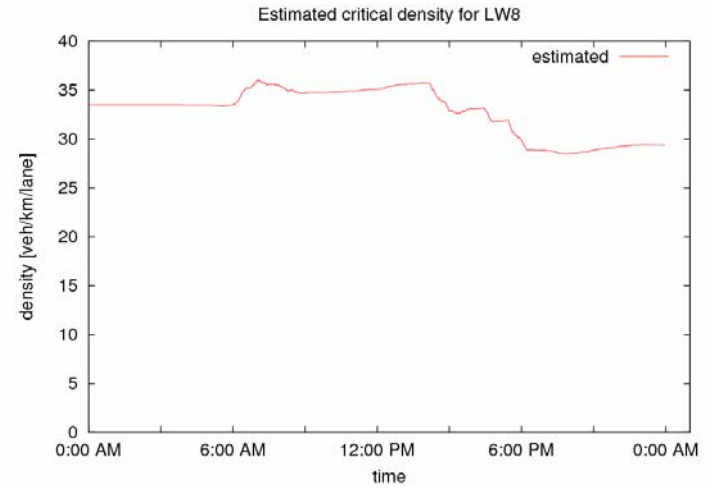
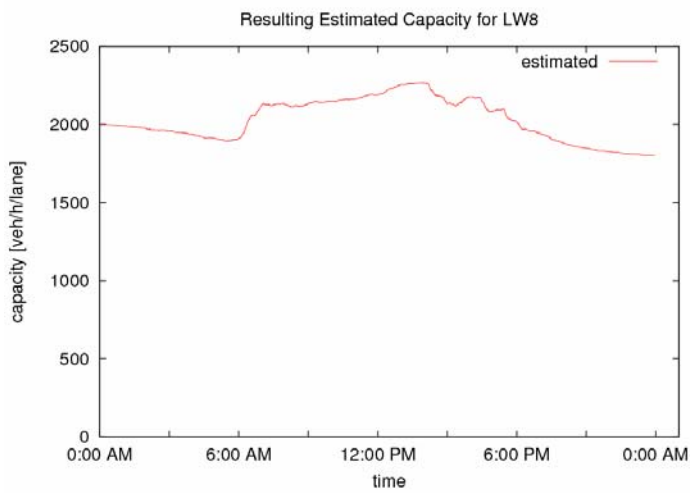
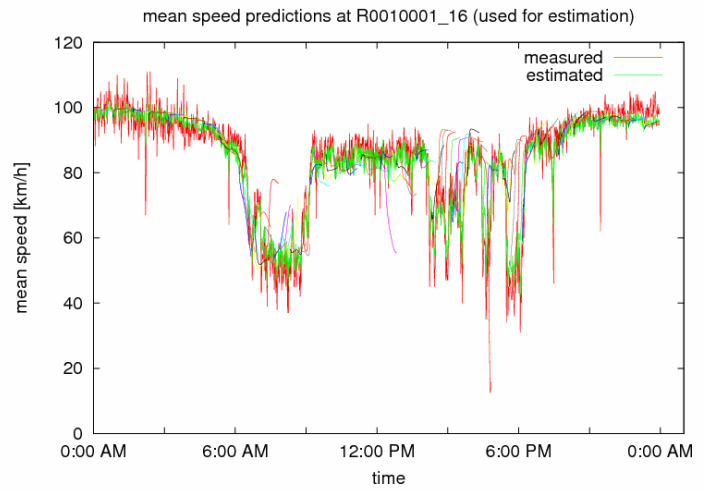
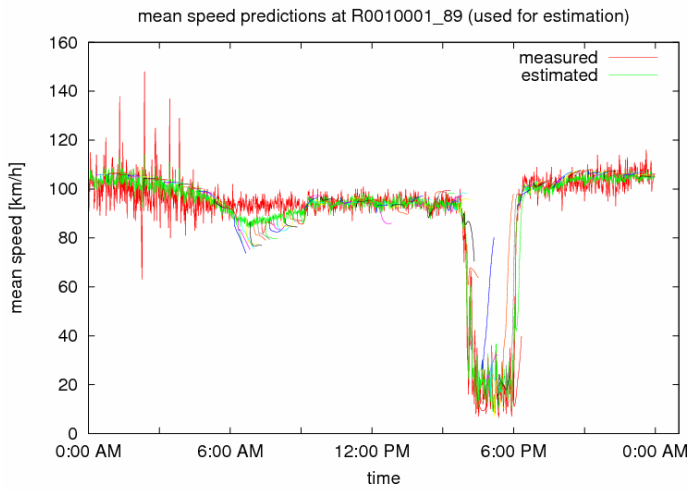
Figure 64: Destination (off-ramp) density predictions with extrapolation only (left column) and with historical data combined with extrapolation (right column).

- Some reduced-speed predictions are visible at the tunnel detectors (_104 and _15) during application of the variable speed limits. This may be due to flow conditions close to capacity that, at some instances, may be slightly exceeded within the RENAISSANCE flow model due to according estimates of the FD parameters. Note, however, the excellent predictions during the afternoon peak period at _15.
- Predictions are seen to be very good during the p.m. peak period congestion at detectors _83, _85 and _89.
- There are two periods of reduced speeds (50-70 km/h) visible at detector _16, one at 6:00-9:00 a.m. and a second at 2:30-4:00 p.m.. The observed low speeds during both periods are due to excessive traffic flow bound for the immediately downstream off-ramp, that exceeds the off-ramp capacity and creates detrimental phenomena on the mainstream, i.e. sensible speed reduction also for the mainstream through lanes. Clearly, these phenomena

cannot be explained by the traffic flow model itself because they act as external events that reduce the mainstream capacity gradually and temporarily. The provided FD parameter estimates for link LW8 indicate indeed a slight decrease of the critical density and capacity during the periods in question. The final prediction outcome at detector _16 is very satisfactory for the a.m. period, as predicted speeds are seen to mostly remain close to the (future) measured values. In contrast, the afternoon period (which features higher speeds than the morning period, with three distinguished but short-lived speed drops) is not reproduced well in the predictions, which are seen to lead to a quick speed recovery.

- The previously mentioned a.m. low-speed period is also visible (due to upstream propagation) at the upstream detectors _94, _95, _17, but does not reach detector _99. The related predictions at _94, _95 are quite good, but the predicted congestion tail does not reach until detector _17, where predicted speeds are seen to recover soon.
- The previously mentioned p.m. low-speed period is not properly predicted at _94. Interestingly, the speed predictions for the same period are quite good further upstream (at _95 and _17), probably due to another congestion commented here below.
- A second afternoon congestion (3:00-6:00 pm) appears at detectors _17 and _99 due to congestion spillback from the off-ramp of node W4 as can be confirmed by inspection of the corresponding off-ramp boundary density in Figure 64. This congestion is reproduced very well in the predictions at _17, thanks to the new bifurcation formula (8) (with $a = 0.9$ here). However, this congestion reaches the further upstream detector _99 only 1 hour later (at around 4:00 pm) while the predicted congestion reaches there much sooner. It might be worth investigating the reasons why the real congestion tail takes 1 hour to cover the 2.3 km between detectors _17 and _99 (and possibly modify the traffic flow model settings accordingly).





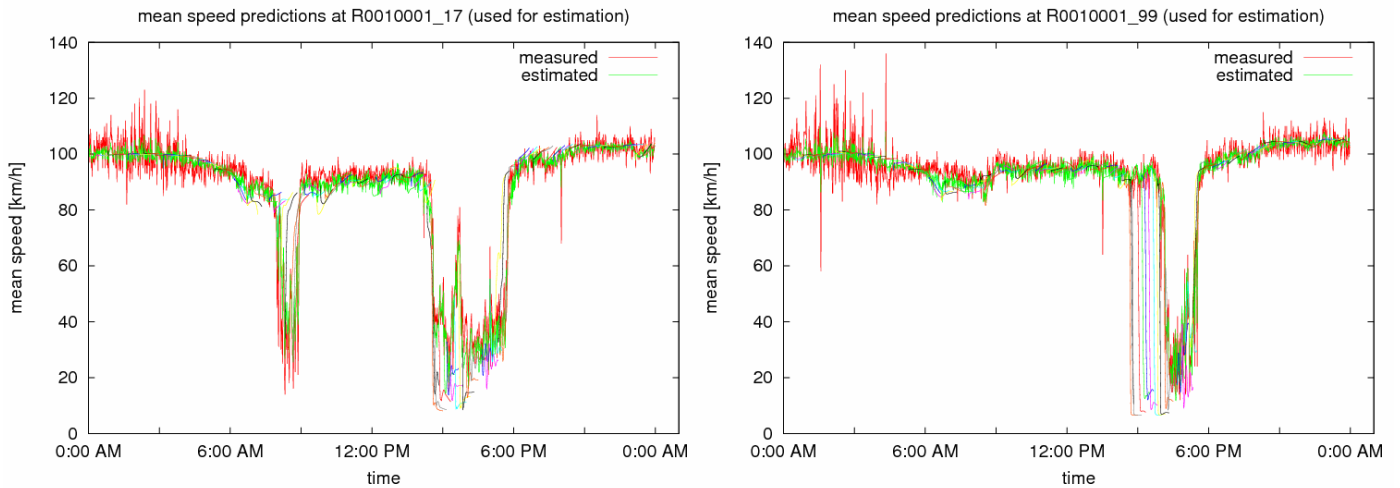
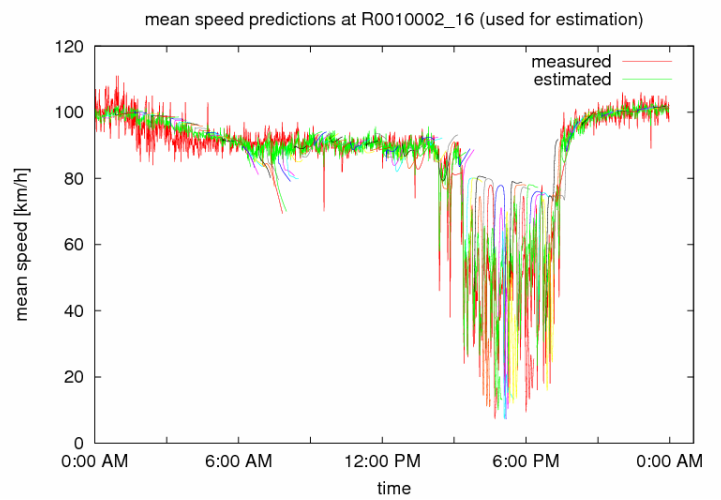
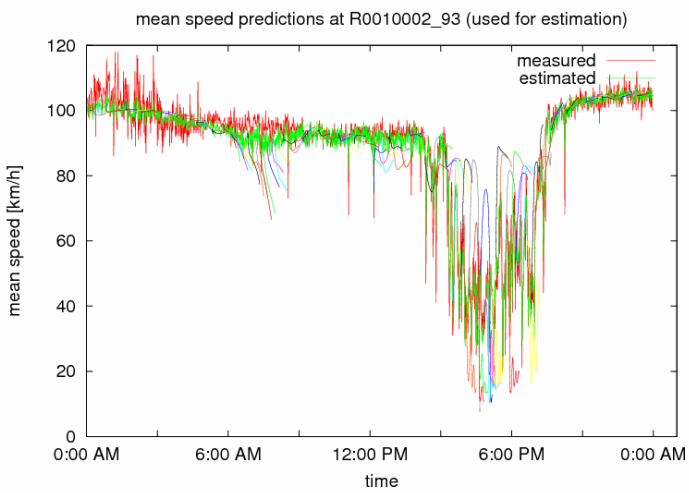
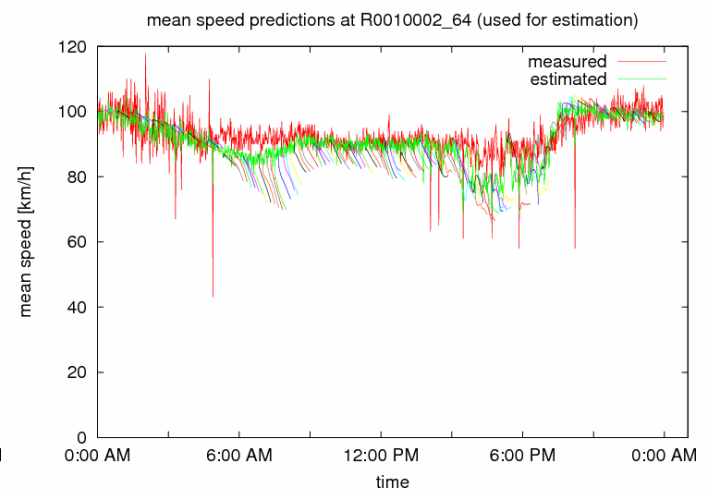
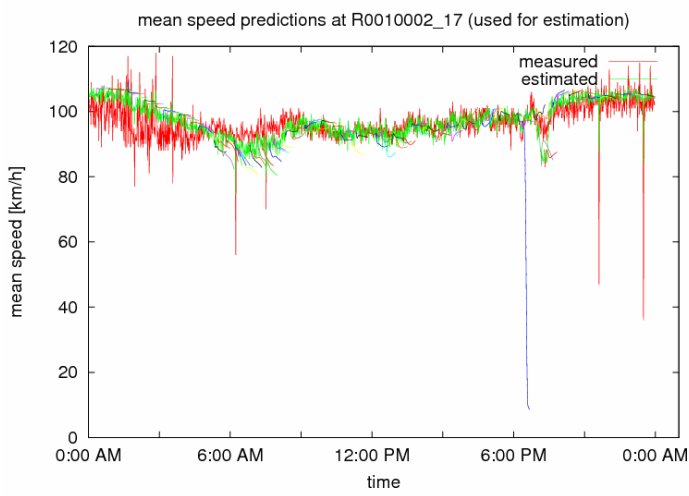
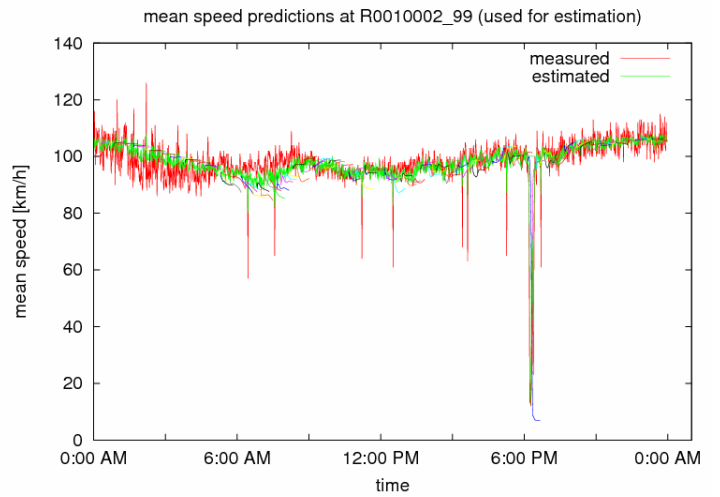
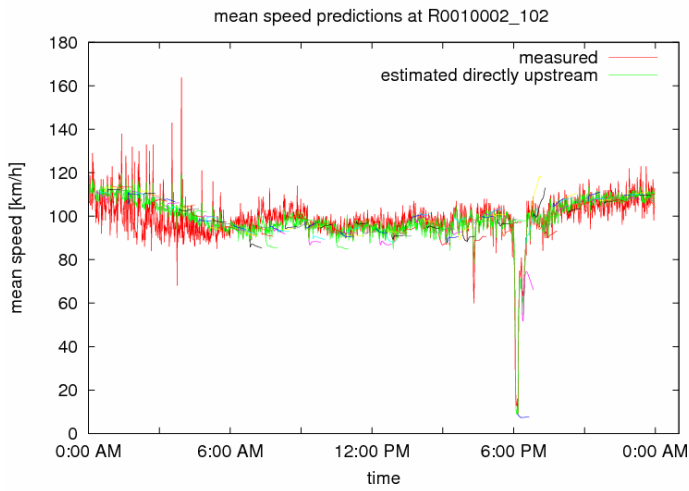


Figure 65: Inner ring prediction results using historical data and extrapolation.

Figure 66 displays the outer ring results (from downstream to upstream), that are commented as follows:

- Predictions are fairly good at those locations that are not explicitly mentioned in the following comments.
- A congestion is spilling back at the off-ramp of node E16 at 3:00-7:00 pm, visible at the detectors _93 and _16. The congestion is seen to have a rather high average speed (around 50 km/h) and to exhibit a very strongly oscillatory behaviour. Despite the use of the new bifurcation formula (8) with $a = 1$, the predictions have a tendency to soon increase the speed to higher values. The origin of this congestion is indeed visible in the boundary density of off-ramp LE16_d in Figure 64. Comparing the boundary density values during spillback at off-ramps LE16_d and LW4_d (Figure 64) it may be seen that the former is clearly lower (around 50 veh/km) and more oscillatory than the latter (around 80 veh/km) which might explain the failure of the prediction to carry this congestion over onto the mainstream. A more detailed investigation of the local circumstances might help to better explain these events and possibly to improve the prediction quality.
- Link LE12 has in reality 6 lanes, albeit with an atypical non-symmetric lane-changing regulation that leads to underutilisation of the right lanes which are not used by through traffic. Link LE12 was modelled in Section 4 as having 5 lanes, but this was further reduced to 4 lanes for this section, without actually affecting the estimation results. In fact, predicted speeds are very good during the strong afternoon congestion at locations _90, _86, _83.
- Predictions are good during the afternoon congestion at locations _15, _14, _77 as well.



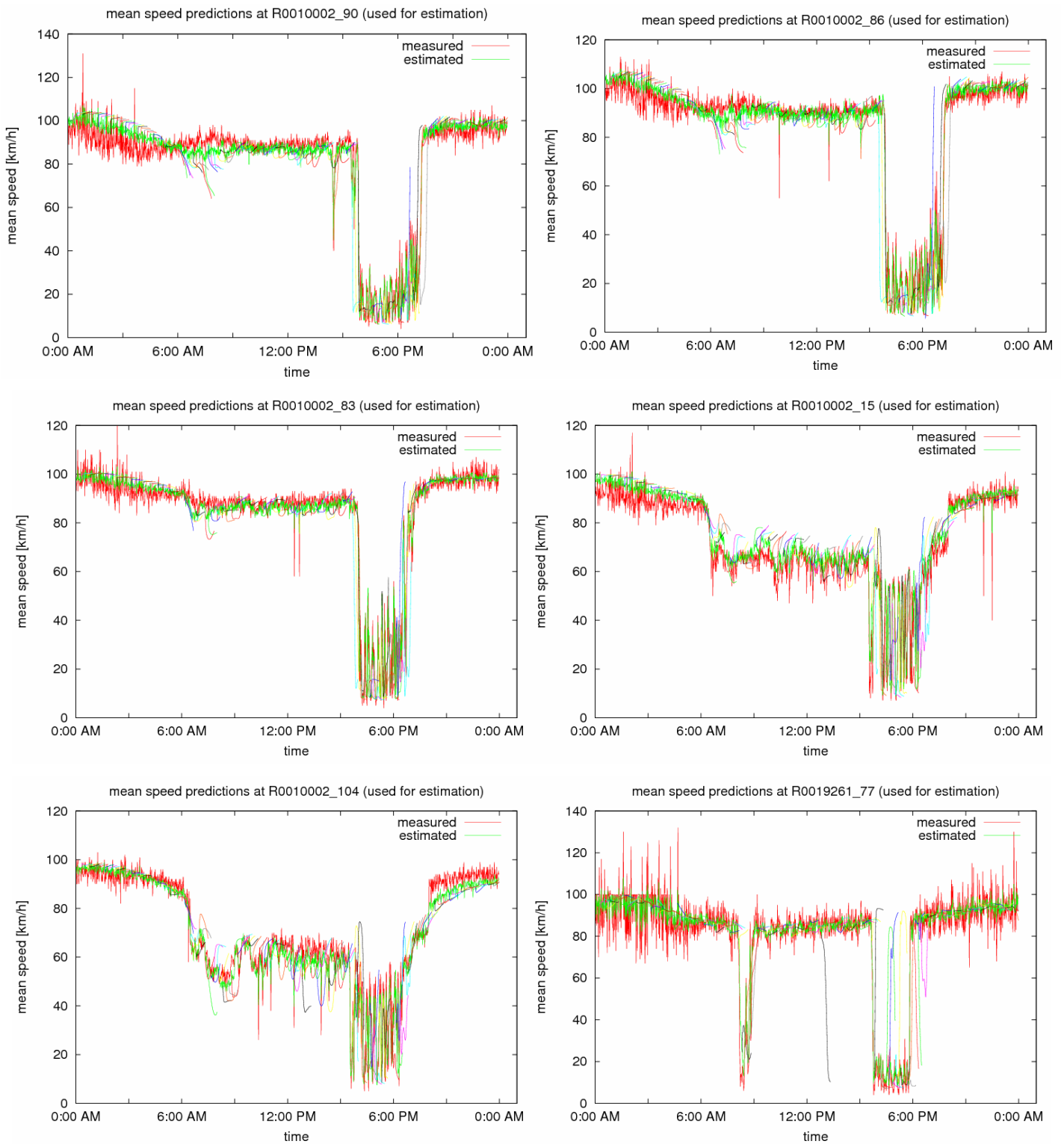


Figure 66: Outer ring prediction results using historical data and extrapolation.

Figure 67 displays the E313 prediction results (from downstream to upstream). The real traffic situation is seen to be quite complex, with very strong but short-lived speed drops. Despite this complex behaviour, predictions are seen to be reasonably good. However, in view of the very strong speed oscillations, the predictions seem sometimes to alternate

between speed recovery (when current speeds are relatively high) and speed drop (when current speeds are low or a modelled congestion arrives from downstream).

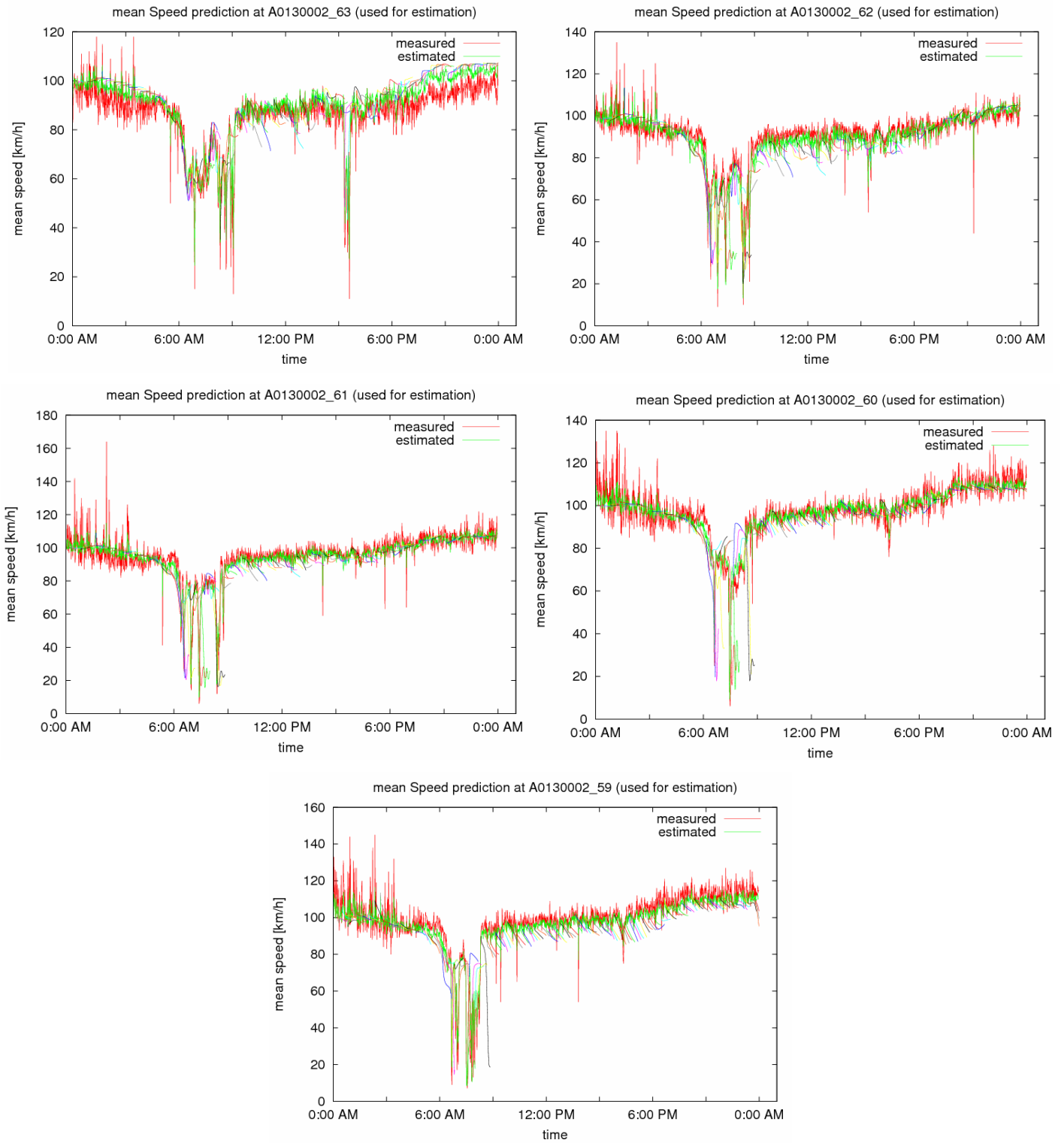
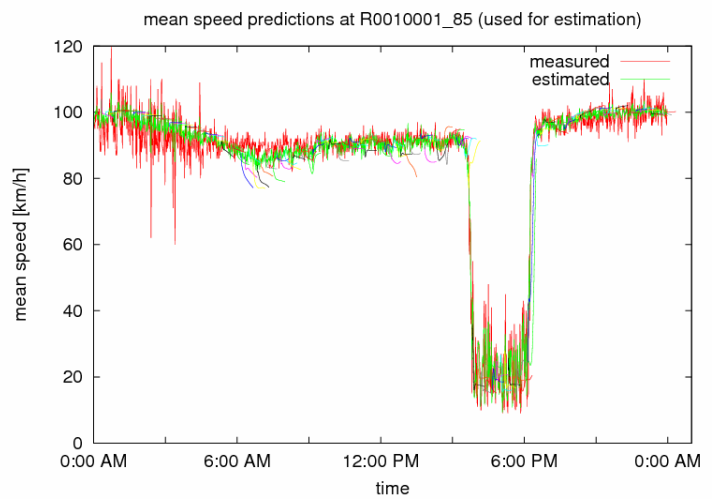
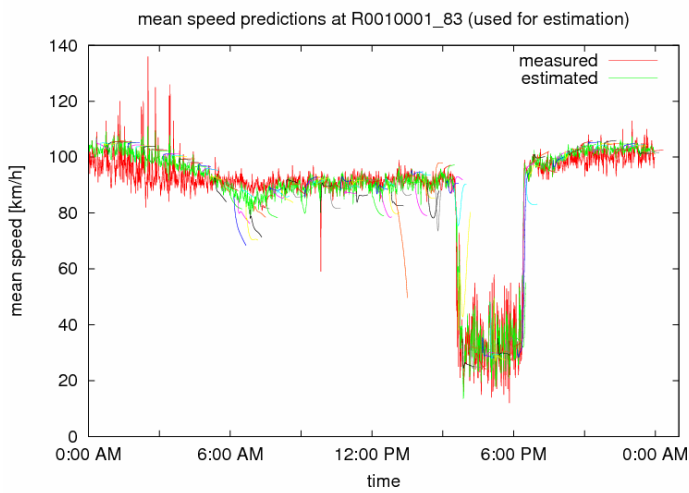
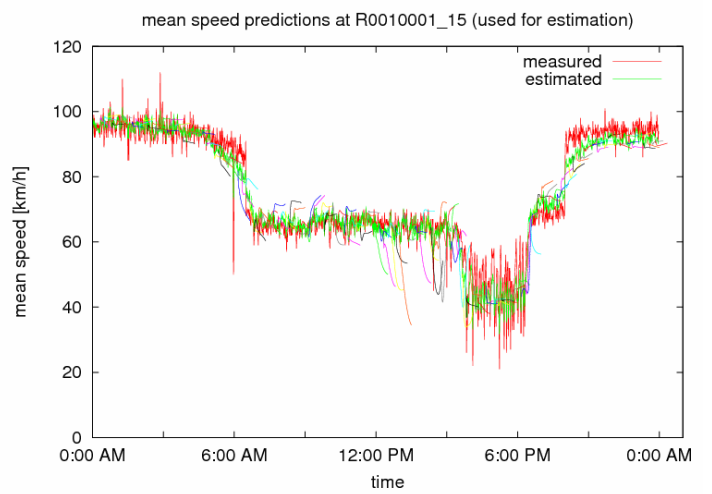
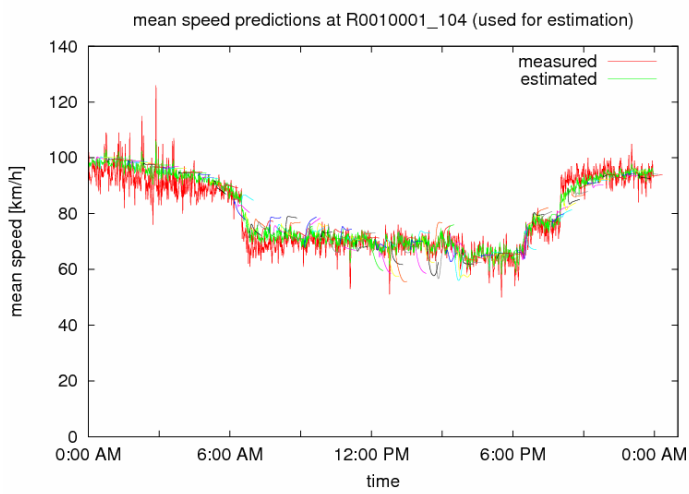
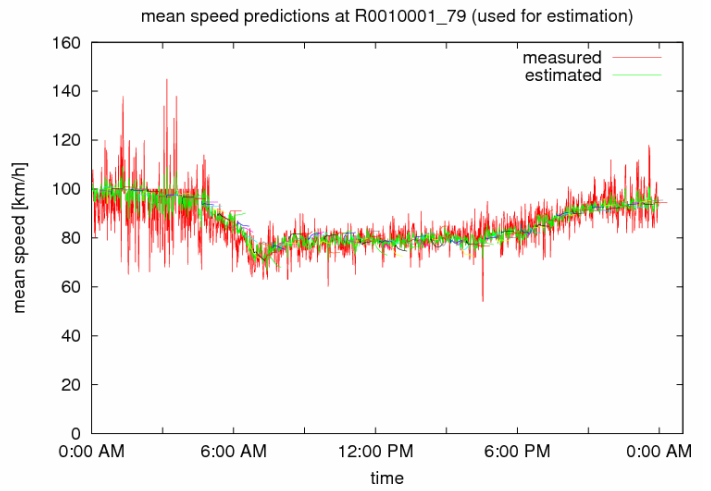
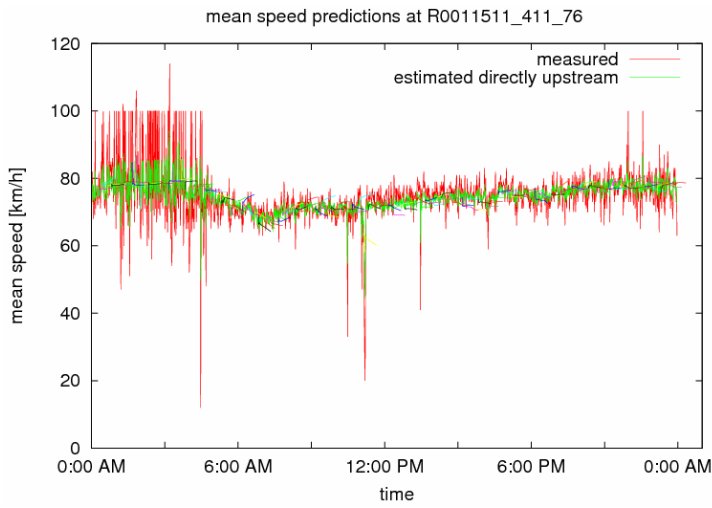


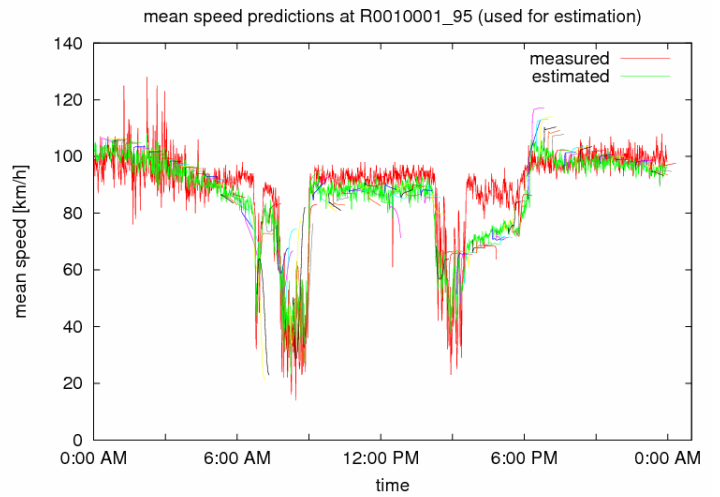
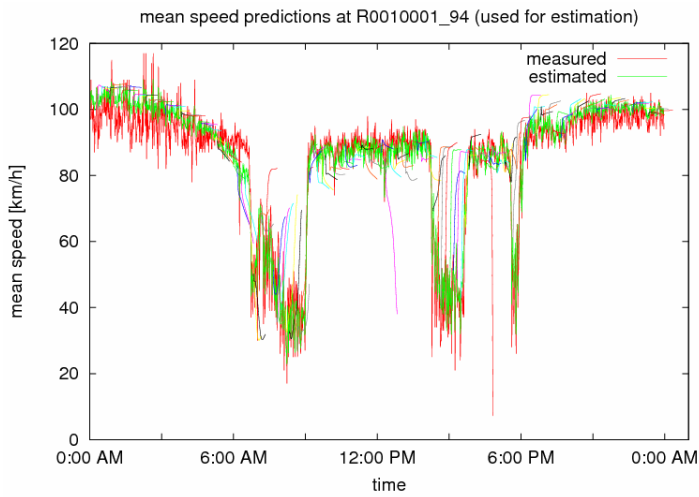
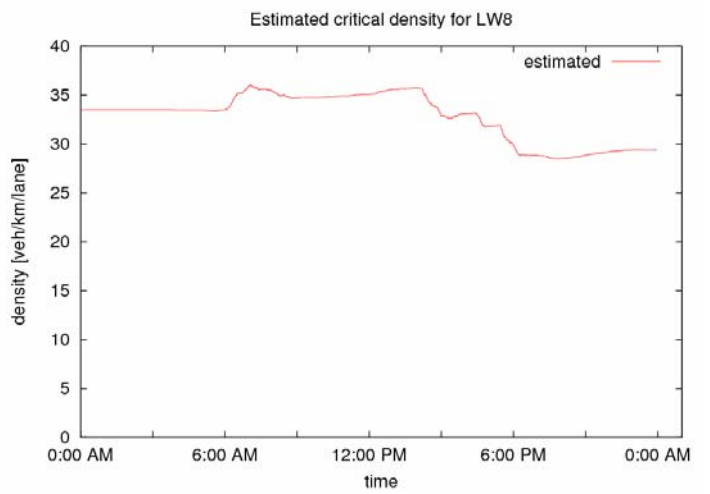
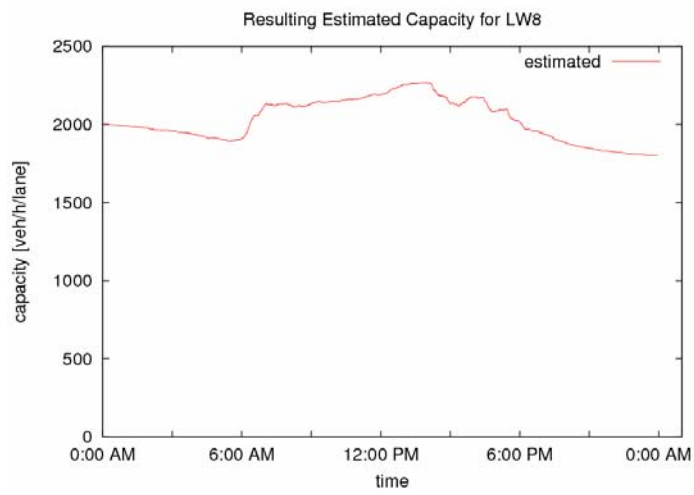
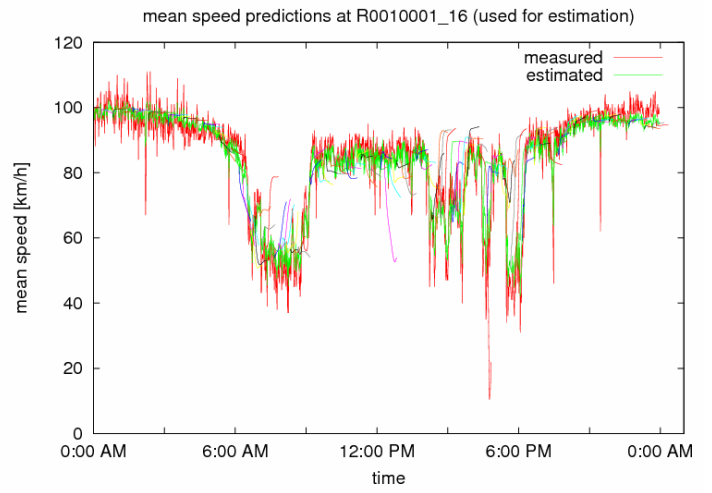
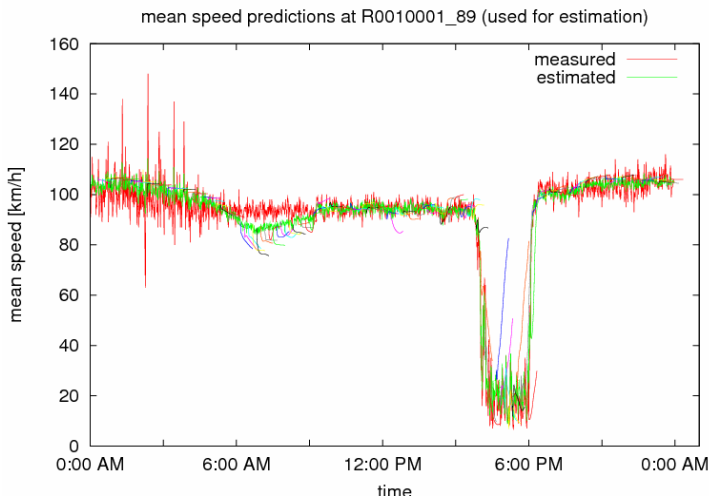
Figure 67: E313 prediction results using historical data and extrapolation.

5.4. Prediction Results with Extrapolation Only

Figures 68-70 display the prediction results when only extrapolation (without historical data) is used for the boundary variable prediction. Contrasting Figures 68-70 with Figures 65-67, one by one, it may be concluded that the prediction results are very similar in nature and interpretation, with a very slight deterioration at some locations and instances when only extrapolation is used.

Summarizing the achieved prediction results for the short-term evolution of the internal network traffic state, we may state that the prediction accuracy is very reasonable in most network parts. Some identified difficulties leading to poor prediction results at some network locations are likely due to particularly complex or specific traffic situations that are apparently not captured well by the traffic flow model of RENAISSANCE. A more focused investigation of the reasons for this complex traffic behaviour might lead to corresponding modifications of the model or of its parameters or of its geometric specifications (segmentation, number of lanes etc.) that could lead to a better prediction quality. Last not least, prediction results might improve via a more targeted positioning of detectors in the problematic network parts.





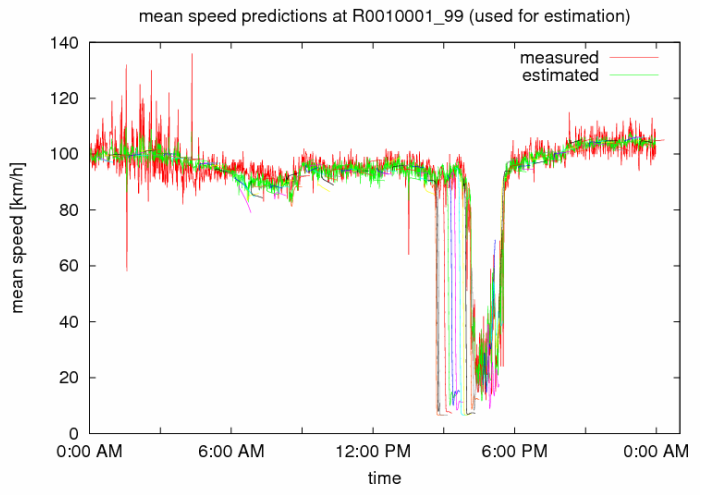
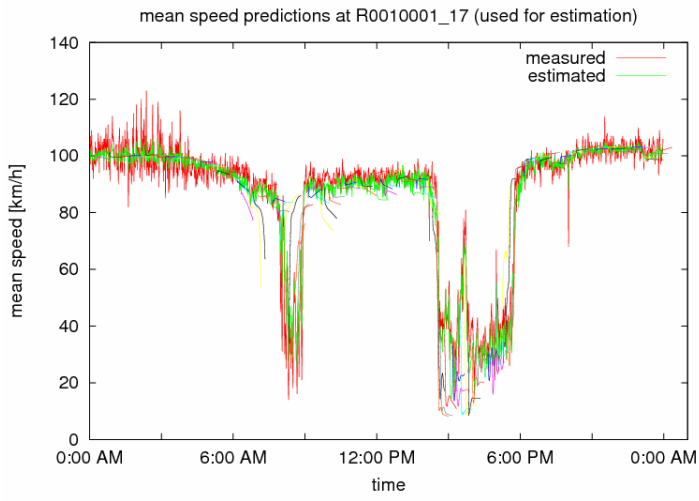
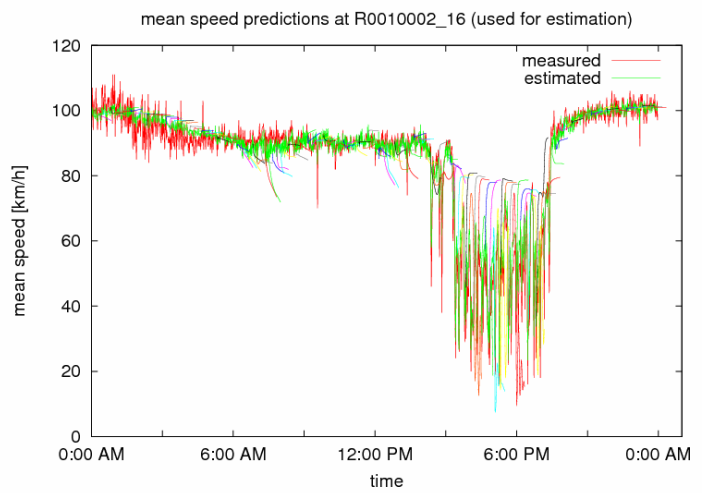
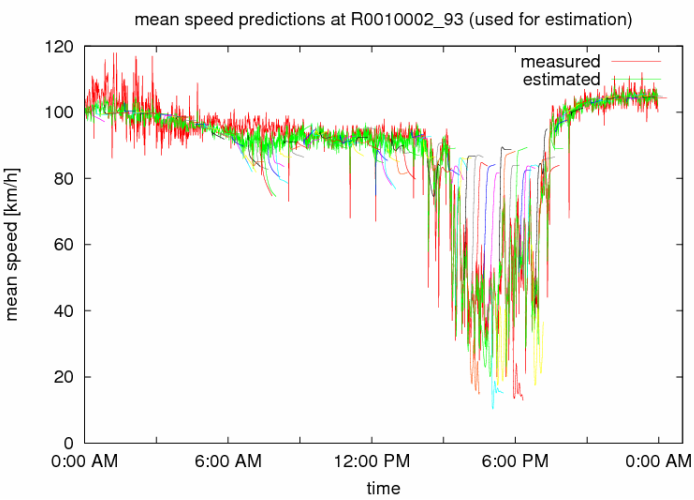
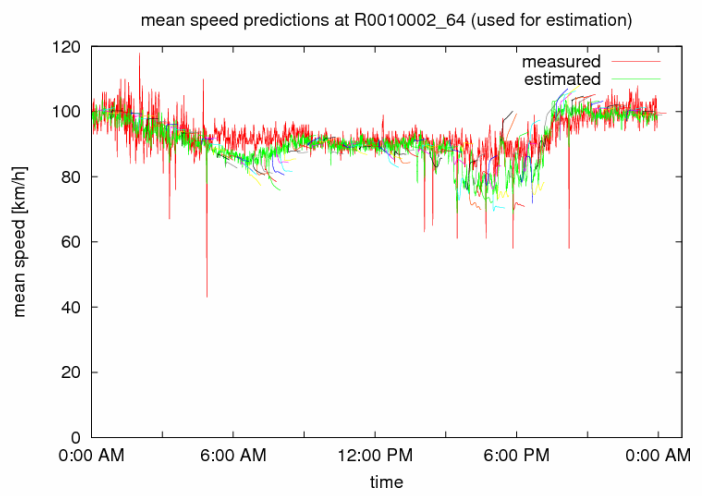
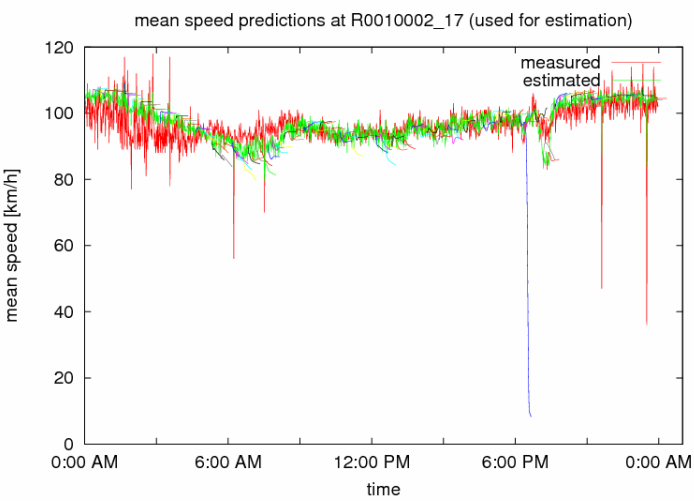
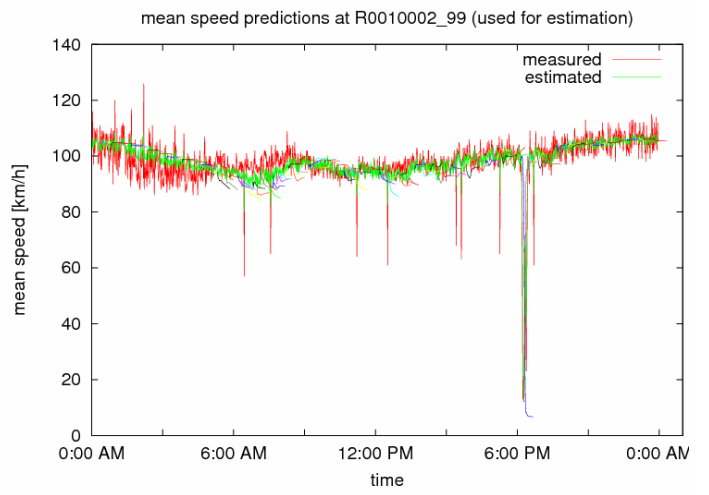
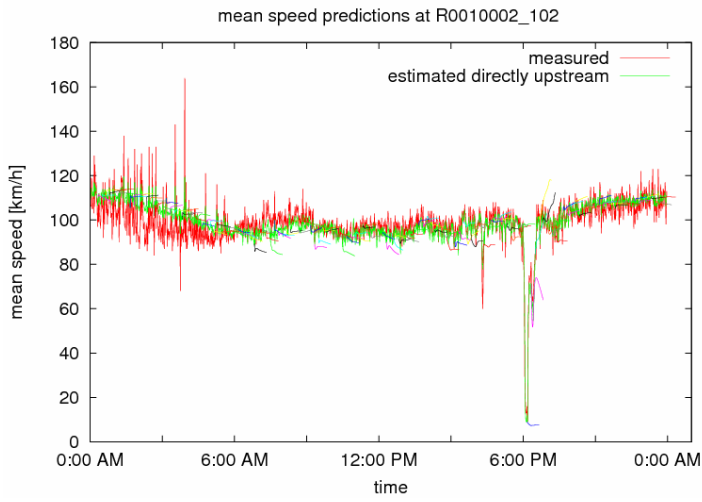


Figure 68: Inner ring prediction results using extrapolation only.



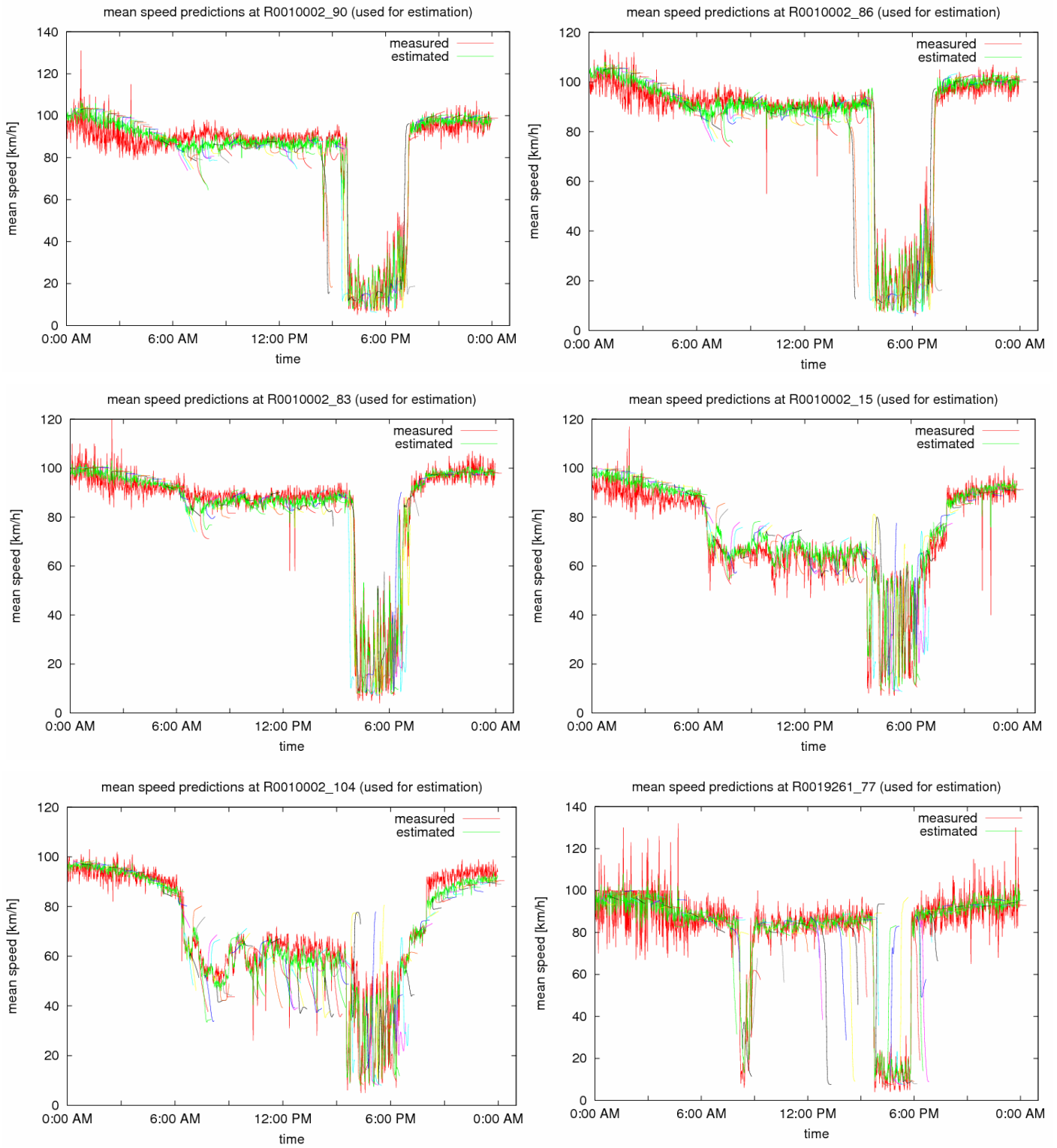


Figure 69: Outer ring prediction results using extrapolation only.

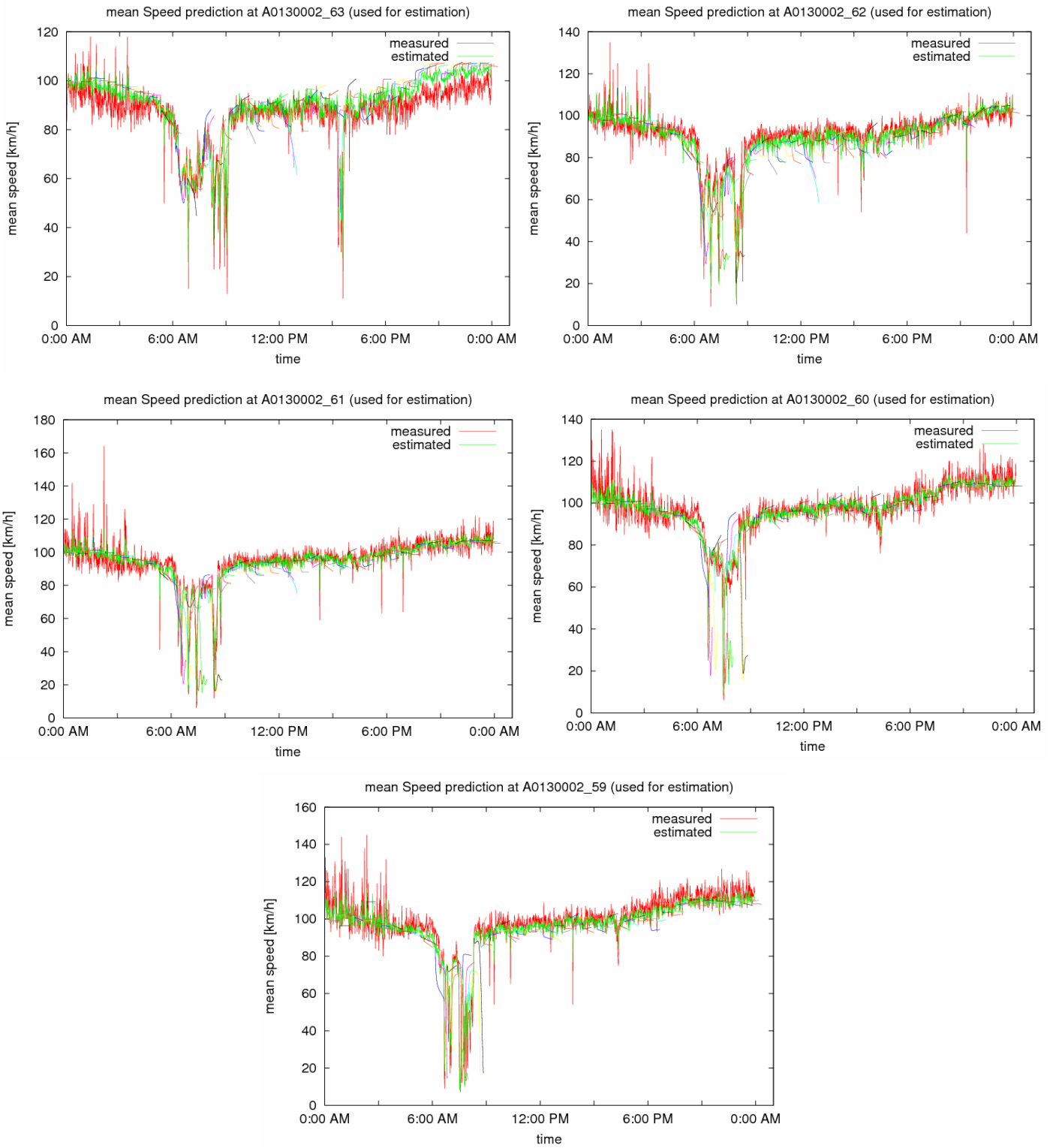


Figure 70: E313 prediction results using extrapolation only.

5.5. Travel Time Prediction

Figure 71 displays the trajectories of travel times on the three network routes (inner ring, outer ring and E313) for 24 h of 23 November 2007, when historical data are used in combination with extrapolation for boundary variable prediction (as in Section 5.3); while Figure 72 displays the same travel times with extrapolation only (as in Section 5.4). Note that each diagram in Figures 71 and 72 contains 2 curves reflecting, respectively,

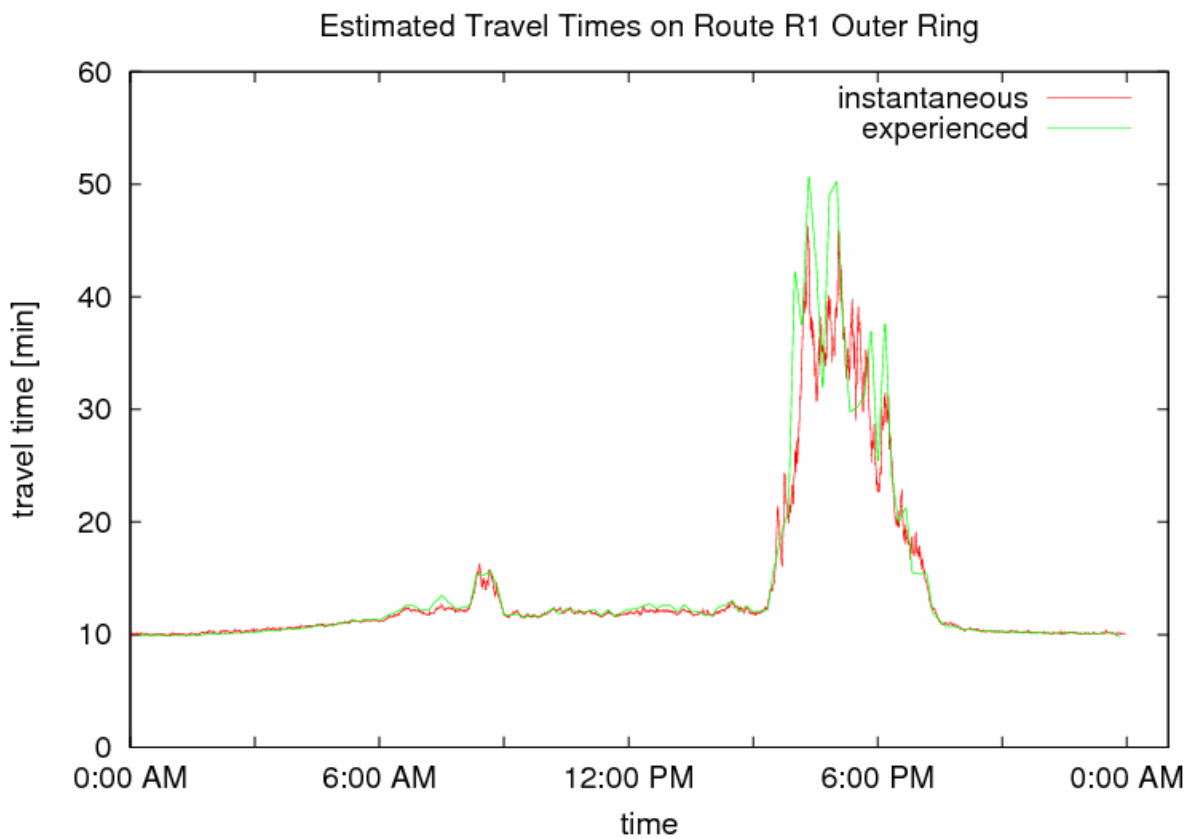
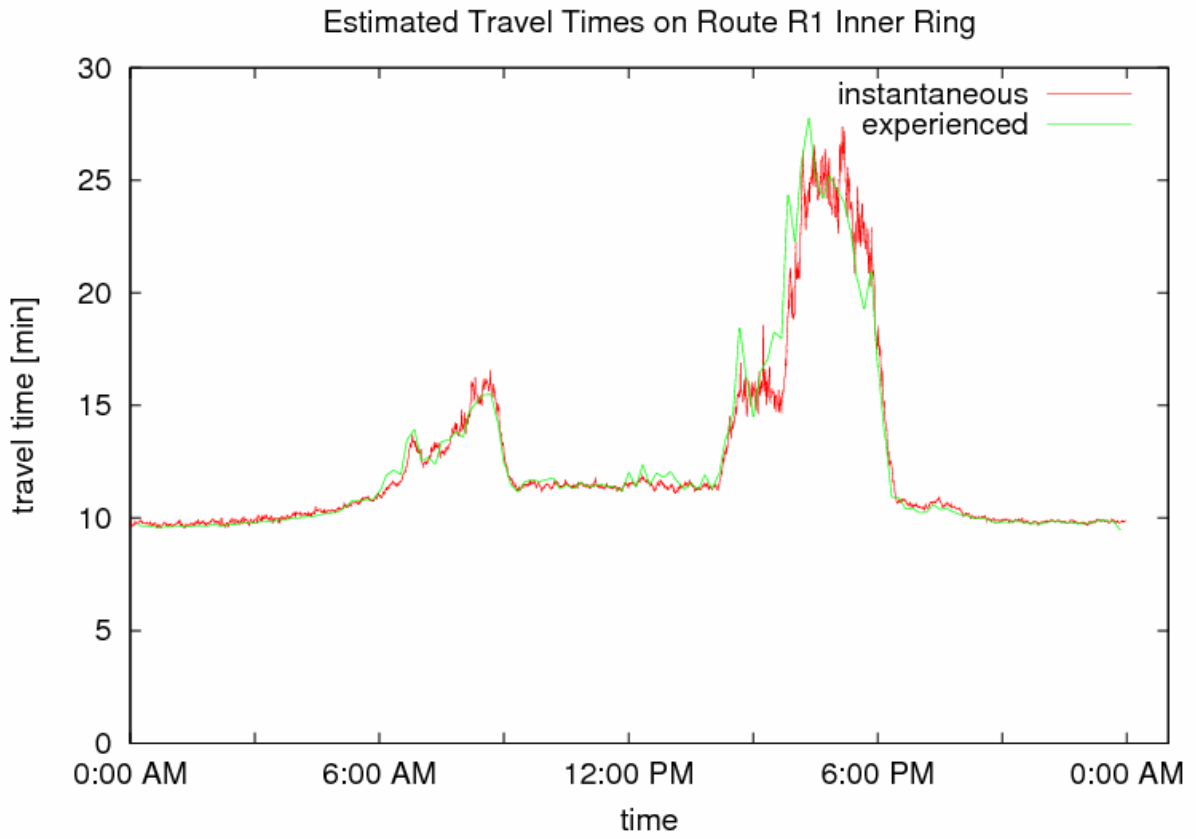
- Instantaneous travel times calculated on the basis of the current speed estimation results according to Section 2.
- Predicted travel times calculated on the basis of the predicted speed results using a virtual-car approach according to Section 2.

In lack of information about the ground truth, the produced travel time estimations/predictions cannot be fully assessed. However, some useful conclusions on the pertinence of these calculations may be drawn by contrasting both types of travel time as follows:

- Instantaneous and predicted travel times are seen to have very similar values during stationary periods, e.g. during off-peak but also during quasi-stationary (congested) peak periods, which is a good indication for reasonable results.
- At periods of increasing or decreasing travel times, the predicted travel times are seen to anticipate the instantaneous travel times which is in full compliance with the nature of both types of travel time and hence a good indication as well.

Clearly, the instantaneous travel times displayed on Figures 71 and 72 are the same for each route because they are only based on estimated speeds and do not depend on the prediction method. Note also that travel time predictions may be better than mean speed predictions (provided that mean speed estimations are reasonably good), because the calculation of predicted travel times via the virtual-car approach makes use of (partially) early speed predictions (e.g. for speeds of segments that are in the upstream part of the travel time route) which are likely to be more accurate than late speed predictions (i.e., those towards the end of the prediction horizon).

In conclusion, the produced travel time predictions appear quite reasonable, but an ultimate quantitative assessment is not possible without ground truth details.



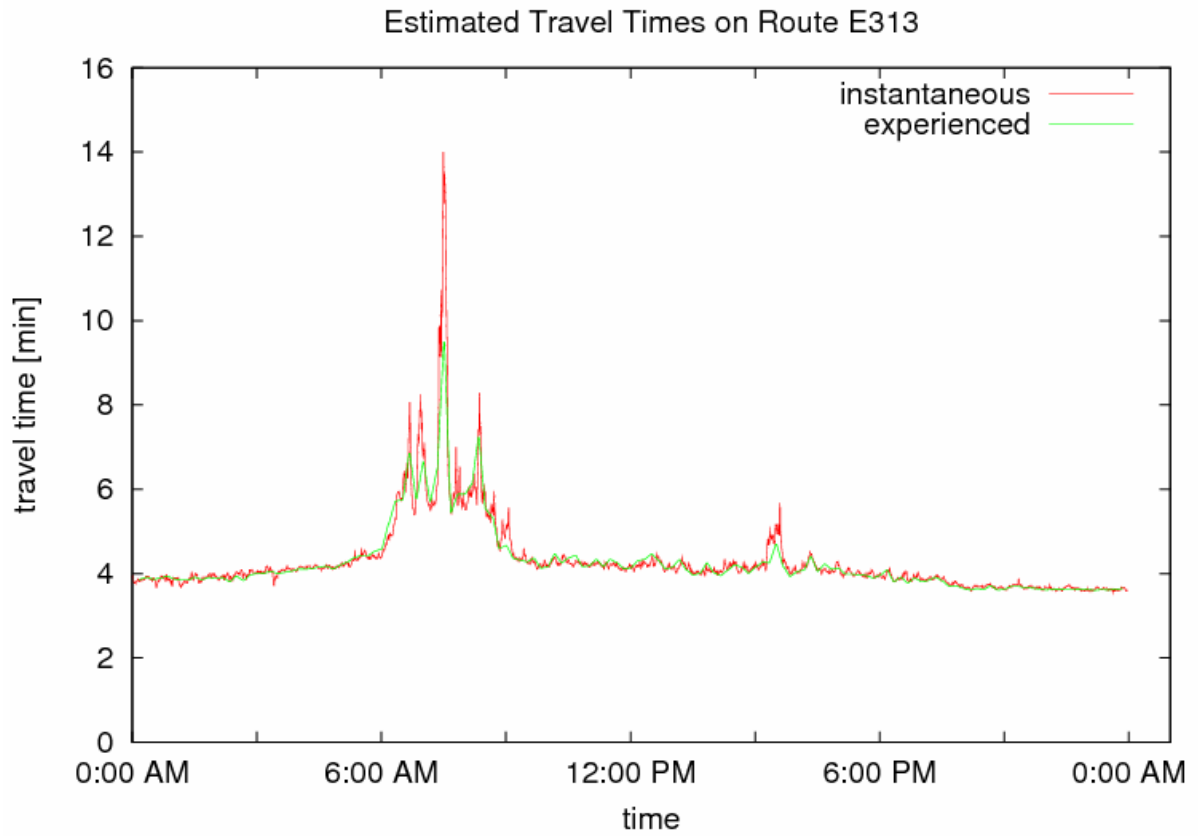
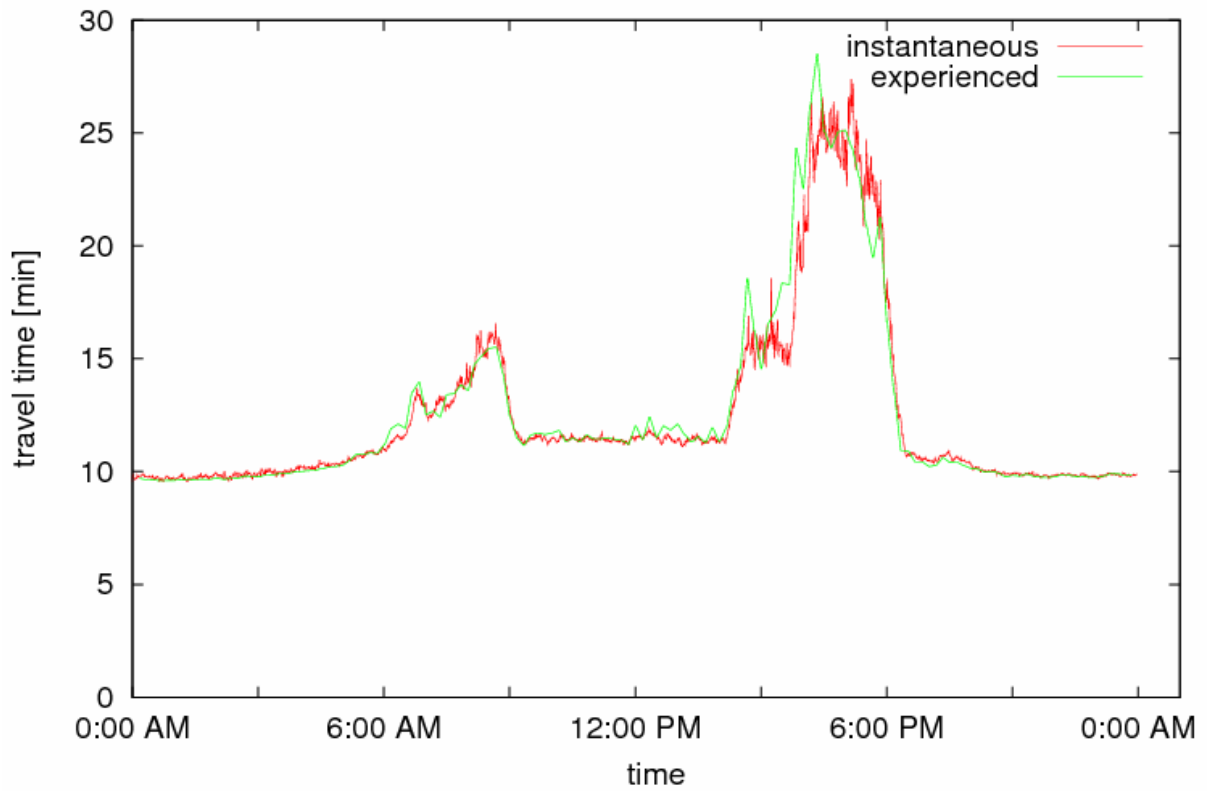
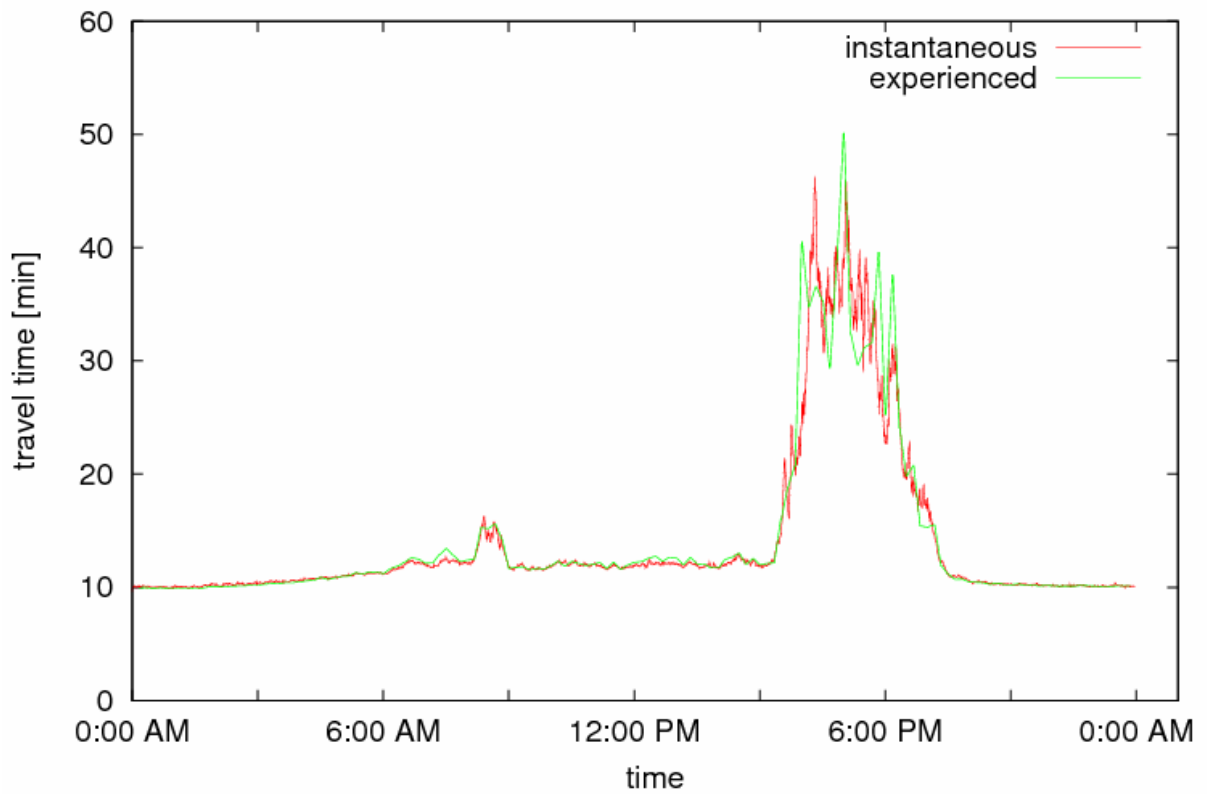


Figure 71: Instantaneous and predicted travel times on 3 network routes with use of historical data and extrapolation.

Estimated Travel Times on Route R1 Inner Ring



Estimated Travel Times on Route R1 Outer Ring



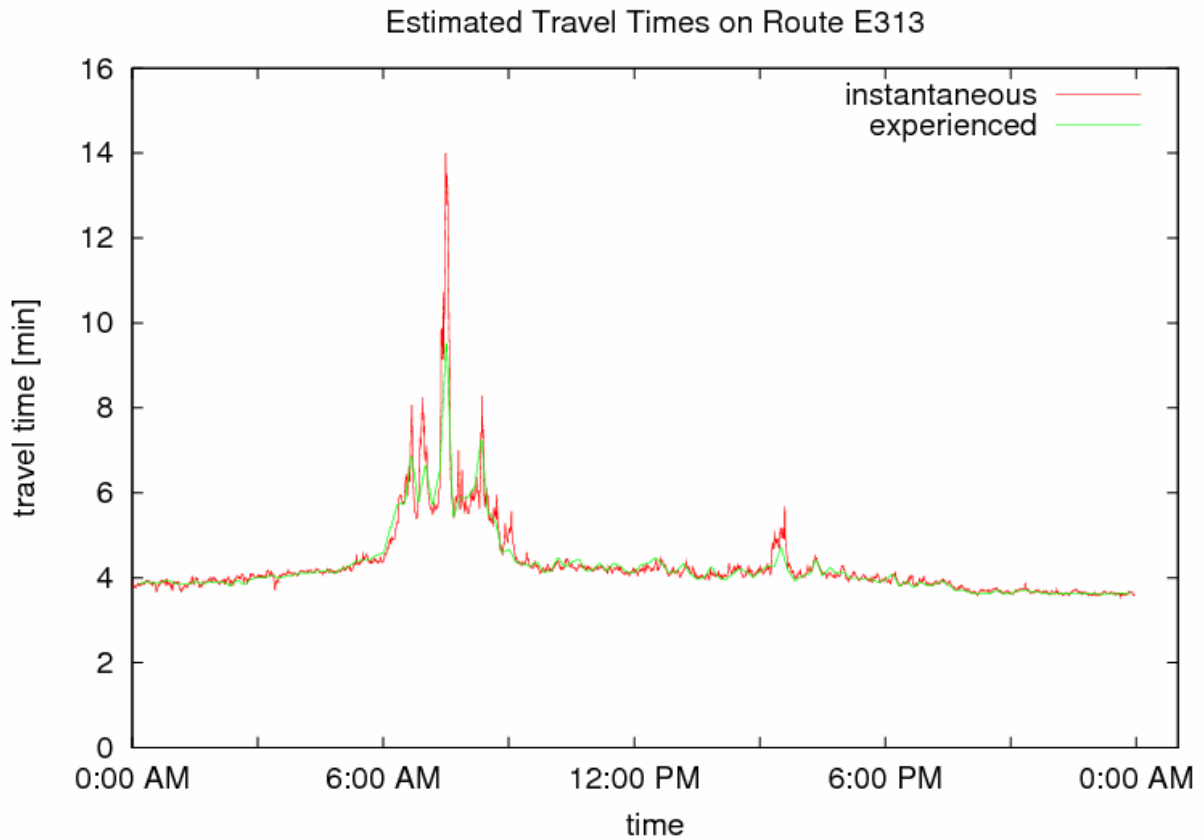


Figure 72: Instantaneous and predicted travel times on 3 network routes with use of extrapolation only.

5.6. Prediction under Incidents

5.6.1 General considerations

In presence of an incident, a reasonably accurate prediction of the future state evolution may have a special value as it could assist the operators in making urgent decisions about possible measures to take, informing drivers etc. There are in principle two ways for producing predictions in presence of incidents.

The first one is to modify the RENAISSANCE traffic flow model appropriately (as in the METANET simulator) so as to enable the traffic flow simulation (into the future) in presence of an incident. To this end, an operator should enter into RENAISSANCE the incident location, the incident severity (rate of capacity reduction) and the estimated time of incident removal, i.e. the incident must be known or verified (after a possible automatic detection or a relevant road user call etc.). If the incident led to a strong change of FD parameter estimates, the FD parameter values must be reset to their pre-incident values for the prediction. The main advantages of this first approach are prediction accuracy, due to known incident data and reasonable modelling accuracy under incident. The main disadvantages are the need for

external (operator) intervention as well as the fact that the incident data must be known and verified, which may delay the production of sensible predictions after the actual incident occurrence.

The second possibility is to let the RENAISSANCE predictions be automatically produced (as usual). The idea here is that, if the estimated FD parameter values were significantly affected by the incident (as in several examples of Section 4.6), then the automatically produced RENAISSANCE predictions will reflect the presence of this incident. The main advantages of this second approach is that it does not need neither an operator intervention nor incident data, hence the predictions can be produced promptly, as no incident verification (e.g. by use of mobile cameras) is needed. The main disadvantage is the reduced accuracy of the produced predictions due to several possible reasons:

- To start with, this approach does not include the possibility of considering incidents that were not detected by RENAISSANCE (but are known to the operators, e.g. via road user calls or other information sources); moreover, incidents that were detected by RENAISSANCE thanks to the strongly negative time-derivative of capacity estimates but did not significantly alter the values of the estimated FD parameters (as in some examples of Section 4.6) will have a correspondingly minor impact on predictions.
- Even if the FD parameter estimates were drastically changed due to the incident, the incident-affected parameter estimates may not accurately reflect the real traffic conditions; for example, Incident 1 of Section 4.6 was found to reduce the capacity estimates from 2000 veh/h to 1200 veh/h, but this latter value may not accurately reflect the real incident-affected highway capacity. In other words, RENAISSANCE may be successful in detecting the incident via the triggered changes of the FD parameter estimates, but it may not be able to also estimate accurately the rate of capacity drop due to the incident.
- Even if the incident-affected FD parameter estimates are accurate, the accordingly modified fundamental diagram would apply to the whole corresponding link cluster rather than to the actual incident-affected segment only (as in the first approach), and this is likely to produce less accurate predictions.

In view of these advantages and disadvantages of both approaches a combined procedure appears reasonable; i.e. to let the automatic RENAISSANCE prediction run which would deliver a “quick and dirty” prediction under the incident; but to manually trigger the first approach as soon as the necessary incident data become available.

Since the exact occurrence time, location, severity and duration of the incidents of Section 4.6 are unknown, the prediction results presented in the next sections are based on the second approach and are therefore expected to suffer from the corresponding accuracy-related disadvantages mentioned above. The incident numbers in the following sections are as in Section 4.6.

5.6.2 Prediction Results for Incident 1

Figure 73 displays the mean speed measurements, estimations and predictions for day 1 of the multiple-day data (Section 4.4) for the outer-ring detectors _102, _99, _17, _64. Incident 1 occurred (see Section 4.6) at around 7:00 a.m. between detectors _102 and _99 and led to a strong non-recurrent congestion that propagated backwards and is visible at the upstream detectors _99, _17, _64 and beyond. Unfortunately, despite the significant drop of capacity estimate from 2000 veh/h/lane to 1200 veh/h/lane (reported in Section 4.6) and reasonably good speed estimates of Figure 73 (that serve as an initial state for the predictions), the predictions displayed in Figure 73 do not fully support the strong real speed drop down to 10 km/h. As a matter of fact, the total mainstream flow at the time of the incident occurrence is around 4000 veh/h on 4 lanes at detector _99 and around 2500 veh/h at detector _102 (there are one on-ramp and one off-ramp between both detectors), see Figure 74. Thus, the estimated capacity reduction to 1200 veh/h/lane is not sufficient to create the full non-recurrent congestion in the predictions. In other words, the real incident apparently reduced the motorway capacity more strongly than estimated as can be seen in the flow measurements at _99 that drop to a total mainstream flow of some 3000 veh/h (for 4 lanes) after the incident occurrence.

5.6.3 Prediction Results for Incident 3

Figure 75 displays the mean speed measurements, estimations and predictions for the inner-ring detectors _16 and _99 on 17 January 2008. Incident 3 occurred (see Section 4.6) at around 7:00 p.m. close to detector _16 and led to a strong non-recurrent congestion that propagated backwards. Although the incident could be detected via the negative peak of the time-derivative of the capacity estimates (Figure 45), the actual drop of the capacity estimate is minor (Figure 44). Thus, despite the good speed estimates visible in Figure 75 (that provide a good initial state for the predictions), the traffic flow model cannot maintain the congestion, and the predicted speeds are seen (Figure 75) to recover very soon.

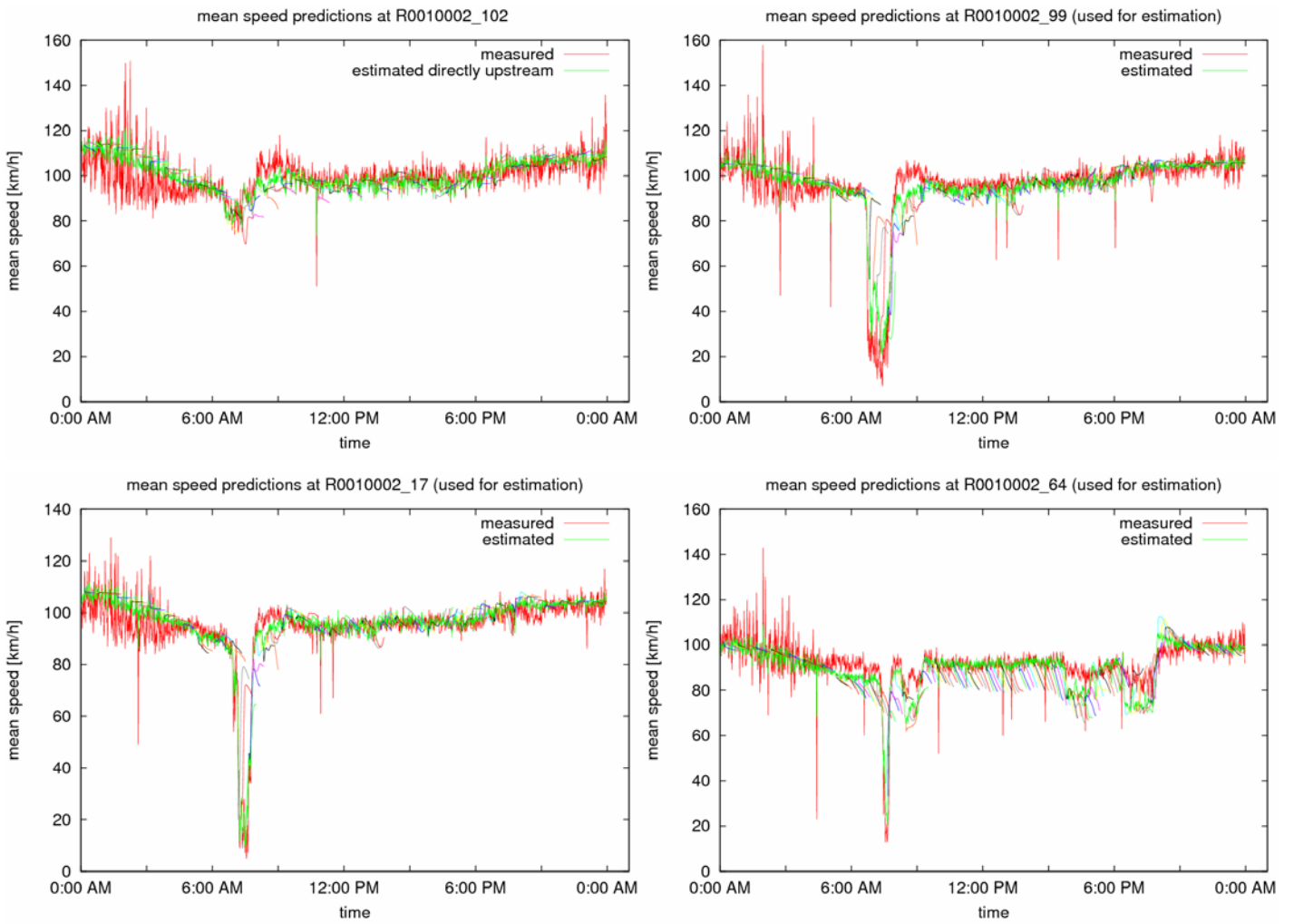


Figure 73: Mean speed predictions for Incident 1.

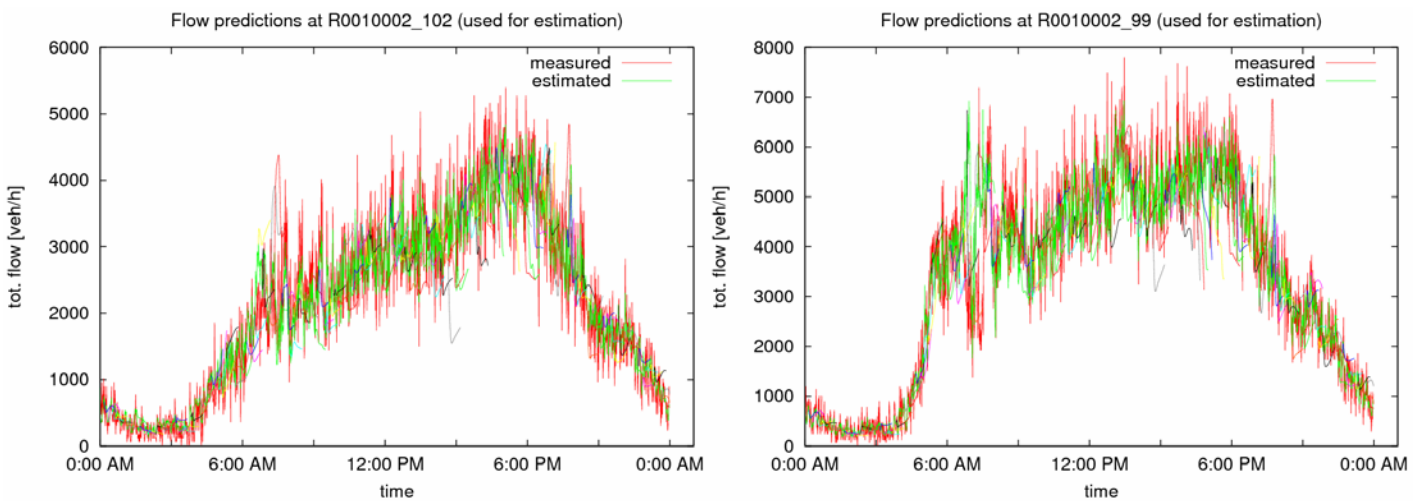


Figure 74: Flow measurements and estimates for Incident 1.

5.6.4 Prediction Results for Incident 4

Figure 76 displays the mean speed measurements, estimations and predictions for the inner-ring detectors _85 and _89 on 6 February 2008. Incident 4 occurred (see Section 4.6) at around 7:00 a.m. close to detector _83 and led to a strong non-recurrent congestion that propagated backwards. Despite the incident detection via the time-derivative of capacity estimates (Figure 49), the estimated capacity drop from 1900 veh/h/lane to 1500 veh/h/lane (Figure 48), and the good speed estimates visible in Figure 76, the predictions do not really reproduce the non-recurrent congestion. The reason is clear by inspection of the flow measurements at _89 (Figure 47): The real flow after the incident occurrence reduces almost to zero, i.e. the motorway was almost completely blocked by the incident.

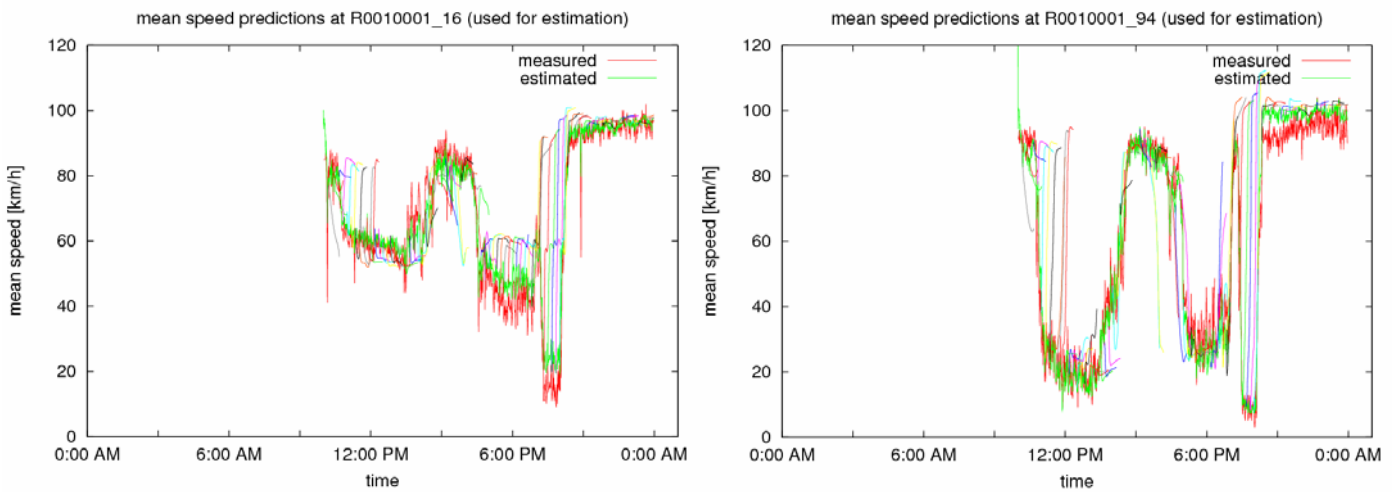


Figure 75: Mean speed predictions for Incident 3.

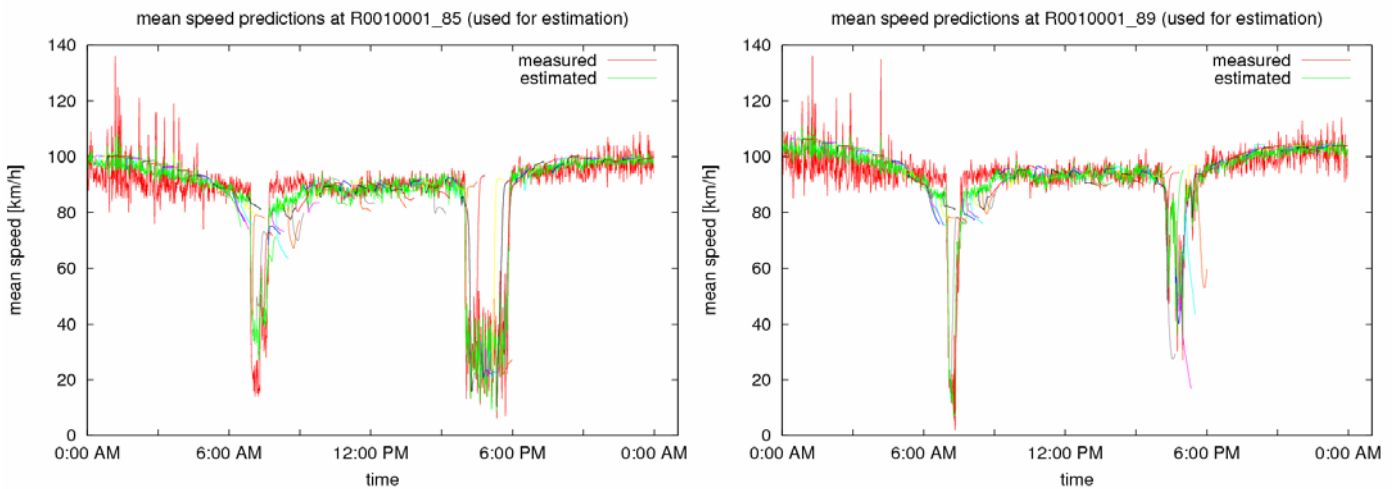


Figure 76: Mean speed predictions for Incident 4.

5.6.5 Conclusions on Prediction under Incidents

The results in this section indicate that, despite the successful incident detection and the good mean speed estimates during the incident (that serve as initial state for the predictions), the produced predictions under incidents fail to capture the resulting non-recurrent congestion. The reason for this is also quite clear. Even if the estimated capacity drops significantly (which is not always the case), it does not drop sufficiently to predict a non-recurrent congestion.

Upon a second thought, this is not really surprising. RENAISSANCE seems to detect the incidents (via the time-derivative of the estimated capacity), to avoid false alarms and even (in some cases) to produce significant drops in the estimated capacity value. However, the latter does not occur to a sufficient degree to also predict the non-recurrent congestion. As a matter of fact, there is no known tool (and, in fact, no known attempt to develop a tool) that would, not only detect incidents, but also estimate correctly the related capacity drop.

A practically useful way to enable significantly better predictions under incidents via a more accurate estimation of the related capacity drop would be to look at the flow measurements after the incident detection. In fact, Figure 74 indicates a flow drop to 3000 veh/h at detector _99 after occurrence of Incident 1; Figure 43 indicates a flow drop to 2000 veh/h at detector _94 after occurrence of Incident 3; and Figure 47 indicates a flow drop to 500 veh/h at detector _89 after occurrence of Incident 4. These reduced flows reflect roughly the real capacity under the incident impact and could be used as a much more accurate capacity estimate when an incident is detected. This possibly is not included in RENAISSANCE at this stage.

6. Conclusions and Recommendations

6.1. Traffic state estimation and travel time prediction capabilities of RENAISSANCE on the Antwerp Ring network in regular conditions

As a reference for state estimation performance, two data sources were available: loop detector data (the same that was used to correct the traffic model) and independent speed measurements by closely spaced AID cameras. Comparing both references to the estimation results, it appeared that both flow and speed estimates were mostly very good, both at the detector locations (where the estimation was corrected using the data) and in between these locations. Estimation is accurate both in free flow conditions (night, between peak periods) and during congestion, where both the contours and the internal structure of congestions (stop & go pattern, speed level) are reproduced pretty accurately. Speed drops and rises are propagated according to expectation between successive detector locations, and also at intermediate locations, both the time and amplitude of these oscillations and waves correspond to those independently observed by the AID cameras.

At some specific locations, like for instance the Kennedy tunnel entrance on the Outer R1 and the weaving area upstream of the E19/A12 exit near Berchem, estimation is slightly less accurate. These are two situations where traffic flow is complex, in the sense that flows are not homogeneous over the lanes and lane changing activity acts as a bottleneck, while a suitably located detector that would allow accurate capacity estimation is lacking. It is recommended to add detectors here in order to improve estimation results (and herewith also prediction results, see further).

The clustering of road segments in several clusters with multiple fundamental diagrams increased estimation accuracy with respect to one single diagram considerably. Estimation of fundamental diagram parameter values shows reasonable values that are mostly stable, also during a 5- and 10-day investigation. However, some parameters may exhibit some drift that is corrected at irregular time intervals. The aspect of the dynamic behaviour of fundamental diagram parameters in the long run therefore needs careful consideration when the model will be tested over longer time periods either off- or online.

The model appears reasonably robust with respect to faulty detector data. As long as flow observability is guaranteed, faulty detectors do not substantially affect estimation accuracy; otherwise, results in affected sections are biased but outside the affected area, estimations remain rather unchanged. A similar observation holds when less detectors are installed, as

long as the mainline detectors are available. This requirement might contradict other requirements to the monitoring system as set by the Antwerp authorities.

6.2. Incident detection capability of RENAISSANCE on the Antwerp Ring network

RENAISSANCE was found to produce excellent results regarding the detection of incidents². In fact, both unknown and known incidents were seen to produce sufficiently strong (or durable) negative peaks of the time-derivative of capacity estimates to be detected. Most importantly, the detected incidents produce time-derivative peaks that are much stronger (or more durable) than the time-derivative values encountered in absence of incidents, which indicates an accordingly low (virtually zero) false alarm rate. Note that high false-alarm rates are the main obstacle towards operational use of virtually all known incident detection algorithms to date. Note also that the RENAISSANCE mechanism for detection of incidents does not call for detector installation every 500 m as most known incident detection algorithms; nor does it call for the absence of on-ramps and off-ramps between the adjacent (upstream and downstream) detectors of the incident location. The detected incidents in this report were mostly included between two mainstream detectors at a distance of some 2 km, with on-ramps and off-ramps between them. On the other hand, the exact location of the detected incidents may not be based on a 500 m-resolution as with usual incident detection algorithms, since it is the parameter estimation for an entire cluster that triggers the incident alarm. The model does not provide exact positioning information of the incident with respect to the detector that is used as a reference for the clusters. Finally, the time-to-detect is deemed very satisfactory and, in several cases, actually quasi-instantaneous.

It is also interesting to note that an exponential smoothing of the time-derivative signal could increase the distance between incident and non-incident cases, at least for incidents of a certain duration. This is because the negative time-derivative values in cases of incidents persist over a period of time while other occasional negative peaks are very short-lived and would be reduced by the smoothing.

² Note that not only real incidents are detected, but also events outside the modelled network that cause congestion spillback onto the modelled network – be it regular or incidental – might be detected as incidents.

6.3. Traffic state estimation capability of RENAISSANCE on the Antwerp Ring network in incident conditions

The traffic state estimation capability of RENAISSANCE in incident conditions is largely comparable to that in regular conditions, with the following limitation. The location of the queue head is only accurate up to the spatial resolution of detectors, because it is the first detector upstream of the incident that fully contains the state information inside the incident-affected queue. As a consequence, congestion upstream of this detector is estimated well, but there might be some distance downstream of this detector (and up to the real incident location) for which state estimation is too optimistic (free flow instead of congestion).

6.4. Traffic state prediction capability of RENAISSANCE on the Antwerp Ring network in regular conditions

Summarizing the achieved prediction results for the short-term evolution of the internal network traffic state and travel times, we may state that the prediction accuracy of RENAISSANCE for this network is overall reasonably good (as in the overall views of **Error! Reference source not found., Error! Reference source not found., Error! Reference source not found.** and travel time predictions of Figure 71); however, zooming on some particular space-time windows reveals some prediction weaknesses. More specifically, congestion patterns at some important bottlenecks in the Antwerp network are not well predicted, in that congestion either consistently disappears (Antwerp-South: Inner ring for exit E19/A12), or is exaggerated (Antwerp-East: Inner ring for exit E313) or alternates between these extremes (E313, Antwerp-East: Outer ring for exit E313). It should be emphasized, however, that all these locations feature quite complex traffic behaviour with congestion spillback from off-ramps and/or lateral inhomogeneities across lanes or quasi-stochastic emergence of shockwaves.

Nonetheless, predictions of the queue upstream of Kennedy Tunnel on the Inner ring show that good predictions are feasible, given that the bottleneck itself and the queue upstream of it are internal to the network. Note also that these encouraging results can still be improved if (i) prediction of conditions upstream is improved, since this determines the inflow of this queue, and (ii) if after that improvement some fine tuning is done for the sections involved in this queue.

From in-depth analysis into the causes of the less satisfactory results, it appears that it may be the way the network was delineated that inhibits RENAISSANCE to produce better

predictions. In all of the problematic predictions, one or a combination of the following causes could be identified:

- The bottleneck (head of the queue) is outside the modelled network
- Traffic demand for the bottleneck could not be identified because the upstream boundary of the network lies within the congested region or due to questionable boundary prediction quality.
- Capacity of a bottleneck inside the modelled network cannot be accurately estimated for lack of a suitably positioned detector allowing such capacity estimation.

Identification of these conditions of lower accuracy is therefore an important lesson learned from this first large-scale RENAISSANCE application in which prediction results were studied in such extent and depth. Although one should be careful in drawing conclusions based on this single application network, it is anticipated that the above findings may be of more general character. The preliminary conclusion is that in general, in order to obtain better predictions with online prediction tools like RENAISSANCE, the following conditions may need to be fulfilled at least for complex bottlenecks:

(i) the bottleneck is internal to the model,

AND

(ii) there is a detector located such that good capacity estimates of this bottleneck are possible,

AND

(iii) the most upstream detector of the important flows feeding the queue are outside the congested area.

These findings lead to the following concrete recommendations for the Antwerp site:

- Inner Ring, Antwerp-South: consider divergence point more upstream (where physically flows on R1 mainline and exiting traffic are actually not yet separated) AND install detector here allowing capacity estimates specifically for the exiting lanes.
- Inner Ring, Antwerp-East / Outer Ring, Antwerp-East: extend modelled network so as to include beginning of E313 outbound AND verify if some existing detector there is suitable for capacity estimation OR install extra detector for this purpose.

- E313: extend the network way upstream; since queues are very long here, additional experiments are needed to see whether extension should really go beyond the tail of the queues, or whether some intermediate extension covering enough entry points (on-ramps, merge E34/E313) are included.

6.5. Traffic state prediction capability of RENAISSANCE on the Antwerp Ring network in incident conditions

Despite the successful incident detection and the good mean speed estimates during the incident (that serve as initial state for the predictions), the produced predictions under incidents fail to capture the resulting non-recurrent congestion if the current software of RENAISSANCE is used unaltered. The reason for this is quite clear. Even if the estimated capacity drops significantly (which is not always the case), it does not drop sufficiently to predict a non-recurrent congestion.

In the future, improved capacity estimation under incident conditions may be achieved by considering the flow measurements after the incident detection. The reduced flows downstream reflect roughly the real capacity under the incident impact and could be used as a much more accurate capacity estimate when an incident is detected. Although, this possibility is not included in RENAISSANCE at this stage, a corresponding software extension would require only moderate effort. Preliminary prediction results when incorporating this possibility were found to be very good.

6.6. Conclusion and recommendations on applicability of RENAISSANCE on the Antwerp Ring network

Overall, the performance of RENAISSANCE on the Antwerp network is satisfactory for traffic state estimation, both in regular and incident-affected conditions. Also the detection of incidents performed remarkably well on the (still limited) set of incidents that was analyzed. It is advisory to continue the analysis of estimation and incident detection performance on a more elaborate data set, for instance in an online context. Special issues to be examined in such long run analysis are:

- Stability of parameter estimates, and related to that, stability of estimation performance;
- Statistical performance of incident detection (detection rate, false alarm rate);
- Validation of travel times versus independent ground truth.

The current prediction performance of RENAISSANCE on the Antwerp network is less satisfactory. In-depth analyses revealed that it is mainly the way in which the network was defined that causes the prediction problems, not necessarily inherent limitations of the model itself. More precisely, it was found that the main regular queues in the network had either their head or tail outside of the modelled network, so that either the capacity constraint or the traffic demand for the queue was external to the model and needed to be predicted through the simplified prediction methods for network boundaries. This would inhibit any online traffic flow model to produce stable prediction results, and therefore also RENAISSANCE. The next steps in improving prediction performance can therefore be either offline or online experiments, involving:

- Some variants of configuration for Inner ring queue upstream of Antwerp-South;
- Extension of network to include beginning of E313 outbound;
- Extension of network upstream of E313 inbound.

Overall, the successful state estimation and incident detection justifies further experimenting with RENAISSANCE application on the Antwerp network, which – apart from some technical issues – should give insights in the added value of the tool for the traffic operators, for traffic information and for deploying traffic management strategies. Furthermore, the prediction results and the insights gained into potential for substantial improvement of the currently less sufficient prediction performance, motivate further experiments as well. The more since for operational purposes, predictions would have added value with respect to already available systems and tools, making a RENAISSANCE model for Antwerp with improved prediction capability a unique tool in the traffic management centre.